THE UNIVERSITY
of EDINBURGH

Characterization Of The Role Of Angiopoietin-Tie Signalling In Haematopoietic Stem Cell Development In The Murine Embryo

Sara Tamagno

Thesis submitted for the degree of Doctor of Philosophy

The University of Edinburgh

2017

Abstract

Haematopoietic stem cells (HSCs) are capable of self-renewing and multi-lineage reconstitution of the haematopoietic system of irradiated recipient mice. In the mouse embryo, HSCs originate in a step-wise manner from the haematogenic endothelium. The first HSC precursor has been detected at E9.5 in the dorsal aorta, while HSCs emerge in the aorta-gonad-mesonephros (AGM) region around E11. To date, the molecular mechanisms regulating these events are poorly characterized. Through the activating role of Angiopoietin1 (Ang1) on Tie2 receptor, the Ang-Tie signalling pathway plays a critical role in HSC maintenance in the adult bone marrow niche. Tie2 ligand Angiopoietin2 (Ang2) is described as being a Tie2 inhibitor, however its role is unknown. The aim of this thesis was to characterise the role of Ang-Tie signalling pathway in HSC formation in the mouse embryo. First, I used an *ex vivo* aggregate system to culture with angiopoietins cells derived from the AGM region at stages of development preceding HSC formation (E9.5-E11). Ang2-treated cells were able to reconstitute the peripheral blood of recipient mice to a higher extent compared to control, indicating a role for Ang2 in promoting HSC maturation. Then, I characterized the expression pattern of Ang-Tie molecules in the AGM region. Ang2-expressing cells were identified as perivascular and sub-aortic mesenchymal cells located in the ventral side of the aorta and in proximity of intra-aortic haematopoietic clusters. Finally, I performed an RNA-seq analysis with the aim of unravelling the molecular mechanisms involved in Ang2-mediated HSC maturation. Pre-HSC-I were cultured in presence or absence of Ang2 and their transcriptional profiles were compared, revealing a number of genes and pathways up-regulated or down-regulated in presence of Ang2, which might indicate a role for Ang2 in increasing cell proliferation, favouring cell migration, and regulation of other signalling pathways involved in HSC development. All together, these data support Ang2 as a novel regulator for HSC formation.

Lay Summary

Blood stem cells (or haematopoietic stem cells) can produce all the cells in the blood, such as red blood cells, white blood cells and platelets. Researchers are currently trying to find ways to grow these cells in the lab for two main reasons. Firstly, these cells could be used to derive red blood cells for transfusions. Secondly, they could be used to replace the aberrant cells of patients affected by leukaemia and other blood malignancies. However, in order to understand how to produce blood stem cells in the lab, it is necessary to know how they originate in the embryo. Although the time and place these cells first appear are known, little is known about what signals control their emergence. My thesis focussed in understanding the role of a new set of molecules that were never studied in embryonic blood stem cell formation before. Adding these molecules to the culture of the immature precursors of blood stem cells showed that one of these molecules, named Angiopoietin2, was able to improve the efficiency of blood stem cell formation. Further study focussed in understanding the specific cell types which produced Angiopoietin2 and the mode of action that it works through. This discovery has provided a new piece of information that will hopefully contribute to the production of blood stem cells in the lab.

Declaration

I declare that this thesis was composed by myself, that the work contained herein is my own except where explicitly stated otherwise in the text, and that this work has not been submitted for any other degree or professional qualification except as specified.

Sara Tamagno
Edinburgh, 2017

Acknowledgements

Firstly, I would like to thank my supervisor Professor Alexander Medvinsky for giving me the opportunity to undertake my PhD studies under his guidance. I am grateful for his vast knowledge and genuine passion for science, as well as for providing both encouraging and critical feedbacks as a scope for creative thinking. Special thanks to my mentor Dr Stanislav Rybtsov for the scientific guidance he provided through teaching, insightful discussions and advice, and especially for his extreme patience.

I would also like to thank all the members of the Medvinsky lab. I am particularly grateful to Dr Vincent Frontera for being my second mentor during his permanence in the lab and for his genuine willingness to help every time he could. To Dr Antoniana Batsivari for technical advice and scientific discussions on the project and on this thesis. To Dr Javier G. Lendinez for the after lab discussions in front of a pint. To Dr Alison McGarvey for the scientific advice on RNA-sequencing. To Dr Jennifer Easterbrook for sharing the joys and pains of writing. To my fellow twin PhD student Anahí Binagui-Casas for embarking this journey together in the lab and in Espionage. To all current and previous members of the lab: Dr Anna Liakhovitskaia, Dr Jordi Senserrich, Dr Céline Souilhol, Dr Lucia Morgado-Palacin, Dr Andreys Ivanovs, Dr Natalia Rybtsova, Dr Sabrina Gordon-Keylock, Dr Boni Afouda, Dr Daria Paruzina, Dr David Hills, Dr Yiding Zhao, Heather Wilson, Suling Zhao, Kateryna Bilotkach, Edie Crosse, Nneka Nnadi.

I am grateful to Professor Elisabetta Dejana for giving me the opportunity to pursue an internship in her lab. The scientific guidance and passion of Dr Costanza Giampietro and the rest of Elisabetta's team has been a driving force for my project and motivation. Further thanks go to Drs Fiona Rossi, Claire Cryer and Bertrand Vernay for technical assistance with flow cytometry and imaging, to Ron Wilkie for support with the histology and to Carol Manson, John Agnew and all the animal unit staff.

To the many PhD students, colleagues and friends in Edinburgh, with whom I shared a lot of hilarious and unforgettable moments, travels and chats, which made these four years in Edinburgh a lot warmer. Special thanks go to Antonella for always encouraging me to continue further in my path. To my flatmate Luca for being like a brother to me. To Matina for being by my side along this journey, for always cheering me up during the difficult moments, and for making the good moments wonderful. To my parents and my grandmother for their unconditional love and support.

Non chiederci la parola che squadri da ogni lato
l'animo nostro informe, e a lettere di fuoco
lo dichiari e risplenda come un croco
perduto in mezzo a un polveroso prato.

Ah l'uomo che se ne va sicuro,
agli altri ed a se stesso amico,
e l'ombra sua non cura che la canicola
stampa sopra uno scalcinato muro!

Non domandarci la formula che mondi possa aprirti,
sì qualche storta sillaba e secca come un ramo.
Codesto solo oggi possiamo dirti,
ciò che *non* siamo, ciò che *non* vogliamo.

———

Do not ask us for the word that gives shape from all angles
to our formless soul, and in letters of fire
declares it, and stands out like a crocus,
lost in the middle of a dusty field.

Ah, the man who goes on confidently,
to others and to himself a friend,
unfazed by his own shadow which the dog days
stamp over a decrepit wall!

Do not demand from us the formula unfolding worlds before you,
rather a few crooked syllables - and dry like a twig.
That alone today we can tell you,
who we are *not*, what we *do not* want. [1]

(Eugenio Montale, Ossi di Seppia, 1923)

[1] *Translation adapted from LiteraryJoin*

Abbreviations

7AAD	7-Amino-Actinomycin D
AGM	Aorta-Gonad-Mesonephros
Ang1	Angiopoietin1
Ang2	Angiopoietin2
Ao	Aorta
AoD	Dorsal domain of the aorta
AoV	Ventral domain of the aorta
BFU-E	Burst Forming Unit -Erythroid
BM	Bone marrow
bp	Base pair
Ca^{2+}	Calcium
CFU-C	Colony Forming Unit - Culture
CFU-GEMM	Colony Forming Unit - Granulocyte Erythroid Monocyte Megakaryocyte
CFU-GM	Colony Forming Unit - Granulocyte Macrophage
CFU-S	Colony Forming Unit - Spleen
CLP	Common Lymphoid Progenitor
CMP	Common Myeloid Progenitor
CP	Caudal part
DAPI	4,6-diamidino-2-phenylindole, dihydrochloride
E	Embryonic day
EDTA	Ethyelediamine tetra-acetate
ee	Embryo equivalent
EHT	Endothelial to Haematopoietic Transition
ES	Embryonic stem
FACS	Fluorescence activated cell sorting
FCS	Foetal Calf Serum
FL	Foetal liver
Flt3-l	Fms-like tyrosine kinase 3-ligand
GFP	Green Fluorescent Protein
HSC	Haematopoietic Stem Cell
HSPC	Haematopoietic Stem and Progenitor cell
IAHC	Intra-Aortic Haematopoietic Cluster
IL3	Interleukin 3
IMDM	Iscove's Modified Dulbecco's Medium
iPSC	Induced Pluripotent Stem Cell
KO	Knock Out
Lin	Lineage

LMPP	Lymphoid-primed Multipotent Progenitor
LT	Long Term
Mg	Magnesium
MPP	Multipotent Progenitor
P-Sp	Para-aortic Splachnopleura
P/S	Penicillin/Streptomycin
PB	Peripheral Blood
PBS	Phosphate Buffered Saline
PCA	Principal Component Analysis
Pre-HSC	Haematopoietic stem cell precursor
qRT-PCR	Quantitative Reverse-Transcription Polymerase Chain Reaction
RT	Room Temperature
SCF	Stem Cell Factor
SLAM	Signalling Lymphocyte Activation Molecule
sp	somite pair
ST	Short Term
UGR	Urogenital Ridge
VC	VE-Cadherin
VEGF	Vascular Endothelial Growth Factor
WT	Wild Type
YS	Yolk Sac

Contents

List Of Figures

List of Tables

Chapter 1 Introduction

1.1 The concept of haematopoietic stem cell

Haematopoietic stem cells (HSCs) are multipotent cells that are responsible for maintaining the adult blood system throughout the life of an organism through a process called haematopoiesis. The haematopoietic system is responsible for a series of fundamental functions for the organism, such as oxygen transportation, immune defence against pathogens, blood clot formation. In this section, haematopoietic stem cells are introduced through their history and properties, their hierarchical model, and the unique detection methods used for their characterization.

1.1.1 History of haematopoietic stem cells or: how I learned to stop worrying and love the bomb

Haematopoietic stem cells (HSCs) were historically discovered in the 1950s, concurrently with the advent of the atomic bomb. At the time, research aimed at understanding how medical intervention could revert the devastating effect of ionizing radiations (Eaves 2015). This led to the discovery that the bone marrow is one of the most radiosensitive tissues and that recovery of the damaged tissue could be mediated by intravenous bone marrow transplantation, which would restore the total amount of myeloid and lymphoid cells of irradiated rodents (Lorenz et al. 1952). While it was initially believed that haematopoietic tissue recovery was mediated by a "substance of a noncellular nature" (Jacobson et al. 1951), Lorentz *et al* were the first to assume that injection of haematopoietic tissue would contribute to survival by creating "new areas of haematopoiesis" (Lorenz et al. 1952). However, it wasn't until four years later that Ford and colleagues established that cellular repopulation was the mechanism by which tissue damage could be reverted (Ford et al. 1956). This discovery led to the idea that the bone marrow tissue contains a class of haematopoietic cells with regenerative capacity.

The empirical demonstration that cells with regenerative capacity are multipotent came with the observation that bone marrow transplanted cells could

give rise to colonies in the spleen (CFU-S) (Till & McCulloch 1961) that were proportional to the number of cells transplanted (Becker et al. 1963). Splenic colonies contained proliferative cells (Till & McCulloch 1961) of myeloid, erythroid and lymphoid origin (Wu et al. 1967; Wu et al. 1968) and could form colonies in secondary recipients (Siminovitch et al. 1963). Thus, these cells held self-renewal and differentiation capacities, the two defining properties of stem cells.

While transplanted cells forming CFU-S were proliferative, further research revealed that in the adult marrow the stem cell population was found in a quiescent state (Becker et al. 1965). Thus, it was proposed that the bone marrow contains a quiescent population of self-renewing haematopoietic stem cells that are capable to differentiate and give rise to all blood lineages.

1.1.2 The haematopoietic stem cell hierarchy

In the widespread hierarchical model of the haematopoietic system, HSCs sit atop of the hierarchy (Figure 1.1). HSC differentiation results in the production of a multipotent progenitor (MPP), which has limited self-renewal capacity but retains the multilineage ability of HSCs of giving rise to all the blood hierarchy. Further downstream, MMPs give rise to both the common myeloid progenitor (CMP), which exclusively differentiates into the myeloid lineage, and the common lymphoid progenitor (CLP), with a restricted differentiation potential towards lymphoid cells. The CLP directly differentiates into committed precursors that result into NK, B and T cell production. By contrast, CMPs give rise to a series of intermediate progenitors: the myeloid-erythroid progenitor (MEP), that generates erythrocytes, and megakaryocytes; and the granulocyte macrophage progenitor (GMP), that results in the production of granulocytes and monocytes (Seita & Weissman 2010).

The understanding of the canonical haematopoietic hierarchy has mainly been achieved by cell surface antigen phenotype analysis by flow cytometry, which has allowed the isolation of sub-populations of blood cells. However, it is possible that phenotypically homogeneous populations might be functionally distinct. An alternative model proposed by Jacobsen's group suggests the existence of a lymphoid-primed population of MPPs (LMPP) (Adolfsson et al. 2005). According to this model, HSCs differentiate into MEP and LMPP. LMPP give rise to the lymphoid

lineage (B/T cells), as well as granulocyte and monocyte, while megakaryocytes and erythrocytes derive from MEPs. Myeloid potential of the LMPP was determined by *in vitro* cultures, while lymphoid potential was assessed by co-culture with OP9-Dll4. However, lineage tracing studies later suggested that megakaryocytes and erythrocytes can also arise from LMPPs (Forsberg et al. 2006), claiming that LMPPs are a more committed subset of MPPs and leaving this model subject to debate.

The advent of new lineage tracing methods has allowed a reinterpretation of the hierarchical structure and proposed alternative routes. A transposon-mediated technique that allowed *in situ* barcoding of approximately 30% of HSC, MMPs and myeloid progenitors suggested that the main drivers of steady state haematopoiesis are multipotent and lineage-restricted progenitors, while HSCs have minimal contribution to blood production (Sun et al. 2014). In human, it has been proposed that while in the foetus many stem and progenitor cells are multipotent, progenitors in the adult are mainly unipotent and oligopotent intermediates are very few (Notta et al. 2016).

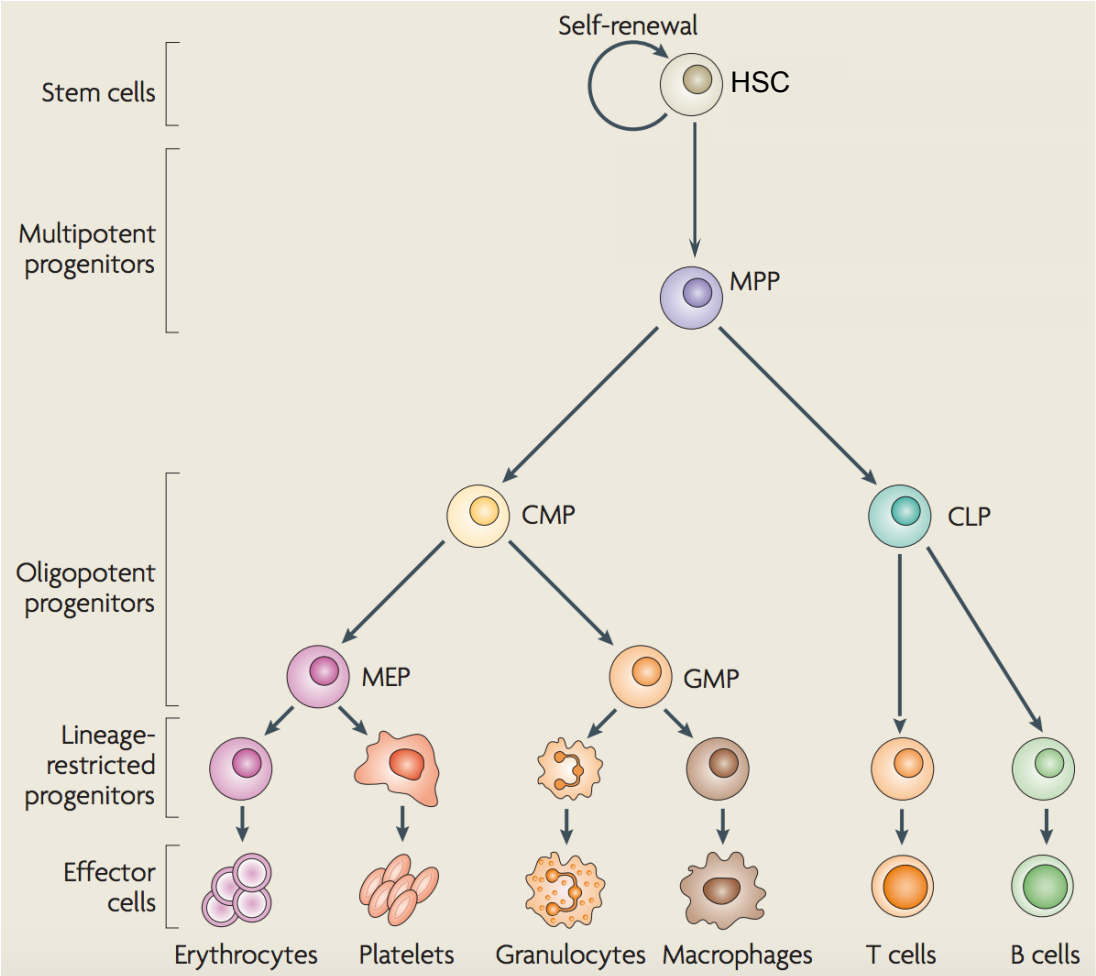

Figure 1.1 | The classical hierarchical model of the haematopoietic system.
General model of the haematopoietic system showing a haematopoietic stem cell (HSC) atop of the hierarchy, which can self-renew or differentiate to gradually produce lineage-restricted cells. MPP: multipotent progenitor; CMP: common myeloid progenitor; CLP: common lymphoid progenitor; MEP: myeloid-erythroid progenitor; GMP: granulocyte macrophage progenitor. Adapted from (Sharpless & DePinho 2007).

1.1.3 Purification and detection of haematopoietic stem cells

The current limitation in HSC research is represented by the fact that no single gene has been found to be uniquely expressed by HSCs. At present, combinations of immunophenotypic markers have been established in order to allow isolation of a population that is significantly enriched for HSCs, but does not exclusively contain this cell type and includes a mixture of progenitor cells. Isolation of bone marrow HSCs typically combines the use of antibodies that characterize Lin^-

[2] $Sca1^+$ $cKit^+$ $CD34^-$ with antibodies against SLAM markers ($CD150^+$ $CD48^-$) in addition to $Flt3^-$ or $EPCR^+$ (Osawa et al. 1996) (Kiel et al. 2005) (Dykstra et al. 2007; Kent et al. 2009) (Goodell et al. 1997).

Thus, the only method that truly allows identification of HSCs is represented by the transplantation assay, in which a population of cells (donors) is transplanted into irradiated adult recipients/hosts. As HSCs retain the capacity to home the host bone marrow, as well as to self-renew and contribute to all blood lineages in the recipient (Harrison 1980), this test reliably determines HSC functionality through the assessment of their engraftment potential. Thus, the higher the donor contribution to the engraftment, the higher the proliferative and repopulating ability of the HSCs contained in the transplanted pool.

Transplantation experiments are usually carried out by co-transplanting donor cells along with competitor/carrier cells that are phenotypically distinguishable from both donor and recipient cells. These cells are usually isolated from the bone marrow of an adult mouse, hence they constitute a pool of cells that includes HSCs. These cells have several functions. Firstly, by co-injecting carrier cells, the ability of donor HSCs can be tested by their capacity to repopulate the haematopoietic system of the recipient relatively to the competitor (Ema et al. 2005; Harrison et al. 1993). Furthermore, co-injection of these cells provides haematopoietic reconstitution of the host even if donor HSCs are provided in low numbers. Repopulating HSCs can then be quantified by transplantation of donor cells at a limiting dilution for quantitative purposes and their frequency can be determined using a Poisson model (Hu & Smyth 2009).

Transplantation experiments revealed the existence of two distinct subtypes of HSCs: long-term repopulating HSCs (LTR-HSCs), which are detectable for at least 12 months in the recipient and are able to provide repopulation when subsequently transplanted into secondary recipients; and short-term repopulating HSCs (STR-HSCs) which have limited self-renew capacity and are only detectable for 1-2 months after transplantation (Zhong et al. 1996; Harrison & Zhong 1992).

[2] Lineage negative (Lin^-) refers to the exclusion of markers that are expressed by lineage committed haematopoietic cells and includes: CD3, CD4, CD5, CD8, B220, Gr1, Mac1, Ter119 (Boyer et al. 2011)

1.2 Ontogeny of the haematopoietic system

Haematopoiesis is a complex process that involves several organs and occurs across a range of developmental stages in the embryo. The widely accepted model of ontogeny is associated with the concept of a dual wave of haematopoietic cells (Medvinsky et al. 2011). Although seeming paradoxical, this model describes that during embryogenesis members of the haematopoietic hierarchy emerge in the reverse order compared to the adult hierarchy. Accordingly, a primitive wave of haematopoiesis starts in absence of HSCs in the yolk sack and produces a transient population of lineage-restricted blood cells. This wave is followed by a definitive wave, which seeks intra-embryonic production of HSCs. After HSCs are detected at several sites in the mid-gestation embryo, they migrate onto the foetal liver where they expand in numbers (Kumaravelu et al. 2002). At later stages of development and prior to birth, HSCs colonize the adult sites of haematopoiesis: bone marrow, spleen and thymus. It is believed that the only period in which HSCs are generated is *de novo* (Henninger et al. 2017), thus the study of their embryonic development is of crucial importance as it can help establish HSC generation *in vitro* for clinical applications.

1.2.1 The primitive wave of haematopoiesis

The primitive wave of haematopoiesis begins extra-embryonically at E7.5 with the appearance of haematopoietic cells in the yolk sac (Figure 1.2). From this time point, erythrocytes, macrophages and megakaryocyte progenitors (Palis et al. 1999; Xu et al. 2001) are detectable in areas of the yolk sac called blood islands (Maximow 1909; Takahashi et al. 1989), which represent compartments of undifferentiated cells surrounded by the endothelium (Ferkowicz & Yoder 2005).

The primitive wave yields unique blood cells. In contrast to their definitive counterpart, primitive erythrocytes are bigger nucleated cells expressing embryonic and adult haemoglobin types (Leder et al. 1992). Primitive macrophages synthetize and express distinct sets of enzymes, including lysozyme (Faust et al. 1997), and in contrast to their definitive counterpart develop independently of the transcription factor MYB (Schulz et al. 2012). Primitive megakaryocytes present differences in

cytokine sensitivity and mature rapidly to produce platelets with the aim of preventing the forming blood vessels from bleeding (Xu et al. 2001).

The primitive wave is rapidly followed by a second wave of cells that produces erythromyeloid (EMP) and lymphoid progenitors (McGrath et al. 2015; Böiers et al. 2013). These cells emerge in the yolk sac and seed the foetal liver, but do not have long-term potential when transplanted. Although recent reports have shown that yolk sac-derived macrophages are the major source of adult microglia (Ginhoux et al. 2010; Kierdorf et al. 2013), it is believed that the HSC-independent waves are mainly required to meet the initial oxygen circulation and blood function needs for embryonic survival. These are later substituted by a definitive wave of haematopoiesis in which HSCs with long-term potential are produced.

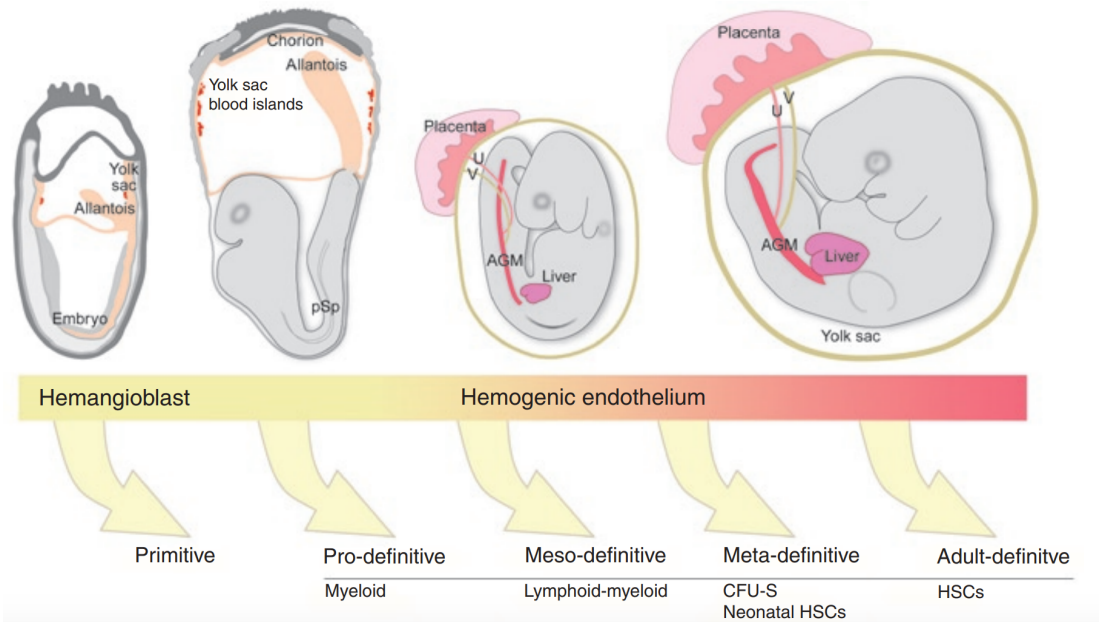

Figure 1.2 | Ontogeny of haematopoiesis in the murine system.

Shows the sequential emergence of haematopoietic cells of the primitive wave, followed by the appearance of more mature progenitors and then the first adult-definitive HSCs. P-Sp: para-aortic splanchnopleura; AGM: aorta-gonad-mesonephros; V: vitelline artery; U: umbilical artery. From (Dzierzak & Speck 2008)

1.2.2 Embryonic origin of definitive haematopoiesis

The identification of the source of the first definitive HSC has been a key challenge in the haematopoietic field due to the intrinsic mobility of HSCs. At E11.5, the aorta-gonad-mesonephros (AGM) region, the yolk sac and the placenta all contain approximately one HSC each (Kumaravelu et al. 2002).

Since the first blood cells develop in the yolk sack, for decades this was considered the source of origin of HSC. This theory was supported by the observation that organ culture of the yolk sac could give rise to multilineage colony forming cells (CFU-C and CFU-S) (Moore & Metcalf 1970). Moreover, trans-placental injection of E9.0 yolk sac cells into embryos had been reported to contribute to erythroid long term repopulation in a small proportion of the recipient animals (Toles et al. 1989). However, it was not clear if the repopulating cells transplanted from the yolk sac originated *in situ* or migrated to the yolk sac from the embryo.

The validity of the yolk sack theory was irremediably questioned with a series of chick-quail grafting experiment (Dieterlen-Lievre 1975). In these experiments, quail embryonic tissue was grafted onto the chick yolk sac at embryonic day 2, before the establishment of vascularization, and the contribution to each of these tissues to adult haematopoiesis was measured after 6-11 days. All the multilineage repopulating cells were of quail type, indicating that the source of haematopoietic stem cell origin must be intra-embryonic. Furthermore, transplantation of cultured cells isolated from both the yolk sac and the caudal part of the embryo at E8.0 (before the onset of circulation) demonstrated long-term repopulation exclusively from the caudal part of the embryo (Cumano et al. 2001).

Thus, these experiments strongly suggested that the source of cells able to sustain the adult haematopoietic system long-term is embryonic and not extra-embryonic.

1.2.3 The aorta-gonad-mesonephros region as the site of definitive haematopoiesis

Once determined that the source of long-term repopulating cells is intra-embryonic, further research was prompted to investigate the tissue of origin of these

cells. Experiments in the avian and amphibian systems were the first to demonstrate that definitive adult haematopoietic stem cells arise from a region of the mesoderm comprising the dorsal aorta (Dieterlen-Lievre & C. Martin 1981; Maeno et al. 1985). In mouse, the direct comparison of CFU-S activity of yolk sac, foetal liver and the aorta-gonad-mesonephros (AGM) (the murine analogue to the intra-embryonic HSC source in chicken and Xenopus) demonstrated that the AGM region contains a higher frequency of CFU-S in comparison to the yolk sac and that CFU-S are contained in the AGM at an earlier developmental stage compared to the foetal liver (Medvinsky et al. 1993). Thus, these experiments indicated the AGM region as the first intra-embryonic site harbouring haematopoietic activity (Figure 1.3).

The ability of the AGM to generate HSCs *in situ* was verified by investigating the long-term repopulating ability of the AGM-derived cells via transplantation into irradiated mice (Müller et al. 1994). These experiments showed that the AGM region at E10 was the first haematopoietic site containing long-term repopulating HSCs, while the yolk sac and the liver had none (Müller et al. 1994). To exclude the possibility that HSC from the AGM might arise from other haematopoietic tissues and migrate onto the AGM through circulation, haematopoietic tissues were isolated at E10.5 and cultured separately using a novel organ culture method before being transplanted into irradiated recipients (Medvinsky & Dzierzak 1996). These experiments showed that the AGM was the only site containing HSC with long-term repopulation ability, while no repopulation was observed from the yolk sac or the foetal liver. This proved that HSC are formed *in situ* in the AGM region and suggested that other haematopoietic sites such as liver and yolk sac are subsequently colonized.

1.2.4 Additional sources of HSC autonomous production currently under debate

Although the AGM was proven to be the first site of autonomous emergence of HSCs, other embryonic and extra-embryonic sites have been linked to HSC activity. Whether the haematopoietic activity in these sites proves autonomous formation of HSC is a subject of debate.

The mouse extra-embryonic placenta contains haematopoietic progenitors as early as E8.5 and by E10 the number of progenitors are higher compared to the yolk sac and foetal liver (Alvarez-Silva et al. 2003). However, transplantation experiments have shown the presence of HSCs in this organ only at later stages. By E10.5-E11, concomitantly with HSC emergence in the AGM region, between 1-2 HSCs can be found in the placenta (Gekas et al. 2005; Ottersbach & Dzierzak 2005). This number increases by E12.5 and declines by E15.5, suggesting migration of HSC to the foetal liver by that time point (Gekas et al. 2005; Ottersbach & Dzierzak 2005). While explant cultures of E10 placentas were not able to repopulate transplanted irradiated mice (Robin et al. 2006), indicating that no HSC could be found in the placental tissue *per se*, it is also possible that explant culture conditions were not optimal to support HSC maintenance and expansion. Thus, whether the placenta has the ability to initiate *in situ* production of HSC or only supports maturation of exogenous HSC is still a subject of debate.

HSCs are also contained in extra-embryonic vessels. At E10.5, the vitelline and umbilical arteries were shown to contain HSCs at a similar frequency to the AGM region (de Bruijn et al. 2000). Accordingly, it was shown that these extra-embryonic vessels contained HSC precursors (HSC precursors will be discussed in section X) that could be expanded in culture and mature into HSCs (Gordon-Keylock et al. 2013), suggesting that extra-embryonic vessels are a site of HSC emergence. However, it still needs to be elucidated whether HSC precursors emerge *in situ* or migrate from another region.

Recent reports explored the possibility that the embryonic head might be a site for HSC development (Zhuan Li et al. 2012; Zhuan Li et al. 2016). In these experiments, the head was transplanted in parallel to the AGM region and the circulating blood at E10.5 and E11.5. Interestingly, at E10.5 both the head and the AGM region repopulated recipient mice at a similar frequency, while repopulation from the blood was detected only at E11.5. Thus the authors claim that since HSCs can be seen in circulation later than they are seen in the head, this suggests that the head is a source of *in situ* production of HSC. However, sub-regional dissection of the head localized the source of repopulating HSCs in the area of the hindbrain and brachial arches, which includes the carotid artery (Zhuan Li et al. 2016). Thus, it

could be postulated that due to the vicinity of the aorta to the carotid artery, aortic HSCs might be source of contamination in that area. In conclusion, it is not clear whether the head harbours autonomous ability to generate HSCs.

1.2.5 The foetal liver as a site of HSC expansion

After HSCs are detected in the embryo at several locations, they can be found in the foetal liver, which contains the largest number of haematopoietic stem cells in the mid-gestation embryo. At E12.5, one day after HSCs first appear in the AGM region, around 50 cells can be found in the foetal liver (Kumaravelu et al. 2002). This pool continues to expand in the following days (Ema & Nakauchi 2000) until E15.5, when the frequency of this population falls dramatically (Morrison et al. 1995) as HSCs seed the bone marrow (Coşkun et al. 2014), the main adult niche. It is not clear whether HSC colonize the foetal liver through circulation or by alternative ways, however HSC migration seems to be dependent on adhesion molecules such as β1-integrin (Hirsch et al. 1996; Potocnik et al. 2000).

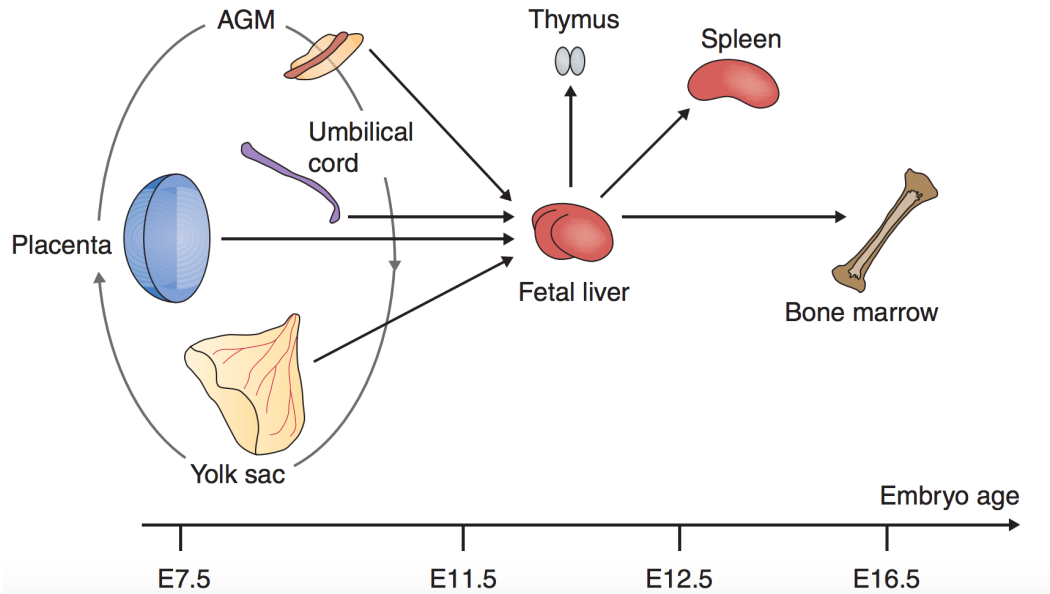

Figure 1.3 | Multisite haematopoietic development.

Representation of the sites of appearance of haematopoietic precursors and HSCs between E7.5 and E11.5. HSCs migrate from the different sites and are found in the foetal liver around E12. HSC expand in the liver and subsequently migrate to the thymus, spleen and bone marrow, the adult HSC niche. Adapted from (Medvinsky et al. 2011).

1.3 Ontogeny of haematopoietic stem cells

In the past decades, several theories have arisen regarding the origin of haematopoietic stem cells. Similarities in the development of the haematopoietic and endothelial lineages have long been observed. No endothelial-specific genes can be exclusively detected in the endothelium but not in the developing haematopoietic lineage. In contrast, haematopoietic cells express a number of lineage-specific markers that are absent from the endothelium. Possible models of HSC ontogeny are discussed in this section.

1.3.1 The haemangioblast

The close association between the endothelium and the first haematopoietic cells forming in the blood islands of the yolk sac has been documented as early as in the 1920s (Sabin 1920). This led to the idea that a common precursor of haematopoietic and endothelial cells might exist, named the haemangioblast.

The haemangioblast was first identified after the observation that embryonic stem (ES)-derived embryoid bodies (EBs) cultured in methylcellulose for 2-4 days in presence of cytokines (VEGF and SCF) could form colonies of immature (blast-like) cells that contained both endothelial and haematopoietic precursors (Choi et al. 1998). Cells with similar properties were later identified in the embryo proper within the posterior primitive streak at E7 (Huber et al. 2004). Interestingly, these cells were shown to have the ability to produce not only endothelial and haematopoietic cells, but also smooth muscle cells. Thus, it is more likely that rather than representing a bi-potent progenitor with endothelial and haematopoietic properties, the haemangioblast as specified could be a multipotent mesodermal cell (Medvinsky et al. 2011). Moreover, a recent study of the *in vivo* clonal analysis of the haemangioblast was able to identify that the majority of the clones in the yolk sac contain either endothelial or haematopoietic cells, but not both (Padrón-Barthe et al. 2014). Thus, this study rejects the idea of a bi-potent cell in the specification of the endothelial and blood lineages and supports the hypothesis of the segregation of those lineages before gastrulation. Accordingly, the existence of a restricted bi-potent precursor of the endothelial and haematopoietic lineage is still open to debate.

1.3.2 Intra-aortic haematopoietic clusters and the haematogenic endothelium

Another theory about the origin of HSCs relies on the hypothesis that they are initiated from a sub-type of endothelial cells that can undergo differentiation into haematopoietic cells, named the haematogenic (or haemogenic) endothelium. This hypothesis is driven by the observation that clusters of haematopoietic cells in the aorta are found in close contact with the endothelium (Jordan 1917) (Smith & Glomski 1982) and that appearance of clusters and emergence of HSCs are correlated in terms of timing and location (Dieterlen-Lievre et al. 2006) (Yokomizo & Dzierzak 2010).

Support for the theory that clusters are generated by endothelial cells has come from the observation that tracing endothelial cells with acetylated low density lipoprotein (AcLDL) (a marker of endothelial cells) at a time point in which clusters are not yet formed, results in labelling of the clusters in both the avian and mouse system (Jaffredo et al. 1998; Sugiyama et al. 2005). However, it was not shown that incorporation of AcLDL is endothelial-specific, thus indicating that other cell types other than endothelial cells might originate the clusters.

Nevertheless, functional evidence suggesting the endothelial origin of HSCs was given by experiments with embryo and ES-derived cells in which an endothelial-like population (VE-Cadherin(VC)$^{+}$ CD45^{-}) was shown to have higher ability to differentiate into myeloid and lymphoid fates over a haematopoietic population (VC^{-} CD45^{+}) (Nishikawa et al. 1998; Hirashima et al. 1999). The endothelial population was then isolated from embryos at E9.5 and was found to provide long-term engraftment in recipient mice (Fraser et al. 2002).

To fulfil the hypothesis that the haematogenic endothelium produces HSCs, studies in mouse have made use of the Sca1 (Ly6a)-GFP reporter (de Bruijn et al. 2002). Using this model it was shown that all functional HSCs in the E11 AGM region co-express Ly6a, a marker of bone marrow HSCs, and CD31, an endothelial cell marker (North et al. 2002). When looking at transverse sections of the AGM, Ly6a-GFP^{+} cells were exclusively found in correspondence of the CD31^{+} endothelial layer, thus suggesting that HSCs are generated from the endothelium and possess both endothelial and haematopoietic characteristics. Endothelial to haematopoietic

transition (EHT) was also shown by live imaging in AGM region slices (with the Ly6a-GFP reporter) (Boisset et al. 2010), in zebrafish (Bertrand et al. 2010; Kissa & Herbomel 2010) and in ES-derived cells (Eilken et al. 2009). In the latter, endothelial colonies derived from ES cells were shown to display morphological characteristics of haematopoietic cells shortly after formation by expressing CD41, an early marker of embryonic haematopoietic progenitor cells, and CD45. Interestingly, among the colonies, some would maintain an endothelial identity without differentiating, indicating that the haematogenic endothelium can also contribute to the structural endothelium. However, the model of the haematogenic endothelium able to generate both endothelial and haematopoietic cells was not supported by a recent report, which shows that the haematogenic endothelium undergoes functional changes over time which confers an increased capacity to generate haematopoietic cells in concomitance with a decrease in the endothelial potential (Swiers et al. 2013) (Figure 1.4).

Thus, both the theory of the haemangioblast and haematogenic endothelium has received experimental evidence. To reconcile the two concepts, it was proposed the idea of the haemangioblast as a precursor of the haematogenic endothelium, which then produces haematopoietic cells (Lancrin et al. 2009).

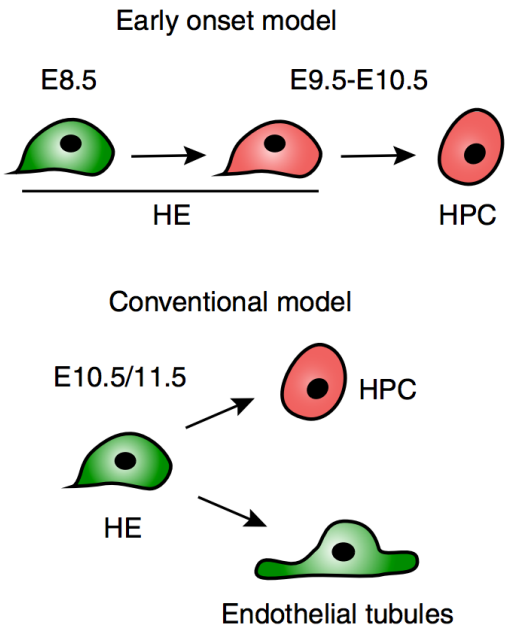

Figure 1.4 | Distinct proposed models of endothelial to haematopoietic transition.
In the early onset model, the haematogenic endothelium (HE) undergoes haematopoietic differentiation (HPC) by losing endothelial potential. In the conventional model, the haematogenic endothelium is equally capable to differentiate into the haematopoietic or endothelial lineage. Adapted from (Swiers et al. 2013).

1.3.3 The HSC precursors lineage

The hypothesis of the existence of a population of HSC precursor cells started from the observation that at E11.5 the embryo contains approximately 3 HSCs, but by E12.5 there are between 50-150 cells in the liver (Kumaravelu et al. 2002; Taoudi et al. 2008). It was then questioned how HSC maturation or expansion can occur in such a rapid fashion. This could possibly occur through rapid proliferation of the HSCs existing pool or maturation of HSC precursors into HSCs. To test these hypotheses, E11.5 AGM cells were labelled with carboxyfluorescin diacetate succinimidyl ester (CFSE) dye to determine the number of divisions cells would undertake in culture and HSCs were found to undergo approximately 4 divisions (Taoudi et al. 2008). This low number of divisions was not compatible with the 150-fold expansion observed in the foetal liver one day later, therefore it was postulated that a HSC precursor population might be present in the AGM region.

Evidence of this population was first observed after the development of a system able to aid maturation of HSCs in culture (Taoudi et al. 2008). This system (referred in this thesis as the re-aggregate culture system) consists of a step in which cells isolated from the AGM region are dissociated and can subsequently be manipulated before being re-aggregated at the gas-liquid interface in presence of growth factors (SCF, IL3, Flt3l) that are required to sustain HSC development. Using this strategy, VC^+ $CD45^+$ cells isolated from the E11.5 AGM region of EGFP mice were re-aggregated with WT AGM cells depleted of this cell type. Transplantation upon culture revealed that the haematopoietic system of recipient mice was repopulated by GFP^+ cells, indicating that VC^+ $CD45^+$ are the precursors of HSCs in the AGM region (Taoudi et al. 2008). Subsequent experiments in which the AGM microenvironment was modified by adding cells of the OP9 stromal line derived from newborn op/op mouse calvaria (Nakano et al. 1994) allowed maturation of HSCs from as early as E9.5, thus allowing to track the phenotype of HSC precursors from an earlier stage (Rybtsov et al. 2011; Rybtsov et al. 2014). These experiment allowed to show functionally that HSCs develop from a VC^+ $CD45^-$ $CD41^+$ $CD43^-$ pro-HSC population at E9.5 (Rybtsov et al. 2014), to a VC^+ $CD45^-$ $CD41^+$ $CD43^+$ pre-HSC-I population at E10.5 (Rybtsov et al. 2011; Rybtsov et al. 2014), to a VC^+ $CD45^+$ $CD41^{low}$ $CD43^+$ pre-HSC-II population at E11.5 (Taoudi et al. 2008; Rybtsov et al. 2014) (Figure 1.5).

Interestingly, VC, a marker of endothelial cells, is expressed by all HSC precursors as well as HSCs (North et al. 2002) (Taoudi et al. 2005). Although it is conceivable that HSC precursors might have an endothelial origin, in agreement with the haematogenic endothelium theory, it is also possible that endothelial markers might be expressed by these cell types transiently during their passage from the mesenchyme to the aortic endothelium lining. This second hypothesis is at the foundation of the sub-aortic patches theory of HSC formation and it is based on the observation that mesodermal structures located below the endothelial lining of the aorta express haematopoietic markers such as Lmo2, Gata3 (Manaia et al. 2000), Runx1 (North et al. 1999), BMP4 and AA4.1 (Godin & Cumano 2002). This theory of origin for HSC precursors is supported by the observation that some of the phenotypic pre-HSC-I at E11.5 reside in the sub-endothelial layers, whereas pre-

HSC-II are located in the endothelium closer to the aortic lumen (Rybtsov et al. 2011). However, these analyses are exclusively based on phenotypic characteristics and only functional lineage tracing assay would help clarifying their spatial and cellular origin.

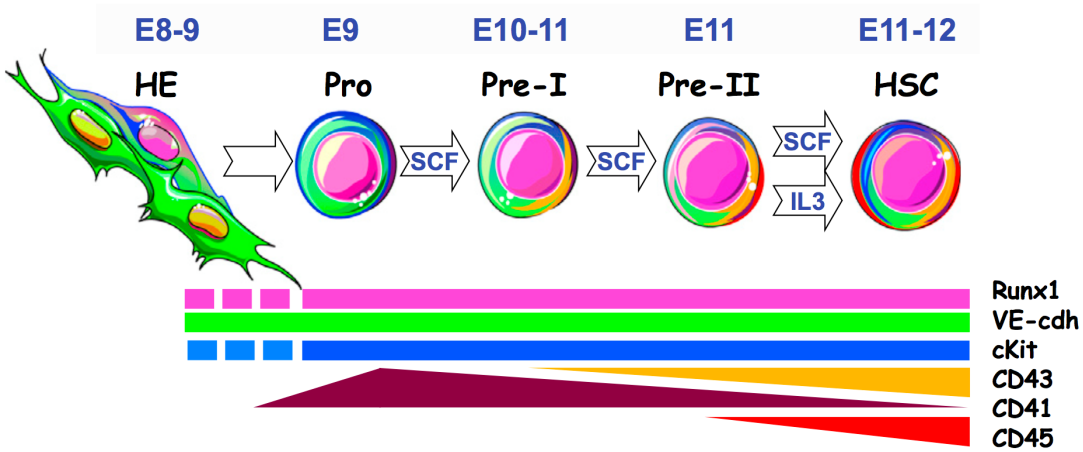

Figure 1.5 | HSCs arise in a step-wise manner in the AGM region.

Diagram showing the maturation of HSC precursor population in the AGM region between E9.5 and E11.5. As they mature, HSCs acquire lineage-specific markers and are dependent on SCF signalling. Pre-HSC-II are also dependent on IL3 signalling. HE: haematogenic endothelium; Pro: pro-HSC; Pre-I: pre-HSC-I; Pre-II: pre-HSC-II. Adapted from (Rybtsov et al. 2014) .

1.4 The haematopoietic stem cell niche

A niche represents a group of cells at a specific tissue location that regulates and supports the self-renewal and differentiation of a stem cell through an interchange of signalling pathways. As the site in which HSC can be located changes along development, thus the characteristics of the niche must also change. Throughout the adult life, HSC can be found in the bone marrow niche, which main function is HSC maintenance. By contrast, the role of the embryonic niche is just temporary and its main aim is to provide the signalling cues necessary for HSC maturation. In this section, the characteristics of both the adult and embryonic niche are discussed.

1.4.1 The adult bone marrow niche

The bone marrow has been postulated to host haematopoietic stem cells since the work of Till and McCulloch (Till & McCulloch 1961). The exclusive property of the bone marrow as a niche that hosts HSCs was first hypothesized by Schofield (Schofield 1978), who observed that putative CFU-S stem cells found in the spleen (nowadays known to be multilineage progenitors) were less capable of multilineage long-term reconstitution compared to bone marrow cells. Thus, further research sought to determine what characteristics of the bone marrow contributed to preserve HSCs and their reconstitutive potential. This led to the discovery that mesenchymal cell culture could maintain HSC *in vitro* (Dexter et al. 1977) and that HSCs were located towards the endosteal margins of long bones, thus leading to the hypothesis that bone cells might regulate haematopoiesis (Lord et al. 1975).

With these studies as a starting point, it is now known that the bone marrow is a heterogeneous environment that harbours a complex mixture of cells, including osteoblasts, adipocytes, perivascular cells, endothelial cells, neural cells (reviewed in (Sean J Morrison 2014)). The osteoblastic niche has been proposed to play a key role in the maintenance of HSC numbers, as an increase in the number of osteoblasts led to an increase of the numbers of HSCs (Calvi et al. 2003; J. Zhang et al. 2003) and transgenic mice whose osteoblasts are ablated presented a reduced number of HSCs and progenitors (Visnjic et al. 2004). It is believed that regulation of HSC maintenance by the osteoblastic niche is maintained via adhesion molecules such as E-cadherin and β-catenin (J. Zhang et al. 2003). However, this was contradicted by depletion studies that resulted in no effect on HSC numbers upon N-cadherin deletion (Kiel et al. 2007; Kiel et al. 2009), suggesting the involvement of alternative mechanisms in this process. Current data supports the idea that HSCs reside in a perivascular niche in which several cell types contribute to express regulatory factors that promote HSC maintenance. Imaging of bone marrow sections revealed presence of HSCs in close proximity to the sinusoidal endothelium (Kiel et al. 2005) and ablation of factors expressed by endothelial and perivascular cells, such as SCF, contributed to HSC ablation (Ding et al. 2012). Therefore, it is likely that several cell types contribute to create the microenvironment suitable for HSC maintenance.

1.4.2 The embryonic AGM niche and its spatial polarization

In contrast to the role of the adult bone marrow niche in maintaining HSC development, the role of the embryonic AGM niche is to provide the functional support necessary to promote maturation of HSC precursors into fully mature, transplantable HSCs. The fact that pre-HSCs in the AGM region cannot provide long term engraftment without fully maturing into HSCs first suggests that the niche provides the necessary cues to support this maturation.

As intra-aortic haematopoietic clusters are preferentially distributed in the ventral aortic endothelium (Jaffredo et al. 1998; Tavian et al. 1996), this led to the hypothesis that the niche supporting HSC development might be located ventrally. This was demonstrated by subsequent dissociation of the AGM region into its dorsal (AoD) and ventral (AoV) domains followed by transplantation, which revealed that HSC can be found four times more frequently in the ventral side of the dorsal aorta (Souilhol, Gonneau, et al. 2016; Taoudi & Medvinsky 2007). Furthermore, co-culture of the AGM with dorsal (notochord) and ventral (gut) tissues showed that tissue positioned ventrally enhances HSC activity (Peeters et al. 2009) and culture of the AGM in presence of the ventrally-located urogenital ridges (UGR) also positively influenced HSC activity (Souilhol, Gonneau, et al. 2016). All together, this data suggests that the microenvironment surrounding the AGM and located ventrally represents the AGM niche and might be the source of supportive cues that are actively contributing to HSC maturation.

1.4.3 Cellular components of the AGM niche

In order to understand how the microenvironment of the niche influences HSC development, it is necessary to understand what type of cells are found in the surrounding of the aorta. Although not all the cellular constituents have been fully elucidated yet, it is likely that niche cells can influence haematopoiesis through the enhancement of physical and chemical signalling (Figure 1.6).

1.4.3.1 The endothelial and perivascular aortic wall

Due to its proximity to the intra-aortic haematopoietic clusters, the endothelium is one of the primary cell types of the AGM niche. It is characterized by

the expression of markers such as VC (Lampugnani et al. 1992) and CD31 (PECAM-1) (Privratsky & Newman 2014). According to the theory of the haematogenic endothelium, endothelial cells are precursors of the haematopoietic lineage. Interestingly, haematopoietic clusters only emerge from arterial and not venous endothelium (de Bruijn et al. 2000; Taoudi & Medvinsky 2007; Gordon-Keylock et al. 2013), suggesting that endothelial cells in the AGM region might retain special properties contributing to HSC emergence. The vasculature endothelium is surrounded by a layer of perivascular cells attached to the vessel wall and in close contact with the endothelium (Armulik et al. 2011). Perivascular cells, referred to as pericytes or smooth muscle cells, were shown to surround the embryonic dorsal aorta and to be characterized by the expression of PDGFRβ, CD146 and NG2 at E11 (Mirshekar-Syahkal et al. 2014). However, little is known about the contribution of perivascular cells to HSC emergence in the AGM region.

Interestingly, the ventral and dorsal domains of both the endothelium and the perivascular layer have been shown to have distinct developmental origins. While the dorsal endothelium originates from the somitic (paraxial) mesoderm, the ventral aspect arises from the later plate (splanchnopleural) mesoderm (Pardanaud et al. 1996). For perivascular cells and the sub-aortic mesenchyme underneath the perivascular layer, between E9 and E10.5 the ventral domain originates from the lateral plate mesoderm and the dorsal domain from the somitic mesoderm (Wasteson et al. 2008; Wiegreffe et al. 2007), as for endothelial cells; however, by E11.5 all lateral plate-derived cells in the ventral part are replaced by somitic-derived cells migrating from the dorsal part (Wasteson et al. 2008; Wiegreffe et al. 2007). Thus, the ventral specificity of these tissues contributes to reinforce the idea that unique cues dependent on the environment might be needed from the niche for HSCs to emerge.

1.4.3.2 The mesonephros and the metanephric mesenchyme

The mesonephros is an organ with a secretory function existing transiently during embryonic development as a precursor of the kidney. The mesonephros derives from the intermediate mesoderm, forms between E9.5 and E11.5 and it is constituted by vascularized glomeruli, proximal and distal tubules, and collecting ducts (Wolffian ducts) (Saxon 1987). It starts to regress by E11.5 in concomitance

with metanephros formation, which forms the adult kidney (Sainio & Raatikainen-Ahokas 1999). Metanephros initiation occurs caudally at E10.5 from the metanephric mesenchyme, a tissue that has been shown to contain multipotent stem cells responsible for the development of the mammalian nephron (Herzlinger et al. 1992). Interestingly, transplantation of cells derived from the foetal kidney and displaying phenotypic markers characteristic of the metanephric mesenchyme were able to produce long-term haematopoietic engraftment (Almeida-Porada et al. 2002). Although the role of these tissues in HSC development remains unclear, the expression of factors related to haematopoiesis has been described. Erythropoietin, Gata3, Sca1 and SCF have been found in the developing tubules and in the mesonephric duct (Wintour et al. 1996; Lakshmanan et al. 1999; Miles et al. 1997; Souilhol, Gonneau, et al. 2016).

1.4.3.3 The gut and primordial germ cells

The developing gut is located ventrally in respect to the aorta. Co-culture of the gut with AGM region explants has been shown to induce HSC development via hedgehog signalling (Peeters et al. 2009). Interestingly, while hedgehog signalling pathway-related molecules were shown to be expressed by the gut, Gli1, a transcriptional target of hedgehog was prominent in the mesenchyme surrounding the aorta, suggesting that the signalling from the gut acts via mesenchymal cells.

The gut also contributes to the AGM niche as a source of primordial germ cells (PGC). These cells are found in the gut between E9-E9.5 and they migrate towards the genital ridges between E9.5-E10.5 (Molyneaux et al. 2001). PGCs had been initially proposed as key players in the formation of HSCs due to the fact that they retain multipotent characteristics of stem cells (Matsui et al. 1992), they co-localize with CFU-S in the embryo (Medvinsky et al. 1993; Medvinsky & Dzierzak 1996) and they contribute to the production of haematopoietic progenitors *in vitro* (Rich 1995). Similarly to HSC precursors, PGC are dependent on SCF signalling (Pesce et al. 1993), which indicates that the AGM region provides the right environment for developmental processes at this stage of development. However, it is unknown if these cells contribute to HSCs development.

1.4.3.4 Other cell types in the AGM region

Among the other cell types that constitute the AGM region, the sympathetic nervous system has been recently depicted as a regulator of HSC formation (Fitch et al. 2012). In this study, impaired production of catecholamines, the mediators of the sympathetic nervous system, obtained via knock out of Gata3 and Th, two factors involved in the synthesis of catecholamines, resulted in reduced functional and phenotypic HSCs compared to control (Fitch et al. 2012).

Haematopoietic cells could also potentially contribute to HSC formation in the AGM niche. Intra-aortic haematopoietic clusters are known to contain a mixture of HSC precursors and progenitor cells (Batsivari et al. 2017) and their close association could result in reciprocal signalling influencing HSC development. On the other hand, cluster cells are in close contact with circulation and they might interact with molecules travelling from distant tissues. Finally, although in the mouse AGM the production of macrophage colony stimulating factor (M-CSF) results in a decreased amount of haematopoietic progenitors and increased production of endothelial cells (Minehata et al. 2002), macrophages have been shown to play a role in haematopoietic stem and progenitor cell (HSPC) mobilization in the zebrafish AGM (Travnickova et al. 2015). Thus, the role of this cell type remains to be elucidated.

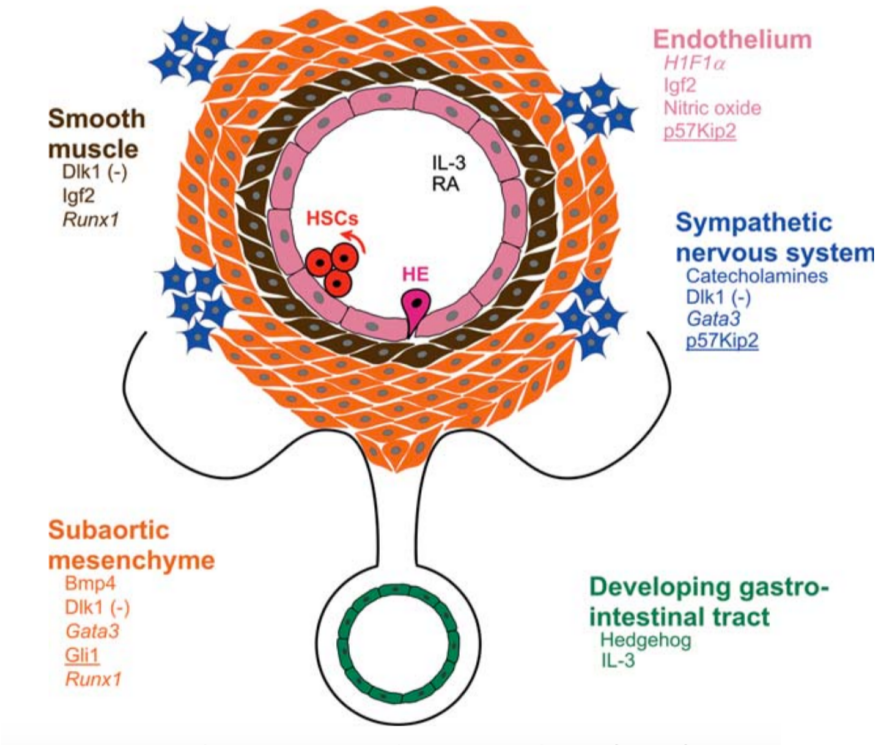

Figure 1.6 | The cell components and main signalling pathways of the AGM niche. Schematic representation of the different cell types in the AGM region and the signalling pathways found to be expressed by or to influencd these cell types. Adapted from (Mirshekar-Syahkal et al. 2014).

1.4.4 Molecular regulators of the AGM niche

In order to understand how niche cell contribute to the development of the embryonic haematopoietic system, it is necessary to understand what molecular events and signalling cues coming from the microenvironments influence HSC development. Disruption of signalling pathways and transcription factors in knockout models has provided meaningful information about how the interaction of the niche with HSCs contributes to their maturation. In this section, some of the main molecular regulators of the niche and HSC development are further discussed.

1.4.4.1 Key transcription factors in the AGM niche

Transcription factors are the regulators of cell identity. A group of transcription factors have been shown to be involved in the endothelial to haeamatopoietic (EHT) transition resulting in maturation of HSCs. Among those, Runx1 is a master regulator of embryonic haematopoiesis. Runx1 deletion did not

affect primitive haematopoiesis, but resulted in embryonic death at E12.5 associated with haemorrhaging, lack of mature haematopoietic cells in the foetal liver and lack of intra-aortic haematopoietic clusters {Sasaki:1996ws, Wang:1996vw, Okuda:1996vx, Mukouyama:2000eb, Liakhovitskaia:2014cj, North:1999ut }, suggesting a specific effect on definitive haematopoiesis. The fact that aortic clusters disappear in absence of Runx1 and that Runx1 is expressed in endothelial and mesenchymal cells in the AGM region (North et al. 1999) suggested that this transcription factor might be necessary for the transition from HSC precursors to mature HSCs. Further experiments have shown that Runx1 is required to promote maturation of pre-HSC-I into pre-HSC-II but not earlier (Liakhovitskaia et al. 2014) and that Runx1 is dispensable for adult HSCs (M. J. Chen et al. 2009).

Among the other transcription factors required for HSC development, Gata2 has been shown to be required for initiation and expansion of foetal liver and bone marrow HSCs (Tsai et al. 1994; Ling et al. 2004). Gata2 knockout embryos die at E10.5 with severe anaemia and a profound deficit in definitive haematopoietic stem and progenitor cells (Tsai et al. 1994). Gfi1 and Gf1b, downstream effectors of Runx1, have also been proposed as regulators of endothelial to haematopoietic transition, as their over-expression was able to trigger down-regulation of endothelial markers and morphological characteristics of EHT (Lancrin et al. 2012).

1.4.4.2 Notch signalling pathway

Notch signalling is an evolutionary conserved pathway involved in the regulation of several developmental processes including tissue homeostasis, stem cell maintenance, cell growth and survival (Koch et al. 2013). Both Notch receptors (Notch1, Notch2, Notch3, Notch4) and ligands (Jagged1, Jagged2, Delta-like1, Delta-like3, Delta-like4) are transmembrane proteins. Notch receptors function as both cell surface and intra-cellular transcriptional regulators; upon activation of the intracellular domain, the RBPjκ transcription factor promotes transcription of Notch targets, including the repressor Hairy, Hey-related targets and the Hes family.

Notch1, Notch4, Jagged1, Jagged2 and Delta-like4 are all expressed ventrally in the endothelium of the dorsal aorta at E9.5 and E10.5, a time point which coincides with HSC development (Robert-Moreno et al. 2005; Moreno et al. 2008). Notch1 null embryos die around E10 and were reported to have impaired HSC

development, including a reduction in the number of CFU-C progenitors (Kumano et al. 2003), thus suggesting that Notch signalling is essential for the regulation of HSC formation. By contrast, inducible expression of DNMAML, a potent inhibitor of Notch signalling, or conditional deletion of RBPjκ resulted in no effect on the long-term potential of adult HSCs, indicating that Notch signalling is dispensable for adult haematopoiesis (Maillard et al. 2008). Recently, using a reporter of the Notch target Hes1, it was possible to show that Notch signalling is active in pre-HSC-I at E10.5, while its activity is decreased at E11.5 in pre-HSC-II and becomes undetectable in mature HSCs (Souilhol, Lendinez, et al. 2016), thus confirming the importance of Notch signalling during the early stages of HSC specification and its redundancy once HSCs have formed.

Other than haematopoiesis, Notch plays an important role in vascular and artero-venous specification. In particular, it was shown that activation of Notch signalling via the VEGF pathway in the endothelium promotes activation of the arterial program and suppression of venous identity (Lawson et al. 2001; Lawson et al. 2002). By contrast, activation of COUP-TFII (F. A. Pereira et al. 1999), a gene with roles in angiogenesis, resulted in the suppression of Notch signalling pathway and maintenance of vein identity (You et al. 2005).

1.4.4.3 BMP signalling pathway

The role of BMP signalling in embryonic HSC development is subject to debate. Bmp signalling is part of the TGF-β superfamily, which expression has been found in active sites of haematopoiesis, such as foetal liver and bone marrow, thus indicating its importance in maintenance and regulation of haematopoiesis (Vaidya & Kale 2015). Bmp4 expression has been detected in the ventral domain of the aorta (Durand et al. 2007) and morpholino knockdown of Bmp4 in zebrafish reduced the number of HSC population ($runx1^+$ cells) (Wilkinson et al. 2009). Moreover, Bmp4 was found to be expressed in stromal lines that support HSCs in culture and when added to E11 AGM explant cultures these were able to repopulate a higher number of mice (77%) compared to control (58%) (Durand et al. 2007). Furthermore, the use of a mouse model reporting the activity of BMP responsive element (BRE) has indicated that all AGM repopulating HSCs at E11.5 are activated by BMP (Crisan et

al. 2015). Thus, all these observations suggest that BMP signalling positively regulate HSC formation.

However, recent studies have shown that re-aggregate culture of E10.5 and E11.5 AGM in presence of Bmp4 generated fewer HSCs and that the BMP inhibitor Noggin was able to rescue the effect of Bmp4 on HSC formation by considerably enhancing production of HSCs (Souilhol, Gonneau, et al. 2016). Moreover, BMPER, an inhibitor of BMP signalling, was shown to induce maturation of pro-HSCs from E9.5 caudal part re-aggregates (McGarvey et al. 2017) and, to a smaller extent, from pre-HSC-II at E11.5, indicating that regulation of HSC formation occurs in a BMP-negative environment.

Although seemingly controversial, these findings about the role of BMP signalling could be reconciled by looking at the precise timing in which BMP signalling is required for HSC development. The details of the BRE-GFP reporter are not stated in full detail, thus making difficult to understand if the GFP expressed at E11.5 reports BMP activity at that exact time or earlier, considering that the half-life of GFP is greater than 24h (X Li et al. 1998). Thus, it is possible that BMP signalling might be needed at earlier stages in the AGM region, while becoming dispensable at E9.5-E10.5. It is also possible that different culture methods used in different studies might have generated discrepancies. Thus, the role of BMP signalling in HSC development is not clear.

1.4.4.4 Wnt signalling pathway

Wnt signalling is an important regulator of several aspects of embryonic development. In embryonic stem cells, Wnt3a has been shown to cooperate with Bmp signalling to induce haemangioblast specification and blood formation (Lengerke et al. 2008). In zebrafish, non-canonical Wnt signalling induced by Wnt16 has been shown to control HSC specification by activating downstream Notch signalling (Clements et al. 2011). In mouse, Wnt signalling has been shown to be required at early stages of development (E10.5), as culture of the AGM region with a Wnt inhibitor resulted in a reduction of HSC development. However, E11.5 AGM region was not affected by inhibition of Wnt, suggesting that the pathway is involved in HSC maturation at early but not later stages of development.

1.4.4.5 Stem cell factor, Interleukin 3 and Flt3-ligand

Stem cell factor (SCF), interleukin 3 (IL3), and Flt3-ligand (Flt3-l) are the three growth factors able to preserve the *ex vivo* capacity of the AGM region to generate HSCs in re-aggregate culture (Taoudi et al. 2008).

Since SCF is the ligand for cKit receptor, which is expressed by all embryonic and adult HSCs (Morrison et al. 1995; Rybtsov et al. 2014; Sanchez et al. 1996), it has been the focus of extensive research to determine the secreted regulators of HSCs. SCF is expressed in the ventral side of the AGM (Souilhol, Gonneau, et al. 2016) and when added to re-aggregate cultures of HSC precursors from E9.5 to E11.5 has been shown to be necessary at E11.5 for HSC expansion and sufficient at E9.5-E10.5 for maturation of HSC precursors into definitive HSCs (Taoudi et al. 2008; Rybtsov et al. 2011; Rybtsov et al. 2014).

The role of IL3 in developmental haematopoiesis has shown to be important as IL3-deficient mice have reduced numbers of HSCs in the AGM region, placenta and yolk sac (Robin et al. 2006). Moreover, addition of IL3 in culture contributed to the progression of E11.5 pre-HSC-II to HSCs and to expansion of the HSC pool in re-aggregate culture (Rybtsov et al. 2014; Taoudi et al. 2008).

Although Flt3l null mice were shown to have a reduction in the number of progenitors, dendritic cells and NK cell (McKenna et al. 2000), foetal liver and adult HSCs were unaffected (Sitnicka et al. 2002; Buza-Vidas et al. 2009). However, supplementation of Flt3l in re-aggregate culture of E11.5 AGM cells together with SCF and IL3 was shown to promote HSC expansion (Taoudi et al. 2008), thus indicating that Flt3l might act synergistically with the other two cytokines.

Although several signalling pathways have been described to have a role in HSC development, only the understanding of the whole combination of molecular cues needed for HSC emergence would fully clarify the mechanism of HSC formation. Studying the ontogeny of HSC at the molecular level will be informative for the production of HSCs *in vitro* for experimental and therapeutic purposes.

1.5 RNA-sequencing technology and its application in the study of HSC ontogeny

The field of transcriptomics has made a significant impact in the understanding of the molecular properties of a cell type by quantification of the expression of every gene in a cell. In recent years, the advent of the transcriptomics technology has allowed to perform whole-genome screenings for the identification of new defining properties of HSC and their precursors, as well as for the characterization of novel genes and pathways with an implication in HSC development. In this section, I will briefly describe how the field of transcriptomics has evolved in the last decade, how bioinformatics analysis has allowed the gain of useful insights from RNA-seq studies and how these studies have been applied to the field of HSC ontogeny.

1.5.1 Development of transcriptome technologies

Experimental techniques allowing the quantification of gene expression were developed many decades ago with the introduction of northern blot (Alwine et al. 1977) and quantitative polymerase chain reaction (qPCR) (Gibson et al. 1996). However, these techniques have the limitation of the number of genes that can be tested simultaneously. One of the earliest techniques enabling identification of a large-scale of gene expression products simultaneously is microarray (Lipshutz et al. 1995; Schena et al. 1995). With this technique, a set of probes representing short sequences of known transcripts is fixed on a chip. When the sample of interest is applied in the form of fluorescently labelled cDNA, this hybridizes to the probes (Lockhart et al. 1996; Schena et al. 1995). After washing off non-specific sequences, only strongly paired strands remain hybridized, thus the relative quantity of RNA transcripts in the sample is measured by the resulting fluorescent signal on the chip at each probe's spot. Although microarrays have been widely applied in many different areas of biology research, one of the main limitations of this technique is inferred by the inability to detect new RNA species, as microarray probes are designed based on previously known genes (Z. Wang et al. 2009).

This issue was overcome by the introduction of RNA-seq, which is not limited to detecting transcripts that correspond to existing genomic sequences and provides information about how two exons are connected at the single base resolution (Z. Wang et al. 2009). Thus, this technique is suitable for the characterization of poorly annotated genomes, as well as for identification of new splice isoforms and genome variations, such as single nucleotide polymorphisms (SNPs) (Z. Wang et al. 2009). Moreover, in comparison with microarray, RNA-seq does not have an upper limit for quantification, thus can detect high fold changes between genes expressed at very low and very high level (Z. Wang et al. 2009). Additionally, RNA-seq experiments give an absolute measure of the abundance of genes/transcripts.

Thus, RNA-seq is the first sequencing method that allows analysis of the transcriptome in a high throughput and quantitative manner (Z. Wang et al. 2009; Mortazavi et al. 2008).

1.5.2 RNA-seq data analysis pipeline

RNA-seq allows the identification of the transcriptional changes occurring genome-wide by converting input cDNA onto reads of genomic sequences that can be computationally mapped to a reference genome to determine their gene identity and quantify their abundance. RNA-seq experiments consist of a three-step process: firstly, a library of cDNA fragments is prepared; secondly, the sequence of all cDNAs in the library is determined through a data analysis step; lastly, differences between groups are statistically identified to gain insight into biological systems (Figure 1.7).

Library preparation consists in converting the isolated RNA into a library of cDNA fragments, which is typically achieved through a controlled heated digestion of the RNA with magnesium or zinc (Head et al. 2014). After cDNA conversion, adapters and barcodes are ligated to one or both ends and cDNA is amplified. Then, the library is assessed for its quality and sequenced.

The result of a sequencing run consists of millions of raw reads, which represent the starting point for downstream data analysis. The first step of the bioinformatics analysis consists of quality control, which serves to assess whether

the sequenced raw reads can be used for downstream analysis. Depending on the parameters that qualify the reads as poor, it is possible to discriminate whether problems have arisen (1) during the library preparation step (strong bias in the percentage of some DNA bases over others, indicating presence of adapters or overrepresented sequences), (2) because of contamination (altered percentage of GC content; high level of duplication) or (3) during the sequencing process (low per base sequence quality). To overcome some of the issues causing the data to be of poor quality, it is possible to undergo a pre-processing step in which low quality reads are filtered out, while adapters and overrepresented sequences are trimmed.

After quality assessment, reads are aligned to a reference genome. When the nucleotide sequence of a read significantly overlaps to a coordinate on the reference genome, then it is considered as mapped to the reference. RNA-seq reads alignment is a very complex process, as genes contain introns and reads might not contiguously map to the genome. To address this problem, a number of computational aligner tools such as TopHat, STAR and HISAT (Trapnell et al. 2009; Dobin, C. A. Davis, Schlesinger & Drenkow 2013; D. Kim et al. 2015) incorporate models that can deal with splice junctions and non-contiguous alignment. Another issue arising during alignment is that of reads that map to multiple coordinates on the reference genome (or multi-mapping reads). A common solution to this problem is to set user-defined cut-offs to limit the number of possible multi-mapping reads and discard reads that exceed the cut-off to avoid ambiguity. However, this solution has the disadvantageous result that repetitive elements will never be detected. Mapped reads are then used for quantification at the gene or transcript level. The quantification process consists of measuring the read abundance of a genomic region corresponding to a gene. Thus, at the end of this step each gene is associated with a number corresponding to its abundance.

In order to identify genes that show a significant change in the abundance with respect to a particular condition, differential expression analysis is performed by comparing the gene expression levels across different conditions. Different tools such as EdgeR, DEseq2 and limma (Robinson et al. 2010; Love et al. 2014; Ritchie et al. 2015) can be used to apply a statistical model for the purpose of distinguishing between changes in gene expression that are significant compared to those that are

inferred by variation in the gene count measurements. Currently, none of these models has shown to outperform the others, thus they are all commonly used for RNA-seq analysis (Rapaport et al. 2013). The output list of differentially expressed genes serves as a starting point to gain biological insight into the tested experimental conditions. Downstream analysis of these genes can be performed at the level of gene ontologies or pathway analysis in order to understand if differentially expressed genes are associated with a certain biological process or molecular function (Garber et al. 2011; Han et al. 2015).

1.5.3 Application of RNA-seq approaches in the study of HSCs ontogeny

In recent years a number of studies have applied RNA-seq to elucidate the transition of HSC precursors into HSCs in the AGM region. In two studies, the transcriptional profiles of HSC and progenitor populations (defined by the expression of Ly6a-GFP) were compared to endothelial cells or haematogenic endothelial cells (Yan Li et al. 2014; Solaimani Kartalaei et al. 2015). These studies identified new regulators of HSC development. The cell population including the developing HSCs ($CD31^+$ VC^+ $ESAM^+$ $cKit^+$ $Ly6aGFP^+$) was found to express genes involved in inflammation (Yan Li et al. 2014). The importance of inflammatory signals was tested experimentally by observing the phenotype of Ifngr1-null mice, which were found to have a 4-fold reduction in the number of HSCs in the AGM region, umbilical cord and vitelline arteries, suggesting the requirement of interferon gamma during embryonic HSC development (Yan Li et al. 2014). With a similar strategy, Kartalaei and colleagues identified the expression of the core HSPC regulators (Wilson et al. 2010) in HSCs and haematogenic endothelial cells compared to endothelial cells. This study also identified Gpr56, a novel surface marker expressed by haematopoietic clusters, and found that its knock down in zebrafish reduced the number of HSCs (Solaimani Kartalaei et al. 2015). Moreover, a third study made use of single cell RNA-seq to compare E11 AGM endothelial cells, pre-HSC-I, pre-HSC-II with E12 and E14 HSCs (Zhou et al. 2016). The study confirmed that core HSPC regulators are expressed by pre-HSCs and HSCs, but not endothelial cells.

Interestingly, more genes were expressed in pre-HSCs compared to endothelial cells, but as pre-HSCs mature to HSCs, this number decreases again (Zhou et al. 2016).

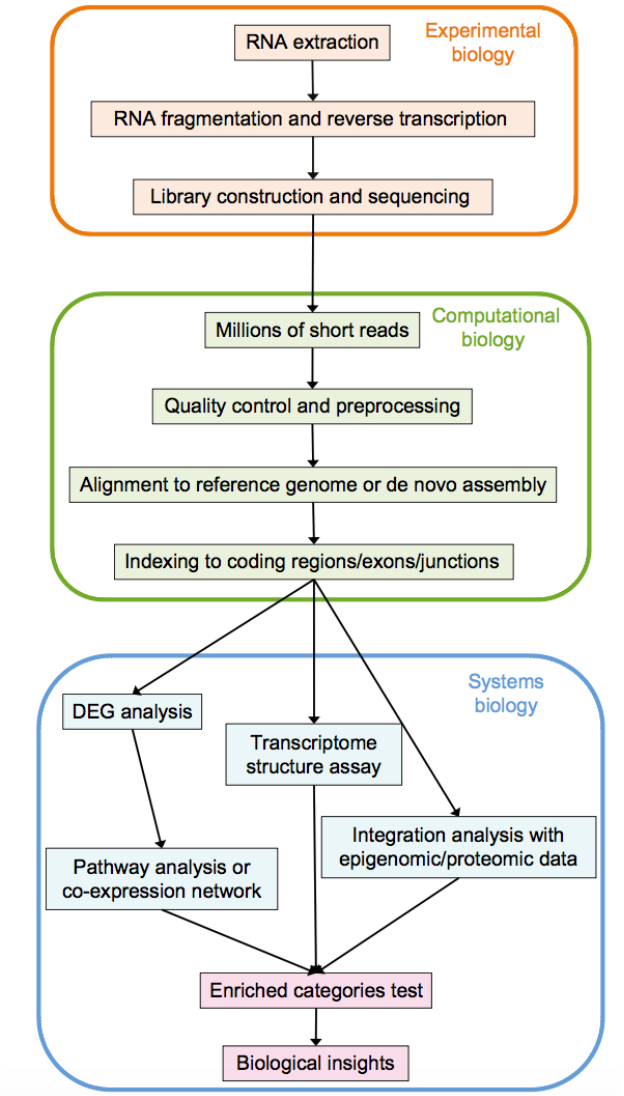

Figure 1.7 | Overview of a RNA-seq experimental workflow.
Schematic representation of the three main steps required for any RNA-seq experiment. The pipeline starts from the experimental preparation of the library, followed by the sequencing and computational step until the systems biology step, which allows to gain biological insigths in the analysis. Adapted from (Han et al. 2015).

Microarray and RNA-seq were also used to yield important insights on the niche signalling microenvironment in which HSCs appear. In a microarray study, gene expression changes were elucidated temporally and spatially in the AGM

region to characterize supportive signals within the AGM niche (Mascarenhas et al. 2009). The AGM gene expression profile was compared before and after HSC emergence (E9.5 vs E11) and along the rostral-caudal axis (middle AGM vs rostral+caudal). This analysis revealed expression of the cyclin-dependent kinase inhibitor p57Kip2 and Gata3 in the HSC supportive niche (Mascarenhas et al. 2009). HSCs in p57Kip2 heterozygous mice were unable to migrate to the foetal liver, suggesting a role for this kinase in HSC proliferation or migration. In a follow up study, Gata3 was shown to regulate HSC maturation via the production of catecholamines (Fitch et al. 2012). Thus, this study has provided insightful information about the HSC regulators in the niche. Recently, a RNA-seq based study focussed on the differences between the ventral (AoV) and dorsal (AoD) domains of the AGM region at E9.5 and E10.5 in order to capture the key signals in the *in vivo* environment supporting HSC development (Figure 1.8) (McGarvey et al. 2017). The E9.5 and E10.5 AGM region was sub-dissected in AoV and AoD and genes expressed at E10.5 vs E9.5 in the AoV compared to the AoD were identified as key candidates responsible for HSC development in the AGM niche. Several genes and pathways were uniquely expressed in the E10.5 AoV. Among them, Bmper, an inhibitor of Bmp signalling, was found to be up-regulated. Supplementation of Bmper in cultured AGM regions at E9.5 significantly improved the maturation efficiency of E9.5 HSC precursors into HSCs, identifying Bmper as a novel regulator of HSC formation and suggesting that inhibition of Bmp signalling is required during development (McGarvey et al. 2017). Thus, the transcriptome analysis in this study represents a valuable resource of signalling molecules as potential candidates for HSC development.

Interestingly, the authors created a publicly accessible graphical interface (http://agmniche.stembio.org/homepage.html) that enables data exploration (McGarvey et al. 2017). Through exploration of secreted molecules in the dataset that could represent novel molecular regulators of HSC development, angiopoietins (Ang1 and Ang2), a novel class of non-well studied ligands involved in angiogenesis, were found to be up-regulated in the AoV at E10.5.

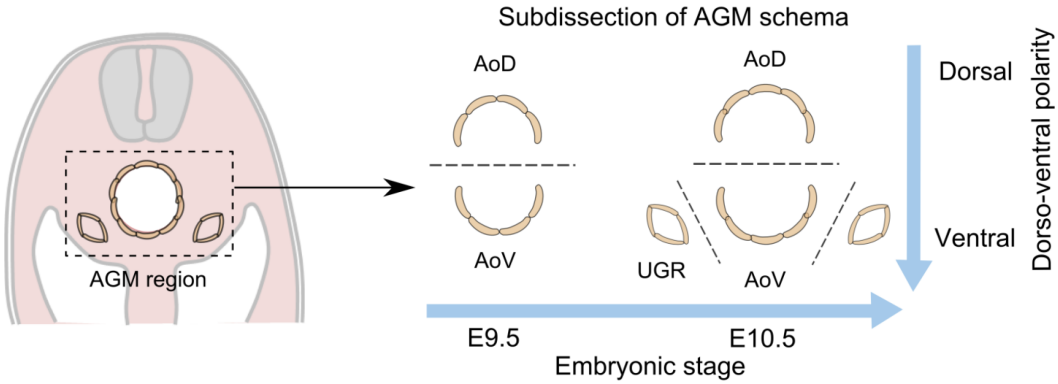

Figure 1.8 | AGM dissection strategy for sequencing and identification of AoV-specific gene signatures.

Schematics of the sub-dissection method for the AGM region. At E9.5, the AGM was sub-dissected into the dorsal (AoD) and ventral (AoV) domains. At E10.5, urogenital ridges (UGRs) were also sub-dissected from the ventral area and compared to the aortic domains. Adapted from (McGarvey et al. 2017).

1.6 Angiopoietin-Tie signalling pathway and its role in haematopoietic stem cells

As discussed in section 1.3, there is growing evidence suggesting a close developmental relationship between the early cells that give rise to the vasculature and the haematopoietic lineage. This evidence raises the possibility that there might be overlapping molecular pathways that regulate both HSCs and endothelial cells. The Angiopoietin-Tie signalling pathway was first identified in the field of vascular biology as a pathway responsible for vessel development and angiogenesis and only in recent years has been linked to the haematopoietic field. In this section, the main components of the pathway, their role and tissue expression, as well as the consequences of the pathway activation are introduced before specifically talking about the role of the pathway in embryonic and adult haematopoiesis.

1.6.1 Molecular components of the Angiopoietin-Tie pathway

The key components of the Angiopoietin-Tie pathway are represented by two receptors, Tie1 and Tie2 (also known as Tek), and two ligands, Angiopoietin1 (Ang1; also known as Angpt1) and Angiopoietin2 (Ang2; also known as Angpt2)

(Figure 1.9). The two receptors are single transmembrane molecules that present a high degree of structural homology (T. N. Sato et al. 1993). They both contain an extracellular portion, constituted by an immunoglobulin (Ig)-like domain, followed by three EGF-like domains, another Ig-like domain and finally three fibronectin type III domains (Augustin et al. 2009; Thurston & Daly 2012). In the cytoplasmic portion, both proteins contain tyrosine kinase domains. Despite of the structural similarities, the two receptors retain different functional properties. Tie2 has the ability to bind directly to angiopoietins, which results in activation of strong kinase activity. Upon activation, Tie2 becomes phosphorylated and downstream PI3-kinase/AKT and ERK signalling pathways are induced(Thurston & Daly 2012). By contrast, Tie1 does not directly bind to angiopoietins, but retains the ability to form a complex with Tie2 upon angiopoietin induction, which results in weak kinase activity (Saharinen et al. 2005). Interestingly, knockdown studies have shown that Tie1 is not required for activation of AKT and ERK pathways, thus the role of Tie1 stimulation is still unclear (Yuan et al. 2007).

Angiopoietins are secreted proteins that exist in dimers and can be further assembled to form multimeric complexes. They are constituted of an N-terminal region that serves to cluster dimers into variable-sized multimers, a central coiled-coil domain used to promote dimerization, and a C-terminal fibrinogen-like domain responsible for receptor binding (S. Davis et al. 2003; Barton et al. 2005). Apart from Ang1 and Ang2, Ang3 and Ang4 were subsequently discovered as the human and mouse orthologue, respectively (Valenzuela et al. 1999).

A family of ligands that share similar structure to angiopoietins was later identified as “angiopoietin-like proteins” (Angptl) and includes seven genes (Angptl1-7) (Augustin et al. 2009). Despite all possessing an N-terminal coiled-coil domain and a C-terminal fibrinogen-like domain, none was shown to bind Tie2 nor Tie1, thus remain orphan ligands (Hato et al. 2008).

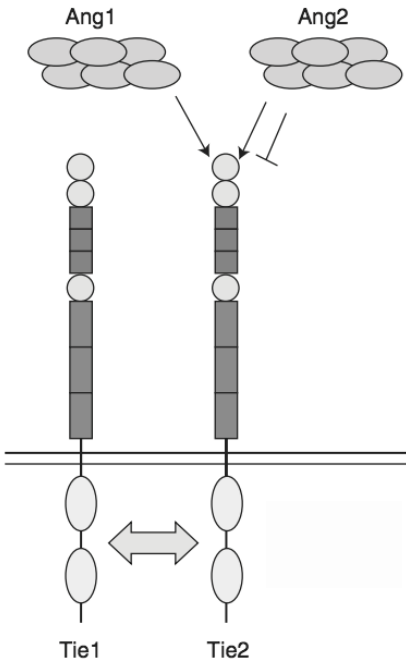

Figure 1.9 | Ligands and receptors of the Angiopoietin-Tie signalling.
Schematics of the structure of the receptors Tie1 and Tie2 and binding dynamics of the ligands angiopoietin1 (Ang1) and angiopoietin2 (Ang2). Adapted from (Thurston & Daly 2012).

1.6.2 Tissue and cell localization of Tie receptors

Tie receptors have been long described as vascular and lymphatic endothelial cell specific receptors in both the adult and the embryo (Thurston & Daly 2012; Korhonen et al. 1995). To date, no endothelial cell population has been described to only express Tie1 or Tie2 (Augustin et al. 2009). In the embryo, Tie2 was first shown to be expressed at E7.5 in both the extraembryonic mesoderm and embryonic mesoderm. At E8.0, Tie1 and Tie2 expression was shown to be expressed in vascular structures at E8.0 (after formation of blood islands) (Korhonen et al. 1994) (Dumont et al. 1994) and spread in the paired aorta, heart, allantois and in the yolk sac at E8.5-E9.0 (Dumont et al. 1994; Puri et al. 1995). By E9.5-E10, Tie receptors can already be observed in all the major blood vessels including the dorsal aorta and intersomitic vessels, as well as smaller vessels of the head region (Puri et al. 1995). While Tie2 is constitutively expressed, Tie1 is tightly regulated and it is often up-regulated at sites of turbulent blood flow or at sites of growth of new capillaries (Augustin et al. 2009).

Despite having been initially described as endothelial cell specific, Tie receptors are also expressed by the blood compartment, including haematopoietic

stem cells, as well as circulating haematopoietic cells, megakaryocytes, monocytes and macrophages (Tang et al. 2010; Puri et al. 1995; De Palma et al. 2005). Moreover, Tie2 has also been described on other cell populations, including dorsal root ganglia (Kosacka et al. 2005), glial cells and several types of tumour cells (O.-H. Lee et al. 2006; Brown et al. 2000).

1.6.3 Tissue and cell localization of Ang ligands

In contrast to the wide co-expression of Tie receptors in endothelial cells, angiopoietins present distinct expression patterns. In an effort to understand the biological processes in which Ang ligands are involved, it is necessary to make a clear distinction between the adult and embryonic scenarios. In the embryo, Ang1 expression can be detected in the heart myocardium between E9 and E11 (Suri et al. 1996; Gale et al. 2002) and in the neural tube at E10.5 (Nagase et al. 2005). In later stages of development, Ang1 becomes much more widely expressed in the mesenchyme surrounding the vessels and in close association with endothelial cells (S. Davis et al. 1996). Interestingly, in the chicken embryo Ang1 was found to be selectively expressed by veins but not arteries at E4 (Moyon et al. 2001). As a result from these studies, Ang1 has widely been recognised to be expressed by perivascular cells surrounding Tie1/Tie2 positive endothelial cells (S. Davis et al. 1996; Eklund & Saharinen 2013; Thurston & Daly 2012; Augustin et al. 2009). However, these conclusions are mainly based on *in situ* hybridization comparisons of single Ang1 and Tie1 (or Tie2) probes on parallel sections (S. Davis et al. 1996), in which Tie receptors are shown to be localized around the vessels, while Ang1 presents a more spread pattern of expression. Thus, co-localization studies are needed to provide full evidence of Ang1 embryonic expression by the perivascular layer at the mRNA and protein level. In the adult, Ang1 was found to be expressed in pericytes (Y. S. Park et al. 2003), endothelial cells (Fan et al. 2004), osteoblasts (Arai et al. 2004; Kasama et al. 2007), fibroblasts (Scott et al. 2005), astrocytes (Acker et al. 2001), epithelial cells (Hangai et al. 2001) and cancer cells (FU et al. 2006). Interestingly, Ang1 is also stored in platelets and released in presence of thrombin (Jian-Jun Li et al. 2001). Although Ang1 expression tends to be up-regulated during angiogenesis, in the adult Ang1 is constitutively produced and can be found in circulation.

Ang2 is predominantly expressed by endothelial cells in the adult (Stratmann et al. 1998; Hackett et al. 2000). Unlike Ang1, expression of Ang2 is tightly regulated. It is normally low in quiescent mature vessels, while it is strongly increased in many inflammatory and angiogenic settings (Augustin et al. 2009). Ang2 expression in cultured endothelial cells is transcriptionally induced in response to TNF, VEGF, hypoxia and shear stress (Stratmann et al. 1998; Mandriota & Pepper 1998; I. Kim, J. H. Kim, et al. 2000) and can be detected in circulation. Ang2 is stored in intracellular granules called Weibel-Palade bodies and it can be liberated in seconds to minutes to control rapid endothelial responses upon inflammatory stimuli (Fiedler et al. 2004). In turn, Ang2 transcriptional repression is mediated by the transcription factor Klf2 as well as by poorly characterized repressor elements of the Ang2 promoter (Augustin et al. 2009); this repression results in endothelial cell quiescence.

In the embryo, Ang2 can be detected in the perivascular layer of cells surrounding the dorsal aorta at E12.5 (Maisonpierre et al. 1997). By E14.5, Ang2 activity can predominantly be observed in all the major arteries including the aorta (Gale et al. 2002). At this time point, Ang2 expression can also be detected around venules and small vessels at sites of vascular remodelling, but not in the surroundings of quiescent vessels (Gale et al. 2002). For this study, the authors used an Ang2-LacZ reporter mouse and based their observations on LacZ-stained images. They affirm that Ang2 is expressed by perivascular cells (around arteries) and endothelial cells (around veins). However, further co-localization studies with endothelial and perivascular markers are needed in order to describe with a higher level of precision the cell types expressing Ang2. Although it is still debatable what cell types express Ang2 in the embryo, the observation that Ang2 is predominantly expressed around the arteries was confirmed by studies in the avian system, in which Ang2 was selectively found in proximity of the aorta and omphalomesenteric artery, but not the cardinal vein (Moyon et al. 2001).

Protein Name	Developmental Stage	Expression Pattern
Ang1	Embryonic	E9-E11: heart myocardium (Suri et al. 1996; Gale et al. 2002) E10.5: neural tube (Nagase et al. 2005) E13: mesenchyme surrounding veins (S. Davis et al. 1996; Moyon et al. 2001)
	Adult	Pericytes (Y. S. Park et al. 2003) Endothelial cells (Fan et al. 2004) Osteoblasts (Arai et al. 2004) Fibroblasts (Scott et al. 2005) Astrocytes (Acker et al. 2001) Epithelial cells (Hangai et al. 2001) Cancer cells (FU et al. 2006) Platelets (Jian-Jun Li et al. 2001)
Ang2	Embryonic	E12.5: perivascular layer surrounding aorta (Maisonpierre et al. 1997) E14.5: around all major arteries including aorta; venules and small vessels (Gale et al. 2002; Moyon et al. 2001)
	Adult	Endothelial cells (Stratmann et al. 1998; Hackett et al. 2000)
Tie1 & Tie2	Embryonic	E7.5: extraembryonic and intraembryonic mesoderm E8.0: vascular structures (Korhonen et al. 1994; Dumont et al. 1994) E8.5-E9.0: paired aortas, heart, allantois, yolk sac (Dumont et al. 1994; Puri et al. 1995) E9.5-E10: all major vessels including aorta, intersomitic vessels, small vessels of the head (Puri et al. 1995)
	Adult	Vascular and lymphatic endothelial cells (Thurston & Daly 2012; Korhonen et al. 1995) Blood compartment: haematopoietic stem cells, circulating haematopoietic cells, monocytes, macrophages, megakaryocytes (Tang et al. 2010; Puri et al. 1995; De Palma et al. 2005)

Table 1 | Expression pattern of angiopoietins and their receptors in embryonic and adult tissues.

1.6.4 Phenotype of loss-of-function mice of the Ang-Tie system

Loss-of-function studies have highlighted Tie2 as the core receptor of this signalling pathway and have given insight in the relevance of these proteins in haematopoiesis. Genetic deletion of Tie2 resulted in embryonic lethality between E10.5 and E12.5. The embryos presented severe cardiac and vascular abnormalities with 75% fewer endothelial cells at E9.5, as well as fewer supporting pericytes and

smooth muscle cells (Dumont et al. 1994). Null embryos also displayed abnormalities in haematopoiesis, with absence of lymphomyeloid cells at E8.5 and lack of cKit+ cells in the vitelline artery at E9.5 (Takakura et al. 1998). Although the authors claim that these defects suggest a role of Tie2 in definitive haematopoiesis, it should be taken into account that no definitive HSCs are produced earlier than E10.5 and that absence of lymphomyeloid could be related to primitive haematopoiesis.

By contrast, Tie1 deficient embryos are perturbed later during development and die between E13.5 and birth. In these animals, the major blood vessels appeared normal and embryonic angiogenesis was not affected; however, integrity and survival of endothelial cells was lost, especially in the regions of capillary growth, leading to widespread oedema (Puri et al. 1995). Haematopoiesis in these embryos was not affected. In the E15.5 foetal liver, the total cellularity was comparable to wild-type animals, progenitors were able to give rise to lymphoid and myeloid colonies and transplanted cells were able to long-term reconstitution of the bone marrow of recipient animals (Rodewald & T. N. Sato 1996). Thus, this indicates that Tie1 is dispensable for haematopoietic stem cell engraftment and self-renewal.

Genetic deletion of Ang1 results in embryonic death around E12.5, with severe heart and vascular defects which phenocopy the lethal phenotype of Tie2-null mice, although being less severe (Suri et al. 1996). In fact, the blood vessels in these mice form but exhibit defects in the remodelling of their vasculature, with a simplified vasculature and fewer branches. The most relevant defects in these mice seem to be in the heart endocardium and myocardium, were Ang1 is prominently expressed at early stages of development.

Mice genetically deficient for Ang2 present embryonic and postnatal lymphatic, vascular and postnatal angiogenesis defects (Gale et al. 2002). These mice also fail to elicit a rapid inflammatory response upon TNFα stimulation, thus recruitment of leukocytes is impaired (Fiedler et al. 2006). Ang2-null pups are born at normal Mendelian ratios, however they develop chylous ascites and oedema and die within 14 days (Gale et al. 2002). However, when bred in the C57Bl/6 genetic background, postnatal mortality is reduced to 10% (Fiedler et al. 2006).

1.6.5 Genetic over-expression and binding dynamics of angiopoietins

Gain-of-function experiments in which Ang ligands are over-expressed have given insight onto the role of Ang1 and Ang2 in mediating Tie2 signalling. Transgenic over-expression of Ang1 in the skin of mice results in formation of enlarged dermal vessels (Suri et al. 1998) associated with an increased amount of endothelial cells (Baffert et al. 2004). Moreover, vessels exposed to Ang1 are resistant to leak induced by inflammatory agents and VEGF and present a reduced vascular activation (Thurston et al. 1999; Thurston et al. 2000). Thus, all together these studies have proposed a role for Ang1 in the activation of Tie2 signalling in order to maintain a quiescent vascular endothelium.

By contrast, over-expression of Ang2 led to embryonic lethality at E9.5-E10.5 caused by severe disruption in blood vessel and heart formation (Maisonpierre et al. 1997). The effects of Ang2 over-expression were found to be very similar to the phenotype of Ang1- and Tie2-deficient mice, thus suggesting that Ang2 acts as a natural antagonist of Ang1 in Tie2 signalling.

Following these studies, the model has been proposed of Ang1 as an activator of Tie2 signalling pathway, while Ang2 as an inhibitor of Ang1-mediated action. Although Ang1 and Ang2 have been shown to retain similar affinity binding to Tie2, Ang1 was shown to induce strong phosphorylation of Tie2 receptor, while addition of exogenous Ang1 and Ang2 reduced the levels of phosphorylation compared to Ang1 alone, thus leading to the conclusion that Ang2 is an antagonist of Tie2 signalling (Hanahan 1997). However, in several other experimental scenarios Ang2 was proven to be an agonist of Tie2. In fact, high concentrations of exogenous Ang2 were able to induce weak phosphorylation of Tie2 in endothelial cells (I. Kim, J. H. Kim, et al. 2000). In another study, endogenous Ang2 expression was induced by low AKT signalling via the transcription factor Foxo and resulted in the activation of Tie2 that could only be inactivated by antibodies against Ang2 (Daly et al. 2006). Ang2 is also considered to promote Tie2 activation in neoplastic settings, where blocking antibodies against Ang2 were found to inhibit tumour growth and angiogenesis by suppressing endothelial cell proliferation, significantly reducing the size of vessels and decreasing Tie2 activity (Falcón et al. 2009). Thus, the effects of Ang2 on Tie2 signalling seem to be context- and concentration-dependent. One of

the possible explanation for these contrasting effects of Ang2 on Tie2 signalling could be that while Ang1 ligand is predominantly found in the form oligomers, Ang2 molecules are usually distributed as dimers. High order oligomers were indeed shown to be activators of Tie2 signalling, whereas dimers were found to antagonize Tie2 activation (S. Davis et al. 2003). Thus, it is possible that at high concentrations Ang2 organises in oligomers and behaves as an activator for Tie2.

1.6.6 Cellular changes promoted by Tie2 receptor activation

Activation of Tie2 receptor via ligand binding has been extensively studied in the context of endothelial cells. This section provides a summary of those findings with the aim to elucidate the cellular functions of the Ang-Tie pathway.

One of the main consequences of Tie2 activation is cell survival and maintenance. Tie2 phosphorylation leads to the activation of AKT signalling which activates survival promoting pathways, such as nitric oxide synthase and survivin, and suppresses several components of the apoptotic pathway, including caspase 9 (Augustin et al. 2009). Activation of Akt also leads to inactivation of Foxo1, which targets Ang2. Thus, activation of Tie2 signalling induces a negative-feedback loop that inhibits production of Ang2 (Daly et al. 2004). By contrast, activation of Foxo1 leads to increased Ang2 production that is associated with endothelial cell destabilization (Tsigkos et al. 2006).

Tie2-mediated activation of AKT signalling can also result in cell migration by inducing the angiogenic cascade, which results in proliferation and increased expression of basement-membrane degrading proteases (Koblizek et al. 1998; Kanda et al. 2005). Migration is induced by increased expression of PI3K, which promotes the recruitment of the adaptor protein Grb14 and the tyrosine phosphatase Shp2 to Tie2 receptor (I. Kim, H. G. Kim, et al. 2000).

Moreover, Tie2 signalling is also responsible for maintenance of permeability between the perivascular and endothelial layer through the establishment of adherens and tight junctions. Tie2 activation induced by Ang1 results in limited permeability through sequestration of the tyrosine kinase Src (Gavard et al. 2008). Finally, Tie2 stimulation acts as an anti-inflammatory signal through the suppression of NF-κB signalling and the recruitment of Abin2 and A20 (Hughes et al. 2003).

1.6.7 The importance of Tie2 receptor in embryonic haematopoiesis

Tie2 null embryo die between E10.5 and E12.5. As this developmental period corresponds to the emergence of haematopoietic stem cells, it has been hypothesized that Tie2 might play a role in this process. The use of a Tie2-Cre;Rosa26R-EYFP reporter mouse revealed abundant expression of EYFP in correspondence to precursors of blood islands at E7.5 (Tang et al. 2010). By E9.5, expression of EYFP in the vast majority of haematopoietic progenitor ($CD41^+$) and erythroid ($Ter119^+$) compartment of the yolk sac suggested that most primitive cells are Tie2-derived (Tang et al. 2010). With these observations in mind, the first hypothesis investigated was about Tie2 being a marker of the bi-potent haemangioblast cell. This hypothesis was reinforced by the remark that after co-culture of E8.5 para-aortic splanchnopleura of Tie2-null embryos with OP9 cells, no haematopoietic cells apart from mast cells developed (Takakura et al. 1998). Moreover, co-culture of E10.5 AGM $Tie2^+$ cells with OP9 resulted in the production of both haematopoietic and endothelial cells (Hamaguchi et al. 1999). However, these studies lack of the evidence that a single Tie2+ cells can give rise to both endothelial and haematopoietic cells.

A second hypothesis was advanced about Tie2 being expressed by the haematogenic endothelium. *In vitro* culture of the haemangioblast followed by time-lapse photography captured Tie2 expression one day after culture (Lancrin et al. 2009). At 48h, a sub-population of $Tie2^+$ cells was found to co-express cKit. Culture of $Tie2^+$ $cKit^+$ $CD41^-$ cells was able to give rise to $CD41^+$ haematopoietic cells (Lancrin et al. 2009), but was unable to give rise to haemangioblast-derived blast colonies and did not express the mesodermal marker brachyury (Lancrin et al. 2009). Thus, this indicated that Tie2 marks a haematogenic endothelial population that is distinct from and downstream of the haemangioblast.

Evidence of the importance of Tie2 in definitive haematopoiesis is well documented. $Tie2^+$ cells in the E10.5 AGM region were found to be part of a population of cells that co-express CD34 and cKit (Hamaguchi et al. 1999), a marker of HSCs. When cultured in presence of cytokines, $Tie2^+$ (but not $Tie2^-$) cells were shown to produce haematopoietic colonies, thus indicating that the $Tie2^+$ population

marks multipotent progenitor cells (Hamaguchi et al. 1999; Takakura et al. 1998). This was confirmed when supplementation of the AGM explant culture with a Tie2-Fc chimeric protein (to prevent free ligands to bind Tie2) resulted in a dose-dependent suppression of haematopoietic progenitors formation (Takakura et al. 1998). Moreover, analysis of Tie2 deficient embryos at E9.5 showed these lacked cKit+ cells in the vitelline artery (Takakura et al. 1998), thus suggesting that Tie2 might be expressed by developing HSCs. To prove that, Runx1, which is required for endothelial to haematopoietic transition (M. J. Chen et al. 2009), was selectively deleted in the Tie2 compartment by Cre-recombinase and most embryos died around E12.5 with a phenotype similar to Runx1-null mice (Zhe Li et al. 2006). Restoration of Runx1 expression in the Tie2 compartment rescued definitive haematopoiesis by producing long-term reconstituting HSCs (Liakhovitskaia et al. 2009), thus indicating that $Tie2^+$ cells give rise to definitive haematopoietic stem cells.

Expression of Tie2 was found in a sub-population of Lin^- $Sca1^+$ $cKit^+$ $AA4.1^+$ HSCs in the E14 foetal liver, representing 7% of the total HSC population. This population was shown to have an increased ability to form colonies *in vitro* and the exclusive capacity to reconstitute recipient mice in the long-term, thus indicating that $Tie2^+$ is a marker of HSCs in the foetal liver (Hsu et al. 2000). Interestingly, chimeric embryos injected with normal cells and cells with double deletion of both Tie1 and Tie2 were still able to produce haematopoietic progenitors in colony assays (Puri & Bernstein 2003). Thus, the authors concluded that expression of these receptors in embryonic HSCs is not required for the emergence of HSCs from the haematogenic endothelium. However, the functional ability of chimeric double null embryos to produce HSCs was not tested by transplantation.

1.6.8 Role of Ang-Tie signalling in the adult HSC niche

As discussed in section 1.4.1, interaction of HSC with their niche is crucial for their maintenance. In the bone marrow, around 30% of Lin^- $Sca1^+$ $cKit^+$ (LSK) cells were found to express Tie1 and Tie2 and both populations were found to retain long-term multilineage engraftment ability (Yano et al. 2007). A study with chimeric mice composed of both normal embryonic cells and cells lacking both Tie1 and Tie2 showed that these receptors are not required for bone marrow homing from the foetal

liver during ontogeny, however they are required for HSC maintenance in the adult bone marrow microenvironment (Puri & Bernstein 2003). As Tie1 deficient cells expressing normal level of Tie2 were able to contribute to haematopoiesis (Rodewald & T. N. Sato 1996), it was suggested that Tie2 alone might be required for the maintenance of HSC in the bone marrow niche. Arai and colleagues (Arai et al. 2004) were able to show that $Tie2^+$ LSK cells are a population of quiescent cells tightly associated to the endosteal surface of the bone marrow, in close contact with osteoblasts. Ang1, which has been previously shown to promote HSC adhesion to fibronectin and collagen *in vitro* (A. Sato et al. 1998; Takakura et al. 1998), was found to be expressed by the osteoblasts of the HSC niche (Arai et al. 2002). Supplementation of Ang1 in co-cultures of $Tie2^+$ LSK with OP9 was shown to reduce HSC mobilization by inducing morphological changes in HSC, which acquire a flattened morphology and start expressing adhesion molecules such as β1-integrin (Arai et al. 2004). Moreover, *in vivo* transplantation of Ang1-over-expressing bone marrow cells was shown to increase cell quiescence and to improve self-renewal (Arai et al. 2002). Thus, Ang1-Tie2 signalling was shown to regulate HSC maintenance on the adult bone marrow niche.

In order to clarify the role of angiopoietins on adult HSCs, further studies have shown that neither Ang1 nor Ang2 altered the production of haematopoietic progenitor colonies derived from LSK cells, however transplantation of LSK cultured in presence of Ang2 resulted in a lower percentage of donor cells in irradiated recipients 3 months post transplantation (Gomei et al. 2010). Moreover, intravenous administration of Ang2 resulted in an increased number of HSCs in circulation and in the spleen (Kuo et al. 2008). Thus, these findings suggest that Ang2 antagonizes the role of Ang1 by increasing mobilization and affecting the self-renewal properties of HSCs. However, cells expressing Ang2 in the adult bone marrow niche have not been characterized yet.

1.7 Project hypothesis, aims and structure

As described in the introduction, emergence of haematopoietic stem cells in the mouse embryo is strictly regulated by signalling molecules expressed in the AGM microenvironment at the time and place of HSC development. The AGM niche is located in the ventral domain of the aorta and supports HSC development around E10.5. The advent of transcriptome approaches as RNA-sequencing has allowed the exploration of the molecular cues regulating HSC fate at the genome-wide level. Accordingly, a recent study sub-divided the AGM region in its dorsal and ventral domains and examined the molecules over-expressed by the ventral HSC niche at E10.5 by RNA-seq (McGarvey et al. 2017). Angiopoietins were found among the up-regulated molecules in the AGM niche. Although a few reports have characterized the role of angiopoietins in the adult HSC niche, little is known about the function of these molecules in the embryonic scenario.

Given the evidence that angiopoietins were up-regulated at the time and place of HSC development in the AGM region, the driving hypothesis of this study was that the angiopoietin-Tie signalling might play a role in HSC emergence. Thus, the objectives of this thesis were:

- Objective 1: to elucidate the role of angiopoietins during HSC ontogeny in the AGM region
- Objective 2: to characterize angiopoietins expression in the AGM region
- Objective 3: to investigate the mechanism of action of these molecules in HSC development.

To explore the aims, the project was sub-divided as follows:

Chapter 3 focuses on the analysis of the role of angiopoietins in HSC formation through functional experiments in which angiopoietins are added in the culture media of AGM aggregates at different stages of development and transplanted into irradiated recipients to assess angiopoietin ability to improve HSC maturation. Here, I find Ang2 but not Ang1 to be a positive regulator of HSC development.

Chapter 4 describes the cellular expression of the molecules of the Ang-Tie pathway in the AGM region at different stages of development. A deeper focus is given to the characterization of Ang2 ventral polarity through the combinatory use of a mouse model reporting the activity of Ang2 through the expression of GFP and an antibody against Ang2. The correlation between the concentration of Ang2 and the presence of intra-aortic haematopoietic clusters is also described. Here, I find that perivascular and sub-aortic mesenchymal cells in the ventral domain of the aorta express Ang2 and that the concentration of Ang2 is increased in presence of clusters.

Chapter 5 investigates the signalling molecules differentially regulated by Ang2 in HSC precursors and endothelial cells of the AGM region through the use of RNA-sequencing. Here, I find that Ang2 induces changes at the gene expression level mainly on HSC precursors and I discuss some of the differentially expressed genes and pathways with the aim of characterizing the mechanism of action of Ang2 on the maturation of HSC precursors into HSC.

Chapter 2 Materials and methods

2.1 General solutions

Dissection buffer:

Dulbecco's phosphate buffered saline (PBS) solution (with $Mg2^{+}$ and $Ca2^{+}$ ions; Sigma) containing 4% foetal calf serum (FCS) (Gibco, PAA, or Biosera) and 50 units/ml penicillin and streptomycin (P/S; Gibco).

FACS buffer:

Dulbecco's PBS (without $Mg2^{+}$ and $Ca2^{+}$) containing 2% FCS and 50 units/ml P/S.

OP9 culture medium:

Iscove's modified Dulbecco's medium (IMDM) (Invitrogen), 20% FCS, L-glutamine (4 mM), P/S (50 U/ml)

Aggregate culture medium:

IMDM (Invitrogen), 20% heat-inactivated FCS (PAA/HyClone), L-glutamine/pyruvate (4 mM), P/S (50 U/ml), 0.1mM β-mercaptoethanol, 100 ng/ml SCF, 100 ng/ml IL3 and 100 ng/ml Flt3l (termed 3GF), unless otherwise indicated (all purchased from Peprotech).

2.2 Animals

2.2.1 Animal husbandry

Wild type and transgenic mice were housed and bred in animal facilities at the University of Edinburgh in accordance with the Home Office regulations. Animals were provided with constant supply of water and chow food and exposed to a 14 hours light/10 hours dark cycle. Litters were weaned 3 weeks after birth by separating the parents from the offspring. Only females older than 6 weeks and males

older than 8 weeks were used for matings. For this study, C57BL/6 (purchased from Jackson Laboratories) and Ang2-GFP (purchased from MMRRC) were used. Ang2-GFP mice were backcrossed to a C57BL/6 background for 6 generations by mating Ang2-GFP males with C57BL/6 females. All experiments with animals were approved under a project license 60/3916 granted by the Home Office (UK), University of Edinburgh Ethical Review Committee, and conducted in accordance with local guidelines.

2.2.2 Animal genotyping by PCR

During weaning, Ang2-GFP mice were ear-punched by the animal facility staff and ear biopsies used for PCR genotyping. Ear tissues were lysed overnight at 56°C in 100ul lysis buffer containing 10% Tween-20, 10% NP40, and 10 mg/ml proteinase K in PCR buffer (Qiagen). Proteinase K was inactivated at 96°C for 15min. Samples were then used immediately or stored at -20°C. PCR mastermix was prepared by mixing 5µl 10X Buffer, 10µl Q Buffer, 1µl dNTPs (10nM), 1µl Taq polymerse (5units/µl), 0.5µl each of forward and reverse primers (100uM) and 3µl template DNA in MilliQ water. The following primers (sequences obtained from MMRRC) have been used: Ang2-F 5'-GGAAGGAAAGTGATTGATTCGGATAC-3' and eGFP-R 5'-GGTCGGGGTAGCGGCTGAA-3'. PCR was carried on a Biometra T3 Thermocycler with the following protocol:

Step 1: 94˚C for 2min 30sec → Initial denaturation

Step 2: 92˚C for 15sec → Denaturation

Step 3: 55˚C for 15sec → Annealing

Step 4: 72˚C for 30sec → Elongation

Step 5: 72˚C for 3min → Final extension

Step 6: 4˚C forever

(Repeat steps 2 to 4 for 34 times).

Electrophoresis was run at 75V on a 2% agarose gel in 1X TE buffer (Tris, EDTA) followed by labelling DNA with ethidium bromide. Gel pictures were taken with Syngene G:Box with GeneSys software. The amplified sequences, determined by agarose gel in comparison with a 1KB ladder, were 475bp.

2.2.3 Time matings and embryo collection

In order to collect embryos of a specific embryonic stage, matings were setup overnight and females were checked on the next morning to assess presence of a vaginal plug. The day of discovery of the vaginal plug was designated as E0.5. Pregnant females at the correct stage of gestation were culled in accordance with the schedule 1 method of cervical dislocation. Embryos were dissected from the uterus in a Dissection buffer and extra-embryonic tissues such as placenta and yolk sac were removed using forceps. Embryo stage was accurately determined by counting the number of somite pairs, so that E9.5 was attributed to embryos with 25-29sp, E10 to embryos with 30-34sp, E10.5 to embryos with 35-39sp, E11.5 to embryos with 41-45sp.

2.3 Tissue isolation and preparation

2.3.1 Isolation of embryonic tissues

Embryonic organs of interest such as AGM and caudal part were dissected in Dissection buffer under a stereomicroscope (Leica MZ8) using tungsten needles. To dissect the AGM region, head and anterior part of the body above the heart were removed first, then somites, neural tube and ventral tissue (including foetal liver, heart, gut). Ribs and dorsal tissue in excess were cut out, leaving only the aorta and the UGRs. For embryos at E9.5 stage, the caudal part was dissected by removing the head and anterior body of the embryo (including the heart).

2.3.2 Single cell preparation of embryonic tissues

Tissues were pooled in a 5ml polystyrene tube and digested with 1mg/ml Collagenase-Dispase (Roche) in Dissection buffer for 35min at 37˚C on a gently shaking water bath. For NG2 staining of perivascular cells, due to sensitivity to collagenase activity of the proteoglycan NG2, cell suspensions were obtained by incubating samples in 5mM EDTA with 2% FCS in PBS for 20min at 37˚C, with pipetting dissociation carried out every 5min. Immediately after, samples were washed with FACS buffer and centrifuged for 5min at 300g. Supernatant was carefully aspirated and tissues were gently dissociated mechanically by pipetting the

cell suspension in FACS buffer. After a second round of centrifugation and washing, single cell pellets were resuspended in the appropriate volume of buffer/staining solution for further processing.

2.3.3 Isolation and cell preparation of adult tissues

Mice were culled by cervical dislocation. Spleen, thymus, tibias and femur were dissected and placed into FACS buffer. Spleen and thymus were mechanically dissociated with the back of a syringe plunger (BD Plastipak) on a 40μm cell strainer placed on top of a 50ml Falcon tube and filtered down with buffer in order to obtain a single cell suspension. To collect the bone marrow, tibias and femur were flushed and mechanically dissociated with a 26-gauge syringe needle (BD Microlance), then filtered on a 5ml polystyrene tube with cell strainer. Blood was obtained post-mortem by cardiac puncture, placed in a solution of 5mM EDTA with 2% FCS in PBS and centrifuged at 300g for 5min at RT. Pellets were resuspended and mixed in 10% PharM Lyse solution (BD Bioscience) in MilliQ water and incubated for 10min at room temperature (RT) for erythrocyte depletion. After a second centrifugation, samples were washed in FACS buffer and processed for flow cytometry analysis. Adult prepared cell suspensions were kept on ice or at 4˚C until further processing.

2.4 Flow cytometry analysis and cell sorting

Cell suspensions were incubated with 1μg/ml Fc-block and antibody cocktail in FACS buffer for 30min at 4˚C in the dark. After incubation, cells were washed with buffer, centrifuged at 300g for 5min and stained once more with fluorochrome-conjugated streptavidin when appropriate. After washing off the streptavidin, samples were resuspended in buffer with 0.5μg/ml 7AAD viability staining solution for exclusion of dead cells. Table 2 lists all the antibodies used for flow cytometry. For all experiments, FMOs (fluorescence-minus-one) controls where all antibodies of the panel were added except one, were prepared in order to set the gates and identify any spread of the fluorochromes into the channel of interest. Flow cytometry analysis was performed using a 4 or 5-laser LSR Fortessa (BD Bioscience) or a dual laser FACS Calibur (BD Bioscience). Sorting was carried out by Dr Fiona Rossi or Dr

Claire Cryer on a FACSAria II or Aria Fusion (BD Bioscience). Compensation was calculated by using single stained beads (OneComp and UltraComp eBeads, Thermofisher). Cells for OP9 co-aggregate culture were sorted in FACS buffer in 5ml polystyrene tubes at RT; for RNA extraction, samples were sorted in Buffer RLT (Qiagen) supplemented with 1% β-mercaptoethanol (14.3M) in 0.2µl PCR tubes at 4˚C. Data was analysed with FlowJo (v10.1, LLC) or FACSDiva software (BD Bioscience).

Antigen	Clone	Isotype	Working Conc.	Conjugate	Supplier
CD16/CD32 (Fc block)	93	rIgG2b	1 µg/ml	N/A	eBioscience
CD45	30F-11	rIgG2b	2 µg/ml	V450, V500	BD Horizon
CD41	MWReg30	rIgG1	10 µg/ml	BV421, PE	Biolegend
CD43	eBioR/60	rIgM	1 µg/ml	PE, Biotin, FITC	eBioscience
VC/CD144	eBioBV13	rIgG1	2 µg/ml	ef660	eBioscience
c-Kit/CD117	2B8	rIgG2b,k	2 µg/ml	BV421	Biolegend
CD45.1	A20	mIgG2a	2 µg/ml	APC, V450	Biolegend
CD45.2	104	mIgG2a	2 µg/ml	V500, PE	Biolegend
Ter119	TER-119	rIgG2b	2 µg/ml	Biotin, PerCP-Cy5.5, FITC	eBioscience
B220/CD45R	RA3-6B2	rIgG2a	2.5 µg/ml	Biotin, PerCP-Cy5.5	eBioscience
CD3e	145-2C11	hIgG	2 µg/ml	Biotin, PE, PerCP-Cy5.5	eBioscience

Mac1/CD11b	M1/70	rIgG2b	2.5 µg/ml	Biotin, PerCP-Cy5.5	eBioscience
Gr1	RB6-8C5	rIgG2b	1.5 µg/ml	Biotin, PerCP-Cy5.5	eBioscience
CD4	GK1.5	rIgG2b	2 µg/ml	Biotin, PE PerCP-Cy5.5	eBioscience
CD8a	53-6.7	rIgG2b	2.5 µg/ml	Biotin, APC PerCP-Cy5.5	eBioscience
CD146	ME-9F1	rIgG2a	1 µg/ml	PE	Biolegend
Tie2	TEK4	rIgG1	2 µg/ml	PE	eBioscience
NG2/AN2	1E6.4	rIgG1	10 µg/ml	Biotin	Miltenyi Biotec
Streptavidin	N/A	N/A	0.1µg/ml	BV421, BV650, BV711, V500	Biolegend
7AAD	N/A	N/A	0.5 µg/ml	N/A	Mol. Probes

Table 2 | List of antibodies used for flow cytometry.

2.5 *In vitro* clonogenic assays

2.5.1 CFU-C assay

Following 5-7 day aggregate culture, cell suspensions were plated at a concentration of 0.01 embryo equivalents (ee) of the starting culture in a methylcellulose based medium containing erythropoietin, IL-3, IL-6 and SCF (MethoCult GF3434; STEMCELL Technologies) and supplemented with 1% P/S. Plates were incubated at 37˚C, 5% CO_2. Haematopoietic colonies were counted and scored after 7-11 days of differentiation following described standard criteria (C. Pereira et al. 2007). The concentration of cells to plate was chosen to avoid saturation of the colonies.

2.5.2 Endothelial assay

Plates were coated with 0.1% gelatine and incubated at 37˚C for 30min. OP9 cells were plated at a concentration of 100,000 cells/well (6-well plates were used) in OP9 culture medium and allowed to set for a minimum of 3 hours. Then, media was removed and cell suspensions of cultured re-aggregates were transferred at a concentration of 0.1ee/well in Aggregate culture medium supplemented with 50ng/ml VEGF (Peprotech) and incubated at 37˚C, 5% CO_2. After 7-11 days, cells were washed in PBS and fixed in 5% DMSO in methanol for 5min at RT, then blocked with 10% FCS/PBS for 30min before incubation with rat anti-mouse CD31 (1:250, MEC13.3, Pharmingen) in 2% FCS/PBS overnight at 4˚C. On the next day, cells were washed in 0.05% Tween-20/PBS and incubated with goat anti-rat alkaline phosphatase (AP) (1:250, Southern Biotech) in washing solution for 2h at RT. After washing, alkaline phosphatase activity was detected using the Blue Alkaline Phosphatase Substrate kit (Vector Labs) following manufacturer's instructions and plates stored in MilliQ water at 4˚C. Endothelial colonies were counted and scored in three different categories: simple, complex, big (details are explained in section 3.2.3).

2.6 *Ex vivo* aggregate culture

Single cell suspensions of embryonic tissues (AGM or caudal parts) (see section 2.3.2) were resuspended in IMDM medium with 20% heat-inactivated (HI) FCS (Hyclone) and placed in 200µl pipette tip sealed with parafilm at the concentration of 1 embryo equivalent (ee)/tip (1ee corresponding to 1 AGM or 1 CP). Tips were centrifuged at 460g for 12min to form a pellet. After gently removing parafilm with forceps, the aggregate pellet was expelled from the tip onto a floating 0.8µm nitrocellulose membrane filter placed on top of culture media. A maximum of 5 aggregates was positioned on a single membrane in order to avoid merging and mixing of neighbour aggregates. Culture at the gas-liquid interface was carried out for 5 days (E11.5 embryos) or 7 days (E9.5-E10 embryos) at 37˚C, 5% CO_2. The medium used for culture was Aggregate culture medium (section 2.1). For 7-day cultures, media was replaced after 24h. For angiopoietins treatment, either Ang1 (10ng/ml or 100ng/ml) (Antibodies-online) or Ang2 (10ng/ml or 100ng/ml) (R&D

Systems) were added to the medium at the beginning of the culture and after 24h (when appropriate). Prior to culture, nitrocellulose membranes were washed on top of IMDM with 20% HI FCS media at 37˚C, 5% CO_2 for a minimum of 30min, then media was aspirated and replaced by culture media.

For OP9 co-aggregate cultures, E11 FACS-sorted pre-HSC-II cells were mixed with 100,000 OP9 stromal cells for each embryo equivalent and spun down at 300g for 5min. The cell pellet composed by a mixture of OP9 and sorted cells was resuspended in IMDM media and distributed in parafilm-sealed 200µl tips at the concentration of 1ee/tip. Tips were centrifuged at 460g for 12min to form co-aggregates and then the procedure was carried out as described above.

After culture, re-aggregates and co-aggregates were transferred to 5ml polystyrene tubes and dissociated to a single cell suspension as described in section 2.3.2.

2.7 Long-term repopulation assay

Cultured or freshly isolated cell suspensions from donor CD45.2/.2 mice were resuspended in FACS buffer and co-injected along with 100,000 bone marrow carrier cells isolated from the femurs of CD45.1/.1 mice. The injected dose of cells was adjusted depending on the culture system and embryonic stage and it is specified for each experiment in Chapter 3. Recipient CD45.1/.2 mice were irradiated prior to transplantation with a dose of 9.5 Gy, split in two doses with a 3-hour gap in between and delivered by a sealed Cs source at a rate of 21.6rad/min. Each recipient was injected with a maximum of 200µl by using a 30-gauge syringe needle (BP Plastipak). All injections were performed in the lateral tail vein of restrained animals according to the procedures described in the project license and the regulations of the Animals Scientific Procedures Act, UK, 1986. In order to assess donor's blood chimerism, blood was collected from recipient mice at 6 weeks post-transplantation for short-term repopulation and 16 weeks for long-term repopulation. Blood was obtained by incision of the tail vein and processed for flow cytometry as described in sections 2.3.3 and 2.4.

2.8 OP9 culture

2.8.1 Thawing and maintenance of OP9 cells

Frozen cells were rapidly thawed (< 1min) in a water bath at 37˚C. Cell vial was wiped with 70% ethanol and vial content was transferred in a 5ml Falcon tube with pre-warmed OP9 medium. Cells were centrifuged at 350g for 5min, then supernatant was removed, fresh OP9 medium added and cell pellets dispersed by gently tapping the tubes and pipetting. Cells were plated at high density in a T-25 flask in order to optimise recovery. Medium was changed in the first 24h to remove debris and dead cells. OP9 medium is described in section 2.1. Cells were maintained at 37˚C, 5% CO_2 in humidified incubators (Sanyo).

2.8.2 Passaging and freezing of OP9 cells

Cells were grown to confluence, then media was aspirated and cells were washed twice with warm PBS. 0.01% trypsin was added and cells were incubated for 5min at 37˚C. FCS-containing medium was added in order to inactivate trypsin and cells were dispersed by gently pipetting before being transferred to a Falcon tube. After centrifugation at 350g for 5min, cells were resuspended in new OP9 medium, counted with a haemocytometer, plated in a new flask and incubated

For freezing, cells were resuspended in OP9 medium with 10% DMSO, transferred to cryovials (Nunc) and placed onto dry ice. Vials were stored overnight at -80˚C and transferred in liquid nitrogen for long term storage.

2.8.3 Doxycycline-inducible OP9 lines

cDNA coding for Angiopoietin2 was cloned into a tetracycline/doxycycline inducible bicistronic pPBhCMV1-cHA-IRES-Venus-pA vector (gift from H. Niwa). The system allows both Ang2 and the Venus reporter proteins to be expressed upon doxycycline induction. 100.000 OP9 cells were electroporated with the plasmid by using NEON transfecting system (Invitrogen) and cells were cultured in presence of 1µg/mL doxycycline (Clontech) for 24h. A control line was electroporated with the bicistronic vector without the Ang2 insertion (Venus-OP9). After culture, OP9 cells expressing Venus were positively selected by FACS-sorting and plated in culture in absence of

doxycycline. After one week of culture, a second sort was performed in order to remove any cells constitutively expressing Venus. Both cell lines were generated by Dr Natalia Rybtsova.

2.9 Immunostaining and confocal microscopy

2.9.1 Embryo embedding and sectioning

Embryos were fixed in 4% PFA overnight at 4˚C on a gentle shaker. After rinsing them twice with PBS, they were placed in a solution of 15% sucrose/PBS for 1-3h (depending on embryonic stage) at 4˚C, until they sank to the bottom of the tube. Samples were transferred to a solution of PBS with 15% sucrose and 7% gelatine and incubated at 37˚C for 1-3h until they sank. Then, they were moved in the same solution to a specimen mount and oriented under a stereomicroscope. Gelatine solution was allowed to set at RT, then specimens were snap-frozen in liquid nitrogen and stored at -80˚C. For cryosectioning, samples were allowed to set for a minimum of one hour at -24˚C. 7μm-thick transverse sections of the AGM region were cut at -24˚C with a Cryotome FSE (Thermo Scientific), mounted on SuperFrost Plus (VWR) slides and allowed to air-dry. Sections were further processed for immunostaining or stored at -20˚C.

2.9.2 Immunostaining and microscopy

Slides were immersed in PBS and placed in a microwave at full power for 30 seconds to remove gelatine. Then, sections were washed twice in PBS, permeabilized and blocked with 5% donkey serum/0.3% triton-X100/PBS and stained with primary antibodies overnight at 4˚C. After a couple of PBS rinses, secondary antibodies were added to a solution of 0.3% triton-X100/PBS for 2hours at room temperature. Slides were washed twice, followed by counterstaining with 10 mg/ml DAPI for 10min at RT. Table 3 contains a list of all primary and secondary antibodies used. Samples were mounted with ProLong Gold Antifade mountant (Life Technologies) and dried at room temperature in the dark for a minimum of 2h, then stored at 4˚C. Secondary antibody only controls were prepared for all new antibodies or combination of antibodies tested. Images were acquired using an inverted confocal microscope

(Leica SP8) and analysed using ImageJ 1.50i (https://imagej.nih.gov/ij/) or Adobe Photoshop CS6.

Antigen	Clone	Isotype	Working Conc.	Conjugate	Supplier
CD31	MEC13.3	Rat	2.5 µg/ml	N/A	Pharmingen
CD146	AF6106	Sheep	2 µg/ml	N/A	R&D Systems
Runx1	EPR3099	Rabbit	10 µg/ml	N/A	Abcam
Tie2	C-20	Rabbit	2 µg/ml	N/A	Santa Cruz Biotech
Ang1	C-19	Goat	4 µg/ml	N/A	Santa Cruz Biotech
Ang2	F-18	Goat	4 µg/ml	N/A	Santa Cruz Biotech
NG2	Polyclonal	Rabbit	2 µg/ml	N/A	Millipore
αSMA	Polyclonal	Rabbit	2 µg/ml	N/A	Abcam
GFP	Polyclonal	Rabbit	2 µg/ml	N/A	Life Technologies
CD44	N/A	Rat	2 µg/ml	N/A	Stratech
COUP-TFII	H7147	Mouse	1 µg/ml	N/A	Perseus Proteomix
cKit	2B8	Rat	0.05 µg/ml	N/A	Biolegend
Goat IgG	NL001	Donkey	10 µg/ml	NL557	R&D Systems

Goat IgG	N/A	Donkey	20 µg/ml	AF647	Invitrogen
Goat IgG	N/A	Donkey	20 µg/ml	AF488	Invitrogen
Rabbit IgG	NL004	Donkey	10 µg/ml	NL557	R&D Systems
Rabbit IgG	N/A	Donkey	20 µg/ml	AF647	Invitrogen
Rat IgG	N/A	Donkey	20 µg/ml	AF488	Invitrogen
Rat IgG	N/A	Donkey	20 µg/ml	AF546	Invitrogen
Rat IgG	N/A	Donkey	20 µg/ml	AF647	Invitrogen
Rat IgG	2A 8F4	mIgG2a	1 µg/ml	AP	Southern Biotech
DAPI	N/A	N/A	0.5 µg/ml	N/A	Biotium

Table 3 | List of primary and secondary antibodies used for immunostaining.

2.9.3 Correlative analysis of intra-aortic haematopoietic clusters

Slides were immunostained as described in section 2.9.2 with a rat anti-mouse CD31 to mark the endothelium and intra-aortic haematopoietic clusters (IAHC) and a goat anti-mouse Ang2 to assess expression of Ang2. Max intensity projections of 7 µm transverse sections were acquired by confocal microscopy. Using a macro specifically created for ImageJ (written by Dr Bertrand Vernay, Imaging Facility Manager), the nuclei of endothelial cells located in the ventral part of the aortic lining were selected as centres. A radius (r) of 12.5 µm (50 pixels) was drawn around each centre. The number of cluster cells contained within the radius was counted manually and the count was assigned to each centre (0 = no cluster cells within the radius). Then, Dr Sergei Zuev performed the statistical modelling. The concentration of Ang2 was calculated within a radius (R) of 25 µm (100 pixels) from the centre of each endothelial cell. The concentration of Ang2 was estimated as the

sum of luminosities of all red pixels within the R. Spearman's rank-order correlation was applied to calculate dependence between clusters and concentration of Ang2.

2.10 Molecular methods

2.10.1 Total RNA extraction, yield and quality control

For total RNA extraction of embryonic tissues, aggregates were cultured for 24h, cells dissociated as described in section 2.3.2 and disrupted in 350µl of Buffer RLT by pipetting. RNA was purified with a silica column-based method using RNeasy Mini Kit (Qiagen) following manufacturer's instructions. RNA yield was measured with NanoDrop ND-1000 Spectrophotometer (LabTech) and samples placed on ice for immediate processing or stored at -80˚C. For total RNA extraction of small numbers of FACS-sorted cells (< 80,000 cells), samples were disrupted in 75µl of Buffer RLT (Qiagen) supplemented with 1% β-mercaptoethanol (14.3M) in RNAse free 0.2µl PCR tubes at 4˚C. Tubes were subjected to vortexing for 1min and RNA was extracted with the RNeasy Micro Kit (Qiagen) including DNA digestion with DNase I (Qiagen), according to manufacturer's instructions. RNA yield was calculated using Nanodrop (Thermo Fisher) or Qubit 2.0 Fluorometer (Thermo Fisher). For RNA-seq samples, RNA integrity number (RIN) was estimated by capillary electrophoresis using Agilent 2200 Tapestation with High Sensitivity RNA ScreenTape, buffer and ladder (Agilent) to ensure all samples had RIN > 7. Samples were immediately processed or stored at -80˚C. Due to the small sample size (100-500 cells) collected after sorting and to ensure the highest amount of RNA could be used for RNA-seq library preparation, RIN was measured on a mock cell population which was sorted at the same time as the samples of interest and processed for RNA extraction simultaneously with the samples.

2.10.2 cDNA preparation

Total RNA was reverse-transcribed using SuperScript III Reverse Transcriptase (Invitrogen). Mastermix was prepared by adding an equal amount of total RNA for each sample (between 1-5ug, varying from experiments), 300ng random primers (3µg/uL) (Invitrogen), 1µl dNTPs (10mM) and volume was

equalised with nuclease-free water. Samples were heated at 65˚C for 5min and incubated on ice for at least 1 minute. Then, tubes were spun down and the following reagents were added: 4µl 5X First-Strand Buffer, 1µl DTT (0.1 M), 1µl RNaseOUT (40 units/µl), 1µl SuperScript III RT (200 units/µl). Reverse-transcription reaction was carried out at 50˚C for 1hour and inactivated at 70˚C for 15 minutes. RNA complementary to cDNA was removed adding 1µl of *E.coli* RNase H (10 U/µl, Ambion) and incubated at 37˚C for 20min. Samples were diluted (1:200-1:500) and immediately processed or stored at -20˚C.

2.10.3 qRT-PCR

2.10.3.1 qRT-PCR reaction

Quantitative real time PCR was performed on a Light Cycler® 480 instrument II 384 well version (Roche Diagnostics) following the Universal Probe Library (UPL) method (Roche). Reaction mix were prepared with 4µl of the diluted cDNA, 5µl of 2x LightCycler® 480 probe Master (Roche Diagnostics), 0.45µl of forward and reverse primers (5µM), 0.1µl of the appropriate UPL probe (10µM) and nuclease-free water to a final volume of 10µl. A control reaction in which cDNA was replaced with water was prepared for each gene transcript. Reactions were generated in duplicates or triplicates in 384-well plates. Plates were sealed, spun down at 500g for 1min and kept in the dark prior to loading onto the machine. The following PCR program was used: pre-incubation at 95˚C for 5min; amplification at 95˚C for 10sec, 55˚C for 10sec, 60˚C for 18sec for 45 cycles; extension at 60˚C for 10min. Experiments were performed in biological duplicates or triplicates.

2.10.3.2 qRT-PCR primer design

Primers were designed using the UPL Assay Design Centre using the transcript ID of the NCBI reference sequence database and selected for intron spanning whenever there was the option. Primers were tested on cDNA derived from positive control tissues of the same stage as for the experiments. Four concentrations of cDNA (each of them diluted 10 times more than the previous concentration) were used as standards. Cp values of each concentration were plotted as standard curve and efficiencies were calculated with the LightCycler® 480 software based on the

slope of the standard curve. Only primers with efficiencies between -1.8 and -2.2 were used. Primers used in this thesis are:

Ang2-F: *ctcaccaccagtggcatcta*

Ang2-R: *cccacgtccatgtcacagta* (UPL probe #60)

Tbp-F: *ggggagctgtgatgtgaagt*

Tbp-R: *ccaggaaataattctggctca* (UPL probe #97)

2.10.3.3 qRT-PCR data analysis

Data was analysed with Microsoft Excel using the $2^{-\Delta\Delta Ct}$ Method (Livak & Schmittgen 2001). Briefly, ΔCt was calculated by normalizing the threshold cycles (Ct) of the target gene to the TATA Binding Protein (Tbp) reference gene:

$$\Delta Ct = Ct_{(Gene)} - Ct_{(TBP)}$$

Then, the ΔCt of the Ang2-treated sample was normalized to the ΔCt of the control sample:

$$\Delta\Delta Ct = Ct_{(Ang2)} - Ct_{(Control)}$$

Finally, the expression ratio calculated as $2^{-\Delta\Delta Ct}$ represents the fold increase (or decrease) of the target gene in the Ang2-treated sample relative to the control sample and is normalized to the expression of the Tbp reference gene.

2.11 RNA-sequencing and analysis

2.11.1 Library preparation

Libraries for RNA-sequencing were prepared using the SMARTer Stranded Total RNA-Seq Kit - Pico Input Mammalian (Takara Bio) following manufacturer's instructions and with slight modifications. Briefly, input RNA (RIN > 7, max 10ng) was mixed to 1µl SMART Pico Oligos Mix, 4ul 5X First-Strand buffer, nuclease-free water to 11µl and fragmented for 4 minutes at 94˚C. Immediately after, 4.5µl of Template Switching Oligo Mix, 0.5µl RNase inhibitor and 2µl of SMARTScribe reverse transcriptase were added to perform first-strand cDNA synthesis for 90 min at 42˚C, followed by inactivation at 70˚C for 10 min. In order to distinguish pooled

libraries from each other after sequencing, indexes were added to the samples by mixing 1µl of Forward (i5) primer and 1µl of Reverse (i7) primer with 2µl of nuclease-free water, 25µl of 2X SeqAmp PCR buffer, 1µl of SeqAmp DNA polymerase. Tubes were heated at 94˚C for 1min, then 5 cycles of denaturation (98˚C, 15sec), annealing (55˚C, 15sec) and elongation (68˚C, 30sec) were performed, followed by final elongation (68˚C, 2min). The amplified RNA-seq libraries were purified twice by immobilization onto AMPure beads (Agencourt) on a magnetic separator with a volume ratio of *1 : 0.9 = sample : beads*, then beads were washed with 80% ethanol and cDNA eluted in nuclease-free water. Ribosomal cDNA was depleted by adding R-probes (1µl) and ZapR (1.25µl) along with 10X ZapR Buffer (2µl). Hybridization of R-probes to ribosomal RNA sequences, followed by enzymatic cut of the sequences by ZapR, was achieved by heating the samples at 37˚C for 1hour and 72˚C for 10 minutes. Next, the library fragments not cleaved by ZapR were further amplified in a second round of PCR. The following mix was prepared: 26µl Nuclease-Free Water, 50µl 2X SeqAmp PCR Buffer, 2µl PCR2 Primer mix, 2µl SeqAmp DNA polymerase. To determine the number of PCR cycles that would amplify the signal without reaching plateau, 9µl of sample were mixed with 1µl of 10X SYBR green (Invitrogen) and qRT-PCR was performed in duplicates following the program described in the kit for the second round of PCR: 94˚C for 1min followed by 25 cycles of 98˚C for 15sec, 55˚C for 15sec, 68˚C for 30sec. Number of cycles for each sample were established by applying the following criteria according to the amplification curves:

$$\text{PCR Cycle}_{(\text{sample})} = \text{Ct}_{(\text{sample plateau})} - 2$$

So for example, if a plateu was reached at Ct 18, sample was amplified by PCR until cycle 16 only. A final step of purification with AMPure beads was performed (*1 : 0.9 = sample : beads)* after PCR.

2.11.2 Library quality control

Library concentrations were quantified using the high sensitivity DNA option on the Qubit 2.0 Fluorometer (Thermo Fisher). Quality control of the generated fragments was performed using the Agilent 2200 Tapestation with D1000 High

Sensitivity DNA reagents (ScreenTape, Buffer and Ladder, Agilent). When adapter dimer peaks were observed in the electropherogram (≈120-140bp length), libraries were cleaned by bead selection (beads were kind concession of Dr Luca Tosti, who helped with library purification) with the ratio (*1 : 0.85 = sample : beads)*.

2.11.3 Sequencing

Sequencing was carried out in the Edinburgh Genomics facility at the University of Edinburgh. 75 base paired-end reads were generated with Illumina HiSeq 3000/4000 (Illumina). Due to low complexity of the libraries, 20% PhiX spike-in control was included.

2.11.4 Sequencing quality control and trimming

Sequencing reads were provided in FASTQ format by the Edinburgh Genomics facility. FASTQ is a text-based file that contains information about the nucleotide sequence and its corresponding quality score for each sequenced read. Quality control of the reads was assessed using FASTQC (S. Andrews 2010) which enables visualization of a report based on analysis modules and gives an evaluation of whether the result for each of the module is normal (green tick), slightly abnormal (orange triangle) or very unusual (red cross). The analysis modules comprise: basic statistics; per base sequence quality; per sequence quality scores; per base sequence content; per base GC content; per sequence GC content; per base N content; sequence length distribution; duplicate sequences; overrepresented sequences; overrepresented Kmers. Universal 3' AGATCGGAAGAGCACACGTCTGAACTCCAGTCAC and 5' AGATCGGAAGAGCGTCGTGTAGGGAAAGAGTGTAGATCTCGGTGGTCGC CGTATCATT adapters were trimmed from the reads using Cutadapt v1.14 (M. Martin 2011) and reads of length inferior than 20bp were discarded.

2.11.5 Sequencing alignment and reads quantification

Sequencing reads were aligned to the mouse reference genome GENCODE M14 mouse reference genome (mm10) using STAR (version 2.5.3ab), an ultra fast

splice aligner tailored for RNA-seq (Dobin, C. A. Davis, Schlesinger & Drenkow 2013). The following filtering options were set: reads containing junctions that did not pass filtering were excluded (--outFilterType BySJout); a maximum of 20 multiple alignments were allowed for a read (if exceeded, the read is considered unmapped) (--outFilterMultimapNmax 20); a read will be considered aligned only if the number of matched bases is higher than or equal to 20 (--outFilterMatchNmin 20). Furthermore, uniquely mapped reads were assigned to genes and quantified as fragments (pair of reads, as the data is paired-end) using featureCounts (Liao et al. 2014).

2.11.6 Statistical and differential expression analysis

All statistical calculations downstream of read quantifications have been performed using the R programming language and environment (R studio version 1.0.143) (Team 2015). Differential expression analysis was performed using the Bioconductor package DEseq2 (Love et al. 2014) (v1.12.4). As DEseq2 internally corrects for library size, the un-normalized estimated counts of sequencing fragments obtained from featureCounts was used as input. In order to estimate dispersion and the log2 fold change in the model, the DEseqDataSet was created including two variables in the design formula: (1) "cell type" categorizes samples into pre-HSCI or endothelial and associates each of them to a culture treatment (Ang2 or control); (2) "experiment" groups the samples based on the sorting batch (exp1 or exp2). Pre-filtering was performed in order to remove genes that have 0 or 1 reads as a way to increase the speed of the transformation and testing functions. In order to compare Ang2 pre-HSCI vs Ctrl pre-HSCI (or Ang2 endo vs Ctrl endo) the function *relevel* was chosen to set up the control group as reference. Differential expression analysis was performed using the function *DESeq*, which models the gene counts in each sample using a negative binomial distribution and assigns a dispersion value to each gene. Genes with a False Discovery Rate (FDR) ≤ 0.05 and an absolute fold change > 1.5 were considered as statistically differentially expressed.

2.11.7 Pathway analysis

Gene ontology (GO) analysis was performed using DAVID database (Database for Annotation, Visualization and Integrated Discovery) (Huang et al. 2007) on the list of previously identified significantly differentially expressed transcripts and using all mouse genes as background. Enriched GO terms were selected based on the p-value ≤ 0.05. Ingenuity Pathway Analysis (IPA) software was utilized for canonical pathway analysis on the list of previously identified significantly differentially expressed transcripts and using all mouse genes as background. Canonical pathways with a p-value ≤ 0.05 were considered significant. A z-score higher than 0 indicated activation, while a z-score less than 0 indicated inactivation. In some occasions, the software could not predict the z-score (NaN) of some of the significantly enriched pathways. The manual of the IPA software doesn't clarify when the z-score cannot be predicted.

Chapter 3 Characterization of the functional role of angiopoietins in HSC formation

3.1 Introduction

In the mouse embryo, the first haematopoietic stem cells (HSCs) emerge from the AGM region around E10.5-E11 (Medvinsky & Dzierzak 1996; Müller et al. 1994). Recent observations indicate that emergence of HSC occurs in a step-wise manner through the expansion and maturation of embryonic HSC precursors, which express markers common to the endothelial lineage, such as VE-Cadherin (VC), and gradually up-regulate haematopoietic markers, such as CD41, CD43 and CD45. Pro-HSCs (VC^+ $CD45^-$ $CD41^+$ $CD43^-$) detected in the E9.5 caudal part of the embryo mature into pre-HSC-I (VC^+ $CD45^-$ $CD41^+$ $CD43^+$) in the E10.5 AGM and finally into pre-HSC-II (VC^+ $CD45^+$ $CD41^+$ $CD43^+$) at E11.5, before becoming HSCs (Taoudi et al. 2008; Rybtsov et al. 2011; Rybtsov et al. 2014). In contrast to HSCs, these precursors are not able to directly repopulate the haematopoietic system of adult irradiated recipients and in order to develop into transplantable HSCs they need a maturation step in an embryonic environment. The development of an aggregate culture system supporting this maturation has enabled the analysis of HSC precursor populations *ex vivo*. As for the explant culture system (Medvinsky & Dzierzak 1996), AGM cells are cultured in isolation from the rest of the embryo, ensuring that changes in cell functionality can be exclusively attributed to the cells of the culture, rather than migration from other regions. Moreover, the dissociation step introduced in this culture reduces the variation between embryos due to slight stage difference, as control and test conditions are taken from the same pool of dissociated tissues derived from multiple embryos. Furthermore, the fact that tissues can be cultured at a stage in which HSC are not yet formed, ensures that the culture system is capturing the maturation process preceding HSC formation. Thus, modification of the culture conditions supporting HSC formation has allowed to inform about the importance of novel molecular cues necessary for HSC development (Rybtsov et al. 2014; Souilhol, Lendinez, et al. 2016; Souilhol, Gonneau, et al. 2016)(McGarvey et al. 2017).

To expand the knowledge of the molecular requirements needed for HSC development, a recent study has focused on determining the genome-wide molecular differences between the ventral domain of the aorta (AoV) and the dorsal domain (AoD) by RNA-sequencing (McGarvey et al. 2017). As HSCs had previously been found to preferentially emerge from the AoV (Taoudi et al. 2008; Souilhol, Gonneau, et al. 2016), molecules that were found to be differentially expressed in the AoV at E10.5 were considered as potential candidates to be tested for their ability to promote HSC development. Angiopoietins were found among the molecules over-expressed at E10.5 in the AoV (see section 3.2.1). Angiopoietins are the ligands of Tie2 receptor and they form part of the Angiopoietin-Tie signalling pathway. The Angiopoietin-Tie signalling pathway was first identified in the field of vascular biology as a pathway responsible for vessel development and angiogenesis (Augustin et al. 2009; Thurston & Daly 2012). Despite a few studies showing the relevance of this signalling pathway in the maintenance of the adult HSC pool in the bone marrow (Arai et al. 2004), the role of this pathway in developmental haematopoiesis is still unknown.

In this chapter, I aim to explore the functional relevance of angiopoietins in HSC development. I will describe two different *ex vivo* aggregate culture systems used to provide supplementation of angiopoietin ligands in AGM cultures; the output of these assays in terms of *in vitro* haematopoietic and endothelial assays, repopulation of irradiated mice, and multilineage engraftment of the repopulated mice; and finally demonstrate that Angiopoietin2 (Ang2) is reproducibly able to increase the efficiency of HSC maturation at early stages of development.

3.2 Results

Aspects of this work were conducted with the help of Dr Stanislav Rybtsov and Dr Natalia Rybtsova. Dr Stanislav Rybstov assisted with the preparation of the first re-aggregate culture and with transplantation of cells for the first few experiments. Dr Natalia Rybtsova generated the OP9 transgenic lines described in this chapter.

3.2.1 Angiopoietins are significantly up-regulated in the AoV at E10.5

The data described in this section was originally produced by Dr Alison McGarvey as a result of the RNA-seq analysis that compared the gene expression profiles of the ventral domain of the aorta (AoV) with the dorsal domain of the aorta (AoD) at different stages of development (McGarvey et al. 2017). The data were downloaded from the publicly accessible data source http://agmniche.stembio.org/homepage.html and commented herein to facilitate the understanding of this thesis project.

Gene expression analysis of the distinct domains of the AGM region revealed a significant enrichment of Angiopoietin1 (Ang1) and Angiopoietin2 (Ang2) in the AoV compared to the AoD at both E9.5 and E10.5 (Figure 3.1A). In particular, at E9.5 and E10.5 Ang1 expression was respectively increased by 2-fold and 1.5-fold in the AoV compared to the AoD (Figure 3.1A). Remarkably, a 5-fold increase of Ang2 expression was detected in the AoV at E9.5, while a 2-fold increase was observed at E10.5 in comparison with the AoD (Figure 3.1A). Angiopoietins receptor Tie1 and Tie2 were also found to be up-regulated in the E9.5 AoV compared to AoD, however both were equally distributed in the AoV and AoD at E10.5 (Figure 3.1A). Moreover, expression of Ang1 and Ang2 in the AoV was increased by 1.5 and 2-fold respectively at E10.5 compared to E9.5, while expression of Tie1 and Tie2 remained unchanged (Figure 3.1B). All together, these results suggested that Ang1 and Ang2 are ventrally polarized in the AGM region and that their expression is more prominent in the AoV at E10.5 compared to E9.5.

As the niche for HSC development is located ventrally (Taoudi et al. 2008) and HSCs are first detected in the AGM region at E10.5 (Müller et al. 1994), enrichment of angiopoietins in the time and place of HSC maturation led to the hypothesis that these molecules might be implicated in the process of HSC emergence. Thus, further investigation was carried out.

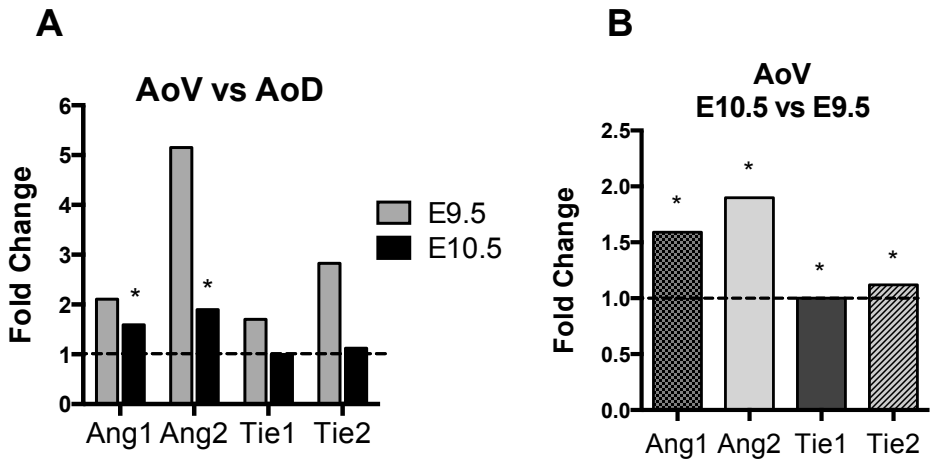

Figure 3.1 | Angiopoietin-Tie expression in the AGM region measured by RNA-seq. **(A)** Fold change of expression between the ventral domain (AoV) and the dorsal domain (AoD) of the aorta of the main components of the Ang-Tie signalling pathway. Grey bars = fold change at E9.5. Black bars = fold change at E10.5. Asterisks indicate AoV vs AoD significance (FDR < 0.05). FDR values could not be retrieved for E9.5 AoV vs AoD comparison. **(B)** Fold change of expression in the AoV between E10.5 and E9.5 of the main components of the Ang-Tie signalling pathway. Asterisks indicate E10.5 vs E9.5 significance (FDR < 0.05). Data were generated by McGarvey et al. 2017 and could be accessed online at **http://agmniche.stembio.org/homepage.html**.

3.2.2 An *ex vivo* culture system able to fully mature HSC precursors into transplantable HSCs to study the role of angiopoietins

In order to investigate the ability of angiopoietins to promote HSC formation at early stages of development, an *ex vivo* re-aggregate culture system was used (Taoudi et al. 2008; Rybtsov et al. 2014). The aim of this system is to enable maturation of HSC precursors contained in the caudal region of the embryo at E9.5 into fully transplantable HSCs. To this extent, the E9.5 caudal part (CP) of the embryo was dissociated at the single cell level and re-aggregated on top of a membrane (Figure 3.2). Cell re-aggregates were cultured at the gas-liquid interface for 7 days in presence of media containing serum and supplemented with SCF, IL3 and Flt3-L (also referred in this thesis as "3GF"). To investigate the contribution of angiopoietins to the HSC maturation process, media was supplemented with Ang1 and/or Ang2 recombinant proteins. Each protein was tested in two different doses,

based on manufacturer's recommendation. At the end of the culture period, re-aggregates were plated for *in vitro* colony assays to determine their clonogenic ability to produce haematopoietic and endothelial progenitors (section 3.2.3 and 3.2.4) and transplanted into sub-lethally irradiated adult mice in order to gain insight into the role of angiopoietins in HSC formation (section 3.2.5).

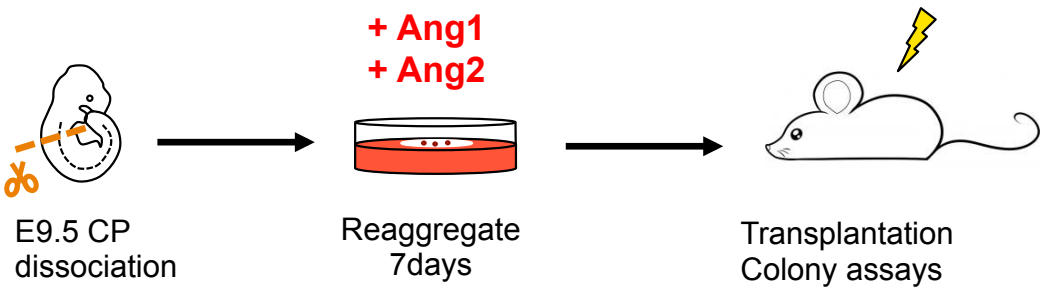

Figure 3.2 | The ex-vivo re-aggregate culture system able to support HSC maturation. Schematics of the culture system used to test the effect of angiopoietins on HSC formation. E9.5 caudal part (CP) is sub-dissected, dissociated to a single cell suspension and re-aggregated on top of a membrane. Re-aggregates are cultured at the gas-liquid interface for 7 days in a media containing serum, SCF, IL3, Flt3-l (3GF) in presence/absence of Ang1 and/or Ang2. At the end of the culture, cells are transplanted to sub-lethally irradiated recipients and plated for *in vitro* haematopoietic and endothelial assay. Ang1 = angiopoietin1; Ang2 = angiopoietin2.

3.2.3 Angiopoietins do not affect *in vitro* haematopoietic colony formation

Haematopoietic stem and progenitor cells retain the ability to differentiate and give rise to lineage-restricted progenitor cells. To test the capacity of angiopoietins to promote haematopoietic specification, an *in vitro* colony-forming unit in culture (CFU-C) assay was set up after 7 days of culture at the gas-liquid interface (Figure 3.2). In this system, cells are allowed to grow for 7-10 days in a methylcellulose-based media in order to stimulate formation of haematopoietic colonies. Based on their morphological characteristics (C. Pereira et al. 2007), colonies are then scored as burst forming unit-erythroid (BFU-E), granulocyte/monocyte (GM) and granulocyte/erythrocyte/monocyte/megakaryocyte (GEMM). Supplementation of the culture with angiopoietins in low concentration

(10ng/ml) had the tendency to increase the number of CFU-Cs, while supplementation with angiopoietins in high concentration (100ng/ml) did not seem to alter formation of CFU-Cs in each of the tested combinations, as the number of colonies was similar to control conditions (Figure 3.3). Of note, when both Ang1 and Ang2 were added at low concentration, the total number of colonies was increased by 3-fold (from 5000 to 15000 CFU-C/ee).

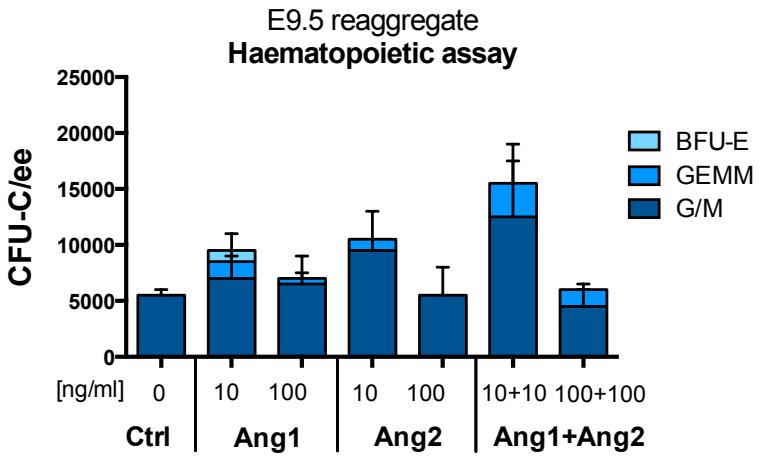

Figure 3.3 | Effect of angiopoietins on CFU-C formation.

Number of haematopoietic colonies (CFU-Cs) formed per embryo equivalent (ee) from cells cultured with the named recombinant protein (Ang1, Ang2 or Ang1+Ang2) or in absence of additional protein (Ctrl), plated in methylcellulose for 7-10 days at a concentration of 0.01ee/dish. The dose of recombinant protein added is displayed in ng/ml. Colonies were scored as: BFU-E = burst forming unit-erythroid, GEMM = granulocyte/erythrocyte/monocyte/megakaryocyte, G/M = granulocyte/monocyte. N = 2 independent experiments, 1 technical replicate each. Error bars represent the standard error of the mean (SEM).

3.2.4 Angiopoietins reduce the number of endothelial progenitors

Angiopoietins are important players in angiogenesis and vasculogenesis (reviewed in (Thurston & Daly 2012)). In order to assess whether the presence of angiopoietins influences production of endothelial progenitors within the AGM microenvironment, an *in vitro* endothelial assay was conducted (see materials and methods, section 2.5.2). To this extent, cells cultured 7 days as re-aggregates were

seeded onto an OP9 stromal cell layer in presence of VEGF, one of the major growth factor involved in vasculogenesis (Carmeliet et al. 1996). OP9 cells provide a favourable environment for the growth of clonogenic endothelial cell progenitors, as they provide support for proliferation, differentiation and formation of clusters of endothelial cells (Hirashima et al. 1999). After 7 to 10 days of co-culture, simple structures (constituted by a single endothelial cell), complex (formed by two or more endothelial cells to form a line of simple structures) and big colonies (a fit network of endothelial cells) (Figure 3.4A) were counted. Re-aggregates treated with angiopoietins had the tendency to produce less endothelial colonies compared to control (Figure 3.4B). Thus, these results suggest that both angiopoietins might play a role in reducing the numbers of endothelial progenitors in the AGM region.

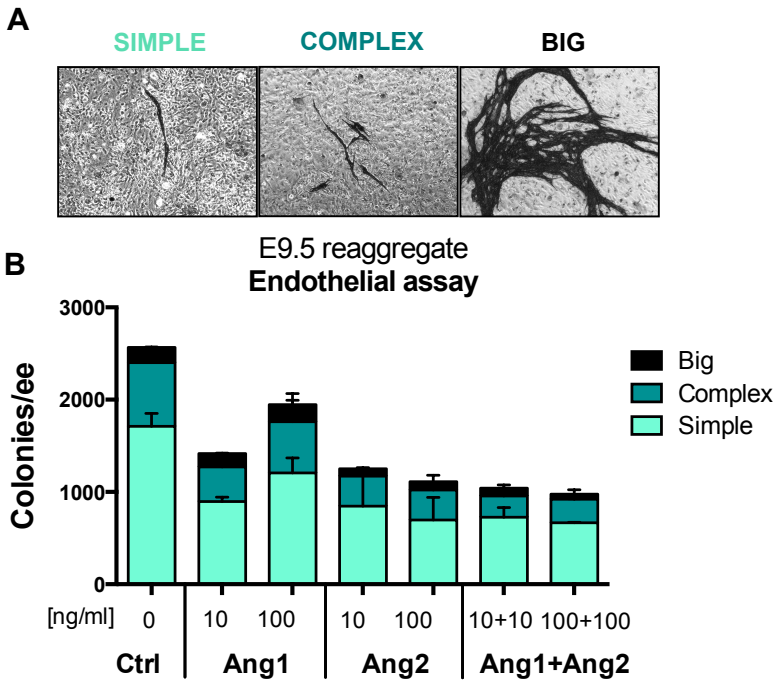

Figure 3.4 | Effect of angiopoietins on endothelial colony formation.

(A) Representative examples of the different type of colonies scored. (B) Number of endothelial colonies scored per embryo equivalent (ee). Cells cultured in presence of angiopoietins at different concentrations (ng/ml) of recombinant proteins (Ang1, Ang2, Ang1+Ang2) or in absence of additional proteins (Ctrl) were plated on top of an OP9 layer in presence of SCF, IL3, Flt3-l and VEGF for 7-10 days. Cells were plated at a concentration of 0.1ee/dish. N = 2 independent experiments, 1 technical replicate each. Error bars represent the SEM.

3.2.5 Long-term repopulation assay functionally validates the role of Ang2 in promoting HSC formation from E9.5 AGM

After culture (Figure 3.2), production of transplantable HSCs mediated by angiopoietins was determined by injecting re-aggregates into the tail-vein of sub-lethally irradiated recipient mice at a dose of 1ee/mouse. Sixteen weeks after transplantation, the long-term repopulation potential of the transplanted HSCs was measured as the percentage of donor cells in the peripheral blood of the recipient. To determine the efficiency of the treatment with angiopoietins in producing HSCs, two factors were taken into account: (a) the level of repopulation of the recipient mice, as an indicator of the quantities of HSCs matured in culture and (b) the number of mice repopulated, which shows whether HSCs were produced in culture (no repopulation indicates no HSCs were produced).

Treatment with Ang2 at a high (100ng/ml) but not at low (10ng/ml) dose significantly increased the level of donor contribution in the peripheral blood of recipient mice compared to control (Figure 3.5). Interestingly, while the average level of donor contribution in control mice was 19%, all the 6 recipients treated with 100ng/ml Ang2 showed a donor contribution level above 45%. By contrast, supplementation of Ang1 to the culture did not significantly improve the levels of repopulation neither at a low or high dose, even if in the latter case 2 out of 6 mice were repopulated at a higher level than control (58% and 71%). However, adding both Ang1 and Ang2 together in low amounts (each at a concentration of 10ng/ml) resulted in a significant improvement of donor blood chimerism.

All together, these results indicated that Ang2 alone is sufficient to support HSC maturation from the E9.5 AGM region. While Ang1 seems to be dispensable in this process, low doses of this protein in combination with Ang2 might act synergistically to improve Ang2-mediated HSC formation. Moreover, as Ang2 had no effect on the number of haematopoietic colonies (Figure 3.3), this suggested that its specific role resides in HSC maturation of HSC precursors from the E9.5 aortic microenvironment, rather then in formation of committed haematopoietic progenitors.

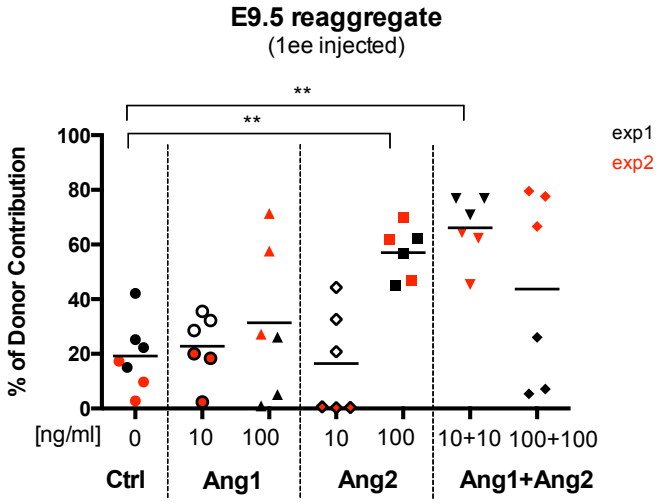

Figure 3.5 | Effect of angiopoietins on HSC formation from E9.5 caudal part.

Percentage of donor contribution in the peripheral blood of recipient mice 16 weeks post-transplantation for E9.5 CP re-aggregated with media supplemented with serum, 3GFs (SCF, IL3, Flt3-l) in presence of the named recombinant protein (Ang1, Ang2, Ang1+Ang2) or in absence of additional protein (Ctrl). 1ee was transplanted into each recipient along with 80,000 BM carrier cells. Donor contribution is measured as percentage of CD45.2/2^{+} cells. Each dot corresponds to a recipient mouse. N = 2 independent experiments with a total of 6 mice per condition. Horizontal bars represent the mean. Different groups of repopulated mice were compared using the Mann-Whitney U statistical test (** $p \leq 0.01$; 100ng/ml Ang2 vs Ctrl: $p = 0.0012$; 10+10ng/ml Ang1+Ang2 vs Ctrl: $p = 0.0012$).

3.2.6 Use of transgenic OP9 as a tool to test HSC formation upon over-expression of Ang2 in culture

To reinforce the notion that Ang2 is a regulator of HSC maturation from the E9.5 AGM, an alternative assay was established in order to deliver Ang2 to the AGM cells in culture. A transgenic OP9 cell line expressing Ang2 upon induction with doxycycline (Ang2-OP9) was generated by Dr Natalia Rybtsova by transfecting OP9 cells with a Piggybac bicistronic vector (gift from H.Niwa) containing the cDNA of Ang2 (Figure 3.6A). Expression of Ang2 was reported by the activation of Venus fluorescent protein, inserted downstream of IRES (Figure 3.6A).

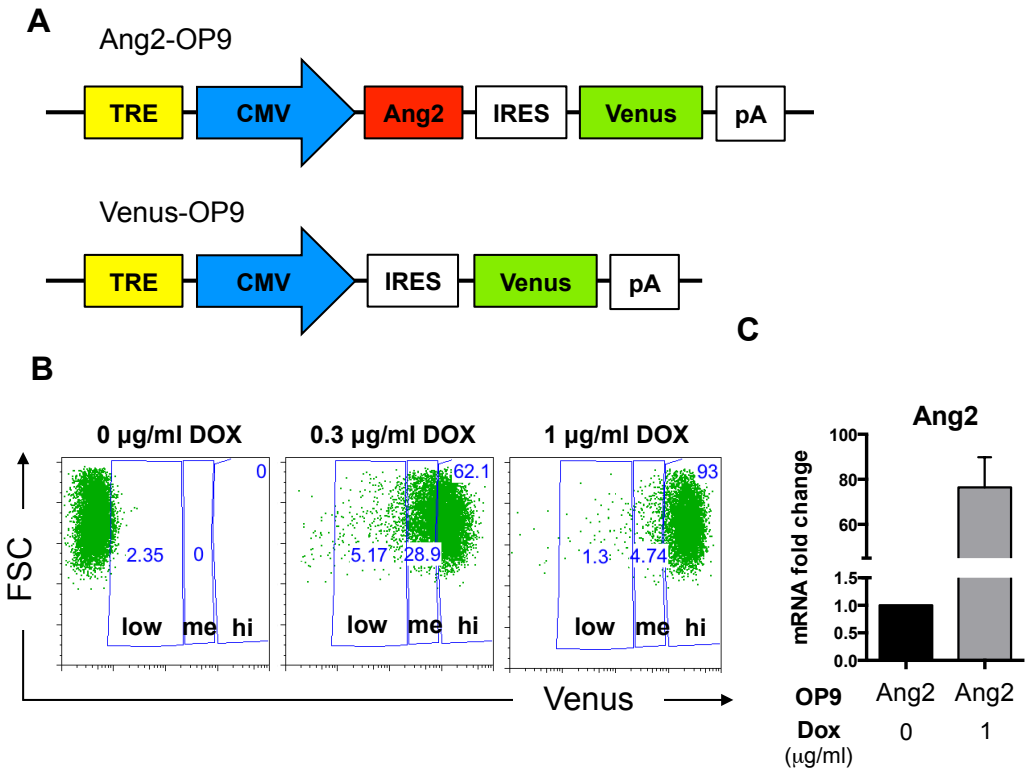

Figure 3.6 | Characterization of the Ang2-OP9 transgenic line.

(A) Schematic representation of the vectors used by Dr Natalia Rybtsova to transfect OP9 cells. Both lines contain a tetracycline-responsive element (TRE) that allows binding of the transactivator (not shown). In presence of Dox (Doxycycline), the cytomegalovirus (CMV) promoter is activated and the downstream sequences are transcribed. In Ang2-OP9, Ang2 is located downstream of the promoter and it is followed by an internal ribosomal entry site (IRES) to allow expression of the Venus reporter. In Venus-OP9, the gene of interest is absent and activation of the promoter results in expression of the Venus protein only. pA = poly A tail. **(B)** Representative flow cytometry plots showing activation of Venus by different doses of Dox 48h after induction. FSC = forward scatter; low = low expression; me = medium expression; hi = high expression of Venus. N = 2 biological replicates. **(C)** qRT-PCR of Ang2-OP9 cultured in presence/absence of Dox for 48h. Expression level of Ang2 mRNA is relative to the housekeeping gene TATA-binding protein (Tbp) in each condition and compares the expression of Ang2 in presence of Dox vs absence of Dox (fold change = 1). N = 2 biological replicates.

Upon stimulation of Ang2-OP9 with increasing doses of doxycycline (Dox), 57 ± 4.9 % of cells expressed Venus at high level (Venus^{high}) in presence of 0.3µg/ml of Dox, whilst 87 ± 5.8 % of cells were Venus^{high} when induced with 1µg/ml of Dox (Figure 3.6B). Doxycycline administration also up-regulated the levels of Ang2

mRNA by 80-fold (Figure 3.6C), proving the efficacy of the OP9 transgenic system as a tool for Ang2 over-expression. As a control for our co-culture experiments, a Venus-OP9 line was generated, which contained Venus without the gene of interest (Figure 3.6A).

E9.5 CP was co-aggregated with Ang2-OP9 (or control OP9) at the gas-liquid interface (Figure 3.7A) and Dox was added to the medium at different concentrations to deliver increasing quantities of Ang2 to the AGM co-culture. As shown in Figure 3.7B, in absence of Dox only 2 out of 6 mice exhibited donor-derived long-term haematopoietic chimerism. By contrast, treatment with 0.3μg/ml Dox repopulated 6 out of 6 mice and significantly increased the level of donor contribution in the peripheral blood of the recipients. Remarkably, when media was supplemented with a dose of 1μg/ml Dox, the average repopulation level increased from 7% (absence of Dox) and 23% (0.3μg/ml of Dox) to 32%, with 3 out of 6 mice repopulated at high level (> 40%), suggesting that Ang2 regulates HSC maturation from the AGM region in a dose-dependent manner.

In the absence of Dox, the number of CFU-Cs was similar to that in the presence of Dox (Figure 3.7C), indicating once again that Ang2 has a specific role in HSC maturation rather than in haematopoietic progenitor formation.

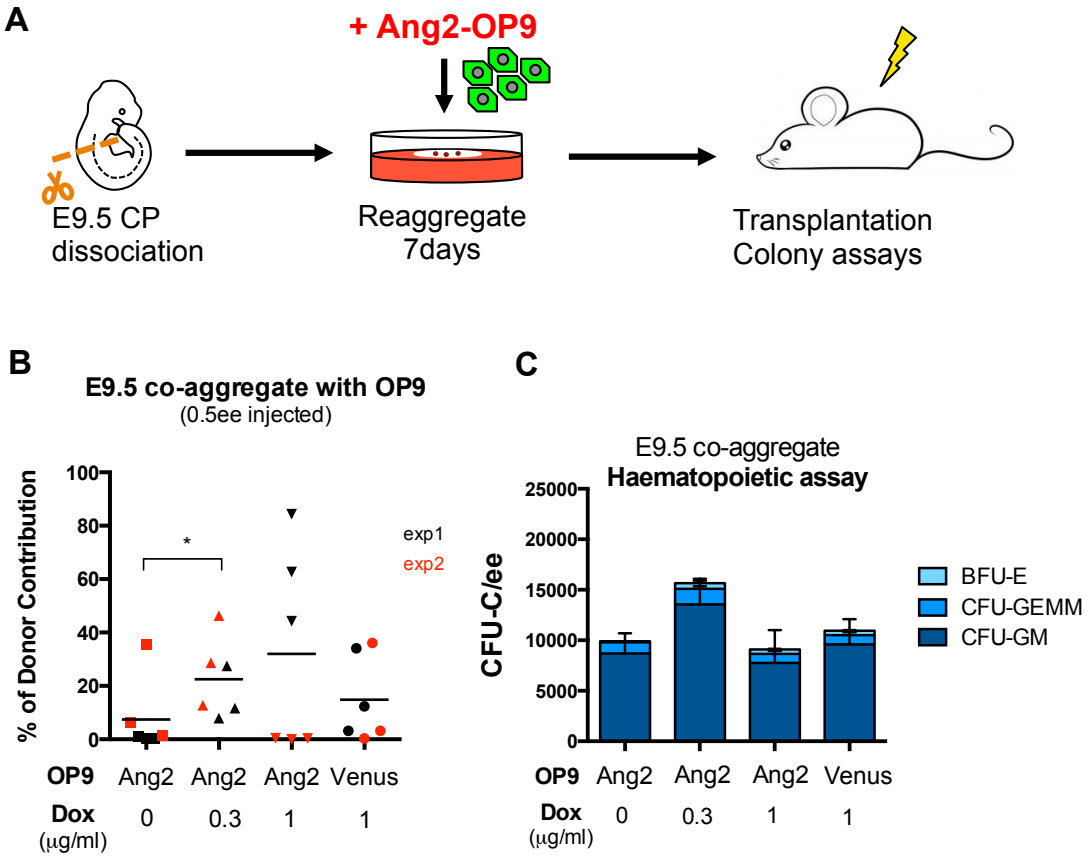

Figure 3.7 | Effect of Ang2 over-expression on E9.5 caudal part mediated by Ang2-OP9. **(A)** Schematics of the co-culture system used to test the effect of Ang2 over-expression on HSC formation. E9.5 caudal part was dissociated to single cell and co-aggregated with 100,000 Ang2-OP9 or Venus-OP9. Media was supplemented with serum, 3GF and increasing doses of Doxycycline (Dox). **(B)** Percentage of donor contribution in the peripheral blood of recipient mice 16weeks post-transplantation (measured as percentage of CD45.2/2^{+} cells). 0.5ee was transplanted into each recipient along with 80,000 BM carrier cells. N = 2 independent experiments. Horizontal bars represent the mean. The different group of repopulated mice were compared using the Mann-Whitney U statistical test (* P = 0.0411). **(C)** Number of haematopoietic colonies (CFU-Cs) formed per embryo equivalent (ee) from cells co-cultured with Ang2-OP9 or Venus-OP9 at different concentrations of Dox. N = 2 independent experiments, 1 technical replicate each. Error bars represent the SEM.

3.2.7 Multilineage reconstitution shows unbiased peripheral blood and bone marrow repopulation of HSCs matured in presence of angiopoietins

To verify the ability of the HSCs generated *ex vivo* in presence of angiopoietins to differentiate towards all blood lineages, the contribution of donor cells to the lymphoid and myeloid compartments of reconstituted mice was assessed. Sixteen weeks after transplantation, peripheral blood, bone marrow, as well as spleen and thymus (data not shown) were analysed by flow cytometry to determine the percentage of putative T cells ($CD3^+$), B cells ($CD19^+$), granulocytes ($CD11b^+$ $Gr1^+$) and monocytes ($CD11b^+$ $Gr1^-$) (Figure 3.8A). Variations in the proportions of each lineage could be observed (Figure 3.8B and C), but no obvious trends were detected, suggesting that HSCs produced in presence of angiopoietins were able to differentiate towards all blood lineages in an unbiased way. Of note, the percentage of T cells in the bone marrow of recipients repopulated with cells co-aggregated with OP9 was remarkably higher compared to the percentage of T cells in recipients that received cells treated with recombinant proteins (Figure 3.8C).

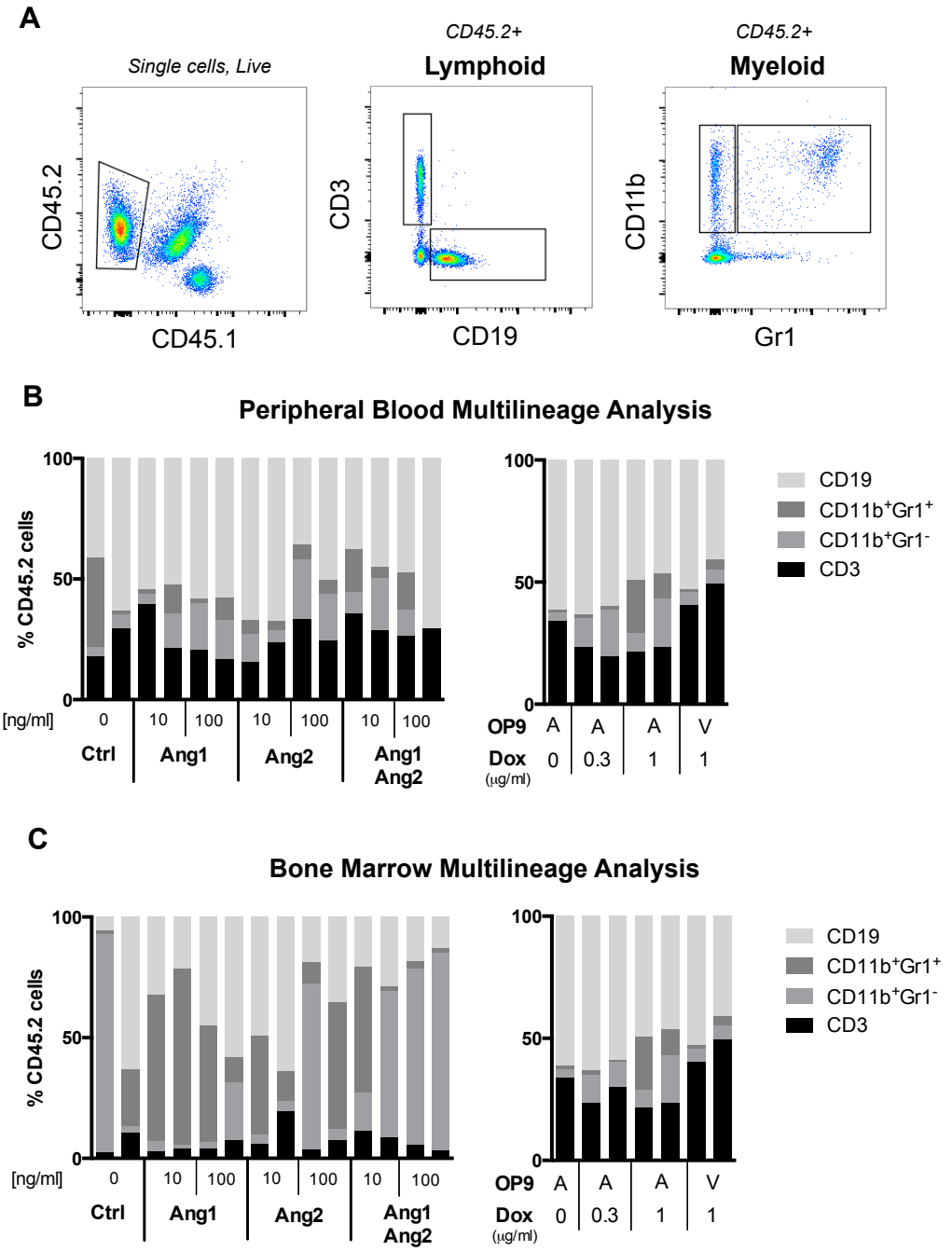

Figure 3.8 | Effect of angiopoietins on multilineage donor contribution.

(A) Representative flow cytometry plots showing the gating strategy used to isolate donor cells ($CD45.2^+$ $CD45.1^-$) and assess their contribution to the lymphoid (T cells: $CD3^+$; B cells: $CD19^+$) and myeloid (granulocytes: $CD11b^+$ $Gr1^+$; monocytes: $CD11b^+$ $Gr1^-$) compartments. **(B)** Percentage of lineage-specific live donor cells ($CD45.2^+$) in the peripheral blood of recipient mice. Assessed 16 weeks post-transplantation of cells cultured with recombinant proteins (left graph) or co-aggregated with OP9 (right graph). **(C)** Percentage of lineage-specific live donor cells ($CD45.2^+$) in the bone marrow of recipient mice. Assessed 16 weeks post-transplantation of

cells cultured with recombinant proteins (left graph) or co-aggregated with OP9 (right graph). 2 representative mice with donor contribution > 5% are shown per condition. A = Ang2-OP9 ; V = Venus-OP9.

3.2.8 Limiting dilution assays suggest a role for Ang2 in the expansion of the pre-existing pool of HSC precursors in culture

The culture of E9.5 caudal part in presence of Ang2 (in the form of recombinant protein or expressed by Ang2-OP9) enabled the identification of Ang2 as a novel regulator of HSC maturation. However, this assay did not clarify whether the increase in repopulation levels of recipients treated with Ang2 can be attributed to (a) *de novo* maturation of HSC precursors from haematogenic endothelium or (b) an expansion in the numbers of pre-existing HSC precursors/HSCs in culture. Consequently, limiting dilution approaches were applied to discriminate between the two possibilities.

At E9.5, the dorsal aorta is populated by pro-HSCs, the first and most immature type of HSC precursors (Rybtsov et al. 2014). The numbers of pro-HSCs in the E9.5 are very limited and range between 0.4 to 2.7 cells/ee (Rybtsov et al. 2016). To evaluate whether Ang2 mediates *de novo* maturation of pro-HSCs from the haematogenic endothelium, a quantitative assay enabling estimation of the number of HSC precursors present in the E9.5 caudal part was used (Rybtsov et al. 2016). E9.5 caudal parts were sub-dissected and pooled (Figure 3.9A). Next, single cell suspensions were split into portions (0.3ee/co-aggregate), and each portion co-aggregated with wild-type (WT) OP9 and independently cultured in presence or absence of Ang2 protein. After 7 days, each co-aggregate was individually transplanted into an irradiated recipient. In this way, each HSC precursor remains contained within a single co-aggregate, matures into HSCs and is transplanted to one recipient, repopulating its peripheral blood (Figure 3.9A). Given that in average the E9.5 CP contains ~1.5 pro-HSCs, it would be expected to see 1-2 recipients repopulated when approximately 1/3 of a CP (0.3ee) is separately transplanted onto 4-5 mice. However, in the hypothesis that Ang2 favours maturation of new haematogenic endothelial cells into HSC precursors, more co-aggregates would be

expected to contain a newborn pro-HSC and therefore more recipient mice would be repopulated after culture with Ang2.

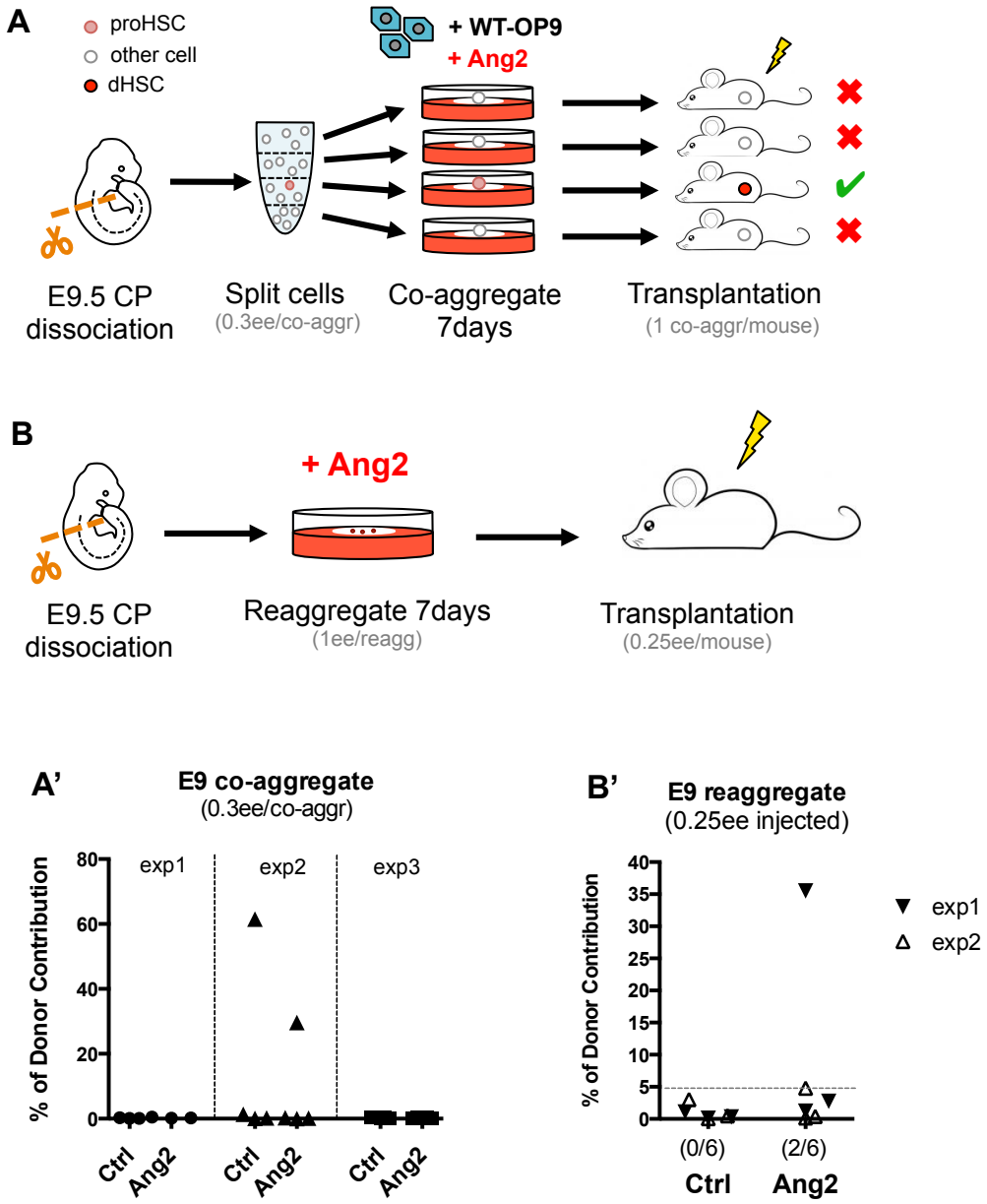

Figure 3.9 | Effect of Ang2 on *de novo* formation vs expansion of pro-HSCs.

(A) Schematic of the limiting dilution culture assay used to determine if Ang2 promotes *de novo* formation of pro-HSCs. Cell suspension of E9.5 caudal parts containing a mix of pro-HSC and other cells were co-aggregated with OP9 at a concentration of 0.3ee/co-aggregate and cultured in presence of serum, 3GF and Ang2. After 7 days, each co-aggregate was injected into a recipient,

but only mice transplanted with a co-aggregate that contained a pro-HSC were expected to be repopulated (green checkmark). **(A')** Percentage of donor contribution assessed 16 weeks after transplantation of cells from (A) in the peripheral blood of recipients (% of CD45.2/2^{+} cells). N =3 independent experiments with a total of 12 mice per condition. **(B)** Schematic of the limiting dilution culture assay used to determine if Ang2 promotes expansion of pre-existing HSC precursors. E9.5 CP is dissociated and re-aggregated in presence of Ang2 for 7 days in presence of serum and 3GF. Only 0.25ee of the original re-aggregate are transplanted into each recipient (along with 80,000 BM cells). **(B')** Long-term repopulation assay (16 weeks) with percentages of donor contribution (CD45.2/2^{+}) in the peripheral blood of recipients. N = 2 independent experiments.

Results in Figure 3.9A' show that in two out of three experiments, none of the mice was repopulated. However, in exp2 1 mouse out of 10 recipients was repopulated from control cells and another one from Ang2-treated cells, suggesting that an equal number of pro-HSCs existed in the culture with Ang2 when compared to the control.

To determine whether Ang2 promotes an expansion in the number of pre-existing HSC precursors/HSCs, a limiting dilution assay was set so that none or little repopulation would be observed in the control. In the hypothesis that Ang2 quantitatively expands the HSC reservoir, some of the mice transplanted with Ang2-treated cells would be repopulated. To achieve this, E9.5 re-aggregates cultured with recombinant Ang2 were injected in irradiated recipients at a dose of 0.25ee/mouse (Figure 3.9B). This dose corresponds to one-quarter of the amount of embryo equivalents required to successfully repopulate recipients transplanted with E9.5 CP cultured for 7 days (Rybtsov et al. 2014)(McGarvey et al. 2017). Sixteen weeks after transplantation, none of the recipients transplanted with control re-aggregates showed donor-derived contribution (Figure 3.9B'). By contrast, 2 out of 6 mice were repopulated by Ang2-treated re-aggregates.

Results from these two experiments suggest that Ang2 might not be involved in production of *de novo* HSC precursors from the AGM region, but rather in expansion of the already existing pool of HSC precursors present in the AGM region.

3.2.9 Ang2 can influence HSC formation from E10 AGM

Despite of the significance of Ang2 in promoting HSC maturation in culture at E9.5, it remains to be elucidated whether Ang2 has the potential to specifically improve expansion of pro-HSCs into HSCs or if Ang2 involvement in the HSC maturation process is also crucial at later stages of the embryonic HSC lineage development. It has been described that at E10 a more mature type of HSC precursors is present in the AGM region, named pre-HSC-I (Rybtsov et al. 2011). To determine the effect of Ang2 on pre-HSC-I, the recombinant protein was supplemented into the media of E10 re-aggregated AGMs (Figure 3.10A) and two different doses of ee were transplanted into irradiated recipients, based on previously published literature (Souilhol, Gonneau, et al. 2016; Souilhol, Lendinez, et al. 2016). Out of the 20 mice that received Ang2-cultured cells, 4 were repopulated (> 5%) (Figure 3.10B). In contrast, cultured control cells did not succeed in producing HSCs, as none of the recipients was successfully transplanted. Since no repopulation was found in the control, this might either indicate that an insufficient dose of ee was transplanted or technical issues might have occurred with the culture system (further examined in section 3.3). Similarly to experiments at E9.5, Ang2 did not seem to influence the number of haematopoietic progenitors at E10, as the number of CFU-C were comparable to control (Figure 3.10C), and slightly reduced the number of endothelial colonies (Figure 3.10D). All together, these results suggest that Ang2 might play a role in HSC but not haematopoietic progenitor maturation from the E10 AGM.

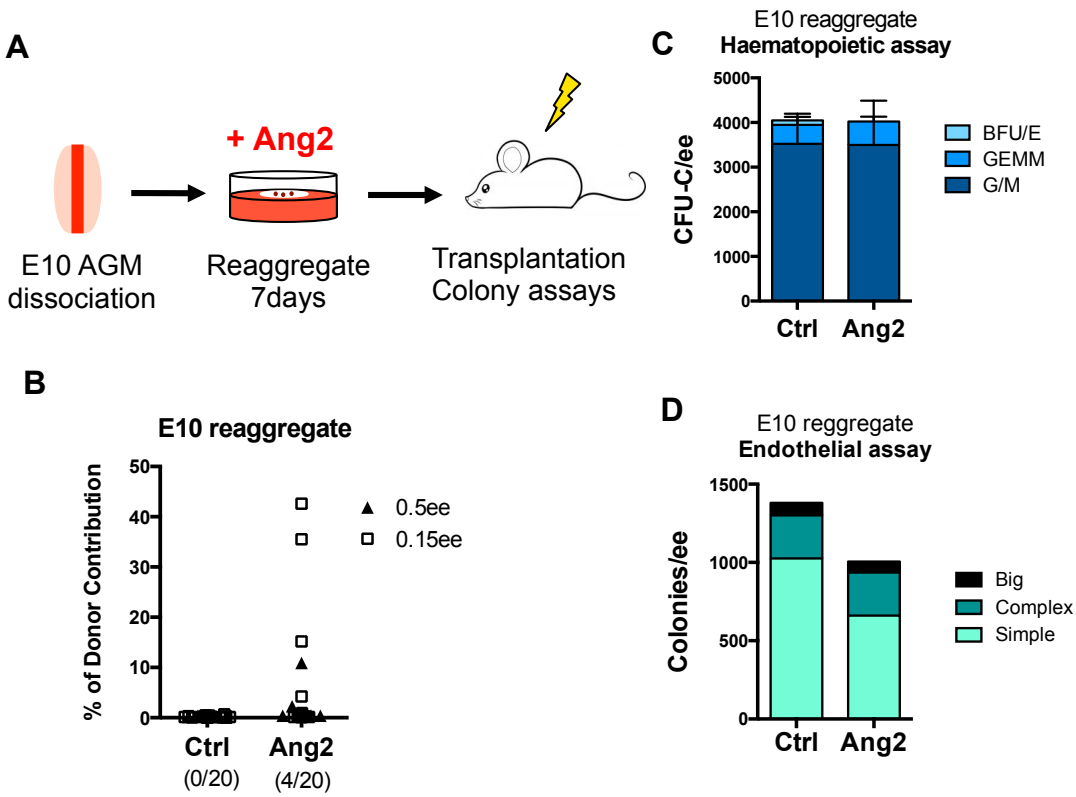

Figure 3.10 | Effect of Ang2 on HSC production from E10 AGM.

(A) Schematic of the re-aggregate culture at E10. E10 AGM was dissociated and re-aggregated in presence of Ang2, serum and 3GF for 7 days. **(B)** Percentage of donor contribution in the peripheral blood of recipients 16 weeks after injection. Each recipient was transplanted with 0.5ee or 0.15ee along with 80,000 BM carrier cells. N = 6 independent experiments (4 experiments with 0.15ee and 2 experiments with 0.5ee). **(C)** Number of haematopoietic colonies (CFU-Cs) formed per ee from E10 cells cultured with Ang2. N = 2 independent experiments, 1 technical replicate each. Error bars represent the SEM. **(D)** Number of endothelial colonies formed per ee from E10 AGM re-aggregates (N = 1).

3.2.10 Ang2 becomes dispensable at later stages of development

The E11 AGM tissue is populated by pre-HSC-II, the most developed type of precursor cell that can be found prior to HSC formation (Taoudi et al. 2008) (Rybtsov et al. 2011). To elucidate the effect of Ang2 on HSC formation at this stage of development, the pre-HSC-II population was sorted from the E11 AGM based on the expression of VE-Cadherin and CD45 (Taoudi et al. 2008) (Figure 3.11B). Subsequently, VE-Cadherin^{+} CD45^{+} cells were co-aggregated with WT-OP9 and cultured in presence of recombinant Ang2 for 5 days to allow maturation of pre-

HSC-II into HSCs (Figure 3.11A). The effect of Ang2 on HSC formation was measured 16 weeks post transplantation by assessing the peripheral blood chimerism of mice. Culture with Ang2 showed a slight increase in HSC production, with 90% of the recipients (9 out of 10) repopulated, compared to only 67% of the control (6 out of 9 mice) (Figure 3.11C). However, no significant difference could be observed in the level of repopulation, with an average of 48% for Ang2-treated cells versus 43% for the control. Once again, Ang2 did not seem to influence formation of haematopoietic colonies (Figure 3.11D). Thus, these results suggest that Ang2 might not be influential in promoting HSC maturation at later stages of development.

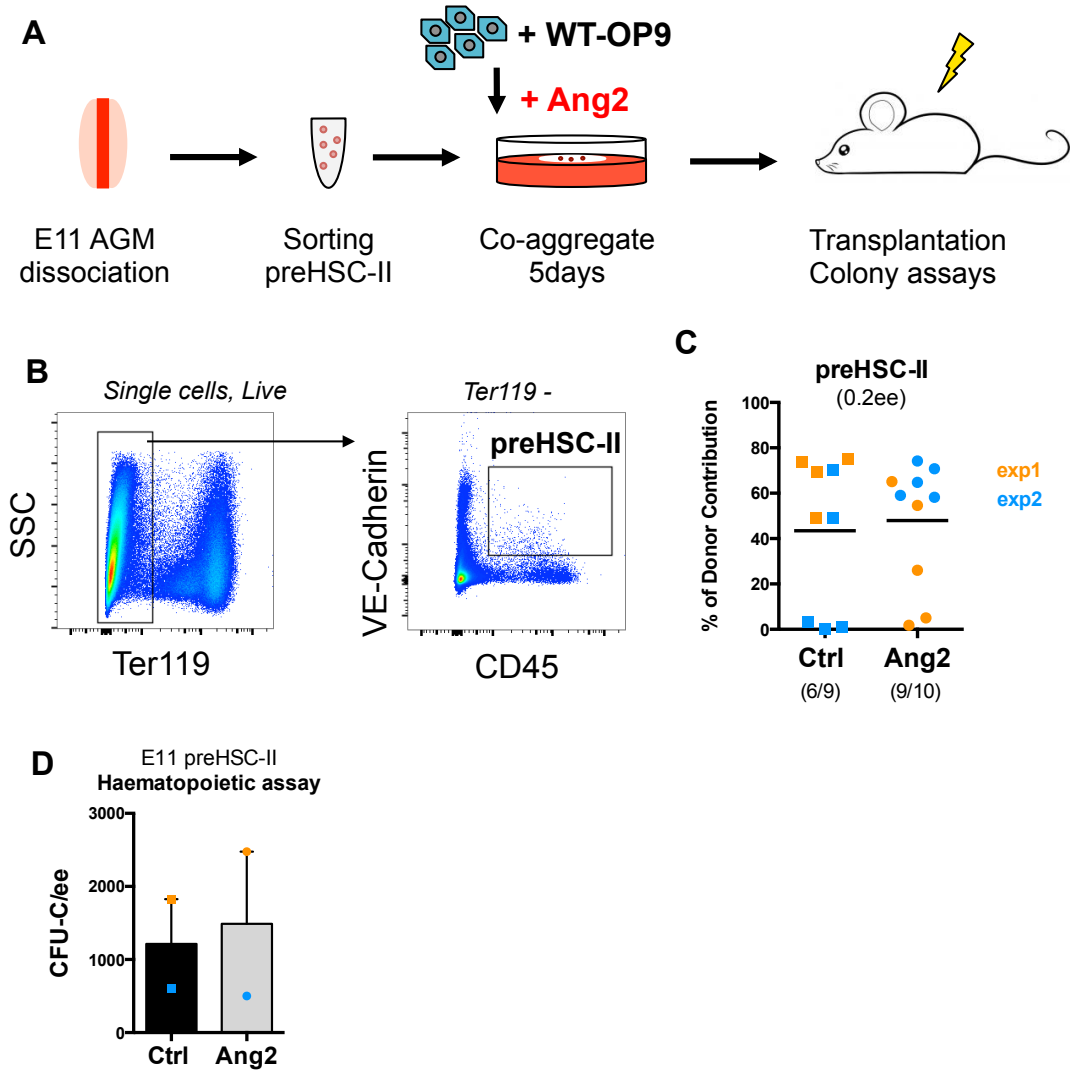

Figure 3.11 | Effect of Ang2 on pre-HSC-II at E11.

(A) Schematic representation of the pre-HSC-II culture. E11 AGM wass dissociated, the pre-HSC-II were sorted and co-aggregated with WT-OP9 for 5 days in media supplemented with serum, 3GF and Ang2. **(B)** Example of the sorting strategy for isolation of the pre-HSC-II population (Live, Ter119^{-}, VE-Cadherin^{+}, CD45^{+}). **(C)** Percentage of donor contribution in the peripheral blood of recipient mice 16 weeks post-transplantation of sorted pre-HSC-II. 0.2ee was transplanted into each recipient along with 80,000 BM carrier cells. Donor contribution is measured as percentage of CD45.2/2^{+} cells. N = 2 independent experiments. Horizontal bars represent the mean. Statistics were calculated by Mann-Whitney U statistical test (**ns** p = 0.8208). **(D)** Number of haematopoietic colonies (CFU-Cs). N = 2 independent experiments, 1 technical replicate each. Error bars represent the SEM and dots represent results from individual experiments (t-Test **ns** p = 0.8350).

3.3 Discussion

This chapter examined the role of angiopoietins in HSC formation. The assay involving the culture of E9.5 caudal part with angiopoietins (Section 3.2.5), as well as the co-aggregate system using a transgenic OP9 stromal line over-expressing Ang2 (Section 3.2.6) enabled the identification of Ang2 as a novel regulator of HSC maturation. This conclusion was reached by observing an increase in repopulation level in the peripheral blood of recipients in the presence of Ang2 compared to control. Further functional testing demonstrated that Ang2 could expand the pool of HSC precursors/HSC. By limiting the dose of cells injected into recipient mice, Ang2-treated cells were indeed able to repopulate 2 out of 6 recipients (Figure 3.9). Unfortunately, it was not possible to determine quantitatively the degree of this expansion using the ELDA software (Extreme Limiting Dilution Analysis;(Hu & Smyth 2009)), as none of the control mice were repopulated. Of note, culture with Ang2 induced a reduction in the number of endothelial progenitors (Figure 3.4B and preliminarily Figure 3.10D), proposing an involvement of Ang2 in the remodelling of the aortic microenvironment to favour HSC emergence.

Since E9.5 CP harbours pro-HSCs capable of maturing in culture over the course of 7 days into fully transplantable HSCs (Rybtsov et al. 2014), and HSC arise in a step-wise manner (Taoudi et al. 2008; Rybtsov et al. 2011; Rybtsov et al. 2014), it was difficult to determine whether Ang2 is exclusively involved in maturation of pro-HSCs or if it is required for the formation of more mature types of HSC precursors. Thus, experiments at later stages of development were carried out to resolve this matter.

Since the AGM at E10 is rich in pre-HSC-I, culture at this developmental stage suggested that Ang2 has a positive effect on pre-HSC-I maturation, as Ang2 successfully induced long-term engraftment in mice (Figure 3.10B). However, control recipients failed to repopulate, thus requiring further experiments to confirm the role of Ang2 on pre-HSC-I maturation. Failure of repopulation in control mice might have originated due to technical issues, such as the use of a different batch of serum for culture, use of out-dated cytokines and alteration of the irradiation dose for recipients. Absence of repopulation in the control could be explained by the transplantation of an insufficient dose of ee. Although the doses were chosen based

on published data (Souilhol, Lendinez, et al. 2016; Souilhol, Gonneau, et al. 2016), our group has observed variations in the efficiency of repopulation in the past, and this has often challenged the reproducibility of transplantation experiments performed with the same dose and conditions.

In contrast to earlier developmental stages, Ang2 seems to become unnecessary at E11 when pre-HSCs-II emerge, as no differences could be observed between conditions (Figure 3.11) when pre-HSCs-II were cultured in presence of Ang2. Thus, the fact that Ang2 specificity in promoting HSC maturation is limited to the early stages of HSC development (E9.5-E10) might indicate a requirement for Ang2 in concomitance with emergence of intra-aortic haematopoietic clusters but not thereafter.

Furthermore, there was a lack of correlation between the CFU-C assay and transplantation results, with the number of haematopoietic progenitors remaining unchanged in presence of Ang2 (Figure 3.3, Figure 3.7, Figure 3.10). This indicates that Ang2 acts exclusively on the developing lineage of HSC precursors, but not on the progenitor lineage. An explanation for this could be the fact that although the CFU-C and HSC lineages emerge concomitantly in the embryo, they represent two different populations that emerge from distinct endothelial populations (M. J. Chen et al. 2011). On a different note, CFU-C assays were designed to include only one technical replicate per condition, thus limiting the statistical power of the experiments. Therefore, further experiments will be performed in order to assess whether Ang2 has an effect on haematopoietic progenitor formation.

In conclusion, this chapter revealed a new role for Ang2 as a regulatory molecule for the maturation of fully transplantable HSCs with multilineage potential. Further investigation regarding characterization of expression of Ang2 in the AGM region and the mechanism of action involved are discussed in Chapter 4 and Chapter 5, respectively.

Chapter 4 Characterization of the expression pattern of Angiopoietin-Tie molecules in the AGM region

4.1 Introduction

The embryonic expression distribution of angiopoietin ligands has been previously described by *in situ* hybridization or reporter activity in the mouse and avian systems (S. Davis et al. 1996; Moyon et al. 2001; Gale et al. 2002). In these studies, both Ang1 and Ang2 were described to be expressed by the perivascular layer surrounding vein or arteries. However, these conclusions were based on analysis of single stained tissues and co-expression of Ang ligands with a perivascular marker was never shown, thus the question remains open about the cell population expressing these ligands. By contrast, angiopoietin receptor Tie2 (Tek) has been described as one of the main receptor expressed by endothelial cells in many studies in both the embryonic and adult scenarios (Thurston & Daly 2012; Dumont et al. 1994). Moreover, Tie2 is also expressed by foetal liver and adult HSCs (Hsu et al. 2000; Yano et al. 2007) and an *in vitro* study suggests it as a marker of the haematogenic endothelium (Lancrin et al. 2009). However, the expression of this receptor by the developing HSC lineage has never been characterized before.

In this chapter I sought to characterize the expression pattern of the molecules of the Ang-Tie signalling pathway in the AGM region at the developmental stages proceeding or overlapping with HSC formation (E9.5-E11.5). As Ang2 was shown earlier in this thesis to play a positive role in HSC formation (Chapter 3), I will describe two different approaches to characterize the expression of Ang2, one using a reporter mouse to characterize the cells expressing Ang2 and the other one using an antibody against Ang2, labelling both cells expressing Ang2 and the secreted form of Ang2. I will investigate the correlation between the presence of intra-aortic haematopoietic clusters and the concentration of Ang2; the difference in protein distribution between Ang2 and Ang1; the expression of Tie2 receptor in the endothelium and HSC lineage of the AGM region. I will demonstrate that Ang2 is

ventrally polarised in the aorta at the protein level, where it is expressed by a sub-population of perivascular and sub-aortic mesenchymal cells; I will show that its concentration increases in proximity of haematopoietic clusters; and finally I will find Tie2 receptor expressed by the developing HSC lineage in the AGM.

4.2 Results

4.2.1 Angiopoietin2 is ventrally polarized within the AGM region at E10.5

The RNA-seq performed by McGarvey et al. 2017 showed an up-regulation of Ang2 in the ventral part of the aorta at E10.5 (section 3.2.1). In order to corroborate these results at the protein level, immunostaining was performed on transverse sections. At E10.5, presence of Ang2 could be predominantly detected in the ventro-lateral side of the aorta, in proximity to the $CD31^{+}$ endothelial layer surrounding the aortic lumen (Figure 4.1). This confirms the RNA-seq results and suggests that both Ang2 expression and protein localization are restricted to the ventral side of the aorta. This prompted further investigation to study the localization of Ang2 in more detail.

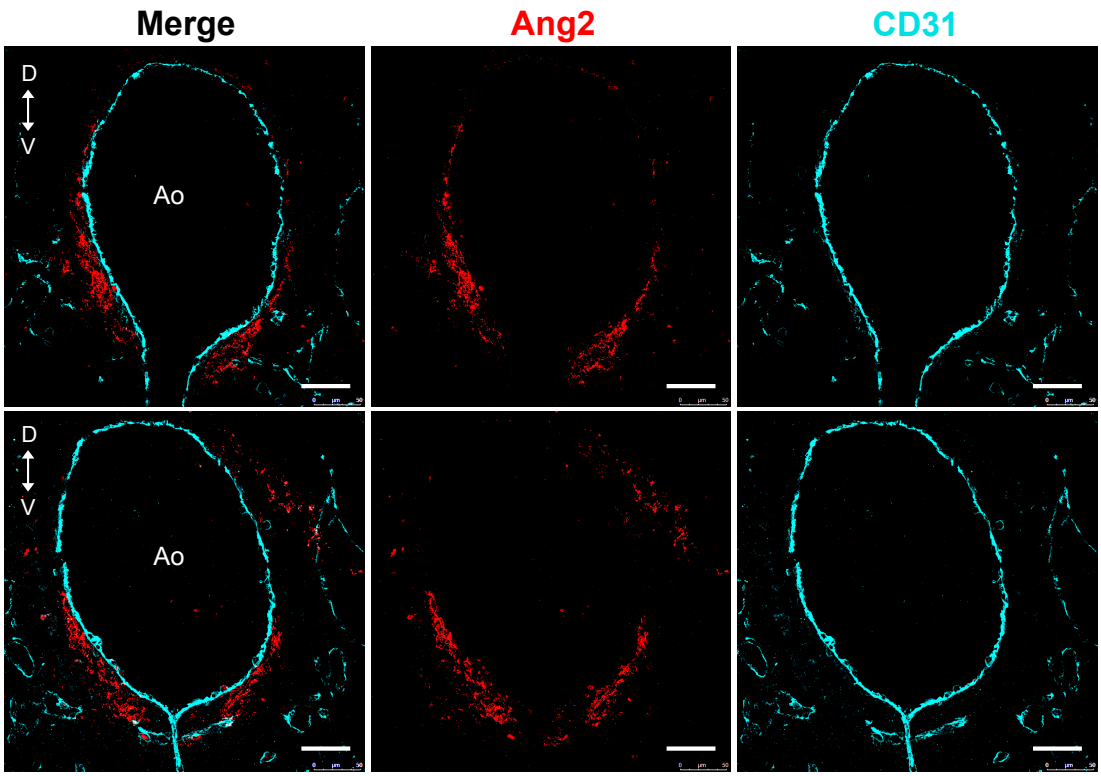

Figure 4.1 | Angiopoietin2 distribution in the E10.5 AGM region.

Expression of Ang2 (red) in the AGM region at E10.5. 7 μm transverse sections were co-stained with CD31 (cyan) to locate the endothelial cells of the dorsal aorta. Scale bar = 50 μm. D = dorsal; V = ventral. Max projections of a Z stack are shown. Ao: aortic lumen. N = 5 different embryos were analysed.

4.2.2 Angiopoietin2 protein is partially contained within the perivascular layer at E10.5

The endothelium represents the first layer of cells that encircles the aortic lumen. The next layer of cells attached to the vessel wall and in close contact with the endothelium is composed of perivascular cells (Armulik et al. 2011). As Ang2 was observed close to the endothelial layer (Figure 4.1), co-staining with perivascular markers was performed in order to understand if Ang2 protein co-localizes with perivascular cells. E10.5 transverse sections were co-stained with NG2, αSMA and CD146. In all the examined cases, Ang2 protein granules could only partially be observed in correspondence of $NG2^{+}$, αSMA^{+} and $CD146^{+}$ perivascular cells (N.B. CD146 also marks endothelial cells) (Figure 4.2). Interestingly, most of the protein seemed to be located within the stroma

neighbouring the perivascular layer, further away from the aortic lumen (Ao), thus prompting further characterization of the cell types expressing Ang2.

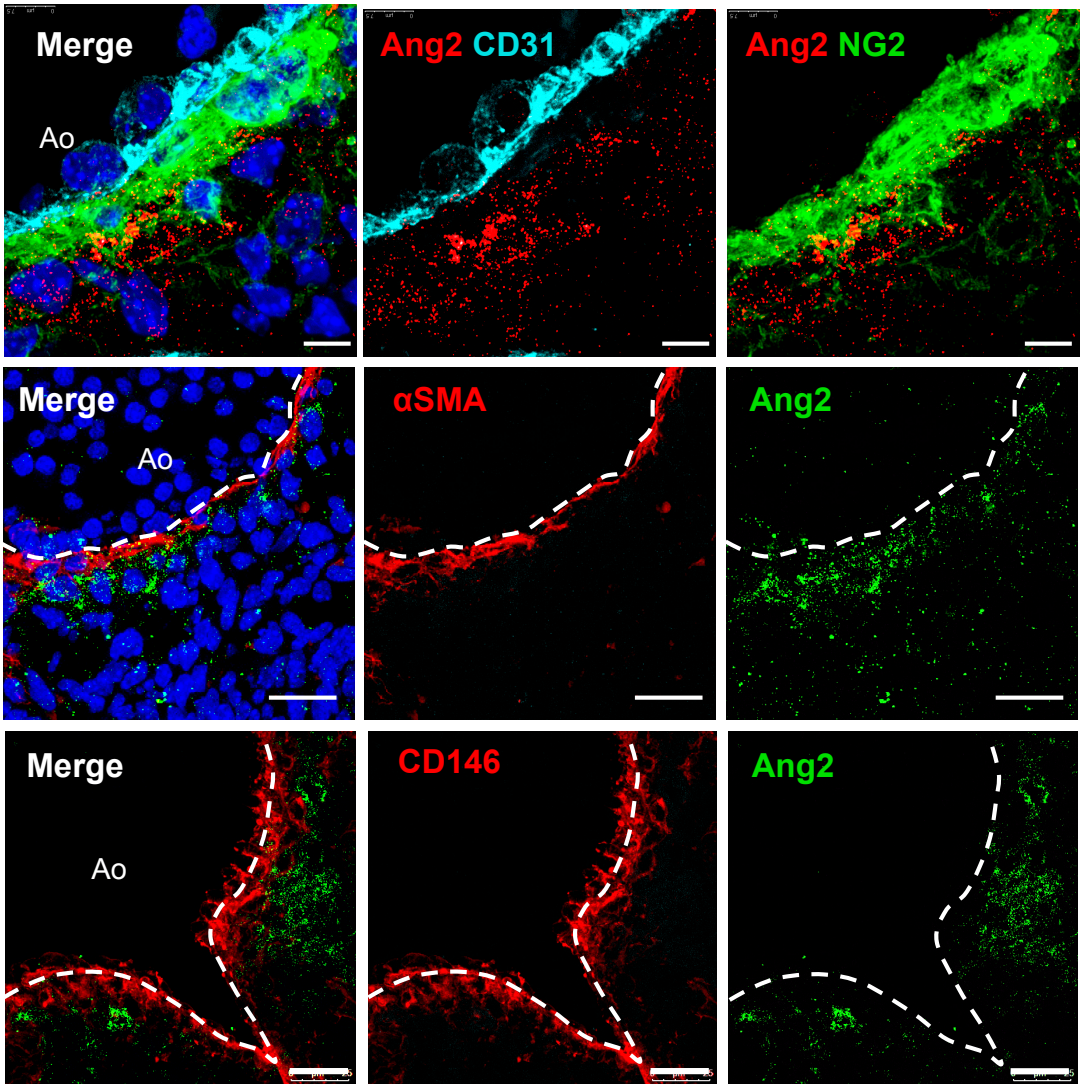

Figure 4.2 | Angiopoietin2 distribution in perivascular cells at E10.5.

Ang2 protein localization in the perivascular layer at E10.5. 7 µm sections were co-stained with three different markers of perivascular cells (NG2, αSMA, CD146). Blue = DAPI. NG2 scale bar = 7.5 µm. αSMA and CD146 scale bar = 25 µm. Dotted line= endothelium. Max projections of a Z stack are shown. Ao: aortic lumen. N = 3 different embryos were analysed.

4.2.3 Ang2-GFP reporter mouse as a tool to characterize Ang2 expression

Angiopoietin2 can be either retained in the cytoplasm of cells or secreted upon stimulation (Thurston & Daly 2012). The use of an anti-Ang2 antibody allowed identification of the protein by immunostaining, however this method doesn't allow to discriminate between (a) cells that express Ang2 and (b) cells that get in contact with secreted Ang2. Therefore, in order to characterize Ang2-expressing cells in the AGM region during the developmental stages preceding HSC formation, a reporter mouse line was used, which reports only the cells expressing Ang2. This line carries a randomly integrated bacterial artificial chromosome (BAC) transgene that contains the Ang2 promoter followed by an enhanced green fluorescent protein (eGFP) inserted upstream of the coding sequence for Ang2 gene (Figure 4.3A). This way, expression of the eGFP reporter is driven by the regulatory sequences of ANG2 gene (without disrupting endogenous Ang2 protein expression). This reporter has been used in several studies that aimed at characterizing Ang2 involvement in vascular remodelling and tumor vasculogenesis (M. Kim et al. 2016; J.-S. Park et al. 2016). In this thesis, this reporter line will be referred to as Ang2-GFP.

Ang2-GFP$^+$ embryos could be genotyped under a fluorescent lamp, as they showed bright GFP expression in the limbs, neural tube and brain (Figure 4.3B). To validate the reporter activity, the GFP$^+$ and GFP$^-$ fractions were sorted from E10.5 embryos and Ang2 expression was validated by qRT-PCR, revealing an enrichment of Ang2 within the GFP$^+$ population (Figure 4.3C).

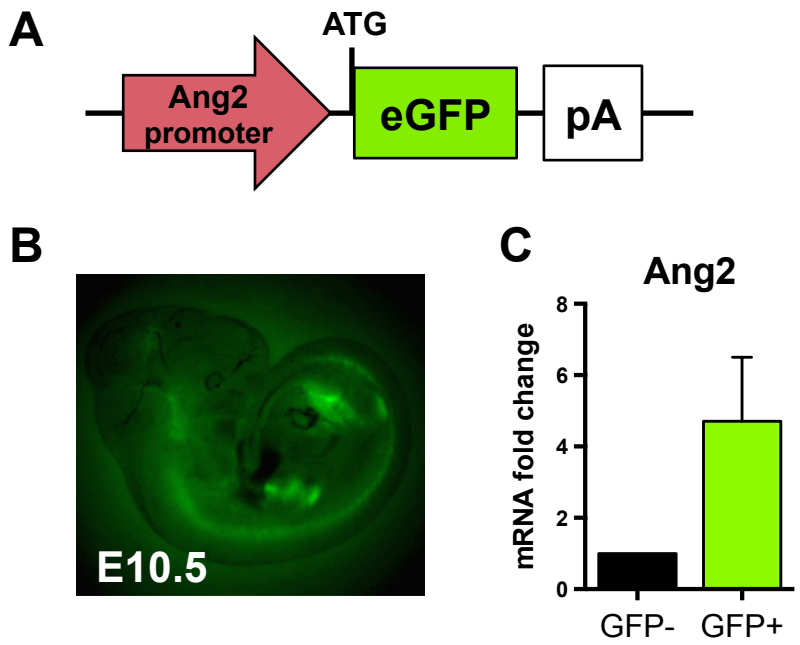

Figure 4.3 | Overview of the Ang2-GFP reporter mouse.

(A) Schematic of the Ang2-GFP transgene. An eGFP-polyA cassette was inserted into the ATG initiation site of the first coding exon of ANG2 gene harbored in a BAC. This was used to produce the transgenic reporter using standard pronuclear injection methods (Gong et al. 2003). **(B)** Representative image of a GFP^+ embryo at E10.5 taken with a stereomicroscope under a fluorescent lamp. **(C)** Ang2 transcript level measured by qRT-PCR as fold change of the GFP^+ population compared to GFP^-. Populations were sorted as live cells based on the expression of GFP from E10.5 embryos. Expression levels are relative to Tbp. N = 2 biological replicates.

4.2.4 Spatial visualization of GFP-expressing cells reveals presence of few ventrally polarized GFP^+ cells around the aortic lumen

In order to spatially locate Ang2-expressing GFP^+ cells, immunofluorescence analysis was performed at E10.5 on Ang2-GFP embryos. Surprisingly, not all the transverse sections analysed contained GFP^+ cells in the AGM region (data not shown). Among those positive for GFP, only a limited number of GFP bright cells could be detected (Figure 4.4A). This suggests there may be limitations with using the reporter to accurately characterize GFP expression, which might affect the detection of $Ang2^{low}$ expressing cells in tissue slices by immunofluorescence (revised in the discussion, section 4.3). Nevertheless, in accordance with the RNA-seq and the anti-Ang2 protein staining, all GFP^+ cells were located in the ventral part of the

aorta. Of note, some of the GFP^+ cells were adjacent to the endothelial layer (Figure 4.4A, white asterisk), while others were found at a greater distance from the aortic lumen (Figure 4.4A, yellow asterisk). This suggests the existence of distinct cell types in the AGM region able to express Ang2; in agreement with the Ang2-antibody staining (Figure 4.2) and based on their position, those might be perivascular (near the endothelium) and stromal cells (further away). Interestingly, granules of Ang2 protein could be observed in concomitance with GFP^- cells, as well as in sections entirely negative for GFP (Figure 4.4B).

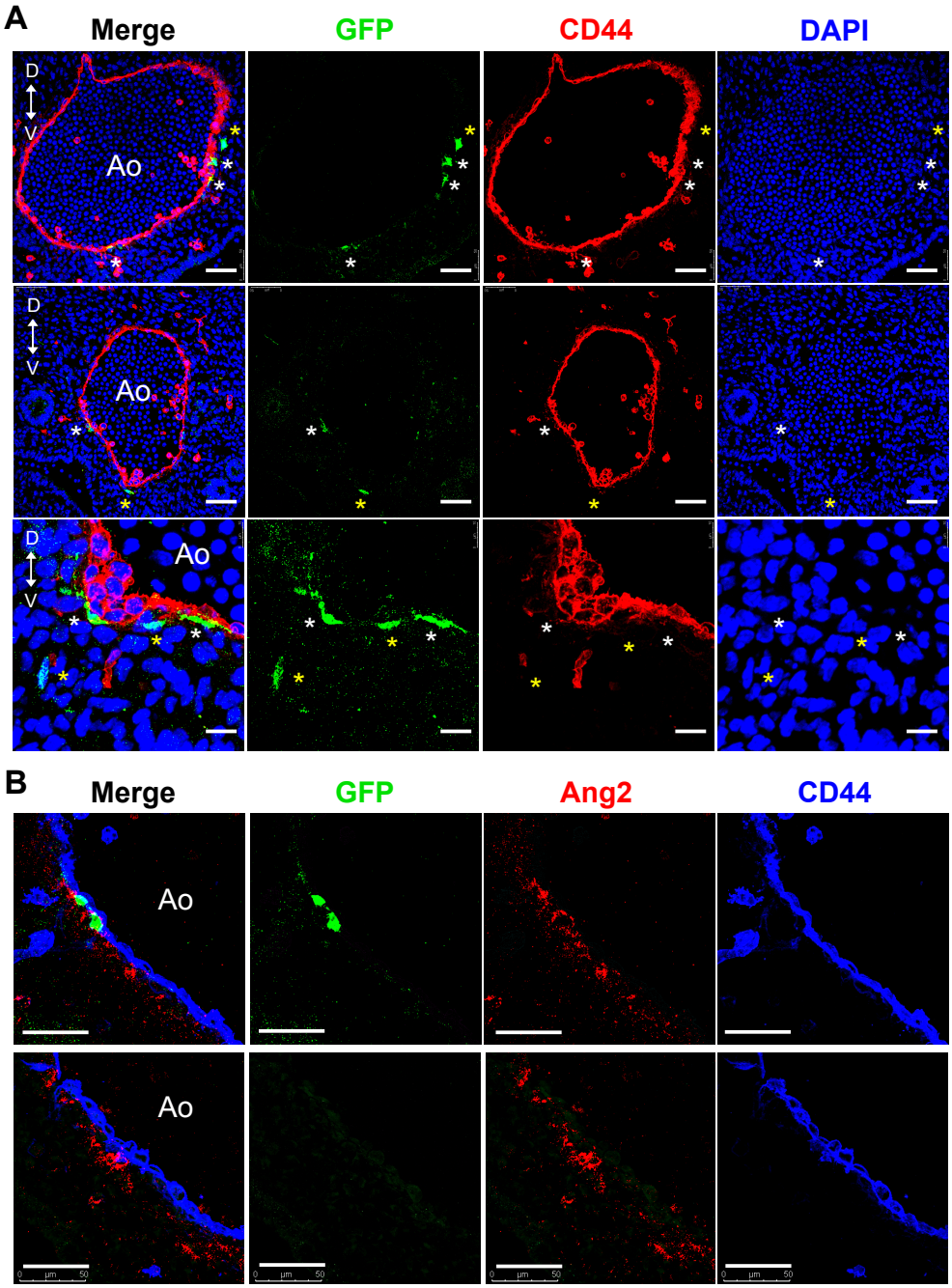

Figure 4.4 | Distribution of GFP in the AGM region at E10.5.

(A) Localization of GFP+ (green) cells in the ventral (V) and dorsal (D) part of the aorta at E10.5. Transverse sections of AGM were co-stained with CD44 (red) to mark the endothelium and DAPI (blue) to mark the nuclei. White asterisk = perivascular-like cells. Yellow asterisk = stromal-like cells. Scale bar (first and second row) = 50 µm. Scale bar (third row) = 10 µm. **(B)** Co-staining GFP (green) with Ang2 (red) and CD44 (blue) reveals presence of Ang2 protein in absence of GFP. Scale bars = 50 µm. Ao = aortic lumen. Max projections are shown. At least 3 independent embryos analysed.

4.2.5 Angiopoietin2 is expressed by perivascular, CD146+ and stromal cells in the AGM region.

To investigate expression of a molecule in a tissue, flow cytometry represents a more practical approach compared to immunostaining, as it allows co-staining of different cell types with multiple antibodies at once. Thus, a spatio-temporal characterization of the cell populations expressing Ang2 in the AGM region was performed between E9.5-E11.5 using the Ang2-GFP reporter and flow cytometry. Little is known about the cell types surrounding the aorta at these developmental stages; therefore, GFP expression was analysed in four broad populations. (a) Endothelial cells were defined by the expression of VE-Cadherin and CD146. CD146 is a marker of both endothelial and perivascular cells (Crisan et al. 2012); however its pattern of expression is wider in the AGM region, where cells located lateral to the aortic lumen and in proximity of the mesonephros are $CD146^{+}$ (Figure 4.5A). Therefore, to distinguish between the different types of CD146-expressing cells, (b) the perivascular population was defined by co-expression of CD146 with NG2 ($VE\text{-}Cadherin^{-}$ $CD146^{+}$ $NG2^{+}$), (c) while the non-endothelial and non-perivascular CD146-expressing cells were classified as $NG2^{-}$ ($VE\text{-}Cadherin^{-}$ $CD146^{+}$ $NG2^{-}$). Finally, (d) the remaining stroma was depicted as the population negative for all the tested markers ($VE\text{-}Cadherin^{-}$ $CD146^{-}$ $NG2^{-}$) (Figure 4.5B). As expression of NG2 in the dorsal aorta starts at E10 (Ozerdem et al. 2001) and cannot be detected at E9.5 (Figure 4.7), expression of Ang2 at this early stage was only characterized in endothelial, $CD146^{+}$ and stromal populations (Figure 4.5C).

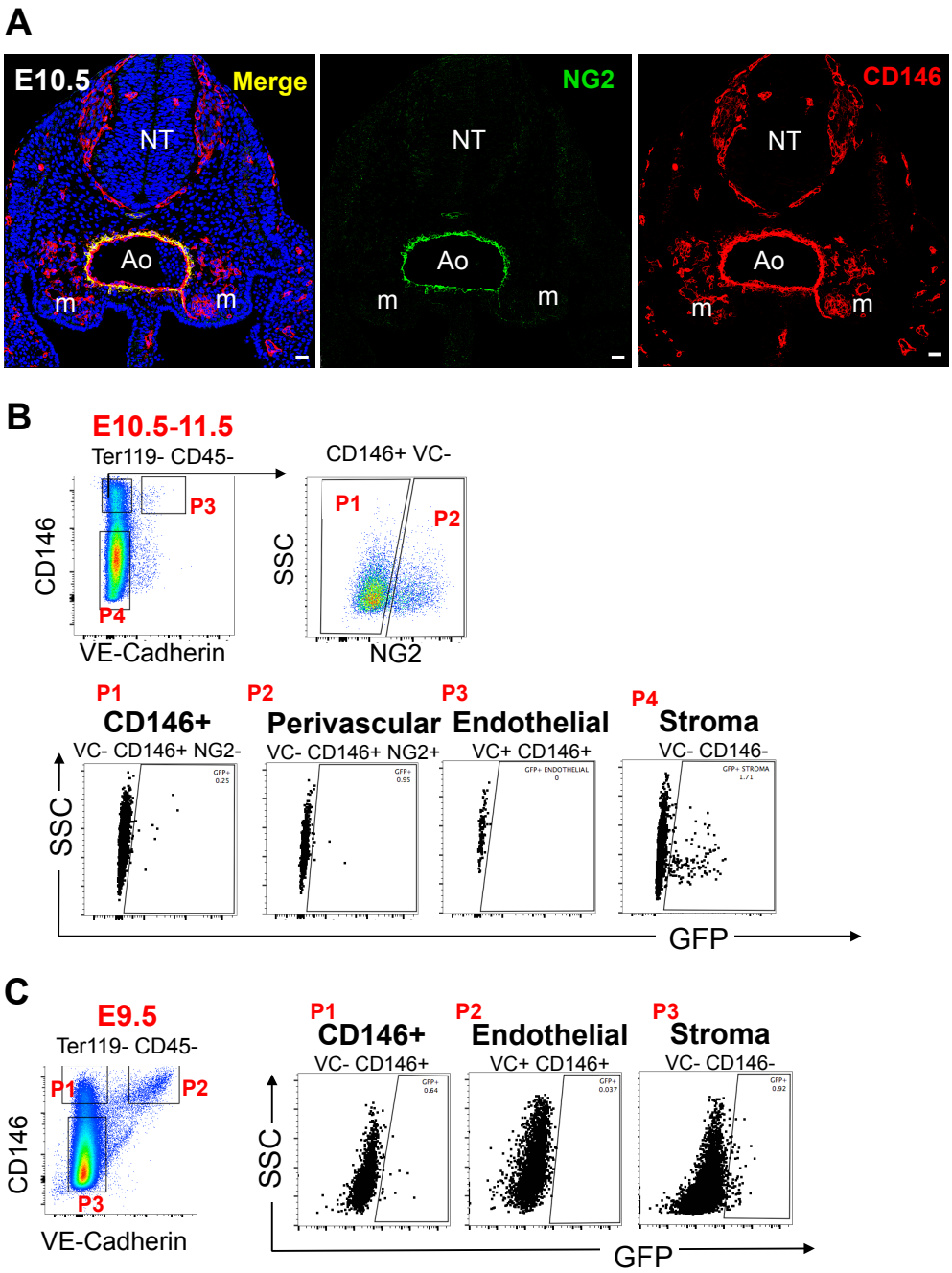

Figure 4.5 | Gating strategy to study Ang2-expressing cells in the AGM region.

(A) Distribution of CD146 and NG2 in the E10.5 AGM region. Both are co-expressed by perivascular cells surrounding the aortic lumen (Ao), however CD146 can be observed laterally to the Ao, in the mesonephros (m) and in proximity of the neural tube (NT). Scale bar = 25 µm. **(B)** Representative plots of the gating strategy utilized at E10.5-E11.5. Single cells Live Ter119$^-$ CD45$^-$ were gated based on the expression of VE-Cadherin (VC), CD146 and NG2. Then, the percentages of GFP$^+$ cells were calculated in each of the following populations: P1 = VC$^-$ CD146$^+$ NG2$^-$; P2 = perivascular (VC$^-$ CD146$^+$ NG2$^+$) ; P3 = endothelial (VC$^+$ CD146$^+$) ; P4 = stroma (VC$^-$ CD146$^-$). **(C)** Representative plots of the gating strategy utilized at E9.5. Single cells

Live Ter119$^-$ CD45$^-$ were gated based on the expression of VE-Cadherin (VC) and CD146. Then, the percentages of GFP$^+$ cells were calculated in each of the following populations: P1 = VC$^-$ CD146$^+$; P2 = endothelial (VC$^+$ CD146$^+$) ; P3 = stroma (VC$^-$ CD146$^-$).

Results in Figure 4.6 show no expression of GFP in endothelial cells at any of the developmental stages studied. At E9.5, 1% of the CD146 population (between 11-12 cells per caudal part) and 1% of the stroma (between 170-938 cells) were the only cell types expressing GFP (Figure 4.6A and B). At E10.5, GFP could be detected in 2% of the perivascular population, represented by 2 to 64 cells per AGM, and in 0.5% of the CD146 population (4-37 cells). However, the vast majority of GFP+ cells were stromal (211-1105 cells, 2%). At E11.5, the percentage of perivascular cells expressing GFP increased up to 5% (31-52 cells), whilst there was a drop in the numbers of stromal cells, with only 139-316 cells expressing GFP (constituting 1% of the total stromal population). Of note, the percentage of GFP$^+$ in CD146 cells remained constant.

In conclusion, although substantial numbers of GFP$^+$ cells were found to be expressed in the perivascular and CD146$^+$ populations, the remaining stromal compartment represented the main source of Ang2 in the AGM region at all developmental stages. Thus, further investigation of this broad cell compartment and its characteristics was carried out separately at each stage of development.

A

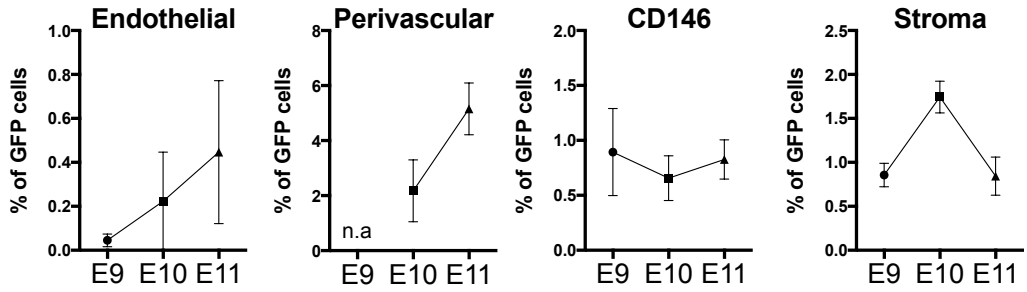

B

(Populations)	**E9** (n. GFP+ events/ee)	**E10** (n. GFP+ events/ee)	**E11** (n. GFP+ events/ee)
Endothelial	0 – 1	0 – 1	0 – 1
Perivascular	n.a.	2 – 64	31 – 52
CD146	11 – 12	4 – 37	13 – 23
Stroma	170 – 938	211 – 1105	139 – 316

Figure 4.6 | Characterization of GFP expression in AGM populations.

(A) Percentages of GFP-expressing cells within the endothelial, perivascular, CD146 and stromal populations in the AGM region at E9.5, E10.5 and E11.5 (abbreviated as E9, E10, E11). Each dot represents the mean. Bars represent the SEM. N = 3 independent experiments for each time point. n.a. = not available. **(B)** Number of GFP+ events per embryo equivalent (ee) in the endothelial, perivascular, CD146 and stroma compartment at E9.5, E10.5 and E11.5 (abbreviated as E9, E10, E11). Numbers displayed are a range showing the lowest-to-highest number of GFP^+ events found in each population. ee were measured as caudal parts at E9.5 and as AGMs at E10.5-E11.5.

4.2.6 Gut and neural tube are sources of stromal Ang2 at E9.5

At E9.5, supplementation of Ang2 protein to cultured caudal part cells supported maturation of HSCs (Chapter 3). To contextualize this behaviour *in vivo*, it was of great interest to localize the endogenous source of Ang2 in more details. As the reporter mouse detected only few GFP^+ cells by immunostaining and only in few sections (Figure 4.4), E9.5 tissue slides were stained with an anti-Ang2 antibody, which allows detection of both Ang2-expressing cells and Ang2 secreted protein.

Interestingly, immunostaining failed to identify Ang2 around the aortic lumen (Figure 4.7A). However, analysis of the tail end of the embryo showed the presence of Ang2 granules along the dorsal neural tube (Figure 4.7Bi) and ventrally in the vicinity of the gut and its epithelium (Figure 4.7B ii and iii). These results suggest that at E9.5 Ang2-expressing cells detected by flow cytometry within the wide-ranging stromal compartment might be confined to the tissues adjacent to the aorta, rather than in the AGM itself.

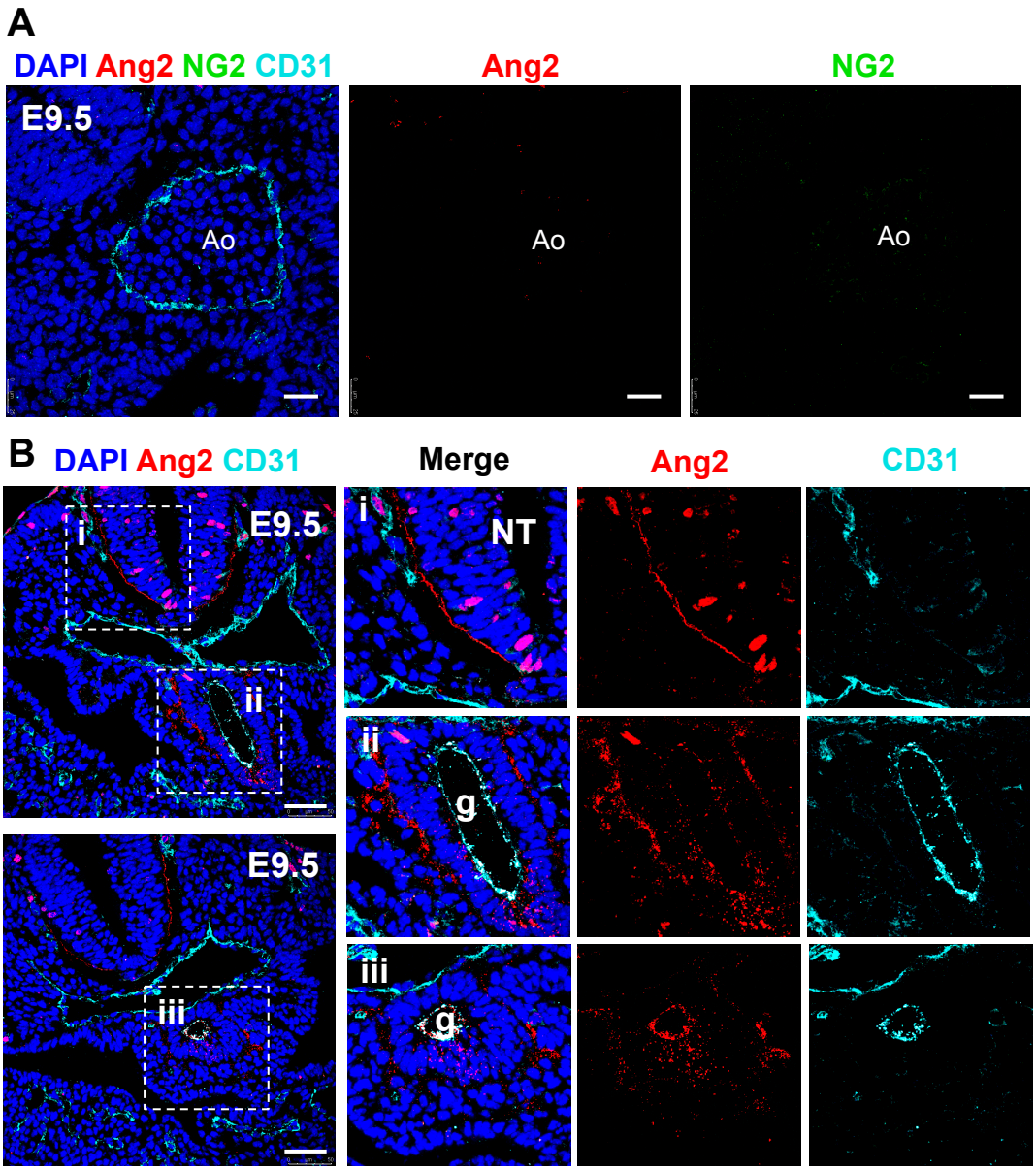

Figure 4.7 | Distribution of Ang2 protein at E9.5.

(A) Representative image shows absence of expression of Ang2 protein (red) and NG2 (green) in proximity of the aorta (Ao) and its endothelial CD31 layer (cyan) at E9.5. Blue = DAPI. Scale bar = 25 µm. **(B)** Distribution of Ang2 in the caudal part of the AGM at E9.5. High magnification shows (i) Ang2 protein along the neural tube (NT), (ii) (iii) Ang2 in the surroundings of the gut (g). Max projections of a Z stack are shown. Merge = DAPI Ang2 CD31. Scale bar = 50 µm. N = 3 embryos.

4.2.7 Angiopoietin2 is distributed in the mesenchyme in the proximity of Runx1 and COUP-TFII-expressing cells at E10.5

The largest number of stromal cells expressing Ang2 was detected at E10.5 compared to E9.5 and E11.5 (Figure 4.6). The AGM microenvironment at this stage of development likely contains a heterogeneous mixture of cells that constitute the mesenchyme surrounding the aortic lumen and to characterize all of them would not be a trivial task. However, as both GFP^+ cells and Ang2 protein could be found in an area of the mesenchyme in close association with the perivascular layer (Figure 4.2 and Figure 4.4), it was of interest to describe the cell types in that area in more detail.

Runx1 is a master regulator of definitive haematopoiesis and it has previously been reported to be expressed at several locations in the embryo, including the sub-aortic mesenchyme (North et al. 1999) (North et al. 2002). It was therefore hypothesized that Runx1-expressing cells located in the mesenchyme might co-express Ang2. Confocal imaging of the E10.5 AGM showed juxtaposition of several layers of $Runx1^+$ nuclei in the AGM region along the aortic lumen (Figure 4.8). Some $Runx1^+$ cells constituted part of intra-aortic haematopoietic clusters or were embedded within the endothelium (Figure 4.8, first panel, arrowheads), while other cells were distributed in the sub-aortic mesenchyme in multiple layers (Figure 4.8, first panel, asterisks). As expected, Ang2 granules were observed in the vicinity of mesenchymal $Runx1^+$ nuclei (Figure 4.8), but not in endothelium or clusters.

The ventral part of the aorta is located in close proximity to the mesonephros and the mesenchymal tissues surrounding the mesonephros. Among the markers characterizing those tissue is COUP-TFII, a transcription factor involved in several developmental processes including arterial-venous specification (You et al. 2005), angiogenesis (Qin et al. 2010), cell fate determination and differentiation of mesenchymal cells (Xie et al. 2011). It was shown to be expressed ventrally between the aorta and the urogenital ridges (UGRs) at E10.5 and in an area defined as the metanephric mesenchyme (Yu et al. 2012), which was shown to contain long-term haematopoietic engraftment activity (Almeida-Porada et al. 2002). In order to understand if the Ang2-enriched sub-aortic mesenchyme is characterized by the expression of COUP-TFII, immunofluorescence analysis was performed. At E10.5, Ang2 protein was found in the surroundings of $COUP\text{-}TFII^+$ nuclei (Figure 4.9A).

Interestingly, COUP-TFII was expressed at lower levels in the sub-aortic mesenchyme compared to the urogenital ridges (UGRs) (Figure 4.9B).

Although co-staining of Runx1 and COUP-TFII will help clarify if these two markers are co-expressed by the same cell type, all together these results suggest the existence of a subpopulation of mesenchymal cells located beneath the ventral side of the aortic lumen in which the presence of Ang2, Runx1 and COUP-TFII can all be detected.

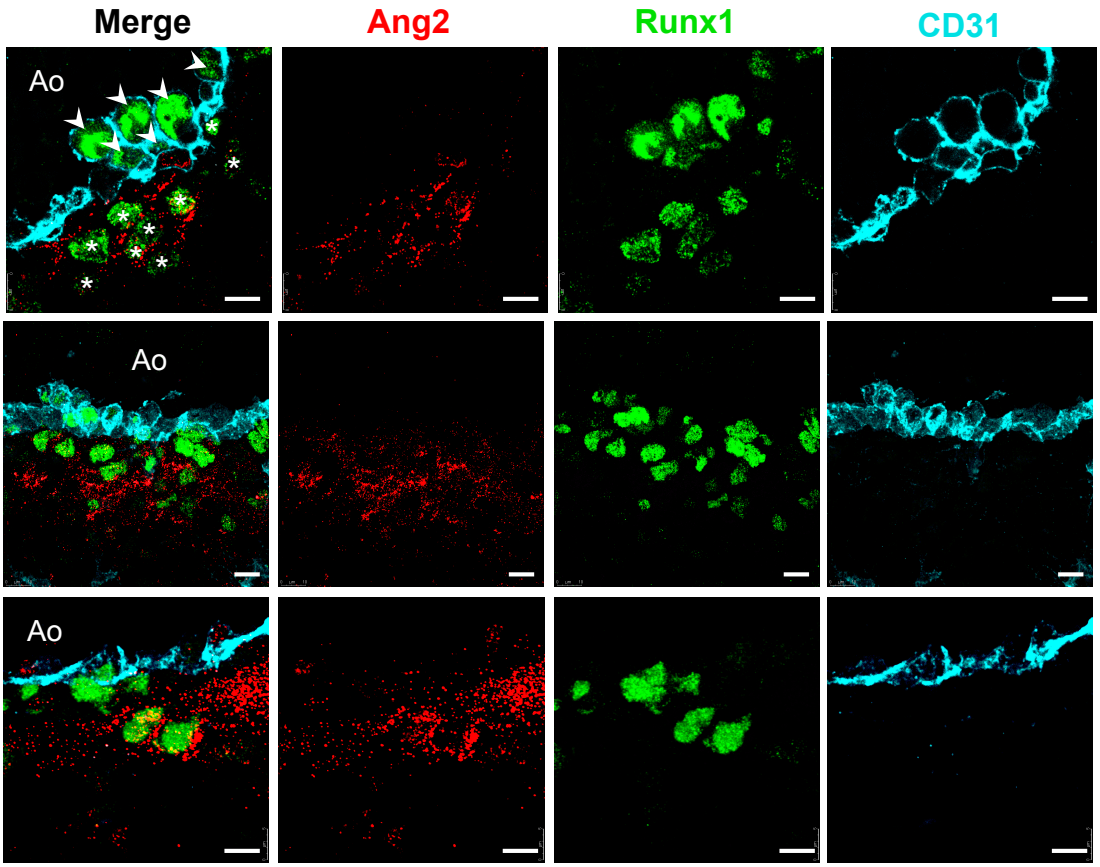

Figure 4.8 | Distribution of Ang2 around Runx1^{+} sub-aortic mesenchymal cells.
Three examples of Ang2 localization in proximity of Runx1^{+} mesenchymal nuclei (asterisks) but not in correspondence of Runx1^{+} endothelial and cluster nuclei (arrowheads) characterized by the expression of CD31. Scale bars: first row = 8 µm ; second row = 10 µm ; third row = 5 µm. Max projection of a Z stack is shown in the second and third row. Ao = aortic lumen. N = 3 embryos.

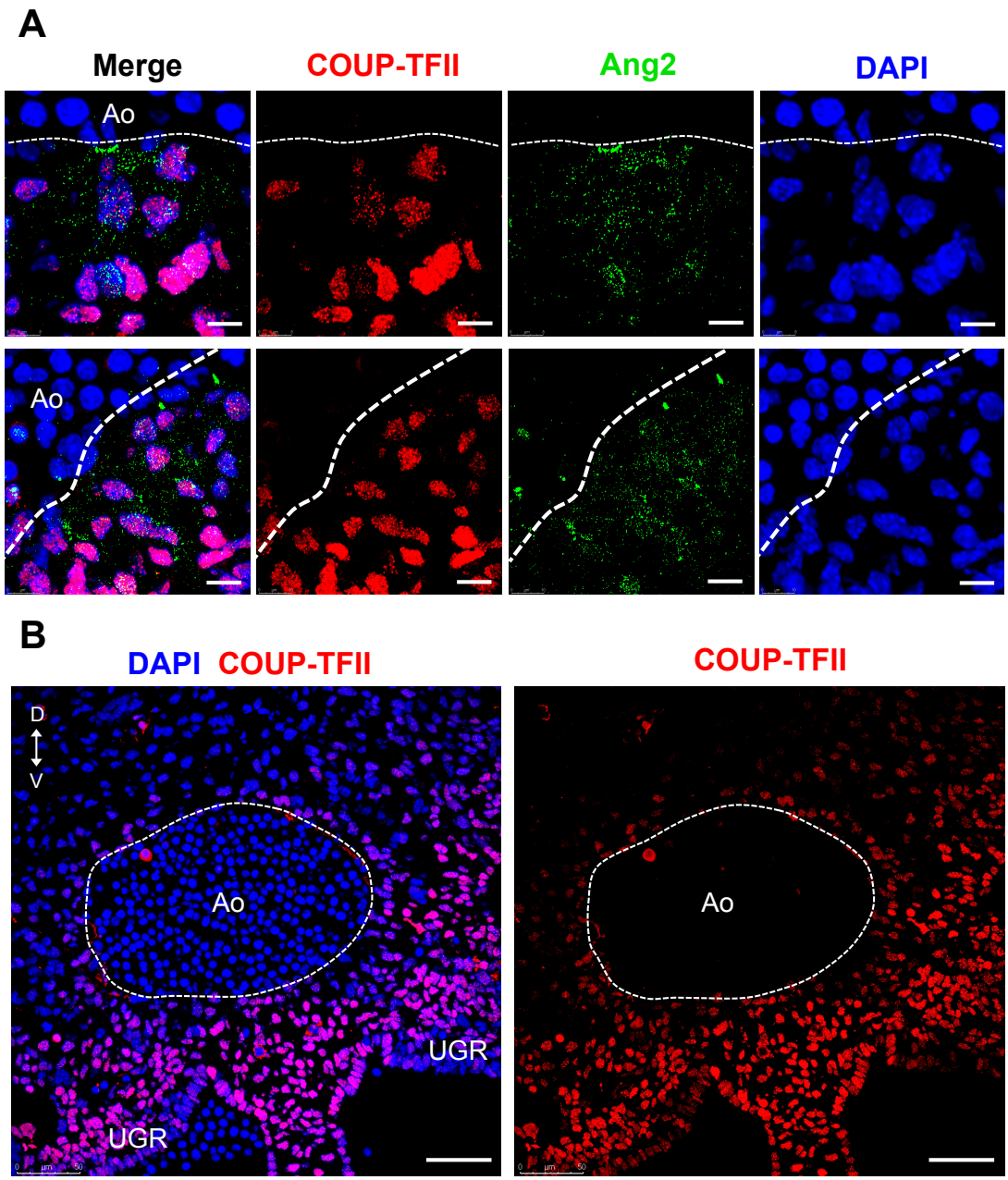

Figure 4.9 | Distribution of Ang2 around COUP-TFII^{low} mesenchymal cells.

(A) Localization of Ang2 in the vicinity of COUP-TFII nuclei in the ventral sub-aortic mesenchyme at E10.5. Scale bar = 8 μm. **(B)** Distribution of COUP-TFII in the aorta at E10.5. COUP-TFII is ventrally polarized and its expression is higher further away from the aortic lumen (Ao). Scale bar = 50 μm. Dotted line = endothelium. D = Dorsal. V = ventral. UGR = urogenital ridges. N = 1 embryo.

4.2.7.1 Expression of Ang2 outside the AGM at E10.5

Despite the inefficiency of the Ang2-GFP reporter in detecting Ang2^{low} expressing cells in sections of the AGM region, at E10.5 GFP bright cells were consistently observed in the neural tube and in dorsal root ganglia extending from the neural tube (Figure 4.10A). In the caudal part of the AGM, bright GFP cells could also be detected in the gut and in the stroma surrounding the gut (Figure 4.10B). Both the neural tube and the gut are usually removed when sub-dissecting the AGM region at E10-E11 and are therefore excluded from expression studies and re-aggregate culture studies. However, it is worth noting that expression of Ang2 in these areas might influence formation of HSCs *in vivo* due to their close proximity to the aorta.

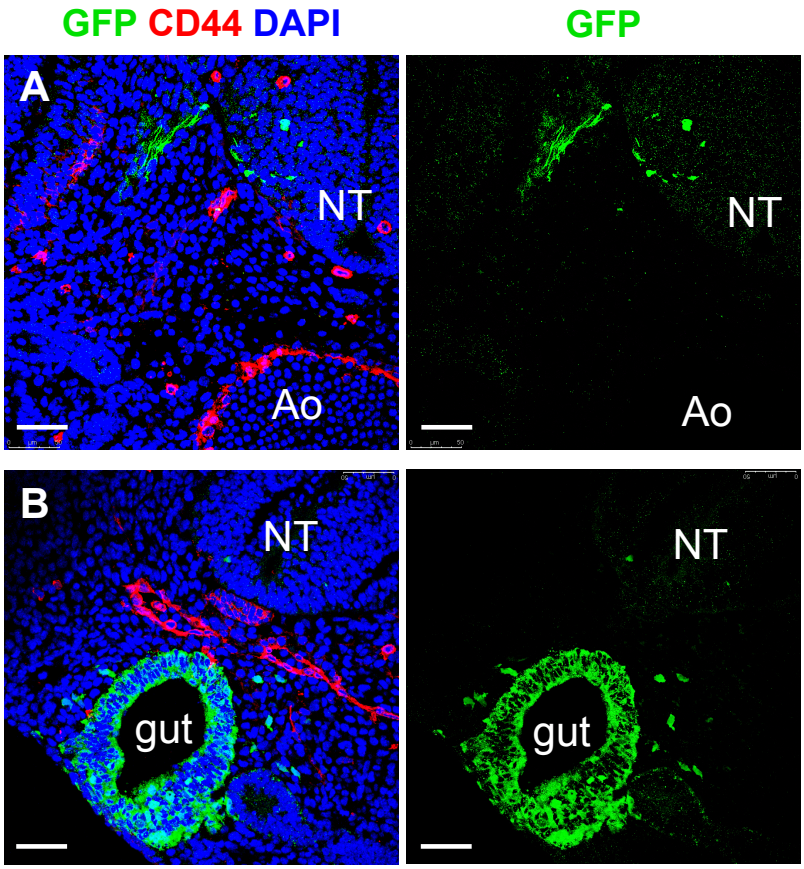

Figure 4.10 | Ang2-GFP expression in tissues neighboring the AGM region at E10.5.
(A) Distribution of GFP expressing cells in the neural tube (NT) and ganglia extending from the NT. Scale bar = 50 μm. **(B)** GFP expression in the caudal part of the AGM in the gut. Few GFP^{+}

cells were also found in the stroma surrounding the gut. Scale bar = 50 μm. Max projections are shown. N = 3 embryos.

4.2.8 The notochord as a source of stromal Ang2 at E11.5

Compared to earlier stages of development, the total number of Ang2-expressing cells appeared to be dramatically reduced at E11.5 (Figure 4.6). In particular, the number of stromal cells was reduced by two thirds compared to E10.5. A spatial investigation of Ang2 distribution pattern in the AGM was conducted by immunofluorescence analysis. Interestingly, Ang2 granules were still ventrally polarized at this stage of development (Figure 4.11). In agreement with the increase in the percentage of GFP-expressing cells in the perivascular compartment detected by flow cytometry, a good proportion of the granules seemed to be located within the perivascular layer (Figure 4.11A). However, Ang2 protein could also be detected in proximity of the notochord (Figure 4.11B, white asterisk), indicating this as a potential source of Ang2-expressing cells in the stromal compartment at E11.5.

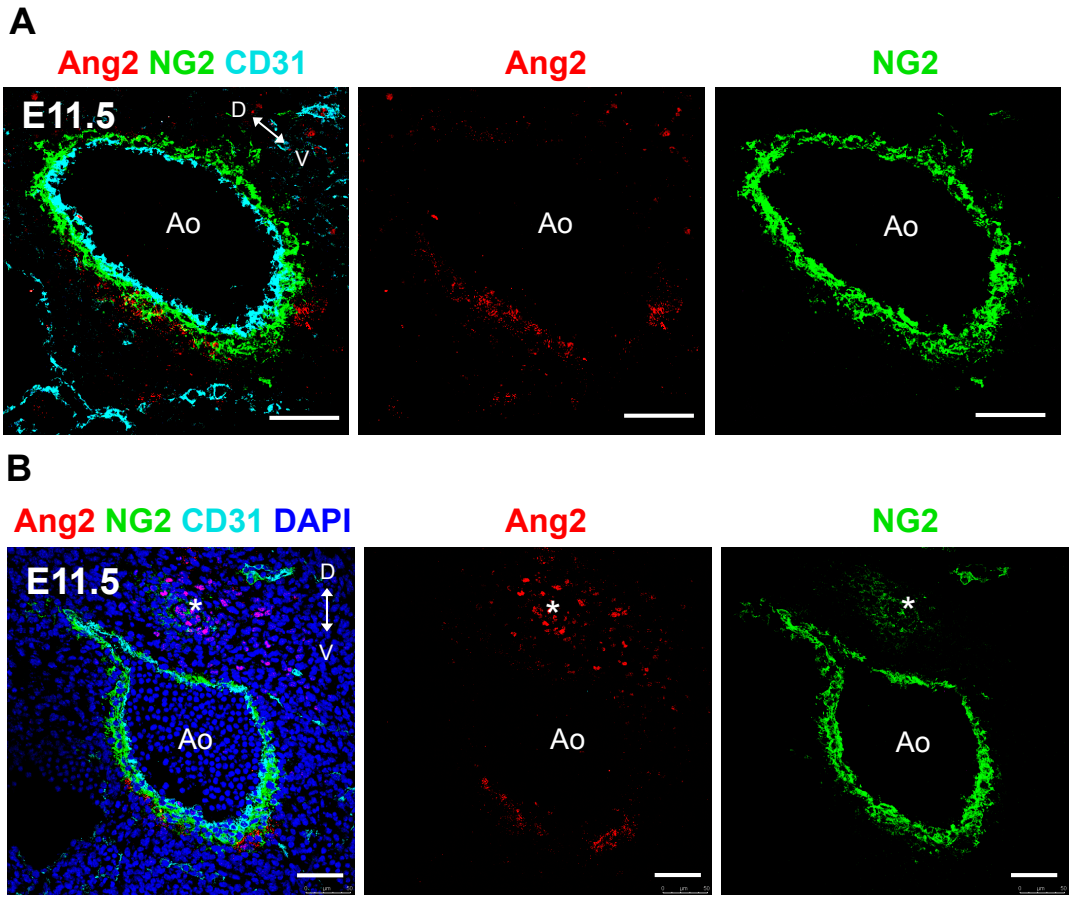

Figure 4.11 | Distribution of angiopoietin2 in the AGM region at E11.5.

(A) Ang2 (red) is ventrally polarized in the AGM region at E11.5. Sections were co-stained with CD31 (cyan) to mark endothelial cells and NG2 (green) to mark perivascular cells. D= dorsal. V = ventral. Scale bar = 50 μm. **(B)** Localization of Ang2 in proximity of the notochord is marked by a white asterisk (*). Scale bar = 50 μm. Ao = aortic lumen. N = 2 embryos.

4.2.9 Angiopoietin2 is correlated with presence of intra-aortic haematopoietic clusters

Ang2 was predominantly detected in the ventral domain of the aorta (Figure 4.1), the site of intra-aortic haematopoietic cluster (IAHC) formation (Jaffredo et al. 1998). As IAHC are believed to host HSC precursors (Rybtsov et al. 2011) and Ang2 was described as a positive regulator of HSC formation (Chapter 3) it was hypothesized that a correlation might exist between Ang2 and presence of clusters. The ventral domain of the aorta contains the highest number of IAHC at E10.5 (Yokomizo & Dzierzak 2010). Therefore, transverse sections of embryos at this time

point were co-stained with Ang2 and CD31, a marker for both endothelial and cluster cells, and Ang2 was found in the vicinity of the clusters (Figure 4.12A). In order to assess if there is a correlation between presence of Ang2 and presence of clusters, an imaging processing strategy (illustrated in Figure 4.12B) followed by statistical analysis was developed in collaboration with Dr Sergey Zuev (also see section 2.9.3 in Materials and methods). The nuclei of cells located in the endothelial lining of the ventral part of the aorta were chosen as centres. The number of cluster cells located within a radius of 12.5 μm from each centre was counted (see Appendix 8.1). Since Ang2 was found to be expressed by perivascular and sub-aortic mesenchymal cells rather than in strict proximity to the clusters, the concentration of Ang2 was quantified as number of positive pixels within a bigger radius of 25 μm from each centre. Dependence between clusters and amount of Ang2 was determined by Spearman rank-order correlation. Out of 21 images analysed, 14 (67% of the total) showed a statistically significant correlation (p-value < 0.05) between the presence of clusters and the concentration of Ang2 in the vicinity of 25 μm from their centre (Table 4). In the remaining 7 images, even if the correlation was not statistically significant, it was positive in 5 out 7 cases (Table 4). These results indicate that in close vicinity to intra-aortic cell clusters, the concentration of Ang2 is increased compared to a point in the aortic lining in which the cluster is absent, thus suggesting that presence of Ang2 in proximity of the clusters might contribute to HSC development.

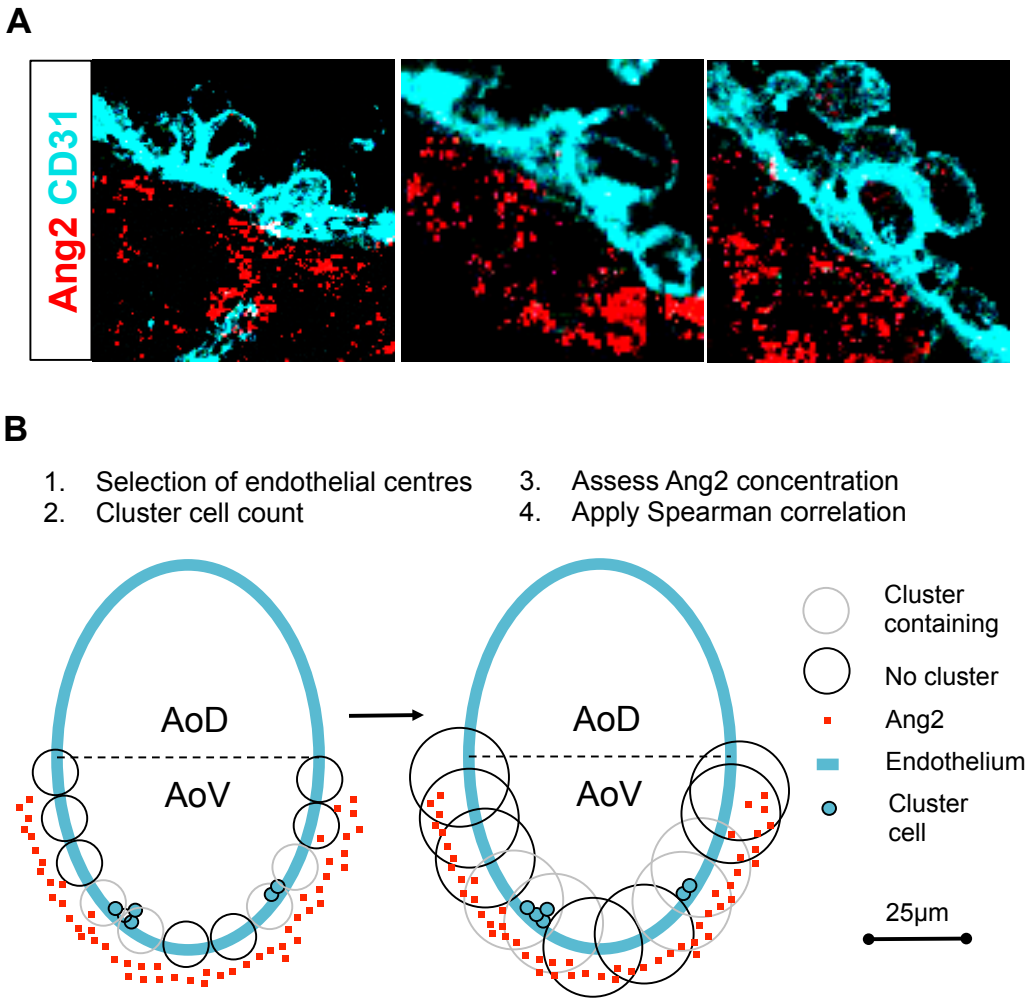

Figure 4.12 | Strategy to determine correlation between Ang2 and aortic clusters.

(A) Representative images showing expression of Ang2 granules (red) in the vicinity of intra-aortic haematopoietic clusters expressing CD31 (cyan) in the AoV at E10.5. **(B)** Schematic representation of the imaging strategy and statistical analysis (the latter performed by Dr Sergey Zuev) used to determine the correlation between Ang2 concentration and presence of clusters in the AGM. AoV = ventral part of the aorta. AoD = dorsal part of the aorta.

Image ID	Spearman correlation	P-value
1A_1	**0.41**	**0.0047**
1A_3	**0.67**	**0.0112**
1A_4	**0.65**	**0.0001**
1A_5	**0.59**	**0.0004**
1A_6	0.00	0.4962
1A_7	**0.39**	**0.0108**
2A_3	-0.18	0.8743
2A_5	0.24	0.0953
2A_6	**0.28**	**0.0805**
2A_8	0.11	0.2906
3A_2	**0.48**	**0.0042**

Image Number	Spearman correlation	P-value
3A_3	**0.58**	**0.0005**
3A_6	0.09	0.3095
4A_6	**0.65**	**0.0000**
4A_7	**0.54**	**0.0000**
5A_2	0.07	n.a.
5A_4	**0.48**	**0.0083**
DEC_1	**0.57**	**0.0028**
DEC_2	0.36	n.a.
DEC_3	**0.80**	**0.0000**
DEC_4	**0.46**	**0.0179**

Table 4 | Spearman rank-order correlation between Ang2 and aortic clusters.

Shows the percentage of Spearman rank-order correlation calculated for each image (1-21) between the concentration of Ang2 and the presence of clusters. For each image a p-value was calculated in order to determine the significance of the correlation. Correlations with p-value < 0.05 were considered statistically significant. N = 2.

4.2.10 Angiopoietin2 is not expressed by HSC precursors

So far in this chapter, Ang2 was shown to be expressed in the ventral part of the aorta by perivascular, CD146^{+} and sub-aortic mesenchymal cells. At E10.5, Ang2 expression was also correlated with presence of intra-aortic cell clusters from which HSC are thought to emerge. However, it was essential to clarify whether HSC precursors express Ang2. In fact, self-expression of Ang2 by developing HSCs would suggest the involvement of a cell-autonomous mechanism in the step-wise process leading to HSC formation. Using the Ang2-GFP reporter, analysis of GFP expression was carried out between E9.5-E11.5 on all populations of the pre-HSC lineage. Cells sub-dissected from caudal parts and AGMs were gated as putative pro-HSCs (VE-Cadherin^{+} CD45^{-}), putative pre-HSC-I (VE-Cadherin^{+} CD45^{-} CD41^{+}

CD43^{+}) and putative pre-HSC-II (VE-Cadherin^{+} CD45^{+}) (Figure 4.13A), based on published literature (Rybtsov et al. 2014; Rybtsov et al. 2011; Taoudi et al. 2008). GFP expression was absent in the gated populations at all developmental stages (Figure 4.13B), suggesting that between E9.5-E11.5 Ang2 is not self-produced by maturing HSCs.

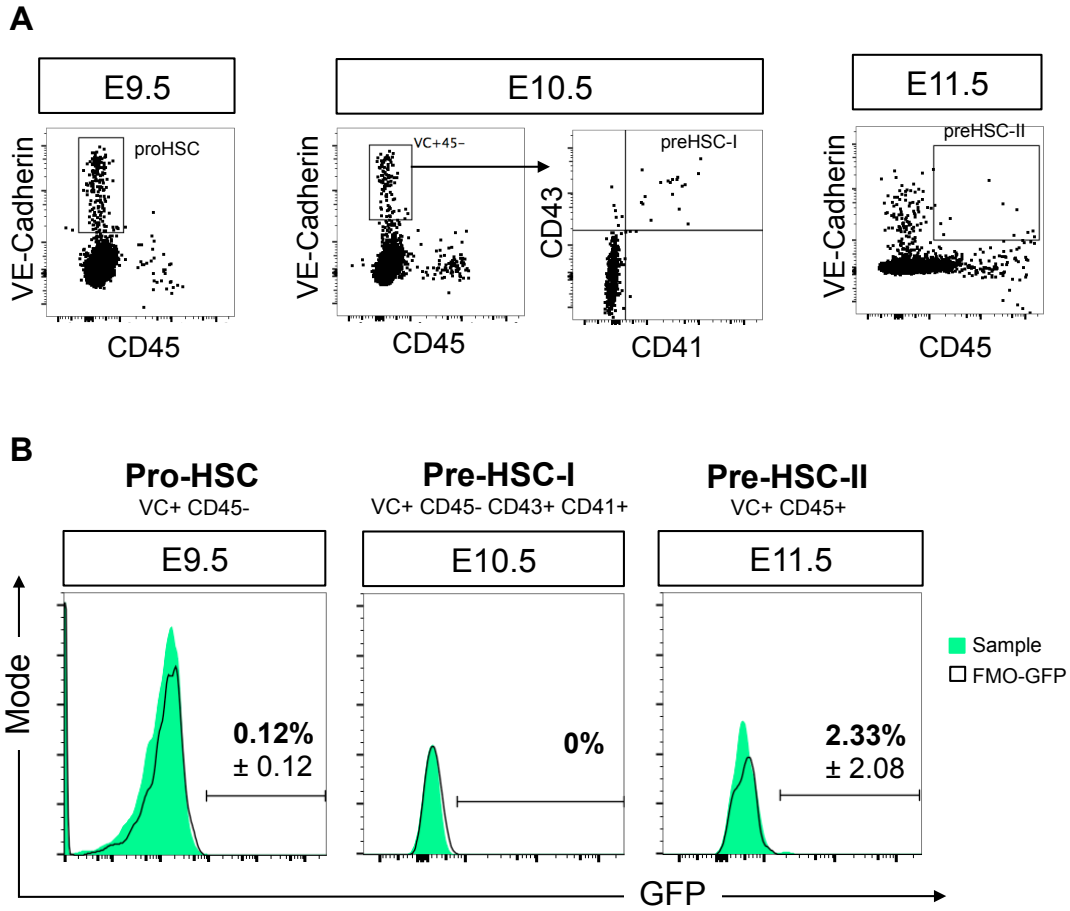

Figure 4.13 | Angiopoietin2 expression by HSC precursors.

(A) Representative plots of the strategy used to gate HSC precursors. Single cells, live, Ter119^{-} B220^{-} CD3^{-} are gated based on the expression of VE-Cadherin (VC) and CD45 at each stage of development. pro-HSCs = VC^{+} CD45^{-} ; pre-HSC-I = VC^{+} CD45^{-} CD43^{+} CD41^{+} ; pre-HSC-II = VC^{+} CD45^{+}. **(B)** Histogram plots showing the percentage of GFP^{+} cells in the pro-HSC (E9.5), pre-HSC-I (E10.5) and pre-HSC-II (E11.5) populations. Percentages are calculated comparing the full stained sample (green) to the FMO-GFP (black line). Mean and SD of 3 independent experiments are shown.

4.2.11 Distribution of Ang1 protein in the AGM region

In Chapter 3 it was shown that supplementation of Ang1 in aggregate cultures of E9.5 caudal part did not affect the production of HSCs (section 3.2.5). However, the RNA-seq results (McGarvey et al. 2017) depicted a significant up-regulation of Ang1 transcript in the ventral part of the aorta compared to the dorsal part between E9.5 and E10.5, with a peak of expression at E10.5 (section 3.2.1). Therefore, immunofluorescence analysis was performed at this time point in order to explore the protein distribution of Ang1 in the aorta. Compared to Ang2, transverse sections contained fewer granules of Ang1 protein in the AGM region (Figure 4.14). This limited the ability to clearly establish whether Ang1 had the tendency to be distributed ventrally. However, Ang1 was consistently observed in the surroundings of round-shaped cells located within the aortic lumen (Figure 4.14A), at the interface between perivascular and endothelial cells (Figure 4.14B) and in the sub-aortic mesenchyme surrounding the aortic lumen (Figure 4.14C). In contrast to the broad distribution of Ang2 in the ventral-later sides of the aorta, these results suggest that expression of Ang1 at the protein level is limited at E10.5.

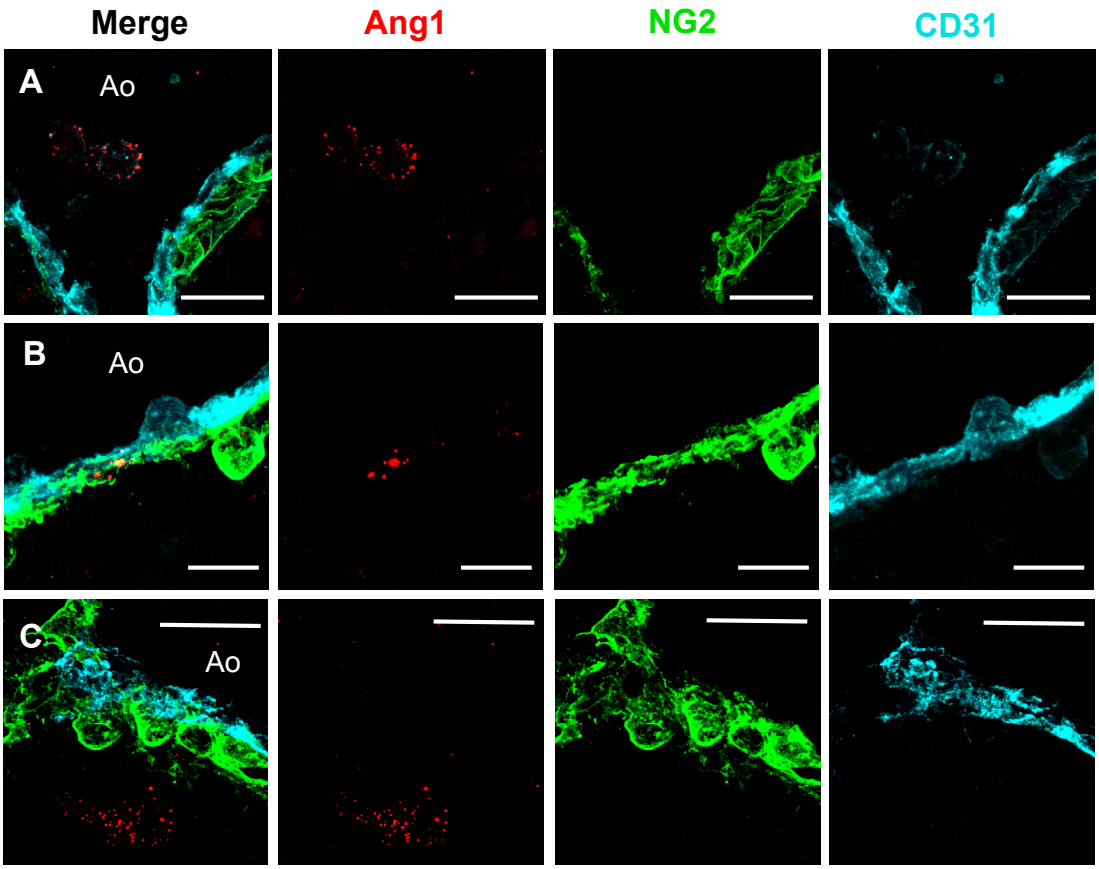

Figure 4.14 | Angiopoietin1 distribution in the E10.5 AGM region.

(A) Localization of Ang1 protein in the surrounding of round-shaped cells in circulation. Scale bar = 25 µm. **(B)** Localization of Ang1 in correspondence of the NG2 perivascular (green) and CD31 endothelial (cyan) layer. Scale bar = 10 µm. **(C)** Localization of Ang1 in the sub-aortic mesenchyme. Scale bar = 25 µm. Ao = aortic lumen. N = 2 independent experiments.

4.2.12 Angiopoietin receptor Tie2 is expressed by endothelial cells and HSC precursors in the AGM region

Tie2 is the main receptor of both angiopoietin1 and angiopoietin2 (S. Davis et al. 1996) (Maisonpierre et al. 1997) and it is mainly expressed by endothelial cells (Thurston & Daly 2012). In order to understand what cell types in the AGM are influenced by Ang2 signalling in the process of HSC emergence, expression of Tie2 was tested at different stages of development by flow cytometry and imaging. Between E9.5 and E11.5, virtually all VE-Cadherin^{+} endothelial cells in the AGM region co-expressed Tie2 (Figure 4.15). Interestingly, at E9.5 and less prominently at E10.5, a subpopulation of non-endothelial VE-Cadherin^{-} Tie2^{+} cells could be

observed on the flow cytometry plot (Figure 4.15A). This population could represent a variety of cell types including glial cells (O.-H. Lee et al. 2006), monocytes and macrophages (Patel et al. 2013). Expression of Tie2 in the endothelial layer surrounding the aorta was confirmed by co-staining with CD31 at E10.5 (Figure 4.15B).

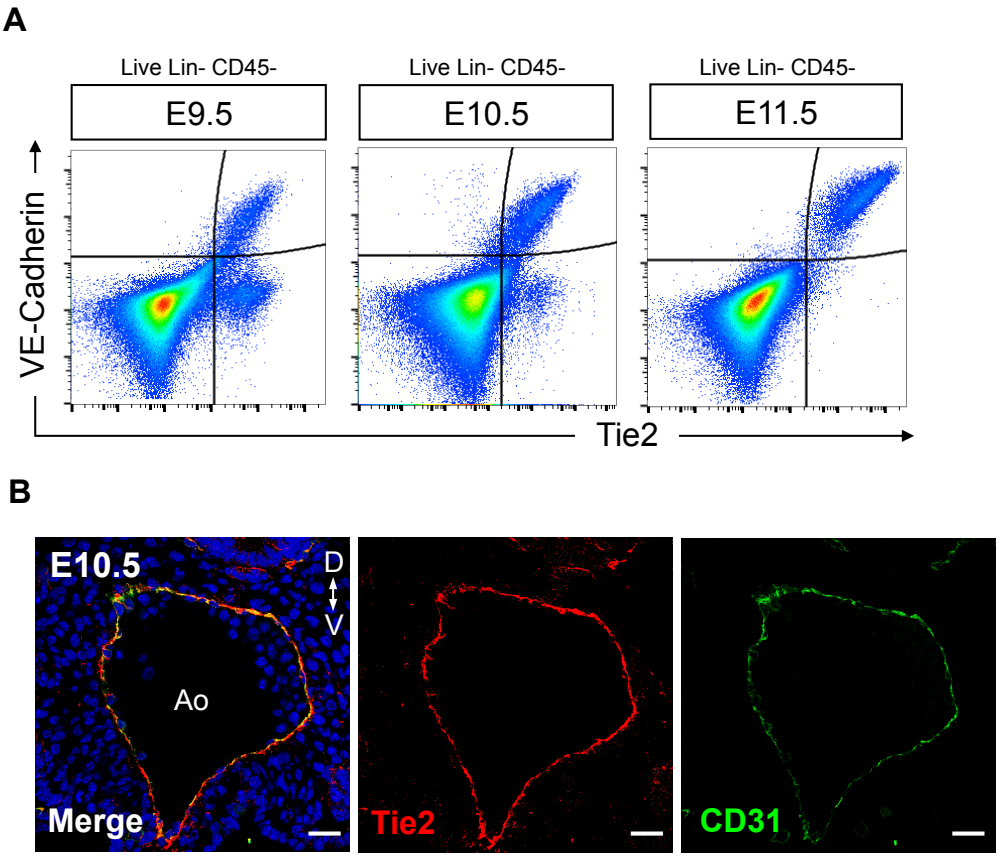

Figure 4.15 | Tie2 expression in the endothelial compartment in the AGM region.
(A) Representative flow cytometry plots showing expression of Tie2 and VE-Cadherin in sub-dissected AGMs at E9.5, E10.5, and E11.5. Single cells were gated as Live Lin$^-$ (Ter119$^-$ B220$^-$ CD3$^-$) CD45$^-$. N = 3 independent experiments. **(B)** Tie2 (red) localization in the CD31 aortic endothelium (green) at E10.5. Scale bar = 25 μm. D = dorsal. V = ventral. Transverse section of a single focal plan is shown. N = 3 embryos.

Moreover, at E10.5 Tie2 was co-expressed with c-Kit, a marker of cluster cells, by rounded cells budding out from the endothelial lining (Figure 4.16A), indicating expression of Tie2 by intra-aortic cell clusters. To investigate the possibility that Tie2 might be expressed by HSC precursors, flow cytometry analysis

was performed in the AGM region between E9.5 and E11.5. Tie2 was found to be expressed by 98.8% ± 1.77 of putative pro-HSCs at E9.5, 91.8% ± 6.29 of putative pre-HSC-I at E10.5 and 96.4%± 0.85 of putative pre-HSC-II at E11.5 (Figure 4.16B), indicating that Tie2 is expressed by the vast majority of cells of the developing HSC lineage.

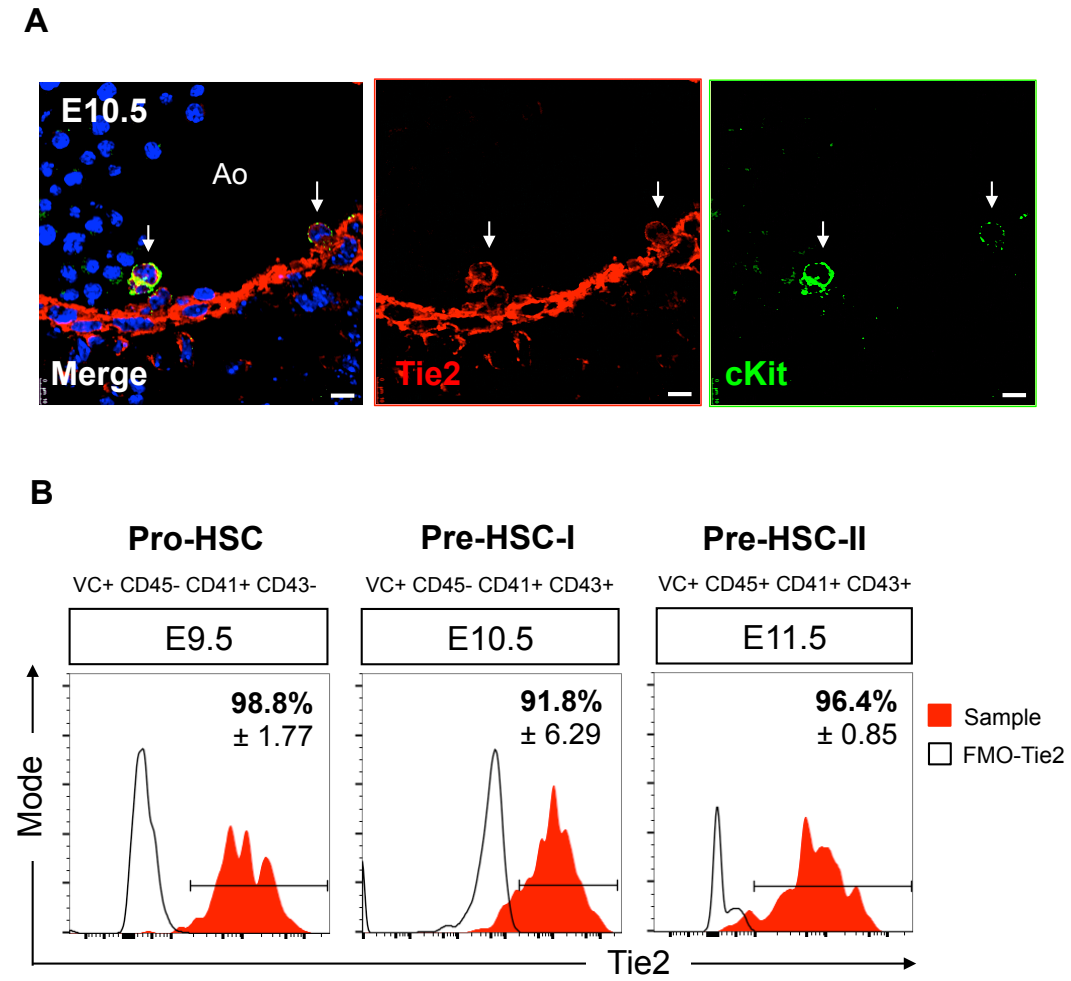

Figure 4.16 | Tie2 expression by HSC precursors and cluster cells.

(A) E10.5 transverse section stained with Tie2 (red), cKit (green) and DAPI (blue) shows expression of Tie2 in intra-aortic cell clusters (arrows). Scale bar = 10 µm. Ao = aortic lumen. A single focal plan is shown. N = 2 embryos. **(B)** Histogram plot showing the percentage of $Tie2^+$ cells in the AGM region between E9.5-E11.5. All cells are gated as live singlets $Ter119^-$ $B220^-$ $CD3^-$. Pro-HSC = VC^+ $CD45^-$ $CD41^+$ $CD43^-$; pre-HSC-I = VC^+ $CD45^-$ $CD41^+$ $CD43^+$; pre-HSC-II = VC^+ $CD45^+$ $CD41^-$ $CD43^+$. Percentage is calculated comparing the full stained sample (red) to the FMO-Tie2-PE (black line). Mean and SD from 3 independent experiments are shown.

4.3 Discussion

The results in this chapter describe the expression of angiopoietins and their receptor Tie2 in the AGM region during the developmental stages that precede HSC formation. Ang2 was found to have a functional role in promoting HSC maturation (Chapter 3); therefore the pattern of expression and distribution of this molecule was characterized at higher resolution compared to the other molecules.

Firstly, both Ang2-expressing cells and Ang2 protein were observed to be ventrally polarized in the AGM region, confirming the RNAseq results (McGarvey et al. 2017) and placing Ang2 in the niche in which HSC are believed to arise from. Some discrepancies could be observed between expression of GFP using the Ang2-GFP reporter mice and the localization of Ang2 protein by immunofluorescence. There were very few GFP-expressing cells detected in the AGM and they were only detected in a low number of tissue sections, while Ang2 protein was distributed along the whole ventral part of the aortic lumen and was present even in GFP negative sections by immunostaining. One possibility to explain this discrepancy is that the BAC transgene might not contain all the regulatory elements of the Ang2 gene, resulting in absence of GFP expression in those cells in which activation of Ang2 is not dependent on Ang2 promoter, but it's rather dependent on distant-acting enhancers. Furthermore, stability of the GFP protein might differ from that of the endogenous Ang2 protein. Ultimately, given that Ang2 is a secreted protein, its distribution in the AGM region might not always correlate with the cells that synthetize and release the protein.

Ang2 was found to be expressed by distinct cell populations located in the aortic microenvironment of the AGM region. Among these, perivascular cells appeared to be a minor but consistent source of expression of Ang2 at E10.5 and E11.5. This is in agreement with previous reports describing Ang2 signal in the smooth muscle layer surrounding the aorta of both E12.5-E14.5 mouse (Maisonpierre et al. 1997) (Gale et al. 2002) and E10 quail embryo (Moyon et al. 2001). Absence of Ang2 expression in the endothelial population was also in line with these studies and contributed to reinforce the notion that a clear distinction should be made between the embryonic and adult scenario, the latter describing Ang2 as predominantly expressed by the endothelium (Fiedler et al. 2004). Another

source of Ang2 was represented by a sub-population of VE-Cadherin$^-$ NG2$^-$ CD146$^+$ cells. These cells are believed to be non-endothelial and non-perivascular and might be located in the mesonephros or laterally to the aortic lumen, however this population still remains poorly characterized. The primary source of Ang2 was represented by the remaining stroma, constituted by all the non-endothelial non-perivascular CD146$^-$ uncharacterized cells. It was not surprising to find the majority of Ang2-expressing cells in this compartment, considering that the components of the microenvironment in which HSC are first formed have not been fully characterized yet (reviewed in (Mirshekar-Syahkal et al. 2014)).

Further investigation of the uncharacterized stromal population at E10.5 revealed Ang2 protein in a sub-perivascular layer of mesenchymal cells characterized by the expression of Runx1 and low levels of COUP-TFII. This does not definitively show whether Ang2 is secreted from outside the sub-aortic mesenchyme or if is produced by cells present there. However, using the Ang2-GFP reporter, Ang2 was shown to be present in the sub-aortic mesenchyme, suggesting that Ang2 is expressed by, or in the vicinity of, Runx1$^+$ COUP$^+$ cells.

An additional interesting observation was the enrichment of Ang2 in correspondence of tissues that are not part of the AGM, such as the gut and neural tube between E9.5-E10.5 and the notochord at E11.5. This is not the first time that a signalling molecule that plays a role in HSC development has been described in the gut (Peeters et al. 2009) or notochord (Echelard et al. 1993), however these findings reinforce the idea that HSC development might require signals from different compartments and distant tissues.

The correlation study between Ang2 and intra-aortic cell clusters suggested a more concentrated distribution of Ang2 in the vicinity of the clusters. It is still undetermined whether clusters form as a chemotactic consequence of higher concentration of Ang2 protein in certain areas of the ventral microenvironment or whether Ang2 concentrates in specific areas of the mesenchyme in response to a stimulus after clusters are formed. Regardless, correlation between Ang2 and clusters might explain the reason why Ang2 exerts a role in HSC development. Interestingly, Ang2 is not produced by HSC precursors, thus dismissing the possibility that pre-HSC-containing clusters might self-sustain their haematopoietic development though

Ang2 and that Ang2-mediated maturation is regulated in a cell-autonomous way. However, as previously discussed Ang2-GFP reporter might not be capturing the whole of the cells expressing Ang2 and thus it might not be a suitable experimental model to report Ang2 expression. Therefore, it cannot be ruled out that HSC precursors express Ang2. Recent literature in which the transcriptome of pre-HSCs and HSCs was analysed did not fully clarify the issue of whether these cell types express Ang2. In {Zhou:2016fi} single cell RNA-seq analysis was performed, but Ang2 is not indicated in any of the "pre-HSC-I", "pre-HSC-II", "E14 HSCs" or "bone marrow HSC" gene signatures, suggesting that the gene is not expressed by these cell types. In {SolaimaniKartalaei:2015go} bulk RNA-sequencing of endothelial cells, haematogenic endothelial cells and HSCs did not result in Ang2 being differentially expressed among these cell types. However, in the bulk RNA-sequencing by {Tober:2018ia} Ang2 is mentioned as one of the differentially expressed genes in pre-HSCs compared to foetal liver HSCs and cultured HSCs (HSC^{ex}), although its levels of expression are only in the range of 1-2 fragments per kilobase million (FPKM) mapped reads, thus indicating low gene expression {Hart:2013iq}. Discrepancies among different studies might be explained by different sorting strategies used for pre-HSCs isolation and by contamination of the putative pre-HSC population with cells of other origins. Future experiments to characterize Ang2 expressing cells will focus on *in situ* hybridization with a probe against Ang2, as well as Ang2 gene expression analysis of sorted pre-HSC populations by qPCR.

In contrast to the effect of Ang2, as Ang1 was not found to have an effect on HSC formation (Chapter 3), the observation that only limited quantities of Ang1 protein are found in the aortic microenvironment might in part explain the lack of efficacy of this molecule in maturation of HSCs.

Finally, the finding that Tie2 receptor is expressed not only by endothelial cells, but also by all the immature cells of the developing HSC lineage between E9.5 and E11.5 indicates that these cells are direct target of Ang2 signalling.

In summary, after Ang2 was described as a positive regulator of HSC formation in Chapter 3, this chapter focused on the investigation of Angiopoietins/Tie2 distribution in the AGM region. Ang2 was mainly localized in

the stromal compartment and in particular in the sub-aortic mesenchyme of the ventral aorta at E10.5. Following the finding that Tie2 receptor is expressed by the functional cells that will mature to become HSCs, further investigation was required to understand the mechanism of action of Ang2 in promoting HSC development. Insights on such mechanism are described in Chapter 5.

Chapter 5 Transcriptional profiling of Ang2-target cells of the AGM region

5.1 Introduction

Several pathways have been implicated in the process of HSC formation, such as Bmp, Notch, SCF, Wnt and Shh signalling, by either exerting an activating or inhibiting function necessary to support HSC formation (Souilhol, Lendinez, et al. 2016; Souilhol, Gonneau, et al. 2016; Rybtsov et al. 2014; Ruiz-Herguido et al. 2012). In recent years, a number of studies have employed genome-wide expression profiling technologies to gain important insight into the processes underlying HSC maturation (Solaimani Kartalaei et al. 2015; Yan Li et al. 2014) (McGarvey et al. 2017). These studies have identified several candidates expressed by the AGM niche that were proven by functional studies as novel regulators of HSC formation such as Gpr56, p57Kip2, Gata3, interferon gamma and Bmper.

The role of the angiopoietin-Tie signalling has never been investigated in the context of embryonic haematopoiesis. Earlier in this thesis, Ang2 was proven to be a positive regulator of HSC formation (Chapter 3) and its concentration was shown to be increased in the vicinity of intra-aortic haematopoietic clusters (Chapter 4). However, it still remain to be elucidated what mechanism of action is exerted by Ang2 on AGM cells in order to promote HSC maturation. As Tie2 was shown to be expressed by endothelial cells and HSC precursors (Chapter 4), it was hypothesised that Ang2 signalling might affect the transcriptome of these cells. Thus, by analysing the genome-wide expression changes produced by the action of Ang2 on these cell types, it could be possible to gain insight into the process of Ang2-mediated HSC formation.

In this chapter, I will describe the RNA-sequencing strategy used for the comparison of HSC precursors and endothelial cells cultured in presence of Ang2 versus control condition. I will list some of the differentially regulated genes and provide description of enriched gene ontologies and canonical pathways enriched in this analysis. I will finally demonstrate that the gene expression changes produced by Ang2 in the pre-HSC-I population might be suggestive of a role for Ang2 in cell

proliferation, cell migration, and regulation of other signalling pathways with a role in HSC development.

5.2 Results

Aspects of this work have been conducted with the help of Dr Matina Fragkogianni and Dr Alison McGarvey, who gave insightful guidance throughout the RNA-seq analysis. Dr Alison McGarvey provided part of the code for trimming of the reads. Dr Matina Fragkogianni provided part of the code for differential expression analysis.

5.2.1 Isolation of angiopoietin2-responsive cells in the AGM region after culture with Ang2

In order to interrogate the mechanism of action of angiopoietin2 contributing to HSC formation in the AGM region, the caudal parts (CP) of E9.5 embryos (between 22 and 42 CP) were sub-dissected, pooled and placed in culture at the gas-liquid interface in presence/absence of recombinant Ang2 protein (Figure 5.1A). As both HSC precursors and endothelial cells express Ang2 receptor Tie2 (Chapter 4, Figure 4.15 and Figure 4.16), it was postulated that alterations at the gene expression level induced by Ang2 would be captured by transcriptome analysis of these cell types. Thus, 24h after culture VE-Cadherin^{+} CD45^{-} CD41^{-} CD43^{-} cKit$^{+/-}$ Lineage^{-} cells were sorted as endothelial cells, while HSC precursors were isolated based on the expression of VE-Cadherin^{+} CD45^{-} CD41^{+} CD43^{+} cKit^{+} Lineage^{-} markers (Figure 5.1B). HSC precursors were sorted with a pre-HSC-I phenotype, the functional HSC precursors at E10 (Rybtsov et al. 2011). This is in accordance with previous findings showing that cultured pro-HSCs (VE-Cadherin^{+} CD45^{-} CD41^{+} CD43^{-}) isolated from E9.5 CP acquire a pre-HSC-I phenotype (characterized by CD43 expression) within the first day of culture and become transplantable HSCs by day 7 (Rybtsov et al. 2014). Interestingly, a slight increase in the percentage of pre-HSC-I could be observed 24h after culture with Ang2 (14.8 ± 8.04 %) compared to control (12.5 ± 7.07 %) (Figure 5.1C). This suggests that presence of Ang2 in culture might contribute to HSC precursor proliferation.

RNA was extracted from the isolated samples and the RNA integrity number (RIN) was calculated in order to determine the overall quality of the RNA. A total of 8 cDNA libraries were barcoded and pooled at an equimolar concentration for sequencing (Table 5).

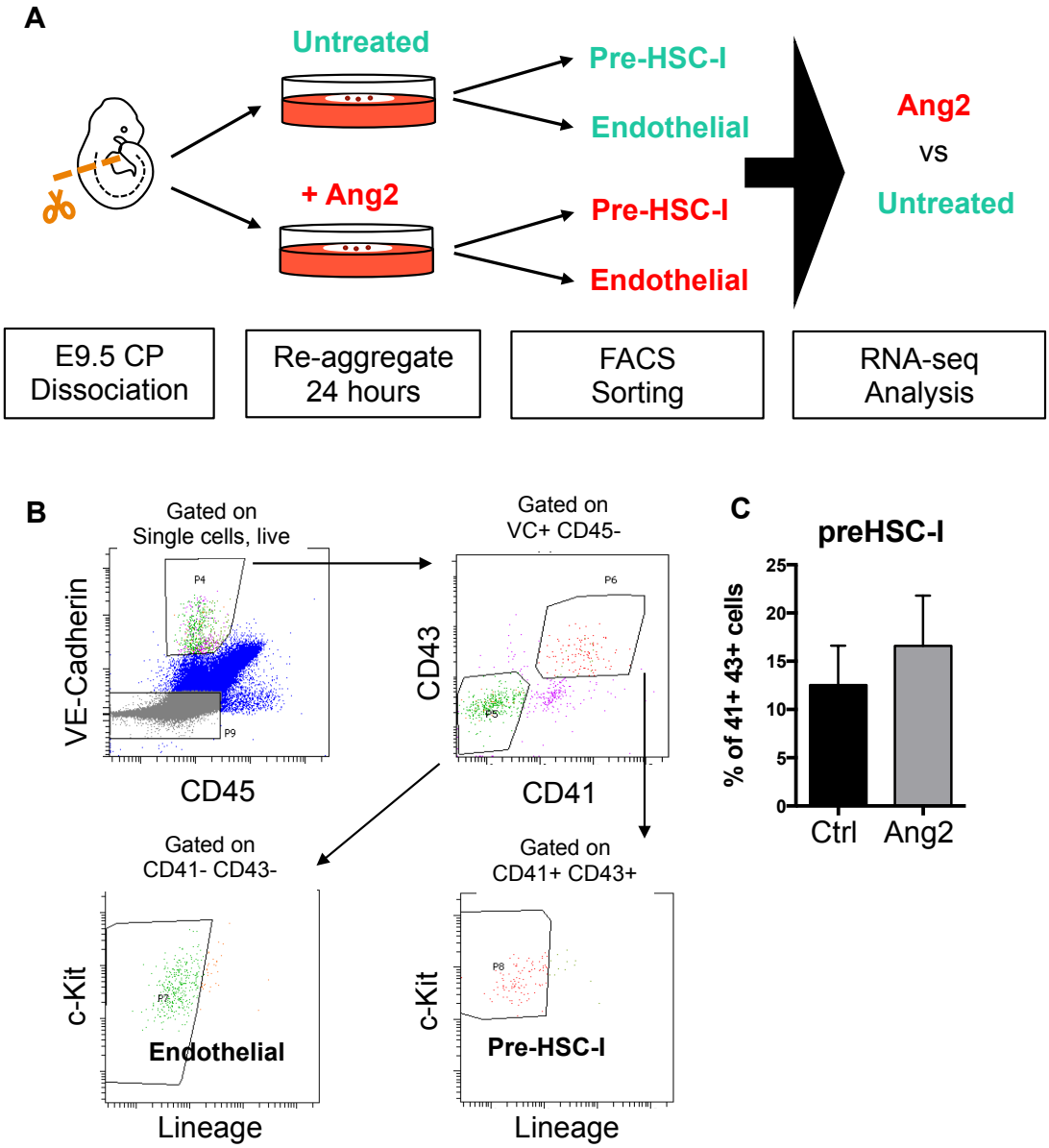

Figure 5.1 | Strategy for RNA-sequencing of HSC precursors and endothelial cells.

(A) Schematic of the strategy employed for the dissection, culture, sorting and sequencing of HSC precursors and endothelial cells derived from the E9.5 caudal part of the embryo. Re-aggregates were cultured at the gas-liquid interface in presence of 3GF and in presence/absence of Ang2 recombinant protein for 24h before sorting. **(B)** Representative plots depicting the sorting strategy for the isolation of pre-HSC-I and endothelial cells 24 after culture. **(C)** Percentage of $CD41^{+}$ $CD43^{+}$ cells (gated according to (B)) 24h after culture in control condition (Ctrl, absence of Ang2) or in presence of Ang2. Mean and SEM are shown. N = 3 independent experiments. VC = VE-Cadherin. Lineage = $Ter119^{-}$ $CD3^{-}$ $B220^{-}$ $CD48^{-}$ $CD11b^{-}$ $Gr1^{-}$.

Sample Number	Experi-ment	Sample Type	Number of cells sorted	RIN	Average Fragment (bp)	cDNA conc (nM)	Volume to use (µl)	Conc in pool (nM)
1	exp1	Ang2 Endo	569	8.0	316	23.2	2.8	5
2	exp1	Ang2 Pre	146	8.0	301	38.5	1.7	5
3	exp1	Ctrl Endo	649	7.9	311	20.6	3.2	5
4	exp1	Ctrl Pre	115	7.9	287	12.1	5.4	5
5	exp2	Ang2 Endo	1098	7.9	342	20.5	3.2	5
6	exp2	Ang2 Pre	365	7.9	325	23.3	2.8	5
7	exp2	Ctrl Endo	879	7.9	334	23.3	2.8	5
8	exp2	Ctrl Pre	255	7.9	290	19.8	3.3	5

Table 5 | Sample information for RNA sequencing.

Columns indicate: "sample number" (used in subsequent figures); "experiment number"; "sample type": Ang2 Endo = endothelial cells cultured with Ang2, Ang2 Pre = pre-HSC-I treated with Ang2, Ctrl Endo = endothelial cells cultured without Ang2, Ctrl Pre = pre-HSC-I cultured without Ang2; "number of cells sorted"; "RIN": indicates the value of the RNA integrity number measured by Tapestation on a mock cell population sorted for each experiment simultaneously with the samples of interest (see Methods, section 2.10.1); "average fragment": measures the length in base pairs of the average fragment estimated by Tapestation; "cDNA conc": measures the concentration of cDNA calculated by Qubit after library preparation; "Volume to use": indicates the volume of each sample that should be added to the library pool, corresponding to an equimolar concentration of 5nM ("Conc in pool").

5.2.2 RNA-seq data obtained from sorted cells is of good quality and can be used for downstream analysis

The bioinformatics pipeline used to analyse the RNA-seq data is depicted in Figure 5.2A. The mean quality value (or phred score) of all reads across each base position in the read was plotted for each sample (Figure 5.2B) using MultiQC (Ewels et al. 2016). The phred score is an estimation of the accuracy of the sequencer in calling the correct nucleobase at a definite position in the read and is logarithmically linked to a base-calling error probability. A low phred quality score of 10 indicates that the sequencer only predicts 90% of the bases correctly, meaning that every 10 bases, 1 might be called incorrectly, while a high phred score of 30 indicates that a

base is accurately called 99.9% of the time, therefore only 1 error every 1000 bases might occur. All samples had a phred score above 30, indicating high accuracy during the sequencing process (Figure 5.2B). Before proceeding with the alignment, trimming was performed in order to reduce the percentage of overrepresented adapter sequences. At the end of this process, the adapter content was reduced to less than 0.3% of all reads at each position (Figure 5.2C).

Sequenced reads were aligned to the genome using STAR (Dobin, C. A. Davis, Schlesinger, Drenkow, et al. 2013). The percentage of reads uniquely mapped to the reference was above 65% and up to 75% for all samples (Figure 5.3A). Around 5% of the reads revealed to be mapped to multiple loci. This might indicate that the ribosomal RNA depletion step during library preparation did not work 100% efficiently, however percentages of multi-mapping reads < 15% are considered normal (Dobin & Gingeras 2015). Approximately 20% of the reads were considered too short by STAR and therefore were not mapped (see Methods section). In order to quantify the number of reads mapping to each gene feature, which is required for downstream analysis, featureCounts (Liao et al. 2014) was used. The number of reads counted varied from a minimum of 10 million for sample 1 up to a maximum of 24 million for sample 6 (Figure 5.3B). Overall, the quality control, alignment and quantification steps suggested that the sequenced data was of good quality; therefore further downstream analysis could be performed.

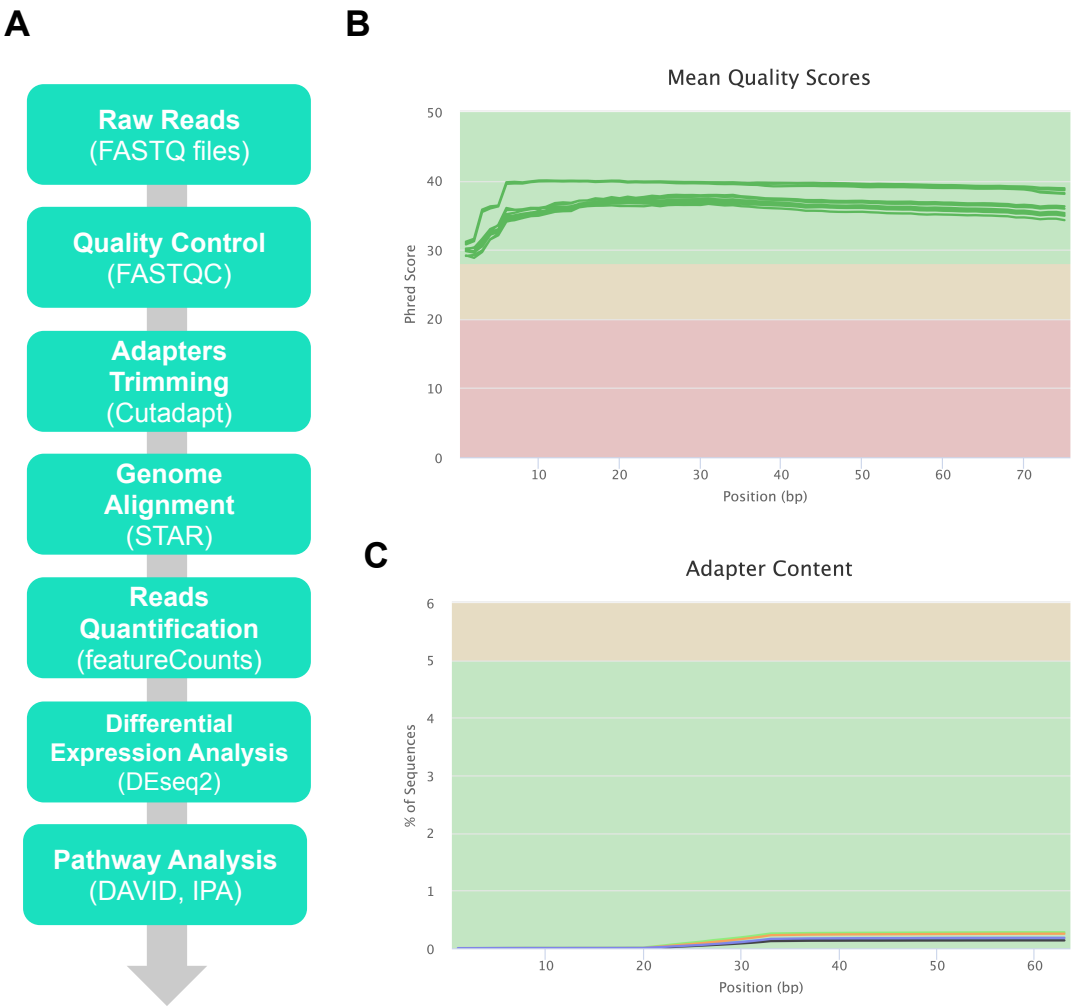

Figure 5.2 | RNA-seq pipeline and sequencing quality control.

(A) Bioinformatics analysis pipeline. Raw reads were quality controlled and aligned to the genome after adapter trimming. Aligned reads were quantified at the gene levels and assessed for differential expression between conditions. Differentially expressed transcripts were used for GO and pathway analysis. **(B)** Mean quality phred score of all reads in each sample for each base position. **(C)** Percentage of adapter sequences at each position for each sample.

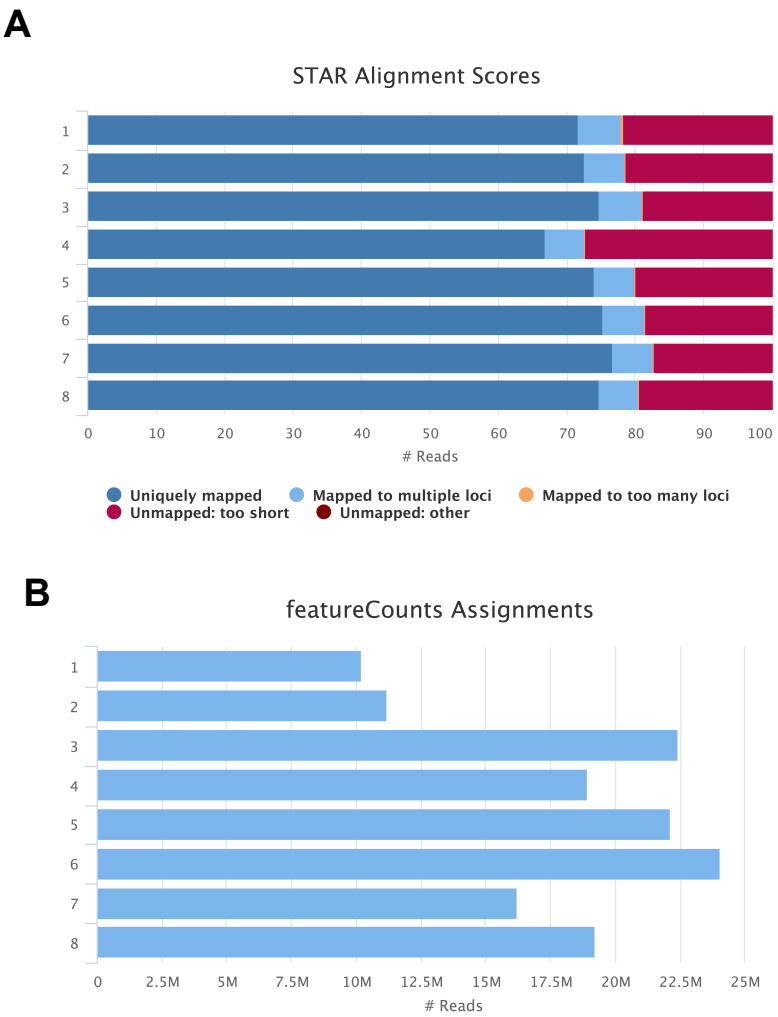

Figure 5.3 | Read alignment and quantification for downstream analysis.

(A) Percentage of reads (x axis) aligned to the reference genome onto a single position (blue), more than one position (light blue), too many loci (yellow) or unmapped because too short (red) or other reasons (purple) are shown for each sample (1-8). **(B)** Number of million (M) reads (x axis) assigned to gene features of the reference genome are shown for each sample (1-8).

5.2.3 HSC precursors but not endothelial cells cluster separately in response to Ang2 culture

To measure variation between samples based on their expression profiles, unsupervised principal component analysis (PCA) on all expressed 19917 genes was performed. The main aim of PCA is to reduce the high-dimensionality of a data set, often represented by many variables. This allows the interpretation of the data set

with just a few variables, called principal components. By reducing the dimension of the data, trends, patterns and outliers can be spotted in the data far more easily than would have been possible without performing the analysis. In order to spot these differences, samples are plotted as points in a graph in which the first and second principal components have been displayed orthogonally. Interestingly, the first principal component (representing 77% of the total variance of the data set) clearly separated the samples based on the cell type by clustering separately endothelial cells (on the left) and pre-HSC-I (on the right) along the horizontal axis (Figure 5.4). Unfortunately, PCA failed to detect differences between endothelial samples treated with Ang2 and untreated, as these two sub-groups clustered together. By contrast, pre-HSC-I cultured with Ang2 clustered separately from control pre-HSC-I (Figure 5.4), suggesting that the culture with Ang2 induced transcriptional changes in this cell type. However, the second principal component (accounting for 10% of the total variance) positioned each of the two Ang2-cultured pre-HSC-I samples at the opposite end of the vertical axis, indicating a high variance between the two replicates (Figure 5.4).

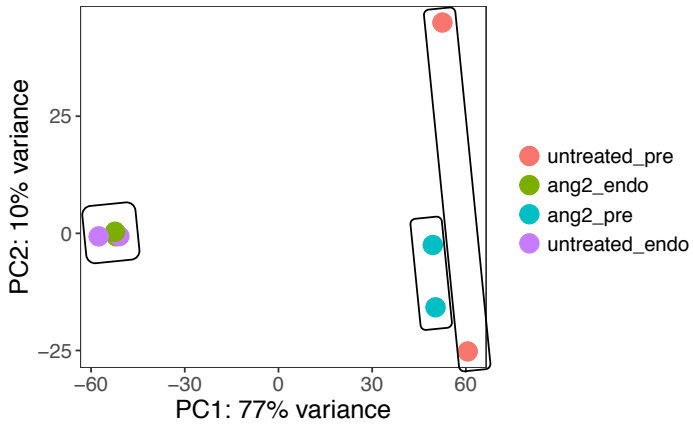

Figure 5.4 | Principal component analysis (PCA) of samples isolated from the AGM region following culture with Ang2.

PCA analysis of Ang2-treated pre-HSC-I ("ang2_pre", cyan dots), Ang2-treated endothelial cells ("ang2_endo", green dots), control pre-HSC-I ("untreated_pre", red dots), control endothelial cells ("untreated_endo", purple dots). The first principal component (PC1) represents the x-axis, while the second principal component (PC2) is shown on the y-axis.

5.2.4 Differential expression analysis of pre-HSC-I cultured with Ang2 compared to control reveals a number of genes up-regulated and down-regulated

In order to investigate the transcriptional changes mediated by Ang2, differential expression analysis was performed on pre-HSC-I cultured with Ang2 compared to untreated pre-HSC-I using DESeq2. Differentially expressed genes were defined as those with a false discovery rate (FDR) ≤ 0.05 and a $\log_2$ fold change ($\log_2$FC) greater than 1.5 (up-regulated genes) or lower than -1.5 (down-regulated genes). Out of 19917 genes, 301 were found to be up-regulated in pre-HSC-I treated with Ang2 vs untreated, while 100 were down-regulated (for a full list of the genes, see Appendix 8.2). Results were illustrated using a volcano plot (Figure 5.5), which shows the relationship between the significance ($-\log_{10}$FDR) and the degree of expression of a gene ($\log_2$FC) compared to control. The larger the degree of expression of a gene in relation to control, the more the gene will lie on the left (if down-regulated) or right (if up-regulated) extreme of the x-axis. The more significant the gene, the smaller the FDR and thus the higher the $-\log_{10}$FDR. Thus, points representing highly significant genes will lie high in the y-axis. Interestingly, although significance was determined by the $-\log_{10}$FDR value of 1.30 ($= \log_{10}0.05$), the plot showed that the vast majority of the significant genes lie above the value 2.50 and up to 10 (Figure 5.5). Likewise, even if a $\log_2$FC of 1.5 was the absolute threshold determining up- and down-regulation, the $\log_2$FC of most of the genes was greater than 4 and up to 8. This suggested that most of the detected differentially expressed genes in this analysis were highly significant and highly up- or down-regulated compared to control.

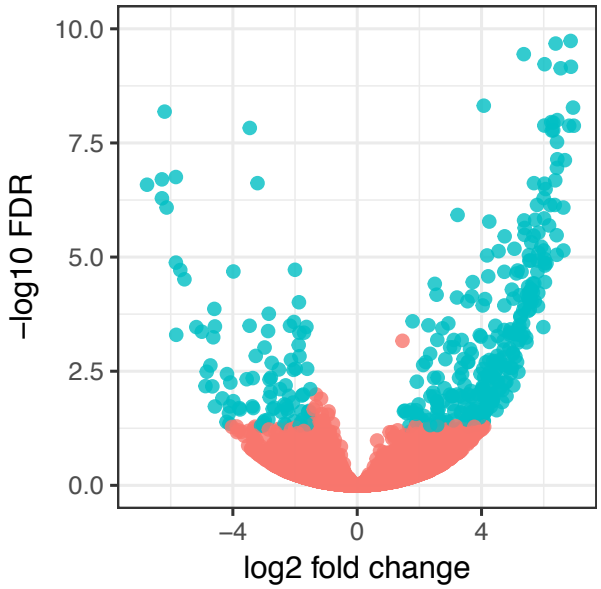

Figure 5.5 | Volcano plot of DE genes obtained from the comparison of pre-HSC-I treated with Ang2 vs control.

Volcano plot representing 19917 genes found to have read count > 1 in pre-HSC-I cultured with Ang2 compared to control. Log_2FC is plotted against the x-axis, while the negative logarithmic transformation of the FDR represents the y-axis. Red dots are not statistically significant genes. Cyan dots below -1.5 Log_2FC are transcripts significantly decreased in pre-HSC-I treated with Ang2 compared to control. Cyan dots above 1.5 Log_2FC are genes significantly up-regulated in pre-HSC-I treated with Ang2 compared to control.

5.2.5 Gene ontology enrichment analysis of pre-HSC-I highlights expression changes associated with cell adhesion and cell shape following culture with Angiopoietin2

Ang2 has been extensively described as a being involved in destabilization and migration of a number of cell types (Scharpfenecker et al. 2005; Thomas et al. 2010; H. S. Lee et al. 2014; Mochizuki et al. 2002). Remodelling of the cytoskeleton (Hakanpaa et al. 2015), enhanced focal adhesion kinase activity (McKinney et al. 2016) and disruption of adherent junctions (Zheng et al. 2014) are among the effectors of Ang2-mediated destabilization and migration. In order to understand whether transcriptome variations mediated by the action of Ang2 involved alterations in the subcellular structure of pre-HSC-I, genes were classified according to their

Gene Ontology (GO) cellular component function using DAVID (Dennis et al. 2003). The largest proportions of genes were assigned to GO terms related to the cytoplasm (150 genes) and the nucleus (133). These terms were also the only two with an FDR < 0.2 (Benjamini correction), indicating statistical significance after a multiple testing correction was applied to the dataset (Table 6).

GO ID	Term	Number of genes	P-value	Benjamini correction
GO:0005737	cytoplasm	150	0.0004	0.1249
GO:0005622	intracellular	48	0.0005	0.0786
GO:0042995	cell projection	25	0.0023	0.2200
GO:0005634	nucleus	133	0.0031	0.2218
GO:0005856	cytoskeleton	33	0.0057	0.3046
GO:0030027	lamellipodium	9	0.0095	0.3956
GO:0005654	nucleoplasm	49	0.0127	0.4391
GO:0005925	focal adhesion	14	0.0242	0.6201
GO:0048471	perinuclear region of cytoplasm	21	0.0254	0.5944
GO:0045121	membrane raft	10	0.0466	0.7778
GO:0005794	Golgi apparatus	30	0.0569	0.8137
GO:0030426	growth cone	7	0.0666	0.8366
GO:0005911	cell-cell junction	8	0.0697	0.8034
GO:0005739	mitochondrion	40	0.0750	0.8058
GO:0043235	receptor complex	6	0.0932	0.8368
GO:0030054	cell junction	19	0.0955	0.8276

Table 6 | Gene Ontology enrichment of Ang2-cultured pre-HSC-I.

Gene ontology terms relative to the cellular component function enriched in pre-HSC-I cultured with Ang2 compared to control. Only GO with p-value < 0.05 were considered significantly enriched. Benjamini correction represents the multiple testing correction used to calculate the FDR.

Despite having a FDR > 0.2, a number of terms related to cytoskeleton components such as “cytoskeleton” and “lamellipodium” were enriched with a p-value < 0.05 (Table 6). Among them, genes such as Carmil2, which is involved in lamellipodial assembly responsible for cell migration (Lanier et al. 2016) and Fer, a regulator of cell adhesion previously shown to induce rounding up and subsequent detachment (Rosato et al. 1998), were found up-regulated (Table 7). Concomitantly, GO revealed enrichment of cell functions associated with adhesion and interaction

such as “cell projection”, “focal adhesion”, “cell-cell junction” and “cell junction” (Table 6). Up-regulated genes included: Robo1, detected on the cell surface of human adult HSC and involved in bone marrow homing (Geutskens & W. D. Andrews 2012); Flrt3, a member of the fibronectin leucine rich transmembrane protein which has been shown to disrupt adhesion and cause cell dissociation (X. Chen et al. 2009); Fgd4 (Frabin), an actin filament binding protein involved in cell shape changes (Obaishi et al. 1998); Itgav, a target of Ang2 signalling known to promote cell destabilization (Thomas et al. 2010) (Table 7). Among the extracellular matrix proteins, tenascin C (Tnc), which over-expression has been reported to enhance cell migration, was up-regulated (Table 7); while laminin β1 (Lamb1) (see Appendix 8.2) was down-regulated. All together, these observations suggest an involvement of Ang2 signalling in the regulation of cytoskeletal and cell adhesion modifications in pre-HSC-I.

Term	Genes
Cell projection	CEP104, BBS5, BBS7, FERMT2, ADCY6, CTNND2, STARD10, **FER**, **ROBO1**, SYNJ2, TMEM185A, **FGD4**, **FLRT3**, 2700049A03RIK, KIF18A, GDPD5, BASP1, EVC2, **CARMIL2**, IQCG, RAB13, IFT88, APBB1, PARVB, IFT74
Cytoskeleton	CEP104, BBS5, BBS7, HIP1R, FERMT2, SSH2, DENND2A, **FER**, SPICE1, CORO2B, CDC42EP1, ANK2, CRMP1, TEK, SYNJ2, **FGD4**, ERCC2, BOD1, 2700049A03RIK, CEP89, ENC1, KIF18A, MID1IP1, EVC2, PHF1, **CARMIL2**, TPPP, IQCG, SYNM, UBXN6, IFT88, PARVB, ACTR10
Lamellipodium	**CARMIL2**, BCAR1, RAPGEF3, **FER**, RAB13, AMOTL1, APBB1, PARVB, FGD4
Focal adhesion	**FLRT3**, CAV2, BCAR1, **TNC**, FERMT2, SSH2, ANXA6, CDC42EP1, **ITGAV**, TEK, YWHAQ, ENG, PARVB, PLAU
Cell-cell junction	PRKD1, PCDHGA12, **FLRT3**, CARMIL2, KIRREL, LCK, TEK, RAB13
Cell junction	**FLRT3**, TMEM204, BCAR1, FERMT2, SSH2, SDK1, CTNND2, UTP15, BASP1, **FER**, AMOTL1, CAMK2N1, KDR, ANK2, **ITGAV**, TEK, SYNM, RAB13, PARVB

Table 7 | Selected GO terms relative to cytoskeleton and cell adhesion modifications. Gene ontologies were selected from Table 5.2. Genes contributing to the enrichment are listed on the right column. Genes highlighted in red are discussed in the text.

5.2.6 Angiopoietin2 induces expression changes of genes associated with signalling pathways involved in HSC emergence

To further discern the mechanism of action of Ang2 in promoting HSC maturation, this study focused on describing differentially expressed genes in Ang2-treated pre-HSC-I compared to control pre-HSC-I, which have been shown in the literature as part of signalling pathways with a role in HSC development. In fact, cooperation between different signalling molecules has been shown to trigger HSC development (Souilhol, Gonneau, et al. 2016).

Firstly, culture with Ang2 promoted down-regulation of Tie2 (Tek) receptor on pre-HSC-I (Figure 5.6). This suggested the existence of an inhibitory mechanism for Ang2-Tie2 signalling following interaction of Ang2 with Tie2. Additional transcripts related to Ang2 signalling were represented by programmed cell death 4 (Pdcd4) and angiopoietin-like 2 (Angptl2). Pdcd4 has been reported to be up-regulated upon suppression of Ang2 (Göke et al. 2015). Accordingly, its expression was decreased in pre-HSC-I upon over-expression of Ang2 in culture (Figure 5.6). By contrast, Angptl2 was found to be up-regulated. This was a notable observation, since Angptl2 promotes HSPC development from the haematogenic endothelium (Lin et al. 2013; Lin et al. 2015) and stimulates expansion of HSC *ex vivo* (C. C. Zhang et al. 2006).

Notch signalling has extensively been shown to play an crucial role in embryonic haematopoiesis (Kumano et al. 2003; Robert-Moreno et al. 2005; Moreno et al. 2008). Notch activity is in fact essential during the early stages of pre-HSC development (pre-HSC-I), but becomes dispensable at later stages (pre-HSC-II) preceding dHSC formation (Souilhol, Lendinez, et al. 2016) and it is not required for maintenance of adult HSCs (Maillard et al. 2008). Accordingly, in this study several genes whose function has been associated with Notch signalling activation, such as Dtx2 (Kishi et al. 2001), Epn2 (H. Chen et al. 2009), Ift88 and Ift74 (Ezratty et al. 2011) were found to be up-regulated in Ang2-treated pre-HSC-I compared to control (Figure 5.6). Interestingly, the Notch inhibitor Dlk1 (Falix et al. 2012) and Notch downstream target Hes1 (Borggrefe & Oswald 2009) were down-regulated.

Up-regulation of genes associated with the TGF-β superfamily/BMP signalling was notable. BMP receptor Bmpr1a, BMP target Id3, the TNF associated

factor 6 (Traf6) and the BMP inhibitor Smad6 were all up-regulated at the transcript level (Figure 5.6). By contrast, endoglin (Eng), Smad1 and activin receptor type 2A (Acvr2a) were down-regulated. BMP signalling has been shown to engage in HSC emergence (Wilkinson et al. 2009). However, recent reports highlighted that precise control of BMP activity mediated by BMP inhibitors is necessary for HSC formation (Souilhol, Gonneau, et al. 2016) (McGarvey 2017). Thus, these gene expression changes might indicate a role for Ang2 in the tight regulation of this signalling pathway.

Furthermore, a number of genes involved in Wnt signalling (Ruiz-Herguido et al. 2012) were also found differentially expressed in Ang2-treated precursors compared to control (Figure 5.6). Prickle, a negative regulator of Wnt (Chan et al. 2006), was up-regulated. Delta-catenin 2, an activator of Beta catenin signalling (H. Kim et al. 2012) and YAP, a target of alternative Wnt signalling that antagonizes Wnt/B-catenin(H. W. Park et al. 2015) were both down-regulated.

Taken all together these results show that treatment with Ang2 triggered modifications at the gene expression level of molecules involved in other signalling pathways relevant to HSC development. The role of these modifications remains unclear and only further investigation might help to clarify their relevance.

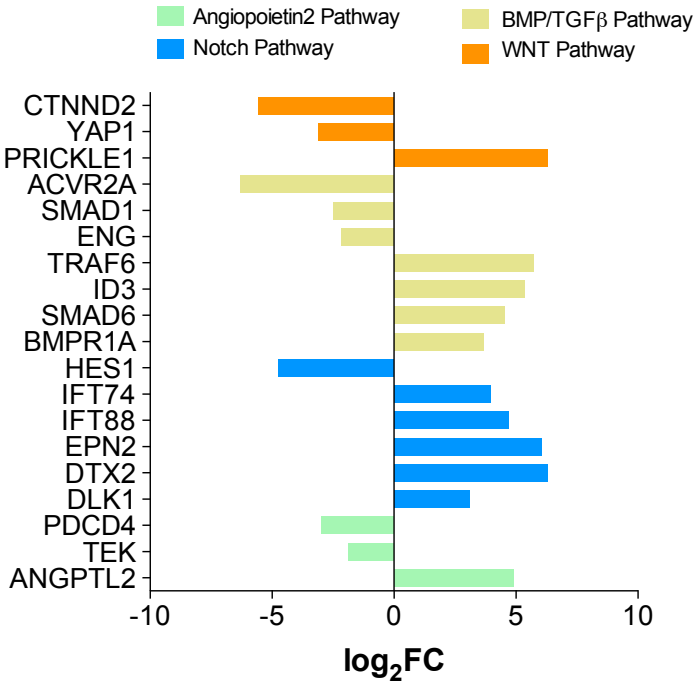

Figure 5.6 | Differentially expressed genes in Ang2-treated pre-HSC-I associated with pathways involved in HSC development.

Log_2FC values of selected genes differentially expressed in Ang2-treated pre-HSC-I vs control pre-HSC-I with an involvement in pathways related to HSC development. All genes shown were statistically significant (FDR < 0.05). Green = genes associated to Ang2 signalling. Blue = genes associated to Notch signalling. Yellow = genes associated to BMP/TGF-β signalling. Orange = genes associated with Wnt signalling.

5.2.7 Enrichment pathway analysis reveals activation of the Renin-Angiotensin signalling and inactivation of TGF-β signalling

To gain a broader understanding of the transcriptome changes produced as an effect of Ang2 signalling on HSC precursors, comparative enrichment analysis of canonical signalling pathways was performed using Ingenuity Pathway Analysis (IPA) (Qiagen). The aim was to identify canonical pathways predicted to be increased or decreased given the observed gene expression changes in Ang2-treated vs untreated pre-HSC-I. Genes with FDR ≤ 0.05 and absolute $log_2FC > 1.5$ were selected and canonical pathways with p-value ≤ 0.05 were considered statistically significant. Canonical pathway analysis revealed an activation of "Renin-Angiotensin signalling" through up-regulation of SHF (Src homology 2), a kinase that plays an important role in ERK activation by angiotensin II (Ishida et al. 1998);

adenylate cyclase 6 (ADCY6) which is involved in the stimulation of renin secretion (Aldehni et al. 2011) and phosphoinositide-3-kinase (PIK3R3) (Yano et al. 2007) (Figure 5.7A). Genes involved in this pathway are normally up-regulated by angiotensin and were up-regulated in pre-HSC-I cultured with Ang2. This was an interesting observation as angiotensin has been shown to promote HSC proliferation (S. Kim et al. 2016) and inhibition of angiotensin-converting enzyme (ACE), involved in the production of angiotensin-I, has been reported to prevent haematopoietic stem cells to enter into cell cycle (Rousseau-Plasse et al. 1998). The present analysis also predicted a significant activation in "Alpha-adrenergic signalling" in Ang2-treated pre-HSC-I (Figure 5.7A). Interestingly, it has been shown that murine HSCs express adrenergic receptors (Muthu et al. 2007). Activated pathways with enriched biological function that were not statistically significant (p-value = 0.052) included "IL8 signalling", which was of particular interest as IL8 is involved in HSC mobilization (Laterveer et al. 1995); and "PTEN signalling", that has been shown to promote HSC self-renewal and expansion in combination with Wnt/β-catenin (Perry et al. 2011) (Figure 5.7A).

Pathways predicted as inactivated in Ang2-treated pre-HSC-I compared to control included "CXCR4 signalling", "TGF-β signalling" and "Nitric oxide signalling in the cardiovascular system" (Figure 5.7B). Nitric oxide (NO) is a regulator of HSC signalling and suppression of the activity of NO synthases (NOS) allows expansion of the number of HSCs (Michurina et al. 2004). One of the down-regulated genes in this pathway was Kdr (Flk1), which has been described to block nitric oxide synthetase (eNOS) (Endo et al. 2003). CXCR4 signalling plays an important role in the homing of HSPC in the bone marrow microenvironment and its disruption results in HSC mobilization (Rettig et al. 2012) (Fricker 2008). TGF-β signalling has been previously implicated in the regulation of HSC expansion and maturation (Crisan et al. 2015) (Durand et al. 2007). Genes that contributed to TGF-β signalling inactivation included SMAD6 and SMAD1 among others (Figure 5.7B). Although not statistically significant, the resulted inactivation of "Thrombin signalling", which induces NO production (Gur-Cohen et al. 2015), was in agreement with down-regulation of NO signalling.

Another group of pathways were shown to be significantly altered (p-value < 0.05) following Ang2 treatment, however the software could not predict their activity pattern (Figure 5.7C). Among others, “Retinoic acid regulation”, “STAT3 pathway” and “Cardiomyocyte differentiation via BMP receptors” were reported.

Thus, the functional enrichment analysis of pre-HSC-I revealed a number of pathways that are significantly enriched following culture with Ang2 and might contribute to Ang2-mediated HSC formation.

(legend refers to the figure displayed in the next page)

Figure 5.7 | Enriched canonical pathways following Ang2 treatment of pre-HSC-I.
(A) Pathways predicted to be activated following Ang2 treatment (IPA z-score > 0). Dark orange indicates enrichments that are statistically significant (p-value < 0.05), light orange not statistically significant pathways. Red = up-regulated genes that contributes to the enrichment. Green = down-regulated genes that contributes to the enrichment. **(B)** Pathways predicted to be inactivated following Ang2 treatment (IPA z-score < 0). Dark blue indicates enrichments that are statistically significant (p-value < 0.05), light blue not statistically significant pathways. Pink = up-regulated genes that contributes to the enrichment. Green = down-regulated genes that contributes to the enrichment. **(C)** Significantly enriched pathways (grey, p-value < 0.05) with unpredicted activity (z-score = NaN). Dotted line corresponds to p-value = 0.05 ($\log_{10}(0.05)$ = 1.30 in the graph) therefore it defines significance. Z-score indicates activation if > 0 or inactivation if < 0.

A **Enriched activated pathways** (z score > 0)

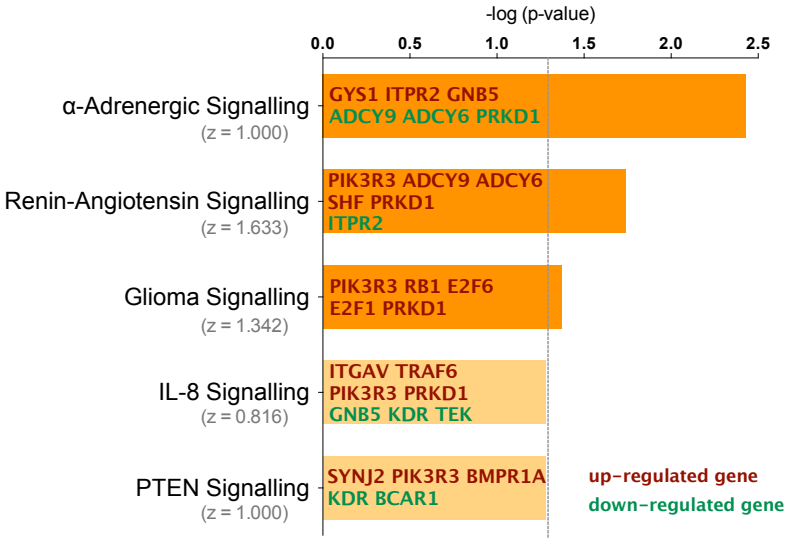

B **Enriched inactivated pathways** (z score < 0)

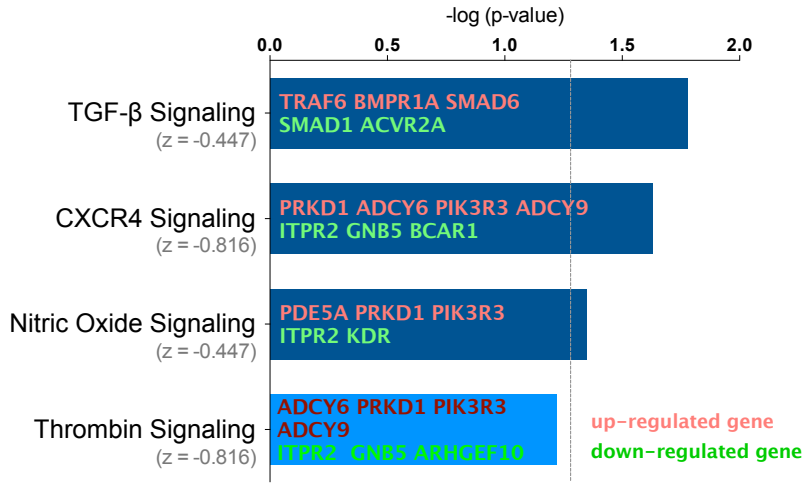

C **Enriched pathways with non-predictable activity** (z score = NaN)

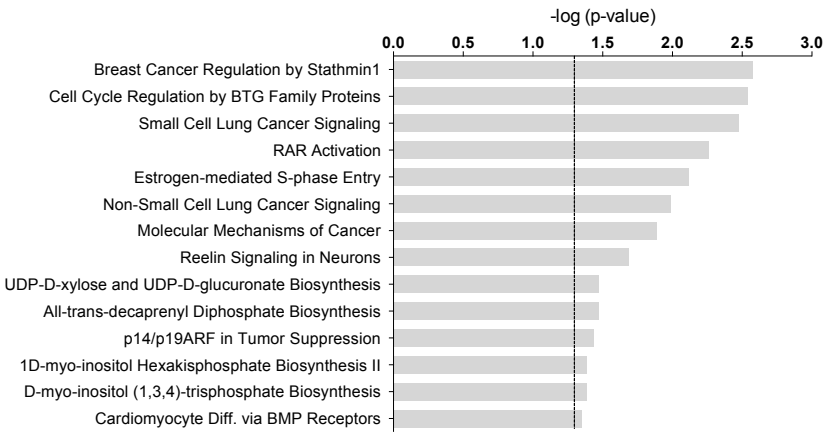

5.2.8 Differential expression analysis of endothelial cells reveals few differences in the endothelium following culture with Ang2

In order to have a broader understanding of the effect of Ang2 in the AGM microenvironment, Ang2 was tested for its ability to induce changes in the transcriptome of endothelial cells, which express Tie2 receptor. Analysis of differentially expressed genes in endothelial cells cultured in presence of Ang2 was tested in comparison to endothelial cells cultured without Ang2. A false discovery rate (FDR) ≤ 0.05 and a $\log_2$ FC > 1.5 (for up-regulated genes) or < -1.5 (for down-regulated genes) were set as parameters to define differentially expressed genes. Interestingly, only a total of 13 genes out of 19917 were found to be differentially expressed (Figure 5.8A). Of those, 8 genes were found to be up-regulated in Ang2-cultured endothelial cells and only 5 of them were down-regulated (Figure 5.8B).

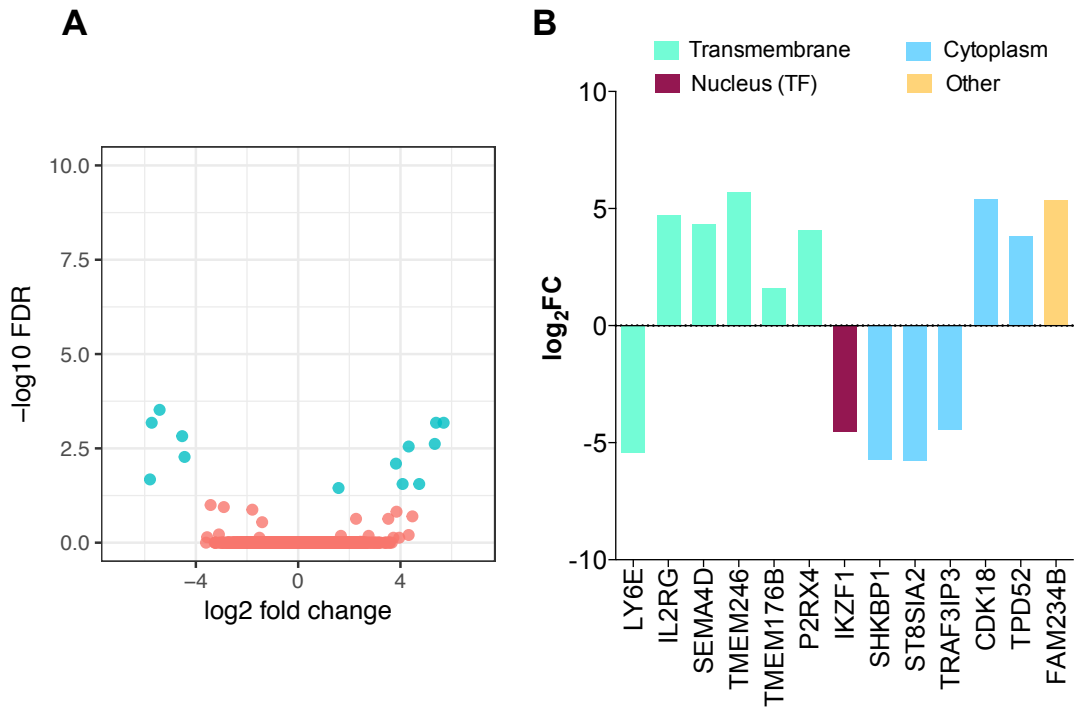

Figure 5.8 | Differential expression analysis results of Ang2-cultured endothelial cells compared to control.

(A) Volcano plot representing 19917 genes found to have read count > 1 in endothelial cells cultured with Ang2 compared to control. Log_2FC is plotted against the x-axis, while the negative logarithmic transformation of the FDR represents the y-axis. Red dots are not statistically significant genes. Cyan dots below -1.5 Log_2FC are transcript significantly decreased in endothelium treated with Ang2 compared to control. Cyan dots above 1.5 Log_2FC are genes

significantly up-regulated in endothelium treated with Ang2 compared to control. **(B)** Differentially expressed genes in the endothelium treated with Ang2 compared to untreated endothelium. Genes are colour-coded based on their cellular localization and function. Green = transmembrane receptors. Purple = transcription factors. Light blue = cytoplasm. Yellow = others.

Five of the up-regulated genes were transmembrane receptors (Figure 5.8B). Sema4d (CD100) and P2rx4, a purinergic receptor that binds ATP in its extracellular domain, were the only two previously described to be expressed by endothelial cells (Luque et al. 2015) (Schwiebert et al. 2002). Among the cytoplasmic molecules, cyclin dependent kinase 18 (CDK18), a molecule involved in the regulation of the actin reorganization (Matsuda et al. 2014) to block cell migration (Matsuda et al. 2017) was up-regulated.

Among the down-regulated genes, Ikaros (Ikzf1) was the only transcription factor (Figure 5.8B). Interestingly, Hoxa3-mediated down-regulation of Ikaros was shown to restrain haematopoietic differentiation of endothelial progenitors (Iacovino et al. 2011). Other down-regulated genes included Traf3ip3, which was previously described to promote activation of the kinase JNK (Dadgostar et al. 2003).

Thus, gene expression analysis of endothelial cells cultured in presence of Ang2 revealed a limited number of transcriptome modifications. This suggests that 24h after culture, the action of Ang2 is almost exclusively HSC precursor specific.

5.3 Discussion

Earlier in this dissertation (Chapter 4), endothelial cells and HSC precursors were found to express Tie2, the main receptor for Ang2. This chapter focussed in unravelling the gene expression changes induced by Ang2 on Tie2-expressing cells isolated from the AGM region by RNA-sequencing, with the aim of understanding the mechanism of action of Ang2 as a positive regulator of HSC maturation.

Using genome-wide transcriptional analysis, this study reported an extensive range of differences between HSC precursors following culture with Ang2. Interestingly, PCA identified two separate clusters characterizing pre-HSC-I treated

with Ang2 and control pre-HSC-I. Furthermore, differential expression analysis allowed the identification of a number of genes differentially regulated by the action of Ang2.

Interestingly, Gene Ontology analysis highlighted an enrichment of genes whose cellular functions are associated with a number of terms related to cytoskeleton and cell-adhesion. Alteration in expression of some of the genes included in these functions, including Carmil2, Fer, Robo1, Flrt3, Fdg4, Tnc, Lamb1 among others, suggested that Ang2-mediated signalling might be accountable for modifications occurring in the cytoskeleton, on the cell surface, at focal adhesions and at the level of extracellular matrix. Genes involved in cell detachment seemed to be up-regulated together with genes promoting alterations of cell shape. Thus, it is possible that in response to Ang2 pre-HSC-I might undergo expression changes orchestrated in order to acquire a migratory phenotype. This hypothesis would be in agreement with the literature relative to the function of Ang2, in which neural crest (McKinney et al. 2016) as well as endothelial cell migration (H. S. Lee et al. 2014; Mochizuki et al. 2002) require active Ang2 signalling.

As part of the mechanism involving cell destabilization and migration, Ang2 signalling has been described to be activated not only by exclusive binding to Tie2 receptor (Scharpfenecker et al. 2005; H. S. Lee et al. 2014), but also via association with integrins (Hakanpaa et al. 2015). Remarkably, up-regulation of αv integrin (Itgav) was observed in the pre-HSC-I following Ang2 stimulation. Interestingly, Ang2 had previously been described to induce formation of a complex between Tie2 and αvβ3 integrin as a starting event leading to endothelial destabilization (Thomas et al. 2010). Thus, it is possible that Ang2 signalling might induce changes in pre-HSC-I via an αv integrin-dependent mechanism.

Analysis of individual genes in pathways of interest could not elucidate whether their transcript alterations resulted into up- or down-regulation of the pathway activity. However, pathway enrichment analysis was able to significantly predict inactivation of TGF-β signalling pathway, which included genes involved in BMP signalling such as Smad1 and Smad6. This inactivation is in agreement with recent studies highlighting the requirement for BMP inhibition in the production of HSC (Souilhol, Gonneau, et al. 2016)(McGarvey et al. 2017) and might indicate a

role of Ang2 in the tight regulation of this signalling pathway to promote HSC maturation.

A further observation when looking at pathway enrichment analysis was the activation of Angiotensin-Renin signalling and IL8 signalling, which have been described to have an involvement in HSC proliferation (S. Kim et al. 2016; Laterveer et al. 1995). Activation of these pathways was concomitant with inactivation of CXCR4 signalling and NO signalling. As suppression of the functions of these inactivated pathways is indicative of mobilization and expansion of the number of HSCs (Rettig et al. 2012; Fricker 2008; Michurina et al. 2004), altogether it could be hypothesized that Ang2 is responsible for increased proliferation of pre-HSC-I. This hypothesis is supported by the observation that following culture with Ang2, the percentage of pre-HSC-I is increased (Figure 5.1C).

Finally, differential expression analysis on endothelial cells did not reveal major differences following treatment with Ang2, with only 13 genes being found as differentially expressed. This might have several explanations; (a) it could indicate that Ang2 mediates HSC formation by selectively interacting with HSC precursors, but not with other cells constituting the aortic microenvironment such as endothelial cells. Even if conceivable, it would seem unlikely that Ang2 protein would selectively bind Tie2 receptor (or αv integrin) on the surface of HSC precursors but not endothelial cells; or that binding of Ang2 on one cell type but not the other would result in no effect in downstream signalling. Therefore, (b) it can be postulated that Ang2 signalling might occur through an unknown receptor expressed by HSC precursors but not endothelial cells. Furthermore, (c) the minimal changes observed in the Ang2-endothelium compared to control endothelium could be explained by the time point chosen for the analysis. While analysis at 24h after culture was able to capture transcriptional changes in pre-HSC-I, it is possible that the changes in endothelial cells mediated by Ang2 might be detectable at an earlier or later time point.

Although the transcriptional analysis described in this chapter successfully documented differences at the gene expression level, the limited number of cells of interest available in the AGM represented one of the main limitations for this approach. VE-Cadherin^{+} cells in the AGM region at E9.5-E10 are around 1% of the

total number of lineage negative cells and only a small proportion of them are pre-HSC-I. For this reason, despite the high number of caudal parts (between 22 and 42) collected, the number of sorted cells was between ~100-1000 and never exceeded 300 cells for pre-HSC-I. Thus, the amount of RNA starting material used for library preparation was very limited and below the detectable amount. As a consequence, library preparation involved an amplification step prior to sequencing. This step can introduce biases due to uneven amplification of transcripts, which can occur by chance in the first cycles of PCR amplification and affect greatly those transcripts that are expressed at lower level at the beginning of the amplification process (Kebschull & Zador 2015); as PCR is a non-linear amplification process, this unevenness can be more prominent by the end of the amplification, resulting in transcripts disproportionately lower than others. This, together with the fact that samples were sequenced at an average depth of approximately 20 million reads/sample, which is below the recommended depth of 36million reads/sample (Sims et al. 2014), might have contributed to the identification of highly expressed transcripts while missing transcripts expressed at lower levels. Deeper sequencing with higher genome coverage is recommended for future follow-up studies that will allow the identification of transcripts expressed at lower levels.

Another limitation in this study was imposed by the small number of replicates. In fact, the high variance between duplicates in control pre-HSC-I might have contributed to the detection of fewer differentially expressed genes in Ang2-treated pre-HSC-I. This variance is easily explainable by the existing biological variability between embryos with similar somite pair counts. However, a higher number of replicates would have allowed a more accurate estimation of the extent of this variability, resulting in a more robust analysis of differential expression.

Finally, another important factor that should be taken into account is the fact that no single gene has so far been found to be uniquely expressed by pre-HSCs. This represent a limitation when the isolation of these cell types is experimentally required. While at E10 around only 10 functional pre-HSC-I have been previously shown to be contained within the AGM region (Rybtsov et al. 2016), the number of cells in freshly isolated AGMs with a pre-HSC-I phenotype (VE-Cadherin^{+} CD45^{-} CD41^{+} CD43^{+} cKit^{+} Lineage^{-}) is around 500-700 (data unpublished from

S.Rybtsov). Thus, it is possible that other cell types might be included within the cell population sorted as pre-HSC-I, thus providing contamination. A solution to this issue would be to perform single cell RNA-seq analysis.

In conclusion, the results summarized in this chapter described the use of genome-wide transcriptional analysis to interrogate the action of Ang2 on HSC precursors and endothelial cells isolated from the AGM microenvironment. Detailed analysis of these transcriptional changes in HSC precursors made possible to observe a number of alterations at the gene and pathway enrichment level mediated by the action of Ang2. Further investigation of these alterations will be necessary to clarify the role of Ang2 in facilitating HSC formation (described in Chapter 6. general discussion).

Chapter 6 General discussion and future perspectives

6.1 Summary

The main goal of this thesis was to investigate the role of angiopoietin-Tie signalling during HSC ontogeny. I have described how angiopoietin2 but not angiopoietin1 selectively contributes to the maturation of HSC precursors into HSCs. I have suggested that the positive role of Ang2 resides in its ability to promote proliferation of the existing population of HSC precursors rather than *de novo* maturation of precursors from the haematogenic endothelium. I have also demonstrated that Ang2 acts selectively on the pre-HSC lineage but does not influence production of haematopoietic progenitors

Through characterization at the gene and protein level, I have observed Ang2 ventrally expressed in the aorta by the perivascular and sub-aortic mesenchymal populations at E10.5. In particular, Ang2 concentration was significantly increased in proximity of intra-aortic haematopoietic clusters, thus indicating Ang2 as a key molecule of the AGM niche for HSC production. Lastly, I observed Tie2 expression in the endothelial and HSC precursor lineage populations, suggesting these cell types as direct targets of Ang2 signalling.

Finally, I analysed the transcriptional profiles of HSC precursors and endothelial cells cultured in presence or absence of Ang2. By comparison of these conditions, I identified major transcriptional changes in pre-HSC-I treated with Ang2 in relation to control, while only minimal differences were observed in endothelial cells cultured with different conditions. I sought to gain biological insight from the large amount of differentially expressed genes obtained by exploring their enrichment in gene ontologies and canonical pathways. Some of these findings suggested a possible role for Ang2 in the alteration of the proliferative status of HSC precursors and of signalling pathways involved in HSC development, which might contribute to promote HSC maturation. Others were in line with previous literature suggesting a role for Ang2 in promoting cell detachment and migration. Those roles

will need to be explored further to understand the mechanism of Ang2-mediated HSC formation.

6.2 The functional role of Ang2 in HSC maturation

This study showed a positive role of Ang2 on HSC maturation using two different aggregate approaches for the 7-day culture of E9.5 caudal parts: a recombinant-protein based assay in which Ang2 is added to the media at defined concentrations and a transgenic OP9-based assay in which increasing concentrations of doxycycline are supplemented to the culture media to induce production of Ang2 by OP9 cells. Both studies proved Ang2 as a novel regulator of HSC formation at early stages of HSC precursor lineage development. This is not the first time that similar approaches have been successfully used to demonstrate the functional role of candidate molecules associated to signalling pathways, such as SCF, BMP4, Shh, Noggin, Dll1, and Bmper (Rybtsov et al. 2014; Souilhol, Lendinez, et al. 2016; Souilhol, Gonneau, et al. 2016)(McGarvey et al.,2017). Hence, both aggregate systems represent useful assays for the study of molecular regulators. However, a main limitation of these screening approaches is that the levels of protein supplemented to the medium (via secretion, in case of the transgenic OP9 culture) might not be representative of the physiological situation. Therefore, to define the *in vivo* role of Ang2, a knockout mouse model for Ang2 could be used and the ability of AGM knockout cells to engraft long-term irradiated recipients should be assessed. Alternatively, a blocking antibody that specifically disrupts the action of Ang2 could also be supplemented in culture to study the impact of Ang2 signalling blockage on HSC development. On the other hand, for the purpose of finding the minimal molecular cues able to support the development of HSC *in vitro*, the physiological relevance of the conditions is not a primary issue.

Furthermore, this study showed that Ang2 does not affect the maturation of haematopoietic progenitors. This finding reinforces the notion that the CFU-C and the HSC lineage are two distinct populations. The differences between these two lineages have been previously established phenotypically and at the cell cycle level (Rybtsov et al. 2014; Batsivari et al. 2017). Indeed, at E9.5 CD43 and cKit markers clearly segregate haematopoietic progenitors (which express CD43 and high levels of

cKit) from HSC precursors (which are CD43 negative and express low levels of cKit) (Rybtsov et al. 2014). Moreover, at E9.5 lineage-committed progenitors are predominantly found in a proliferative status compared to pro-HSCs, the latter being significantly more quiescent (Batsivari et al. 2017). In addition to these studies, the present work indicated that these two cell populations are responsive to distinctive signalling cues, as progenitors are Ang2-insensitive.

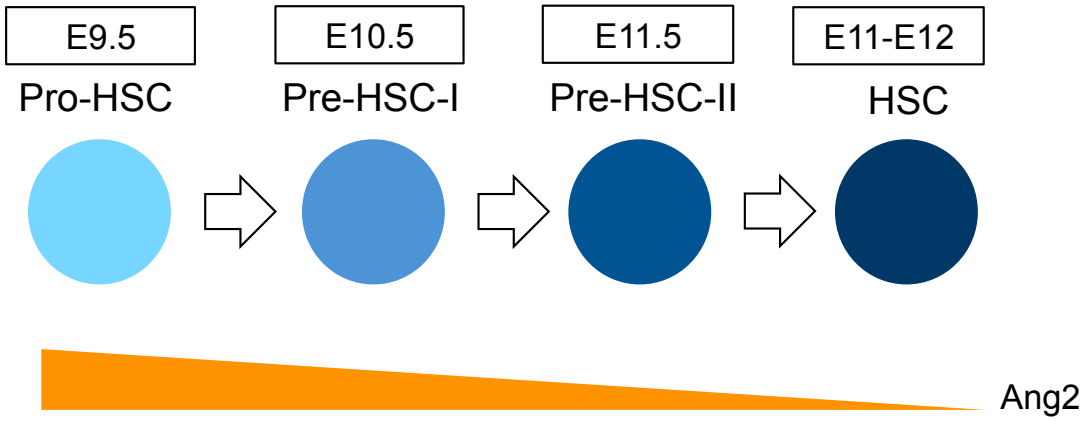

Figure 6.1 | Ang2 requirement along maturation of the developing HSC lineage. Schematic representation of the different types of HSC precursors present at each stage of development (E9.5-E11.5). Ang2 is required for maturation of pro-HSCs and pre-HSC-I into functional HSCs. Ang2 requirement decreases over time and becomes dispensable for maturation of pre-HSC-II at E11. Ang2 = angiopoietin2.

6.3 Ang2 concentration in the ventral sub-aortic mesenchyme in proximity of intra-aortic haematopoietic clusters

In this study, Ang2 was shown to be expressed by a sub-population of perivascular and mesenchymal cells located in the ventral side of the aorta. The presence of Ang2 in this area supports the idea of a ventrally polarised AGM niche {Taoudi:2008cs, Souilhol:2016bs, North:1999ut} (McGarvey et al. 2017). While perivascular cells have been described to provide molecular signals required for HSC maintenance in the adult bone marrow niche (Ding et al. 2012), this study is suggestive of a novel and potentially HSC-supportive role for perivascular cells in the AGM region through the expression of Ang2. As expression of Ang2 is only

detected within a sub-population of these cells, for future studies it would be interesting to characterize the transcriptome of Ang2-expressing perivascular cells in comparison to non-Ang2-expressing perivascular cells. This could be done by sorting the perivascular GFP^+ and GFP^- populations of the Ang2-GFP reporter mouse. This way, it would be possible to elucidate whether Ang2-expressing perivascular cells represent a haematopoietic-supportive sub-population of perivascular cells predisposed to the secretion of other molecules involved in HSC maturation. Such transcriptomic characterization would be challenged by the limited amount of Ang2-expressing perivascular cells contained per AGM (2-64 cells at E10.5, Figure 4.6), thus a single-cell-based RNA-seq approach would be preferred over a bulk-sequencing approach, unless a large cohort of embryos could be used at once.

Expression of Ang2 in the ventral sub-aortic mesenchyme raised the question of what sub-types of mesenchymal cells specifically populate that area and what haematopoietic-supportive properties are distinctive of that region. Although Ang2 was found in proximity of Runx1 and COUP-TFII nuclei, no ventral mesenchymal-specific gene has been so far described in the literature. The identification of such gene would facilitate the isolation of ventral mesenchymal cells. Then, a transcriptome approach could be used to characterize the properties of ventral sub-aortic mesenchymal cells in comparison to dorsal mesenchymal cells, or to evaluate the Ang2-expressing ventral mesenchymal population in relation to the non-Ang2-expressing ventral mesenchyme. One strategy to isolate the ventral mesenchyme at E9.5 could be the use a reporter mouse tracing lateral-plate mesoderm-derived cells, such as HoxB6-Cre (Wasteson et al. 2008), as cells derived from the lateral-plate mesoderm are exclusively located ventrally. However, this strategy would be ineffective at E10.5, as somite-derived cells located dorsally extend ventrally to replace lateral-plate derived mesenchymal cells, as shown by the Meox1-Cre mouse model (Wasteson et al. 2008).

Ultimately, the increased concentration of Ang2 in the vicinity of intra-aortic haematopoietic clusters could explain the *in vivo* supportive effect exerted by Ang2 on developing HSCs. A comparative analysis of cluster size, structure and morphology in Ang2-null versus wild-type embryos at distinct developmental stages

could help clarify the requirement of higher concentrations of Ang2 near the clusters. If the characteristics of cluster cells in the Ang2-null model differ from WT at early stages of development (i.e. early E10), this could indicate that Ang2 is necessary for cluster formation. By contrast, if Ang2-null clusters form indistinguishably from WT embryos, this might suggest that accumulation of Ang2 occurs as a consequence of cluster formation. Similar informative answers to the clusters question could be obtained by looking at the Ang2-over-expressing mouse model; however, the main difficulty would be to choose the appropriate cell compartment to over-express the molecule that would mimic the *in vivo* physiological situation.

6.4 Ang1 is dispensable for HSC formation

The supplementation of Ang1 to the E9.5 culture system failed to detect Ang1 as a regulator of HSC formation. This could reflect the distinct binding dynamics of Ang ligands to Tie2 receptor. While Ang1 has exclusively been described as an activator of Tie2, Ang2 has primarily been shown to antagonise Ang1 signalling, which results in Tie2 inhibition (Augustin et al. 2009; Thurston & Daly 2012). Thus, it is possible that Ang1-mediated activation of Tie2 does not positively influence nor inhibit HSC formation, whereas Ang2-orchestrated inhibition of Tie2 signalling has indeed a beneficial role on HSC maturation. Although Ang1 was shown to be ventrally polarised at the mRNA level by McGarvey et al. 2017, analysis at the protein level failed to reveal a clear distribution of the molecule in the ventral domain of the aorta at E10.5. As Ang1 was found to be present in small quantities in the *in vivo* AGM niche at the time and place of HSC emergence, this could explain why this molecule might be dispensable for HSC development. However, it remains to be investigated whether the amount of Ang1 protein increases at a later stage of development (such as E11) and, in that case, whether supplementation of Ang1 in culture might have a positive effect on HSCs at that stage.

Interestingly, co-supplementation of Ang1 and Ang2 together in small quantities positively affected HSC formation, although the outcome was not different to the effect of Ang2 alone. This phenomenon could be explained by taking into account the structure conformation of angiopoietins. Previously, it was shown that

Ang ligands could organise in multimeric or dimeric structures, with oligomeric structures promoting activation of Tie2, while dimeric structures promoting signalling inhibition (S. Davis et al. 2003). Although Ang1 was preferentially found to be organised in oligomers (S. Davis et al. 2003), it is possible that due to the small quantities of protein added in culture the ligand could only organise in dimers, thus promoting signalling inhibition synergistically with Ang2 dimers at a concentration that was sufficient to block Tie2 receptor and promote HSC development. However, more clarifications on the physiological role of Ang1 could be inferred by transplantation of Ang1-null AGM cells to long-term irradiated recipients.

6.5 Potential Ang2-mediated mechanisms of HSC formation

6.5.1 Ang2 as a potential modulator of HSC precursor proliferation

In this study, through limiting dilution analysis, Ang2-mediated HSC formation was suggested to occur through the expansion of the pre-existing pool of HSC precursors in culture, rather than by maturation of new haematogenic endothelial cells into pre-HSCs. This notion was supported by the observation that 24h after culture with Ang2 a slight increase in the percentage of the pre-HSC-I population was observed in comparison to pre-HSC-I cultured in absence of Ang2. Moreover, pathway analysis suggested an enhancement of the activity of the Angiotensin-Renin and IL8 signalling, which have been shown to be involved in HSC proliferation (S. Kim et al. 2016; Laterveer et al. 1995). To reinforce the notion of Ang2 as a modulator of HSC proliferation, functional assessment of cell proliferation should be performed in the future. This could be carried out by staining cells with CFSE (Parish 1999) to assess the number of cell divisions undergone in culture by the HSC precursor population in presence of Ang2, or by checking their proliferative status through Ki67, which is a marker of actively cycling cells. Additionally, the Fucci mouse model could be used, as it was recently validated for the analysis of the cell status of HSC precursors (Batsivari et al. 2017).

6.5.2 Ang2 as a potential modulator of Notch signalling

The transcriptome analysis in this study showed expression changes on pre-HSC-I of genes involved in signalling pathways with a role in HSC development mediated by the action of Ang2. These results are supportive of the idea that the interplay between several regulatory signals in the AGM is required to induce HSC development (Souilhol, Gonneau, et al. 2016). In this work, a number of genes reported to be associated with Notch signalling activation were found up-regulated (Dtx2, Epn2, Ift88, Ift74). As Notch activation is required for pre-HSC-I development and Notch inhibition on this cell type negatively affects HSC maturation (Souilhol, Lendinez, et al. 2016), this suggests that Ang2 might act upstream of Notch signalling to promote pre-HSC-I development. Moreover, as the transition between pre-HSC-I and pre-HSC-II has been described to involve down-regulation of Hes1 (Souilhol, Lendinez, et al. 2016), down-regulation of Hes1 in this data set might be indicative of a quicker predisposition of pre-HSC-I to mature into pre-HSC-II following culture with Ang2.

Additionally, this thesis showed presence of Ang2 in the ventral sub-aortic mesenchyme in proximity of cells expressing COUP-TFII in their nucleus. Interestingly, COUP-TFII has been identified as an inhibitor of Notch signalling (You et al. 2005). While COUP-TFII is ventrally distributed in the AGM mesenchyme at E10.5, its expression seems to be decreased in sub-aortic mesenchymal cells compared to the UGRs. As inhibition of Tie2 signalling was shown to reduce COUP-TFII (Chu et al. 2016), this could suggest a role for Ang2 in the modulation of Notch signalling during the pre-HSC-I to pre-HSC-II transition via down-regulation of COUP-TFII.

The hypothesis of Ang2 as modulator of HSC development in combination with Notch signalling would fit with previous findings in the literature demonstrating a cross-talk between the two pathways (Gao et al. 2013), also reinforced by the fact that both play a role in angiogenesis (Siekmann & Lawson 2007; Thurston & Daly 2012). Moreover, since it was recently shown that the HSC lineage becomes Notch-independent towards the end of pre-HSC maturation (Souilhol, Lendinez, et al. 2016), this hypothesis would also explain the reason why at E11 Ang2 becomes dispensable. This hypothesis could in future be explored further with functional

experiments to test whether Ang2 is able to rescue HSC formation from pre-HSC-I cultured with a Notch inhibitor.

6.5.3 Ang2 role on endothelial cells

In this study, RNA-seq analysis did not reveal many differences at the transcriptome level in endothelial cells following Ang2 culture treatment. The fact that only a minority of genes were regulated by the action of Ang2 could be attributed to the culture time point chosen for the analysis of the samples. In fact, in the *in vivo* scenario Ang2 is stored in granules and it is released within seconds to control rapid responses upon inflammatory stimuli on endothelial cells (Fiedler et al. 2004). Thus, it is possible that most of the changes at the gene expression level would occur shortly after Ang2 supplementation in culture and that at 24h the transcriptional changes exerted by Ang2 on endothelial cells might not be any longer detectable. The hypothesis of Ang2 exerting a role on the endothelium at a different time point would be in line with the observation that, after culture with Ang2, AGM cells showed an impaired ability to produce colonies of endothelial progenitors *in vitro*. This observation is in agreement with the concept of Ang2 being responsible for endothelial destabilization caused by its inhibitory action on Tie2 receptor (Tsigkos et al. 2006).

6.6 Conclusions

In conclusion, the data presented in this thesis has contributed to expand the knowledge relative to the molecular cues required during the embryonic process of HSC formation in the AGM region. This study elucidated a novel role for the Angiopoietin-Tie signalling pathway in the formation of HSCs. The signals required for the development of HSCs were shown to be exerted through the action of Ang2, which is expressed in the ventral AGM niche. Ang2-mediated inhibition of Tie2 on the developing HSC lineage resulted in transcriptional changes that were suggested to increase the proliferation of the developing HSC precursors and modulate other HSC-promoting signalling pathways. All together, these changes positively improved HSC formation. The discovery of Ang2 as a novel regulator of HSC

maturation may be applicable to protocols for differentiation of ES cells towards an HSC fate. Further analysis of molecules selectively expressed in the ventral aortic niche will be required to unravel the complexity of the AGM signalling landscape. This would contribute to identify additional molecular regulators that can improve HSC maturation *ex vivo* and may lead to the development of novel protocols for the generation of HSCs *in vitro* for clinical applications.

Chapter 7 References

Acker, T., Beck, H. & Plate, K.H., 2001. Cell type specific expression of vascular endothelial growth factor and angiopoietin-1 and -2 suggests an important role of astrocytes in cerebellar vascularization. *Mechanisms of Development*, 108(1-2), pp.45–57.

Adolfsson, J. et al., 2005. Identification of Flt3+ lympho-myeloid stem cells lacking erythro-megakaryocytic potential a revised road map for adult blood lineage commitment. *Cell*, 121(2), pp.295–306.

Aldehni, F. et al., 2011. Stimulation of renin secretion by catecholamines is dependent on adenylyl cyclases 5 and 6. *Hypertension*, 57(3), pp.460–468.

Almeida-Porada, G. et al., 2002. Differentiative potential of human metanephric mesenchymal cells. *Experimental hematology*, 30(12), pp.1454–1462.

Alvarez-Silva, M. et al., 2003. Mouse placenta is a major hematopoietic organ. *Development (Cambridge, England)*, 130(22), pp.5437–5444.

Alwine, J.C., Kemp, D.J. & Stark, G.R., 1977. Method for detection of specific RNAs in agarose gels by transfer to diazobenzyloxymethyl-paper and hybridization with DNA probes. *Proceedings of the National Academy of Sciences of the United States of America*, 74(12), pp.5350–5354.

Andrews, S., 2010. *FastQC: a quality control tool for high throughput sequence data. Available from: h ttp*,

Arai, F. et al., 2002. Mesenchymal stem cells in perichondrium express activated leukocyte cell adhesion molecule and participate in bone marrow formation. *Journal of Experimental Medicine*, 195(12), pp.1549–1563.

Arai, F. et al., 2004. Tie2/angiopoietin-1 signaling regulates hematopoietic stem cell quiescence in the bone marrow niche. *Cell*, 118(2), pp.149–161.

Armulik, A., Genové, G. & Betsholtz, C., 2011. Pericytes: Developmental, Physiological, and Pathological Perspectives, Problems, and Promises. *Developmental cell*, 21(2), pp.193–215.

Augustin, H.G., Koh, G.Y. & Thurston, G., 2009. Control of vascular morphogenesis and homeostasis through the angiopoietin-Tie system. *... reviews Molecular cell ...*.

Baffert, F. et al., 2004. Age-Related Changes in Vascular Endothelial Growth Factor Dependency and Angiopoietin-1-Induced Plasticity of Adult Blood Vessels. *Circulation research*, 94(7), pp.984–992.

Barton, W.A., Tzvetkova, D. & Nikolov, D.B., 2005. Structure of the angiopoietin-2 receptor binding domain and identification of surfaces involved in Tie2 recognition. *Structure (London, England : 1993)*, 13(5), pp.825–832.

Batsivari, A. et al., 2017. Understanding Hematopoietic Stem Cell Development through Functional Correlation of Their Proliferative Status with the Intra-aortic Cluster Architecture. *Stem cell reports*, 8(6), pp.1549–1562.

Becker, A.J. et al., 1965. THE EFFECT OF DIFFERING DEMANDS FOR BLOOD CELL PRODUCTION ON DNA SYNTHESIS BY HEMOPOIETIC COLONY-FORMING CELLS OF MICE. *Blood*, 26(3), pp.296–308.

Becker, A.J., McCulloch, E.A. & Till, J.E., 1963. Cytological demonstration of the clonal nature of spleen colonies derived from transplanted mouse marrow cells. *Nature*.

Bertrand, J.Y. et al., 2010. Haematopoietic stem cells derive directly from aortic endothelium during development. *Nature*, 464(7285), pp.108–111.

Boisset, J.-C. et al., 2010. In vivo imaging of haematopoietic cells emerging from the mouse aortic endothelium. *Nature*, 464(7285), pp.116–120.

Borggrefe, T. & Oswald, F., 2009. The Notch signaling pathway: transcriptional regulation at Notch target genes. *Cellular and molecular life sciences*.

Boyer, S.W. et al., 2011. All Hematopoietic Cells Develop from Hematopoietic Stem Cells through Flk2/Flt3-Positive Progenitor Cells. *Cell stem cell*, 9(1), pp.64–73.

Böiers, C. et al., 2013. Lymphomyeloid Contribution of an Immune-Restricted Progenitor Emerging Prior to Definitive Hematopoietic Stem Cells. *Cell stem cell*, 13(5), pp.535–548.

Brown, L.F. et al., 2000. Expression of Tie1, Tie2, and Angiopoietins 1, 2, and 4 in Kaposi's Sarcoma and Cutaneous Angiosarcoma. *The American journal of pathology*, 156(6), pp.2179–2183.

Buza-Vidas, N. et al., 2009. FLT3 receptor and ligand are dispensable for maintenance and posttransplantation expansion of mouse hematopoietic stem cells. *Blood*, 113(15), pp.3453–3460.

Calvi, L.M. et al., 2003. Osteoblastic cells regulate the haematopoietic stem cell niche. *Nature*, 425(6960), pp.841–846.

Carmeliet, P. et al., 1996. Abnormal blood vessel development and lethality in embryos lacking a single VEGF allele. *Nature*, 380(6573), pp.435–439.

Chan, D.W. et al., 2006. Prickle-1 Negatively Regulates Wnt/β-Catenin Pathway by Promoting Dishevelled Ubiquitination/Degradation in Liver Cancer. *Gastroenterology*, 131(4), pp.1218–1227.

Chen, H. et al., 2009. Embryonic arrest at midgestation and disruption of Notch signaling produced by the absence of both epsin 1 and epsin 2 in mice. *Proceedings of the National Academy of Sciences of the United States of America*, 106(33), pp.13838–13843.

Chen, M.J. et al., 2011. Erythroid/myeloid progenitors and hematopoietic stem cells originate from distinct populations of endothelial cells. *Cell stem cell*, 9(6), pp.541–552.

Chen, M.J. et al., 2009. Runx1 is required for the endothelial to haematopoietic cell transition but not thereafter. *Nature*, 457(7231), pp.887–891.

Chen, X. et al., 2009. A Protocadherin-Cadherin-FLRT3 Complex Controls Cell Adhesion

and Morphogenesis N. A. Hotchin, ed. *PloS one*, 4(12), p.e8411.

Choi, K. et al., 1998. A common precursor for hematopoietic and endothelial cells. *Development (Cambridge, England)*, 125(4), pp.725–732.

Chu, M. et al., 2016. Angiopoietin receptor Tie2 is required for vein specification and maintenance via regulating COUP-TFII. *eLife*, 5, p.4552.

Clements, W.K. et al., 2011. A somitic Wnt16/Notch pathway specifies haematopoietic stem cells. *Nature*, 474(7350), pp.220–224.

Coşkun, S. et al., 2014. Development of the fetal bone marrow niche and regulation of HSC quiescence and homing ability by emerging osteolineage cells. *Cell reports*, 9(2), pp.581–590.

Crisan, M. et al., 2015. BMP signalling differentially regulates distinct haematopoietic stem cell types. *Nature communications*, 6, p.ncomms9040.

Crisan, M. et al., 2012. Perivascular cells for regenerative medicine N. I. Moldovan, ed. *Journal of Cellular and Molecular Medicine*, 16(12), pp.2851–2860.

Cumano, A. et al., 2001. Intraembryonic, but Not Yolk Sac Hematopoietic Precursors, Isolated before Circulation, Provide Long-Term Multilineage Reconstitution. *Immunity*, 15(3), pp.477–485.

Dadgostar, H. et al., 2003. T3JAM, a novel protein that specifically interacts with TRAF3 and promotes the activation of JNK. *FEBS Letters*, 553(3), pp.403–407.

Daly, C. et al., 2004. Angiopoietin-1 modulates endothelial cell function and gene expression via the transcription factor FKHR (FOXO1). *Genes & Development*, 18(9), pp.1060–1071.

Daly, C. et al., 2006. Angiopoietin-2 functions as an autocrine protective factor in stressed endothelial cells. *Proceedings of the National Academy of Sciences of the United States of America*, 103(42), pp.15491–15496.

Davis, S. et al., 1996. Isolation of Angiopoietin-1, a Ligand for the TIE2 Receptor, by Secretion-Trap Expression Cloning. *Cell*, 87(7), pp.1161–1169.

Davis, S., Papadopoulos, N. & Aldrich, T.H., 2003. Angiopoietins have distinct modular domains essential for receptor binding, dimerization and superclustering. *Nature Structural & ...*.

de Bruijn, M.F.T.R. et al., 2000. Definitive hematopoietic stem cells first develop within the major arterial regions of the mouse embryo. *The EMBO Journal*, 19(11), pp.2465–2474.

de Bruijn, M.F.T.R. et al., 2002. Hematopoietic stem cells localize to the endothelial cell layer in the midgestation mouse aorta. *Immunity*, 16(5), pp.673–683.

De Palma, M. et al., 2005. Tie2 identifies a hematopoietic lineage of proangiogenic monocytes required for tumor vessel formation and a mesenchymal population of pericyte progenitors. *Cancer cell*, 8(3), pp.211–226.

Dennis, G. et al., 2003. DAVID: Database for Annotation, Visualization, and Integrated Discovery. *Genome biology*, 4(9), p.R60.

Dexter, T.M., Allen, T.D. & Lajtha, L.G., 1977. Conditions controlling the proliferation of haemopoietic stem cells in vitro. *Journal of Cellular Physiology*, 91(3), pp.335–344.

Dieterlen-Lievre, F., 1975. On the origin of haemopoietic stem cells in the avian embryo: an experimental approach. *Journal of embryology and experimental morphology*, 33(3), pp.607–619.

Dieterlen-Lievre, F. & Martin, C., 1981. Diffuse intraembryonic hemopoiesis in normal and chimeric avian development. *Developmental biology*, 88(1), pp.180–191.

DIETERLENLIEVRE, F. et al., 2006. Are Intra-Aortic Hemopoietic Cells Derived from Endothelial Cells During Ontogeny? *Trends in Cardiovascular Medicine*, 16(4), pp.128–139.

Ding, L. et al., 2012. Endothelial and perivascular cells maintain haematopoietic stem cells. *Nature*, 481(7382), pp.457–462.

Dobin, A. & Gingeras, T.R., 2015. Mapping RNA-seq Reads with STAR. *Current protocols in bioinformatics*, 51, pp.11.14.1–19.

Dobin, A., Davis, C.A., Schlesinger, F. & Drenkow, J., 2013. STAR: ultrafast universal RNA-seq aligner. ....

Dobin, A., Davis, C.A., Schlesinger, F., Drenkow, J., et al., 2013. STAR: ultrafast universal RNA-seq aligner. *Bioinformatics (Oxford, England)*, 29(1), pp.15–21.

Dumont, D.J. et al., 1994. Dominant-negative and targeted null mutations in the endothelial receptor tyrosine kinase, tek, reveal a critical role in vasculogenesis of the embryo. *Genes & Development*, 8(16), pp.1897–1909.

Durand, C. et al., 2007. Embryonic stromal clones reveal developmental regulators of definitive hematopoietic stem cells. *Proceedings of the National Academy of Sciences of the United States of America*, 104(52), pp.20838–20843.

Dykstra, B. et al., 2007. Long-Term Propagation of Distinct Hematopoietic Differentiation Programs In Vivo. *Cell stem cell*, 1(2), pp.218–229.

Dzierzak, E. & Speck, N.A., 2008. Of lineage and legacy: the development of mammalian hematopoietic stem cells. *Nature immunology*, 9(2), pp.129–136.

Eaves, C.J., 2015. Hematopoietic stem cells: concepts, definitions, and the new reality. *Blood*, 125(17), pp.2605–2613.

Echelard, Y. et al., 1993. Sonic hedgehog, a member of a family of putative signaling molecules, is implicated in the regulation of CNS polarity. *Cell*, 75(7), pp.1417–1430.

Eilken, H.M., Nishikawa, S.-I. & Schroeder, T., 2009. Continuous single-cell imaging of blood generation from haemogenic endothelium. *Nature*, 457(7231), pp.896–900.

Eklund, L. & Saharinen, P., 2013. Angiopoietin signaling in the vasculature. *Experimental*

cell research, 319(9), pp.1271–1280.

Ema, H. & Nakauchi, H., 2000. Expansion of hematopoietic stem cells in the developing liver of a mouse embryo. *Blood*, 95(7), pp.2284–2288.

Ema, H. et al., 2005. Quantification of Self-Renewal Capacity in Single Hematopoietic Stem Cells from Normal and Lnk-Deficient Mice. *Developmental cell*, 8(6), pp.907–914.

Endo, A. et al., 2003. Selective Inhibition of Vascular Endothelial Growth Factor Receptor-2 (VEGFR-2) Identifies a Central Role for VEGFR-2 in Human Aortic Endothelial Cell Responses to VEGF. *Journal of Receptors and Signal Transduction*, 23(2-3), pp.239–254.

Ewels, P. et al., 2016. MultiQC: summarize analysis results for multiple tools and samples in a single report. *Bioinformatics (Oxford, England)*, 32(19), pp.3047–3048.

Ezratty, E.J. et al., 2011. A Role for the Primary Cilium in Notch Signaling and Epidermal Differentiation during Skin Development. *Cell*, 145(7), pp.1129–1141.

Falcón, B.L. et al., 2009. Contrasting Actions of Selective Inhibitors of Angiopoietin-1 and Angiopoietin-2 on the Normalization of Tumor Blood Vessels. *The American journal of pathology*, 175(5), pp.2159–2170.

Falix, F.A. et al., 2012. Possible roles of DLK1 in the Notch pathway during development and disease. *Biochimica et Biophysica Acta (BBA) - Molecular Basis of Disease*, 1822(6), pp.988–995.

Fan, F. et al., 2004. Interleukin-1β Regulates Angiopoietin-1 Expression in Human Endothelial Cells. *Cancer Research*, 64(9), pp.3186–3190.

Faust, N. et al., 1997. Different macrophage populations develop from embryonic/fetal and adult hematopoietic tissues. *Experimental hematology*, 25(5), pp.432–444.

FERKOWICZ, M. & Yoder, M., 2005. Blood island formation: longstanding observations and modern interpretations. *Experimental hematology*, 33(9), pp.1041–1047.

Fiedler, U. et al., 2004. The Tie-2 ligand Angiopoietin-2 is stored in and rapidly released upon stimulation from endothelial cell Weibel-Palade bodies. *Blood*, 103(11), pp.4150–4156.

Fiedler, U., Reiss, Y. & Scharpfenecker, M., 2006. Angiopoietin-2 sensitizes endothelial cells to TNF-[alpha] and has a crucial role in the induction of inflammation. *Nature*.

Fitch, S.R. et al., 2012. Signaling from the sympathetic nervous system regulates hematopoietic stem cell emergence during embryogenesis. *Cell stem cell*, 11(4), pp.554–566.

Ford, C.E. et al., 1956. Cytological identification of radiation-chimaeras. *Nature*.

Forsberg, E.C. et al., 2006. New evidence supporting megakaryocyte-erythrocyte potential of flk2/flt3+ multipotent hematopoietic progenitors. *Cell*, 126(2), pp.415–426.

Fraser, S.T. et al., 2002. Definitive hematopoietic commitment within the embryonic

vascular endothelial-cadherin(+) population. *Experimental hematology*, 30(9), pp.1070–1078.

Fricker, S.P., 2008. A novel CXCR4 antagonist for hematopoietic stem cell mobilization. *Expert opinion on investigational drugs*, 17(11), pp.1749–1760.

FU, Y. et al., 2006. Inhibition of gastric cancer cells associated angiogenesis by 15d-prostaglandin J2 through the downregulation of angiopoietin-1. *Cancer letters*, 243(2), pp.246–254.

Gale, N.W. et al., 2002. Angiopoietin-2 Is Required for Postnatal Angiogenesis and Lymphatic Patterning, and Only the Latter Role Is Rescued by Angiopoietin-1. *Developmental cell*, 3(3), pp.411–423.

Gao, W. et al., 2013. Notch signalling pathways mediate synovial angiogenesis in response to vascular endothelial growth factor and angiopoietin 2. *Annals of the rheumatic diseases*, 72(6), pp.1080–1088.

Garber, M. et al., 2011. Computational methods for transcriptome annotation and quantification using RNA-seq. *Nature methods*, 8(6), pp.469–477.

Gavard, J., Patel, V. & Gutkind, J.S., 2008. Angiopoietin-1 Prevents VEGF-Induced Endothelial Permeability by Sequestering Src through mDia. *Developmental cell*, 14(1), pp.25–36.

Gekas, C. et al., 2005. The Placenta Is a Niche for Hematopoietic Stem Cells. *Developmental cell*, 8(3), pp.365–375.

Geutskens, S.B. & Andrews, W.D., 2012. Control of human hematopoietic stem/progenitor cell migration by the extracellular matrix protein Slit3. *Laboratory …*.

Gibson, U.E., Heid, C.A. & Williams, P.M., 1996. A novel method for real time quantitative RT-PCR. *Genome research*, 6(10), pp.995–1001.

Ginhoux, F. et al., 2010. Fate Mapping Analysis Reveals That Adult Microglia Derive from Primitive Macrophages. *Science*, 330(6005), pp.841–845.

Godin, I. & Cumano, A., 2002. The hare and the tortoise: an embryonic haematopoietic race. *Nature reviews. Immunology*, 2(8), pp.593–604.

Gomei, Y. et al., 2010. Functional differences between two Tie2 ligands, angiopoietin-1 and -2, in regulation of adult bone marrow hematopoietic stem cells. *Experimental hematology*, 38(2), pp.82–89.e1.

Gong, S. et al., 2003. A gene expression atlas of the central nervous system based on bacterial artificial chromosomes. *Nature*.

Goodell, M.A. et al., 1997. Dye efflux studies suggest that hematopoietic stem cells expressing low or undetectable levels of CD34 antigen exist in multiple species. *Nature medicine*.

Gordon-Keylock, S. et al., 2013. Mouse extraembryonic arterial vessels harbor precursors capable of maturing into definitive HSCs. *Blood*, 122(14), pp.2338–2345.

GÖKE, A. et al., 2015. The FGFR Inhibitor NVP-BGJ398 Induces NSCLC Cell Death by Activating Caspase-dependent Pathways as well as Caspase-independent Apoptosis. *Anticancer Research*, 35(11), pp.5873–5879.

Gur-Cohen, S. et al., 2015. PAR1 signaling regulates the retention and recruitment of EPCR-expressing bone marrow hematopoietic stem cells. *Nature medicine*, 21(11), pp.1307–1317.

Hackett, S.F. et al., 2000. Angiopoietin 2 expression in the retina: upregulation during physiologic and pathologic neovascularization. *Journal of Cellular Physiology*, 184(3), pp.275–284.

Hakanpaa, L. et al., 2015. Endothelial destabilization by angiopoietin-2 via integrin β1 activation. *Nature communications*, 6, p.ncomms6962.

Hamaguchi, I. et al., 1999. In Vitro Hematopoietic and Endothelial Cell Development From Cells Expressing TEK Receptor in Murine Aorta-Gonad-Mesonephros Region. *Blood*, 93(5), pp.1549–1556.

Han, Y. et al., 2015. Advanced Applications of RNA Sequencing and Challenges. *Bioinformatics and biology insights*, 9(Suppl 1), pp.29–46.

Hanahan, D., 1997. Signaling Vascular Morphogenesis and Maintenance. *Science*, 277(5322), pp.48–50.

Hangai, M. et al., 2001. Angiopoietin-1 Upregulation by Vascular Endothelial Growth Factor in Human Retinal Pigment Epithelial Cells. *Investigative Ophthalmology & Visual Science*, 42(7), pp.1617–1625.

Harrison, D.E., 1980. Competitive repopulation: a new assay for long-term stem cell functional capacity. *Blood*, 55(1), pp.77–81.

Harrison, D.E. & Zhong, R.K., 1992. The same exhaustible multilineage precursor produces both myeloid and lymphoid cells as early as 3-4 weeks after marrow transplantation. *Proceedings of the National Academy of Sciences of the United States of America*, 89(21), pp.10134–10138.

Harrison, D.E. et al., 1993. Primitive hemopoietic stem cells: direct assay of most productive populations by competitive repopulation with simple binomial, correlation and covariance calculations. *Experimental hematology*, 21(2), pp.206–219.

Hato, T., Tabata, M. & Oike, Y., 2008. The role of angiopoietin-like proteins in angiogenesis and metabolism. *Trends in Cardiovascular Medicine*, 18(1), pp.6–14.

Head, S.R. et al., 2014. Library construction for next-generation sequencing: overviews and challenges. *BioTechniques*, 56(2), pp.61–4– 66– 68– passim.

Henninger, J. et al., 2017. Clonal fate mapping quantifies the number of haematopoietic stem cells that arise during development. *Nature cell biology*, 19(1), pp.17–27.

Herzlinger, D. et al., 1992. Metanephric mesenchyme contains multipotent stem cells whose fate is restricted after induction. *Development (Cambridge, England)*, 114(3), pp.565–572.

Hirashima, M. et al., 1999. Maturation of embryonic stem cells into endothelial cells in an in vitro model of vasculogenesis. *Blood*, 93(4), pp.1253–1263.

Hirsch, E. et al., 1996. Impaired migration but not differentiation of haematopoietic stem cells in the absence of beta1 integrins. *Nature*, 380(6570), pp.171–175.

Hsu, H.-C. et al., 2000. Hematopoietic stem cells express Tie-2 receptor in the murine fetal liver. *Blood*, 96(12), pp.3757–3762.

Hu, Y. & Smyth, G.K., 2009. ELDA: Extreme limiting dilution analysis for comparing depleted and enriched populations in stem cell and other assays. *Journal of immunological methods*, 347(1-2), pp.70–78.

Huang, D.W. et al., 2007. DAVID Bioinformatics Resources: expanded annotation database and novel algorithms to better extract biology from large gene lists. *Nucleic acids research*, 35(Web Server issue), pp.W169–75.

Huber, T.L. et al., 2004. Haemangioblast commitment is initiated in the primitive streak of the mouse embryo. *Nature*.

Hughes, D.P., Marron, M.B. & Brindle, N.P.J., 2003. The Antiinflammatory Endothelial Tyrosine Kinase Tie2 Interacts With a Novel Nuclear Factor-κB Inhibitor ABIN-2. *Circulation research*, 92(6), pp.630–636.

Iacovino, M. et al., 2011. HoxA3 is an apical regulator of hemogenic endothelium. *Nature cell biology*, 13(1), pp.72–78.

Ishida, M. et al., 1998. Activation of Extracellular Signal–Regulated Kinases (ERK1/2) by Angiotensin II Is Dependent on c-Src in Vascular Smooth Muscle Cells. *Circulation research*, 82(1), pp.7–12.

Jacobson, L.O., Simmons, E.L. & Marks, E.K., 1951. Recovery from radiation injury. *Science*.

JAFFREDO, T. et al., 1998. Intraaortic hemopoietic cells are derived from endothelial cells during ontogeny. *Development (Cambridge, England)*, 125(22), pp.4575–4583.

Jordan, H.E., 1917. Aortic cell clusters in vertebrate embryos. In Proceedings of the National Academy of ….

Kanda, S. et al., 2005. Angiopoietin 1 Is Mitogenic for Cultured Endothelial Cells. *Cancer Research*, 65(15), pp.6820–6827.

Kasama, T. et al., 2007. Expression of angiopoietin-1 in osteoblasts and its inhibition by tumor necrosis factor-alpha and interferon-gamma. *Translational Research*, 149(5), pp.265–273.

Kebschull, J.M. & Zador, A.M., 2015. Sources of PCR-induced distortions in high-throughput sequencing data sets. *Nucleic acids research*, 43(21), p.e143.

Kent, D.G. et al., 2009. Prospective isolation and molecular characterization of hematopoietic stem cells with durable self-renewal potential. *Blood*, 113(25), pp.6342–6350.

Kiel, M.J. et al., 2009. Hematopoietic stem cells do not depend on N-cadherin to regulate their maintenance. *Cell stem cell*, 4(2), pp.170–179.

Kiel, M.J. et al., 2005. SLAM Family Receptors Distinguish Hematopoietic Stem and Progenitor Cells and Reveal Endothelial Niches for Stem Cells. *Cell*, 121(7), pp.1109–1121.

Kiel, M.J., Radice, G.L. & Morrison, S.J., 2007. Lack of evidence that hematopoietic stem cells depend on N-cadherin-mediated adhesion to osteoblasts for their maintenance. *Cell stem cell*, 1(2), pp.204–217.

Kierdorf, K. et al., 2013. Microglia emerge from erythromyeloid precursors via Pu. 1-and Irf8-dependent pathways. *Nature*.

Kim, D., Langmead, B. & Salzberg, S.L., 2015. HISAT: a fast spliced aligner with low memory requirements. *Nature methods*, 12(4), pp.357–360.

Kim, H. et al., 2012. δ-Catenin promotes E-cadherin processing and activates β-catenin-mediated signaling: Implications on human prostate cancer progression. *Biochimica et Biophysica Acta (BBA) - Molecular Basis of Disease*, 1822(4), pp.509–521.

Kim, I., Kim, H.G., et al., 2000. Angiopoietin-1 Regulates Endothelial Cell Survival Through the Phosphatidylinositol 3′-Kinase/Akt Signal Transduction Pathway. *Circulation research*, 86(1), pp.24–29.

Kim, I., Kim, J.H., et al., 2000. Angiopoietin-2 at high concentration can enhance endothelial cell survival through the phosphatidylinositol 3'-kinase/Akt signal transduction pathway. *Oncogene*, 19(39), pp.4549–4552.

Kim, M. et al., 2016. Opposing actions of angiopoietin-2 on Tie2 signaling and FOXO1 activation. *The Journal of Clinical Investigation*, 126(9), pp.3511–3525.

Kim, S. et al., 2016. Angiotensin II Regulation of Proliferation, Differentiation, and Engraftment of Hematopoietic Stem CellsNovelty and Significance. *Hypertension*, 67(3), pp.574–584.

Kishi, N. et al., 2001. Murine homologs of deltex define a novel gene family involved in vertebrate Notch signaling and neurogenesis. *International Journal of Developmental Neuroscience*, 19(1), pp.21–35.

Kissa, K. & Herbomel, P., 2010. Blood stem cells emerge from aortic endothelium by a novel type of cell transition. *Nature*, 464(7285), pp.112–115.

Koblizek, T.I. et al., 1998. Angiopoietin-1 induces sprouting angiogenesis in vitro. *Current Biology*, 8(9), pp.529–532.

Koch, U., Lehal, R. & Radtke, F., 2013. Stem cells living with a Notch. *Development (Cambridge, England)*, 140(4), pp.689–704.

Korhonen, J. et al., 1995. Endothelial-specific gene expression directed by the tie gene promoter in vivo. *Blood*, 86(5), pp.1828–1835.

Korhonen, J. et al., 1994. The mouse tie receptor tyrosine kinase gene: expression during

embryonic angiogenesis. *Oncogene*, 9(2), pp.395–403.

Kosacka, J. et al., 2005. Angiopoietin-1 promotes neurite outgrowth from dorsal root ganglion cells positive for Tie-2 receptor. *Cell and tissue research*, 320(1), pp.11–19.

Kumano, K. et al., 2003. Notch1 but Not Notch2 Is Essential for Generating Hematopoietic Stem Cells from Endothelial Cells. *Immunity*, 18(5), pp.699–711.

Kumaravelu, P. et al., 2002. Quantitative developmental anatomy of definitive haematopoietic stem cells/long-term repopulating units (HSC/RUs): role of the aorta-gonad-mesonephros (AGM) region and the yolk sac in colonisation of the mouse embryonic liver. *Development (Cambridge, England)*, 129(21), pp.4891–4899.

Kuo, M.-C. et al., 2008. Ischemia-induced exocytosis of Weibel-Palade bodies mobilizes stem cells. *Journal of the American Society of Nephrology : JASN*, 19(12), pp.2321–2330.

Lakshmanan, G. et al., 1999. Localization of distant urogenital system-, central nervous system-, and endocardium-specific transcriptional regulatory elements in the GATA-3 locus. *Molecular and cellular biology*, 19(2), pp.1558–1568.

Lampugnani, M.G. et al., 1992. A novel endothelial-specific membrane protein is a marker of cell-cell contacts. *The Journal of cell biology*, 118(6), pp.1511–1522.

Lancrin, C. et al., 2012. GFI1 and GFI1B control the loss of endothelial identity of hemogenic endothelium during hematopoietic commitment. *Blood*, 120(2), pp.314–322.

Lancrin, C. et al., 2009. The haemangioblast generates haematopoietic cells through a haemogenic endothelium stage. *Nature*, 457(7231), pp.892–895.

Lanier, M.H., McConnell, P. & Cooper, J.A., 2016. Cell Migration and Invadopodia Formation Require a Membrane-binding Domain of CARMIL2. *Journal of Biological Chemistry*, 291(3), pp.1076–1091.

Laterveer, L. et al., 1995. Interleukin-8 induces rapid mobilization of hematopoietic stem cells with radioprotective capacity and long-term myelolymphoid repopulating ability. *Blood*, 85(8), pp.2269–2275.

Lawson, N.D. et al., 2001. Notch signaling is required for arterial-venous differentiation during embryonic vascular development. *Development (Cambridge, England)*, 128(19), pp.3675–3683.

Lawson, N.D., Vogel, A.M. & Weinstein, B.M., 2002. sonic hedgehog and vascular endothelial growth factor act upstream of the Notch pathway during arterial endothelial differentiation. *Developmental cell*, 3(1), pp.127–136.

Leder, A. et al., 1992. In situ hybridization reveals co-expression of embryonic and adult alpha globin genes in the earliest murine erythrocyte progenitors. *Development (Cambridge, England)*, 116(4), pp.1041–1049.

Lee, H.S. et al., 2014. Gln-362 of angiopoietin-2 mediates migration of tumor and endothelial cells through association with α5β1 integrin. *Journal of Biological Chemistry*, 289(45), pp.31330–31340.

Lee, O.-H. et al., 2006. Expression of the Receptor Tyrosine Kinase Tie2 in Neoplastic Glial Cells Is Associated with Integrin β1-Dependent Adhesion to the Extracellular Matrix. *Molecular Cancer Research*, 4(12), pp.915–926.

Lengerke, C. et al., 2008. BMP and Wnt specify hematopoietic fate by activation of the Cdx-Hox pathway. *Cell stem cell*, 2(1), pp.72–82.

Li, Jian-Jun et al., 2001. Thrombin Induces the Release of Angiopoietin-1 from Platelets. *Thrombosis and Haemostasis*, 85(2), pp.204–206.

Li, X et al., 1998. Generation of destabilized green fluorescent protein as a transcription reporter. *Journal of Biological Chemistry*, 273(52), pp.34970–34975.

Li, Yan et al., 2014. Inflammatory signaling regulates embryonic hematopoietic stem and progenitor cell production. *Genes & Development*, 28(23), pp.2597–2612.

Li, Zhe et al., 2006. Runx1 function in hematopoiesis is required in cells that express Tek. *Blood*, 107(1), pp.106–110.

Li, Zhuan et al., 2012. Mouse Embryonic Head as a Site for Hematopoietic Stem Cell Development. *Cell stem cell*, 11(5), pp.663–675.

Li, Zhuan et al., 2016. Subregional localization and characterization of Ly6aGFP-expressing hematopoietic cells in the mouse embryonic head. *Developmental biology*, 416(1), pp.34–41.

Liakhovitskaia, A. et al., 2009. Restoration of Runx1 Expression in the Tie2 Cell Compartment Rescues Definitive Hematopoietic Stem Cells and Extends Life of Runx1 Knockout Animals Until Birth. *Stem cells (Dayton, Ohio)*, 27(7), pp.1616–1624.

Liakhovitskaia, A. et al., 2014. Runx1 is required for progression of CD41+ embryonic precursors into HSCs but not prior to this. *Development (Cambridge, England)*, 141(17), pp.3319–3323.

Liao, Y., Smyth, G.K. & Shi, W., 2014. featureCounts: an efficient general purpose program for assigning sequence reads to genomic features. *Bioinformatics (Oxford, England)*, 30(7), pp.923–930.

Lin, M.I. et al., 2013. Angiopoietin-Like Proteins Stimulate HSC Development Through Direct Interaction With Notch. *Blood*, 122(21), pp.463–463.

Lin, M.I. et al., 2015. Angiopoietin-like proteins stimulate HSPC development through interaction with notch receptor signaling. *eLife*, 4, p.108.

Ling, K.-W. et al., 2004. GATA-2 plays two functionally distinct roles during the ontogeny of hematopoietic stem cells. *Journal of Experimental Medicine*, 200(7), pp.871–882.

Lipshutz, R.J. et al., 1995. Using oligonucleotide probe arrays to access genetic diversity. *BioTechniques*, 19(3), pp.442–447.

Livak, K.J. & Schmittgen, T.D., 2001. Analysis of relative gene expression data using real-time quantitative PCR and the 2(-Delta Delta C(T)) Method. *Methods (San Diego, Calif.)*, 25(4), pp.402–408.

Lockhart, D.J. et al., 1996. Expression monitoring by hybridization to high-density oligonucleotide arrays. *Nature biotechnology*, 14(13), pp.1675–1680.

Lord, B.I., Testa, N.G. & Hendry, J.H., 1975. The relative spatial distributions of CFUs and CFUc in the normal mouse femur. *Blood*, 46(1), pp.65–72.

Lorenz, E., Congdon, C. & Uphoff, D., 1952. Modification of acute irradiation injury in mice and guinea-pigs by bone marrow injections. *Radiology*.

Love, M.I., Huber, W. & Anders, S., 2014. Moderated estimation of fold change and dispersion for RNA-seq data with DESeq2. *Genome biology*, 15(12), p.550.

Luque, M.C.A. et al., 2015. CD100 and plexins B2 and B1 mediate monocyte-endothelial cell adhesion and might take part in atherogenesis. *Molecular immunology*, 67(2 Pt B), pp.559–567.

Maeno, M., Tochinai, S. & Katagiri, C., 1985. Differential participation of ventral and dorsolateral mesoderms in the hemopoiesis of Xenopus, as revealed in diploid-triploid or interspecific chimeras. *Developmental biology*, 110(2), pp.503–508.

Maillard, I. et al., 2008. Canonical Notch Signaling Is Dispensable for the Maintenance of Adult Hematopoietic Stem Cells. *Cell stem cell*, 2(4), pp.356–366.

Maisonpierre, P.C. et al., 1997. Angiopoietin-2, a Natural Antagonist for Tie2 That Disrupts in vivo Angiogenesis. *Science*, 277(5322), pp.55–60.

Manaia, A. et al., 2000. Lmo2 and GATA-3 associated expression in intraembryonic hemogenic sites. *Development (Cambridge, England)*, 127(3), pp.643–653.

Mandriota, S.J. & Pepper, M.S., 1998. Regulation of Angiopoietin-2 mRNA Levels in Bovine Microvascular Endothelial Cells by Cytokines and Hypoxia. *Circulation research*, 83(8), pp.852–859.

Martin, M., 2011. Cutadapt removes adapter sequences from high-throughput sequencing reads. *EMBnet journal*, 17(1), pp.pp. 10–12.

Mascarenhas, M.I. et al., 2009. Identification of novel regulators of hematopoietic stem cell development through refinement of stem cell localization and expression profiling. *Blood*, 114(21), pp.4645–4653.

Matsuda, S. et al., 2014. PCTAIRE kinase 3/cyclin-dependent kinase 18 is activated through association with cyclin A and/or phosphorylation by protein kinase A. *Journal of Biological Chemistry*, 289(26), pp.18387–18400.

Matsuda, S. et al., 2017. PCTK3/CDK18 regulates cell migration and adhesion by negatively modulating FAK activity. *Scientific reports*, 7, p.45545.

Matsui, Y., Zsebo, K. & Hogan, B.L.M., 1992. Derivation of pluripotential embryonic stem cells from murine primordial germ cells in culture. *Cell*, 70(5), pp.841–847.

Maximow, A., 1909. *Relation of blood cells to connective tissue*, Zbl allg Path path Anat.

McGarvey A.C. et al., 2017. A molecular roadmap of the AGM niche reveals BMPER as a

novel regulator of HSC maturation. *Journal of Experimental Medicine*, in press.

McGrath, K.E. et al., 2015. Distinct Sources of Hematopoietic Progenitors Emerge before HSCs and Provide Functional Blood Cells in the Mammalian Embryo. *Cell reports*, 11(12), pp.1892–1904.

McKenna, H.J. et al., 2000. Mice lacking flt3 ligand have deficient hematopoiesis affecting hematopoietic progenitor cells, dendritic cells, and natural killer cells. *Blood*, 95(11), pp.3489–3497.

McKinney, M.C., McLennan, R. & Kulesa, P.M., 2016. Angiopoietin 2 signaling plays a critical role in neural crest cell migration. *BMC biology*, 14(1), p.111.

Medvinsky, A. & Dzierzak, E., 1996. Definitive Hematopoiesis Is Autonomously Initiated by the AGM Region. *Cell*, 86(6), pp.897–906.

Medvinsky, A., Rybtsov, S. & Taoudi, S., 2011. Embryonic origin of the adult hematopoietic system: advances and questions. *Development (Cambridge, England)*, 138(6), pp.1017–1031.

Medvinsky, A.L. et al., 1993. An early pre-liver intraembryonic source of CFU-S in the developing mouse. *Nature*.

Michurina, T. et al., 2004. Nitric Oxide Is a Regulator of Hematopoietic Stem Cell Activity. *Molecular Therapy*, 10(2), pp.241–248.

Miles, C. et al., 1997. Expression of the Ly-6E.1 (Sca-1) transgene in adult hematopoietic stem cells and the developing mouse embryo. *Development (Cambridge, England)*, 124(2), pp.537–547.

Minehata, K.-I. et al., 2002. Macrophage colony stimulating factor modulates the development of hematopoiesis by stimulating the differentiation of endothelial cells in the AGM region. *Blood*, 99(7), pp.2360–2368.

Mirshekar-Syahkal, B., Fitch, S.R. & Ottersbach, K., 2014. Concise review: From greenhouse to garden: the changing soil of the hematopoietic stem cell microenvironment during development. *Stem cells (Dayton, Ohio)*, 32(7), pp.1691–1700.

Mochizuki, Y. et al., 2002. Angiopoietin 2 stimulates migration and tube-like structure formation of murine brain capillary endothelial cells through c-Fes and c-Fyn. *Journal of Cell Science*, 115(1), pp.175–183.

Molyneaux, K.A. et al., 2001. Time-lapse analysis of living mouse germ cell migration. *Developmental biology*, 240(2), pp.488–498.

Moore, M.A.S. & Metcalf, D., 1970. Ontogeny of the Haemopoietic System: Yolk Sac Origin of In Vivo and In Vitro Colony Forming Cells in the Developing Mouse Embryo. *British journal of haematology*, 18(3), pp.279–296.

Moreno, À.R. et al., 2008. Impaired embryonic haematopoiesis yet normal arterial development in the absence of the Notch ligand Jagged1. *The EMBO Journal*, 27(13), pp.1886–1895.

Morrison, S.J. et al., 1995. The purification and characterization of fetal liver hematopoietic stem cells. *Proceedings of the National Academy of Sciences of the United States of America*, 92(22), pp.10302–10306.

Mortazavi, A. et al., 2008. Mapping and quantifying mammalian transcriptomes by RNA-Seq. *Nature methods*, 5(7), pp.621–628.

Moyon, D. et al., 2001. Selective expression of angiopoietin 1 and 2 in mesenchymal cells surrounding veins and arteries of the avian embryo. *Mechanisms of Development*, 106(1-2), pp.133–136.

Mukouyama, Y. et al., 2000. The AML1 transcription factor functions to develop and maintain hematogenic precursor cells in the embryonic aorta-gonad-mesonephros region. *Developmental biology*, 220(1), pp.27–36.

Muthu, K. et al., 2007. Murine hematopoietic stem cells and progenitors express adrenergic receptors. *Journal of Neuroimmunology*, 186(1-2), pp.27–36.

Müller, A.M. et al., 1994. Development of hematopoietic stem cell activity in the mouse embryo. *Immunity*, 1(4), pp.291–301.

Nagase, T. et al., 2005. Angiogenesis within the developing mouse neural tube is dependent on sonic hedgehog signaling: possible roles of motor neurons. *Genes to cells : devoted to molecular & cellular mechanisms*, 10(6), pp.595–604.

Nakano, T., Kodama, H. & Honjo, T., 1994. Generation of lymphohematopoietic cells from embryonic stem cells in culture. *Science*, 265(5175), pp.1098–1101.

Nishikawa, S.I. et al., 1998. In vitro generation of lymphohematopoietic cells from endothelial cells purified from murine embryos. *Immunity*, 8(6), pp.761–769.

North, T. et al., 1999. Cbfa2 is required for the formation of intra-aortic hematopoietic clusters. *Development (Cambridge, England)*, 126(11), pp.2563–2575.

North, T.E. et al., 2002. Runx1 Expression Marks Long-Term Repopulating Hematopoietic Stem Cells in the Midgestation Mouse Embryo. *Immunity*, 16(5), pp.661–672.

Notta, F. et al., 2016. Distinct routes of lineage development reshape the human blood hierarchy across ontogeny. *Science*, 351(6269), pp.aab2116–aab2116.

Obaishi, H. et al., 1998. Frabin, a novel FGD1-related actin filament-binding protein capable of changing cell shape and activating c-Jun N-terminal kinase. *Journal of Biological Chemistry*, 273(30), pp.18697–18700.

Okuda, T. et al., 1996. AML1, the target of multiple chromosomal translocations in human leukemia, is essential for normal fetal liver hematopoiesis. *Cell*, 84(2), pp.321–330.

Osawa, M. et al., 1996. Long-term lymphohematopoietic reconstitution by a single CD34-low/negative hematopoietic stem cell. *Science*.

Ottersbach, K. & Dzierzak, E., 2005. The Murine Placenta Contains Hematopoietic Stem Cells within the Vascular Labyrinth Region. *Developmental cell*, 8(3), pp.377–387.

Ozerdem, U. et al., 2001. NG2 proteoglycan is expressed exclusively by mural cells during vascular morphogenesis. *Developmental Dynamics*, 222(2), pp.218–227.

Padrón-Barthe, L. et al., 2014. Clonal analysis identifies hemogenic endothelium as the source of the blood-endothelial common lineage in the mouse embryo. *Blood*, 124(16), pp.2523–2532.

Palis, J. et al., 1999. Development of erythroid and myeloid progenitors in the yolk sac and embryo proper of the mouse. *Development (Cambridge, England)*, 126(22), pp.5073–5084.

Pardanaud, L. et al., 1996. Two distinct endothelial lineages in ontogeny, one of them related to hemopoiesis. *Development (Cambridge, England)*, 122(5), pp.1363–1371.

Parish, C.R., 1999. Fluorescent dyes for lymphocyte migration and proliferation studies. *Immunology and cell biology*, 77(6), pp.499–508.

Park, H.W. et al., 2015. Alternative Wnt Signaling Activates YAP/TAZ. *Cell*, 162(4), pp.780–794.

Park, J.-S. et al., 2016. Normalization of Tumor Vessels by Tie2 Activation and Ang2 Inhibition Enhances Drug Delivery and Produces a Favorable Tumor Microenvironment. *Cancer cell*, 30(6), pp.953–967.

Park, Y.S., Kim, N.H. & Jo, I., 2003. Hypoxia and vascular endothelial growth factor acutely up-regulate angiopoietin-1 and Tie2 mRNA in bovine retinal pericytes. *Microvascular research*, 65(2), pp.125–131.

Patel, A.S. et al., 2013. TIE2-expressing monocytes/macrophages regulate revascularization of the ischemic limb. *EMBO Molecular Medicine*, 5(6), pp.858–869.

Peeters, M. et al., 2009. Ventral embryonic tissues and Hedgehog proteins induce early AGM hematopoietic stem cell development. *Development (Cambridge, England)*, 136(15), pp.2613–2621.

Pereira, C., Clarke, E. & Damen, J., 2007. Hematopoietic Colony-Forming Cell Assays. In M. C. Vemuri, ed. *Stem Cell Assays*. Stem Cell Assays. Totowa, NJ: Humana Press, pp. 177–208.

Pereira, F.A. et al., 1999. The orphan nuclear receptor COUP-TFII is required for angiogenesis and heart development. *Genes & Development*, 13(8), pp.1037–1049.

Perry, J.M. et al., 2011. Cooperation between both Wnt/{beta}-catenin and PTEN/PI3K/Akt signaling promotes primitive hematopoietic stem cell self-renewal and expansion. *Genes & Development*, 25(18), pp.1928–1942.

Pesce, M. et al., 1993. Stem cell factor and leukemia inhibitory factor promote primordial germ cell survival by suppressing programmed cell death (apoptosis). *Development (Cambridge, England)*, 118(4), pp.1089–1094.

Potocnik, A.J., Brakebusch, C. & Fässler, R., 2000. Fetal and adult hematopoietic stem cells require beta1 integrin function for colonizing fetal liver, spleen, and bone marrow. *Immunity*, 12(6), pp.653–663.

Privratsky, J.R. & Newman, P.J., 2014. PECAM-1: regulator of endothelial junctional integrity. *Cell and tissue research*, 355(3), pp.607–619.

Puri, M.C. & Bernstein, A., 2003. Requirement for the TIE family of receptor tyrosine kinases in adult but not fetal hematopoiesis. *Proceedings of the National Academy of Sciences of the United States of America*, 100(22), pp.12753–12758.

Puri, M.C. et al., 1995. The receptor tyrosine kinase TIE is required for integrity and survival of vascular endothelial cells. *The EMBO Journal*, 14(23), pp.5884–5891.

Qin, J. et al., 2010. COUP-TFII regulates tumor growth and metastasis by modulating tumor angiogenesis. *Proceedings of the National Academy of Sciences of the United States of America*, 107(8), pp.3687–3692.

Rapaport, F. et al., 2013. Comprehensive evaluation of differential gene expression analysis methods for RNA-seq data. *Genome biology*, 14(9), p.R95.

Rettig, M.P., Ansstas, G. & DiPersio, J.F., 2012. Mobilization of Hematopoietic Stem and Progenitor Cells Using Inhibitors of CXCR4 and VLA-4. *Leukemia : official journal of the Leukemia Society of America, Leukemia Research Fund, U.K*, 26(1), pp.34–53.

Rich, I.N., 1995. Primordial germ cells are capable of producing cells of the hematopoietic system in vitro. *Blood*, 86(2), pp.463–472.

Ritchie, M.E. et al., 2015. limma powers differential expression analyses for RNA-sequencing and microarray studies. *Nucleic acids research*, 43(7), pp.e47–e47.

Robert-Moreno, À. et al., 2005. RBPjκ-dependent Notch function regulates Gata2 and is essential for the formation of intra-embryonic hematopoietic cells. *Development (Cambridge, England)*, 132(5), pp.1117–1126.

Robin, C. et al., 2006. An Unexpected Role for IL-3 in the Embryonic Development of Hematopoietic Stem Cells. *Developmental cell*, 11(2), pp.171–180.

Robinson, M.D., McCarthy, D.J. & Smyth, G.K., 2010. edgeR: a Bioconductor package for differential expression analysis of digital gene expression data. *Bioinformatics (Oxford, England)*, 26(1), pp.139–140.

Rodewald, H.R. & Sato, T.N., 1996. Tie1, a receptor tyrosine kinase essential for vascular endothelial cell integrity, is not critical for the development of hematopoietic cells. *Oncogene*, 12(2), pp.397–404.

Rosato, R. et al., 1998. Involvement of the tyrosine kinase fer in cell adhesion. *Molecular and cellular biology*, 18(10), pp.5762–5770.

Rousseau-Plasse, A. et al., 1998. Lisinopril, an angiotensin I-converting enzyme inhibitor, prevents entry of murine hematopoietic stem cells into the cell cycle after irradiation in vivo. *Experimental hematology*, 26(11), pp.1074–1079.

Ruiz-Herguido, C. et al., 2012. Hematopoietic stem cell development requires transient Wnt/β-catenin activity. *Journal of Experimental Medicine*, 209(8), pp.1457–1468.

Rybtsov, S. et al., 2016. Concealed expansion of immature precursors underpins acute burst

of adult HSC activity in foetal liver. *Development (Cambridge, England)*, 143(8), pp.1284–1289.

Rybtsov, S. et al., 2011. Hierarchical organization and early hematopoietic specification of the developing HSC lineage in the AGM region. *The Journal of experimental medicine*, 208(6), pp.1305–1315.

Rybtsov, S. et al., 2014. Tracing the origin of the HSC hierarchy reveals an SCF-dependent, IL-3-independent CD43(-) embryonic precursor. *Stem cell reports*, 3(3), pp.489–501.

Sabin, F.R., 1920. Studies on the origin of blood vessels and of red corpuscles as seen in the living blastoderm of the chick during the second day of incubation. *Contributions to Embryology*, 9, pp.213–262.

Saharinen, P. et al., 2005. Multiple angiopoietin recombinant proteins activate the Tie1 receptor tyrosine kinase and promote its interaction with Tie2. *The Journal of cell biology*, 169(2), pp.239–243.

Sainio, K. & Raatikainen-Ahokas, A., 1999. Mesonephric kidney--a stem cell factory? *International Journal of Developmental Biology*, 43(5), pp.435–439.

Sanchez, M.J. et al., 1996. Characterization of the first definitive hematopoietic stem cells in the AGM and liver of the mouse embryo. *Immunity*, 5(6), pp.513–525.

Sasaki, K. et al., 1996. Absence of fetal liver hematopoiesis in mice deficient in transcriptional coactivator core binding factor beta. *Proceedings of the National Academy of Sciences of the United States of America*, 93(22), pp.12359–12363.

Sato, A. et al., 1998. Characterization of TEK receptor tyrosine kinase and its ligands, Angiopoietins, in human hematopoietic progenitor cells. *International immunology*, 10(8), pp.1217–1227.

Sato, T.N. et al., 1993. Tie-1 and tie-2 define another class of putative receptor tyrosine kinase genes expressed in early embryonic vascular system. *Proceedings of the National Academy of Sciences of the United States of America*, 90(20), pp.9355–9358.

Saxon, L., 1987. *Organogenesis of the Kidney*, Developmental and cell biology series. Cambridge ….

Scharpfenecker, M. et al., 2005. The Tie-2 ligand Angiopoietin-2 destabilizes quiescent endothelium through an internal autocrine loop mechanism. *Journal of Cell Science*, 118(4), pp.771–780.

Schena, M. et al., 1995. Quantitative monitoring of gene expression patterns with a complementary DNA microarray. *Science*, 270(5235), pp.467–470.

Schofield, R., 1978. The relationship between the spleen colony-forming cell and the haemopoietic stem cell. *Blood cells*, 4(1-2), pp.7–25.

Schulz, C. et al., 2012. A Lineage of Myeloid Cells Independent of Myb and Hematopoietic Stem Cells. *Science*, 336(6077), pp.86–90.

Schwiebert, L.M. et al., 2002. Extracellular ATP signaling and P2X nucleotide receptors in

monolayers of primary human vascular endothelial cells. *American journal of physiology. Cell physiology*, 282(2), pp.C289–301.

Scott, B.B. et al., 2005. TNF-α modulates angiopoietin-1 expression in rheumatoid synovial fibroblasts via the NF-κB signalling pathway. *Biochemical and Biophysical Research Communications*, 328(2), pp.409–414.

Sean J Morrison, D.T.S., 2014. The bone marrow niche for haematopoietic stem cells. *Nature*, 505(7483), pp.327–334.

Seita, J. & Weissman, I.L., 2010. Hematopoietic stem cell: self-renewal versus differentiation. *Wiley Interdisciplinary Reviews: Systems Biology and Medicine*, 2(6), pp.640–653.

Sharpless, N.E. & DePinho, R.A., 2007. How stem cells age and why this makes us grow old. *Nature reviews. Molecular cell biology*, 8(9), pp.703–713.

Siekmann, A.F. & Lawson, N.D., 2007. Notch signalling and the regulation of angiogenesis. *Cell adhesion & migration*, 1(2), pp.104–106.

Siminovitch, L., McCulloch, E.A. & Till, J.E., 1963. The distribution of colony-forming cells among spleen colonies. *Journal of Cellular Physiology*, 62(3), pp.327–336.

Sims, D. et al., 2014. Sequencing depth and coverage: key considerations in genomic analyses. *Nature Reviews Genetics*, 15(2), pp.121–132.

Sitnicka, E. et al., 2002. Key role of flt3 ligand in regulation of the common lymphoid progenitor but not in maintenance of the hematopoietic stem cell pool. *Immunity*, 17(4), pp.463–472.

Smith, R.A. & Glomski, C.A., 1982. "Hemogenic endothelium" of the embryonic aorta: Does it exist? *Developmental & Comparative Immunology*, 6(2), pp.359–368.

Solaimani Kartalaei, P. et al., 2015. Whole-transcriptome analysis of endothelial to hematopoietic stem cell transition reveals a requirement for Gpr56 in HSC generation. *The Journal of experimental medicine*, 212(1), pp.93–106.

Souilhol, C., Gonneau, C., et al., 2016. Inductive interactions mediated by interplay of asymmetric signalling underlie development of adult haematopoietic stem cells. *Nature communications*, 7, p.10784.

Souilhol, C., Lendinez, J.G., et al., 2016. Developing HSCs become Notch independent by the end of maturation in the AGM region. *Blood*, 128(12), pp.1567–1577.

Stratmann, A., Risau, W. & Plate, K.H., 1998. Cell Type-Specific Expression of Angiopoietin-1 and Angiopoietin-2 Suggests a Role in Glioblastoma Angiogenesis. *The American journal of pathology*, 153(5), pp.1459–1466.

Sugiyama, D., Arai, K.-I. & Tsuji, K., 2005. Definitive hematopoiesis from acetyl LDL incorporating endothelial cells in the mouse embryo. *Stem cells and development*, 14(6), pp.687–696.

Sun, J. et al., 2014. Clonal dynamics of native haematopoiesis. *Nature*, 514(7522), pp.322–

327.

Suri, C. et al., 1998. Increased Vascularization in Mice Over-expressing Angiopoietin-1. *Science*, 282(5388), pp.468–471.

Suri, C. et al., 1996. Requisite Role of Angiopoietin-1, a Ligand for the TIE2 Receptor, during Embryonic Angiogenesis. *Cell*, 87(7), pp.1171–1180.

Swiers, G. et al., 2013. Early dynamic fate changes in haemogenic endothelium characterized at the single-cell level. *Nature communications*, 4, p.2924.

Takahashi, K., Yamamura, F. & Naito, M., 1989. Differentiation, maturation, and proliferation of macrophages in the mouse yolk sac: a light-microscopic, enzyme-cytochemical, immunohistochemical, and ultrastructural study. *Journal of Leukocyte Biology*, 45(2), pp.87–96.

Takakura, N. et al., 1998. Critical Role of the TIE2 Endothelial Cell Receptor in the Development of Definitive Hematopoiesis. *Immunity*, 9(5), pp.677–686.

Tang, Y. et al., 2010. The contribution of the Tie2+ lineage to primitive and definitive hematopoietic cells. *Genesis (New York, N.Y. : 2000)*, 48(9), pp.563–567.

Taoudi, S. & Medvinsky, A., 2007. Functional identification of the hematopoietic stem cell niche in the ventral domain of the embryonic dorsal aorta. *Proceedings of the National Academy of Sciences of the United States of America*, 104(22), pp.9399–9403.

Taoudi, S. et al., 2008. Extensive hematopoietic stem cell generation in the AGM region via maturation of VE-cadherin+CD45+ pre-definitive HSCs. *Cell stem cell*, 3(1), pp.99–108.

Taoudi, S. et al., 2005. Progressive divergence of definitive haematopoietic stem cells from the endothelial compartment does not depend on contact with the foetal liver. *Development (Cambridge, England)*, 132(18), pp.4179–4191.

Tavian, M. et al., 1996. Aorta-associated CD34+ hematopoietic cells in the early human embryo. *Blood*, 87(1), pp.67–72.

Team, R.S., 2015. *RStudio: Integrated Development for R (RStudio, Inc., Boston, MA, 2015)*, URL: https://www. rstudio. com/products/rstudio.

Thomas, M. et al., 2010. Angiopoietin-2 stimulation of endothelial cells induces alphavbeta3 integrin internalization and degradation. *Journal of Biological Chemistry*, 285(31), pp.23842–23849.

Thurston, G. & Daly, C., 2012. The Complex Role of Angiopoietin-2 in the Angiopoietin–Tie Signaling Pathway. *Cold Spring Harbor Perspectives in Medicine*, 2(9), pp.a006650–a006650.

Thurston, G. et al., 2000. Angiopoietin-1 protects the adult vasculature against plasma leakage. *Nature*.

Thurston, G. et al., 1999. Leakage-resistant blood vessels in mice transgenically over-expressing angiopoietin-1. *Science*, 286(5449), pp.2511–2514.

Till, J.E. & McCulloch, E.A., 2010. A Direct Measurement of the Radiation Sensitivity of Normal Mouse Bone Marrow Cells. *dx.doi.org*, 14(2), p.213.

Toles, J.F. et al., 1989. Hemopoietic stem cells in murine embryonic yolk sac and peripheral blood. *Proceedings of the National Academy of Sciences of the United States of America*, 86(19), pp.7456–7459.

Trapnell, C., Pachter, L. & Salzberg, S.L., 2009. TopHat: discovering splice junctions with RNA-Seq. *Bioinformatics (Oxford, England)*, 25(9), pp.1105–1111.

Travnickova, J. et al., 2015. Primitive macrophages control HSPC mobilization and definitive haematopoiesis. *Nature communications*, 6, p.6227.

Tsai, F.Y. et al., 1994. An early haematopoietic defect in mice lacking the transcription factor GATA-2. *Nature*, 371(6494), pp.221–226.

Tsigkos, S. et al., 2006. Regulation of Ang2 release by PTEN/PI3-kinase/Akt in lung microvascular endothelial cells. *Journal of Cellular Physiology*, 207(2), pp.506–511.

Vaidya, A. & Kale, V.P., 2015. TGF-β signaling and its role in the regulation of hematopoietic stem cells. *Systems and synthetic biology*, 9(1-2), pp.1–10.

Valenzuela, D.M. et al., 1999. Angiopoietins 3 and 4: diverging gene counterparts in mice and humans. *Proceedings of the National Academy of Sciences of the United States of America*, 96(5), pp.1904–1909.

Visnjic, D. et al., 2004. Hematopoiesis is severely altered in mice with an induced osteoblast deficiency. *Blood*, 103(9), pp.3258–3264.

Wang, Q. et al., 1996. Disruption of the Cbfa2 gene causes necrosis and hemorrhaging in the central nervous system and blocks definitive hematopoiesis. *Proceedings of the National Academy of Sciences of the United States of America*, 93(8), pp.3444–3449.

Wang, Z., Gerstein, M. & Snyder, M., 2009. RNA-Seq: a revolutionary tool for transcriptomics. *Nature Reviews Genetics*, 10(1), pp.57–63.

Wasteson, P. et al., 2008. Developmental origin of smooth muscle cells in the descending aorta in mice. *Development (Cambridge, England)*, 135(10), pp.1823–1832.

Wiegreffe, C. et al., 2007. Sclerotomal origin of smooth muscle cells in the wall of the avian dorsal aorta. *Developmental dynamics : an official publication of the American Association of Anatomists*, 236(9), pp.2578–2585.

Wilkinson, R.N. et al., 2009. Hedgehog and Bmp Polarize Hematopoietic Stem Cell Emergence in the Zebrafish Dorsal Aorta. *Developmental cell*, 16(6), pp.909–916.

Wilson, N.K. et al., 2010. Combinatorial transcriptional control in blood stem/progenitor cells: genome-wide analysis of ten major transcriptional regulators. *Cell stem cell*, 7(4), pp.532–544.

Wintour, E.M. et al., 1996. The erythropoietin gene is expressed strongly in the mammalian mesonephric kidney. *Blood*, 88(9), pp.3349–3353.

Wu, A.M. et al., 1967. A cytological study of the capacity for differentiation of normal hemopoietic colony-forming cells. *Journal of Cellular Physiology*, 69(2), pp.177–184.

Wu, A.M. et al., 1968. CYTOLOGICAL EVIDENCE FOR A RELATIONSHIP BETWEEN NORMAL HEMATOPOIETIC COLONY-FORMING CELLS AND CELLS OF THE LYMPHOID SYSTEM. *Journal of Experimental Medicine*, 127(3), pp.455–464.

Xie, X. et al., 2011. Nuclear receptor chicken ovalbumin upstream promoter-transcription factor II (COUP-TFII) modulates mesenchymal cell commitment and differentiation. *Proceedings of the National Academy of Sciences of the United States of America*, 108(36), pp.14843–14848.

Xu, M.-J. et al., 2001. Evidence for the presence of murine primitive megakarycytopoiesis in the early yolk sac. *Blood*, 97(7), pp.2016–2022.

Yano, N. et al., 2007. A novel phosphoinositide 3-kinase-dependent pathway for angiotensin II/AT-1 receptor-mediated induction of collagen synthesis in MES-13 mesangial cells. *Journal of Biological Chemistry*, 282(26), pp.18819–18830.

Yokomizo, T. & Dzierzak, E., 2010. Three-dimensional cartography of hematopoietic clusters in the vasculature of whole mouse embryos. *Development (Cambridge, England)*, 137(21), pp.3651–3661.

You, L.-R. et al., 2005. Suppression of Notch signalling by the COUP-TFII transcription factor regulates vein identity. *Nature*, 435(7038), pp.98–104.

Yu, C.-T. et al., 2012. COUP-TFII is essential for metanephric mesenchyme formation and kidney precursor cell survival. *Development (Cambridge, England)*, 139(13), pp.2330–2339.

Yuan, H.T. et al., 2007. Activation of the orphan endothelial receptor Tie1 modifies Tie2-mediated intracellular signaling and cell survival. *FASEB journal : official publication of the Federation of American Societies for Experimental Biology*, 21(12), pp.3171–3183.

Zhang, C.C. et al., 2006. Angiopoietin-like proteins stimulate ex vivo expansion of hematopoietic stem cells. *Nature medicine*, 12(2), pp.240–245.

Zhang, J. et al., 2003. Identification of the haematopoietic stem cell niche and control of the niche size. *Nature*, 425(6960), pp.836–841.

Zheng, W. et al., 2014. Angiopoietin 2 regulates the transformation and integrity of lymphatic endothelial cell junctions. *Genes & Development*, 28(14), pp.1592–1603.

Zhong, R.K., Astle, C.M. & Harrison, D.E., 1996. Distinct developmental patterns of short-term and long-term functioning lymphoid and myeloid precursors defined by competitive limiting dilution analysis in vivo. *The Journal of Immunology*, 157(1), pp.138–145.

Zhou, F. et al., 2016. Tracing haematopoietic stem cell formation at single-cell resolution. *Nature*, 533(7604), pp.487–492.

Chapter 8 Appendix

8.1 Processed images of statistical correlation between clusters and Ang2 expression

Image: images/1A_1.png

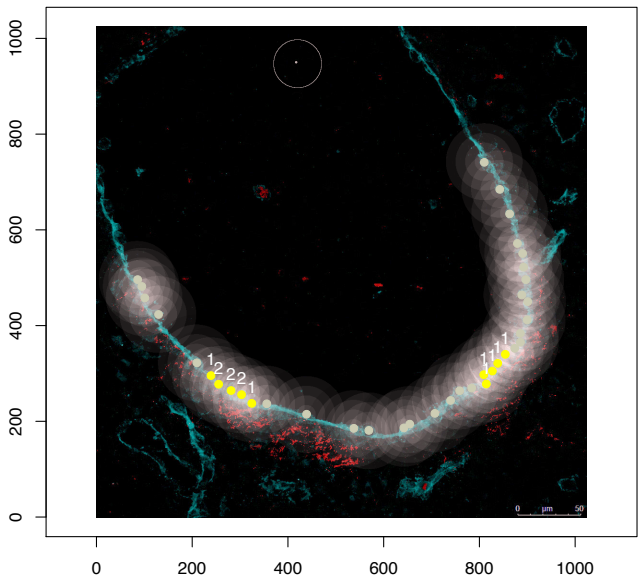

Image: images/1A_3.png

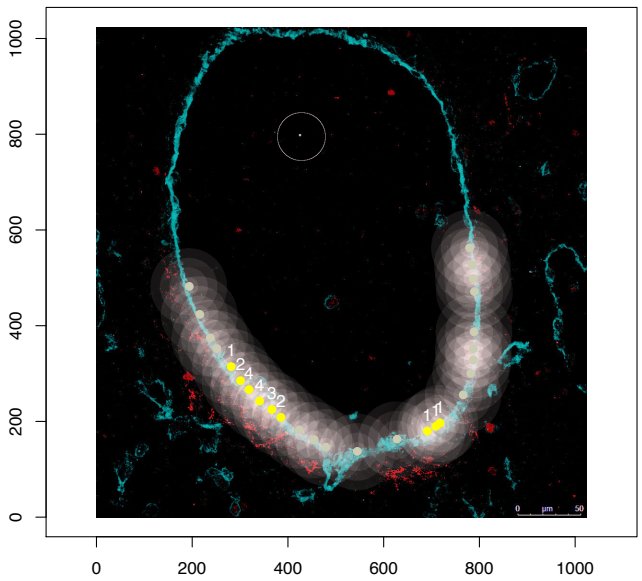

Image: images/1A_4.png

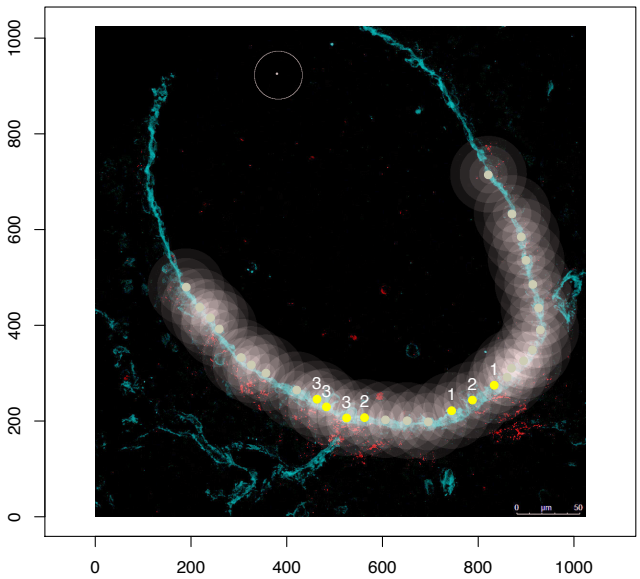

Image: images/1A_5.png

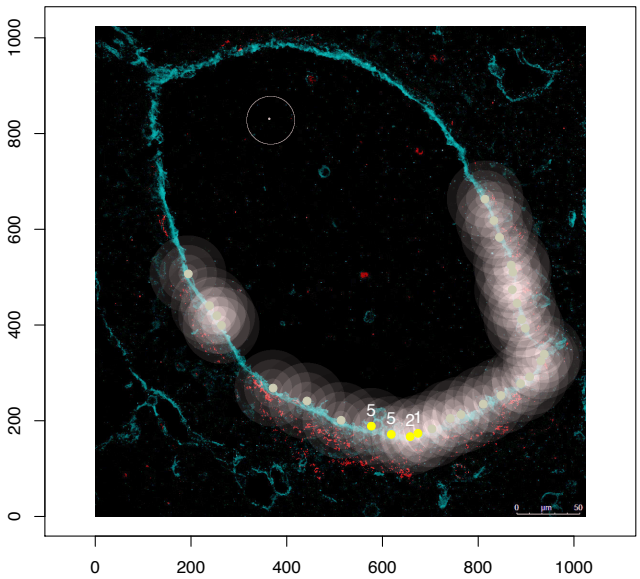

Image: images/1A_6.png

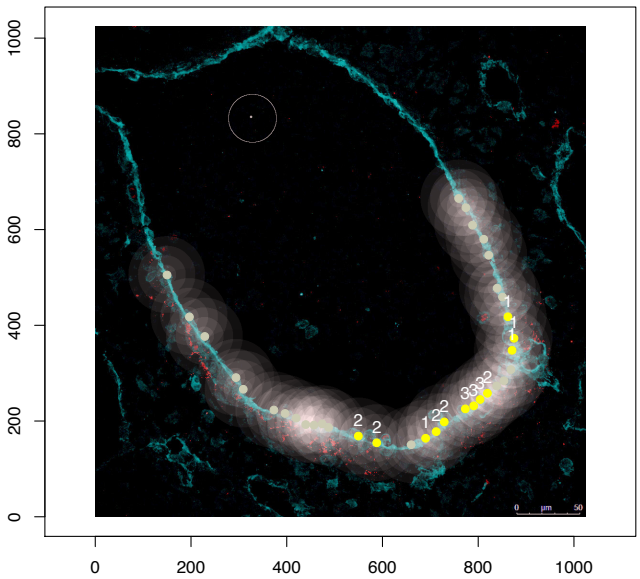

Image: images/1A_7.png

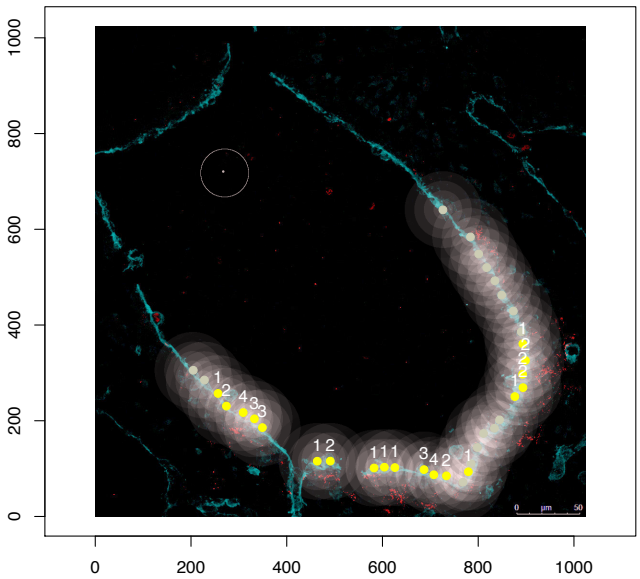

Image: images/2A_3_new.png

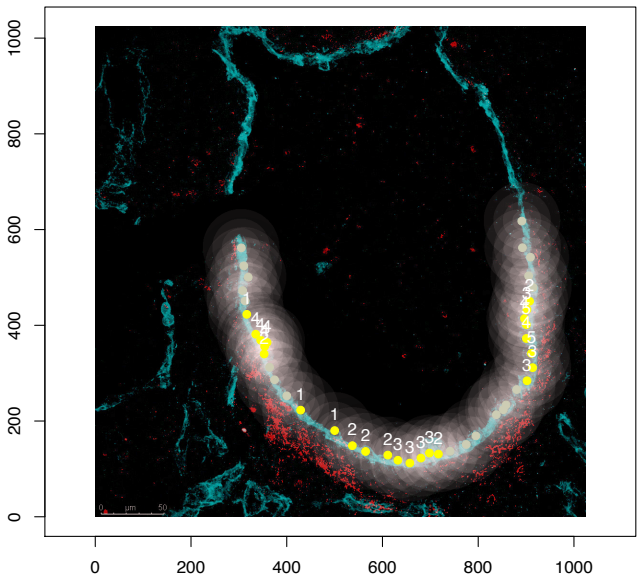

Image: images/2A_5.png

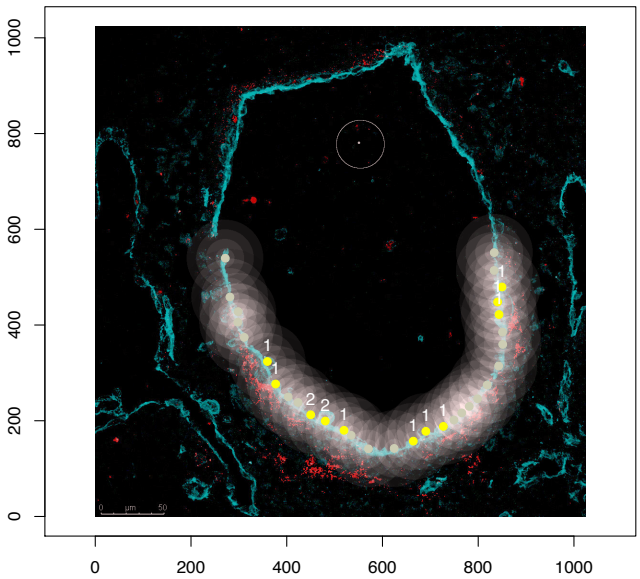

Image: images/2A_6.png

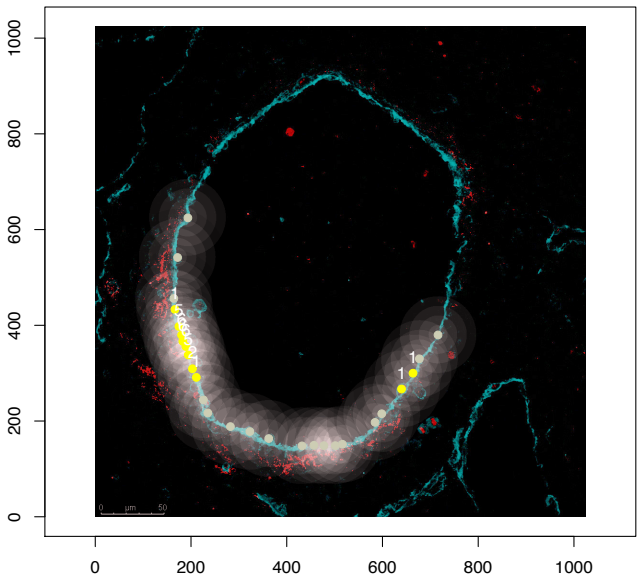

Image: images/2A_8.png

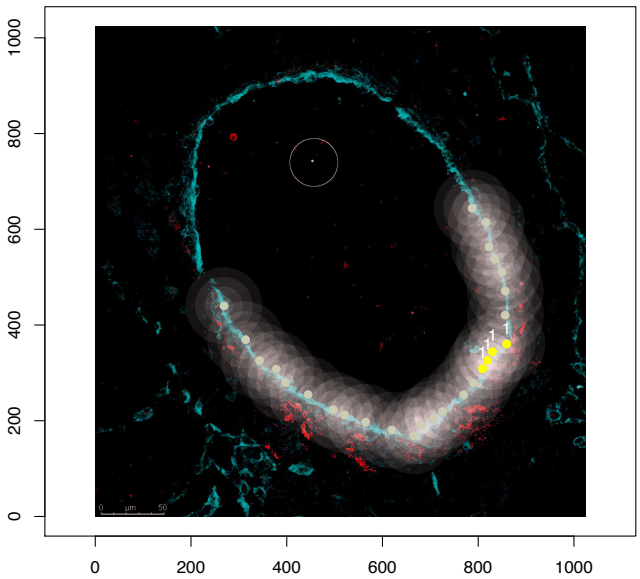

Image: images/3A_2.png

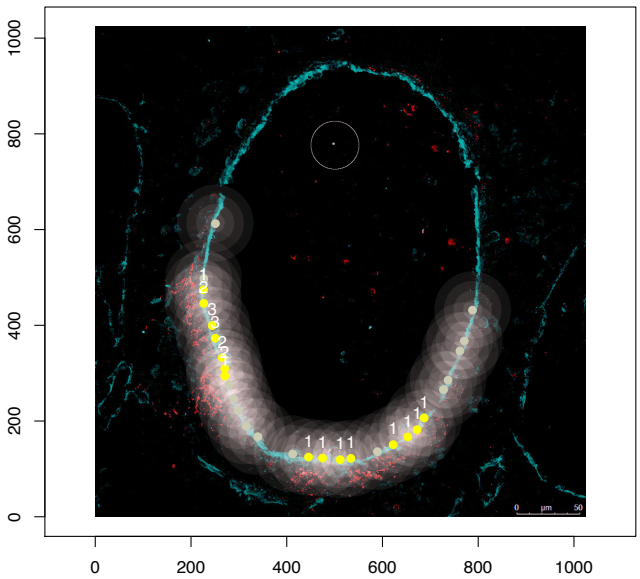

Image: images/3A_3.png

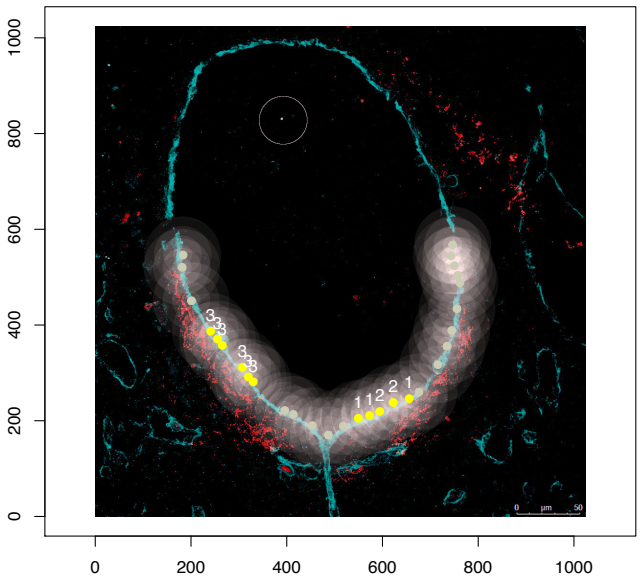

Image: images/3A_6.png

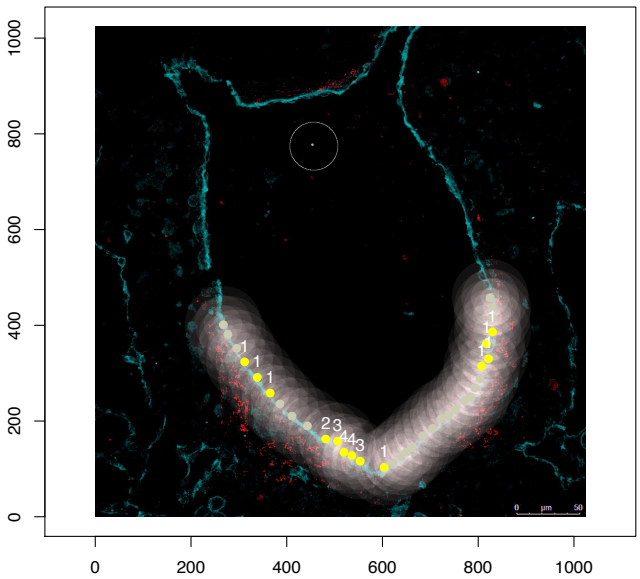

Image: images/4A_6.png

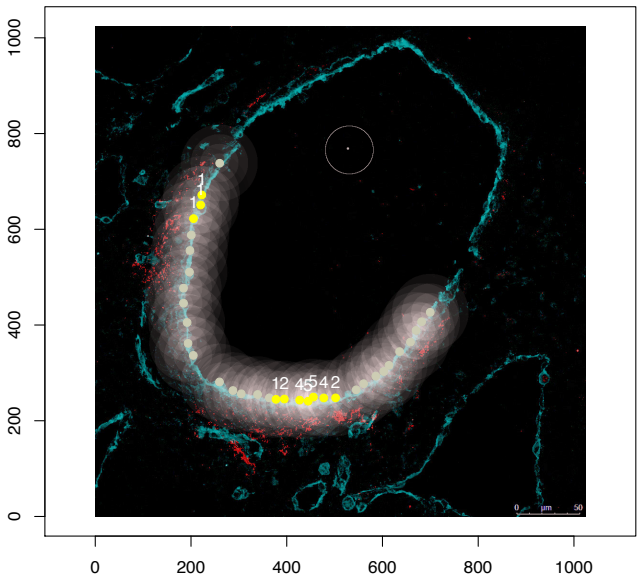

Image: images/4A_7.png

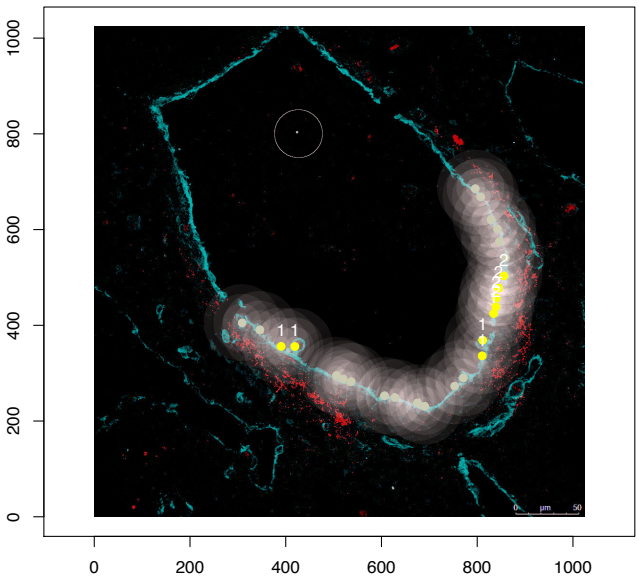

Image: images/5A_2.png

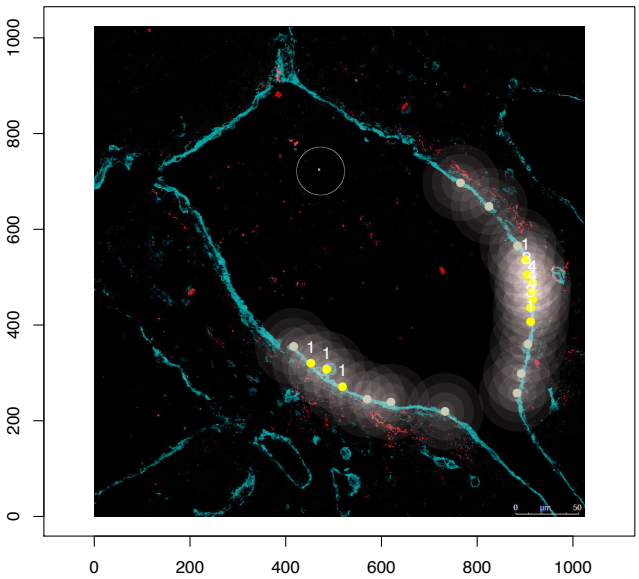

Image: images/5A_4.png

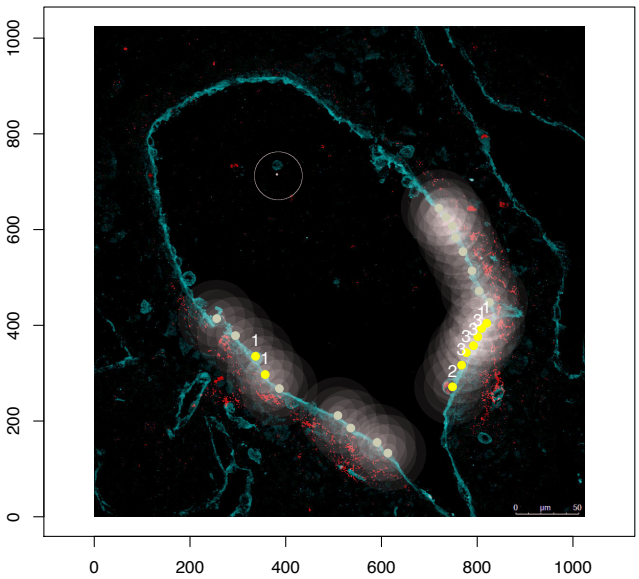

Image: images/DEC_1.png

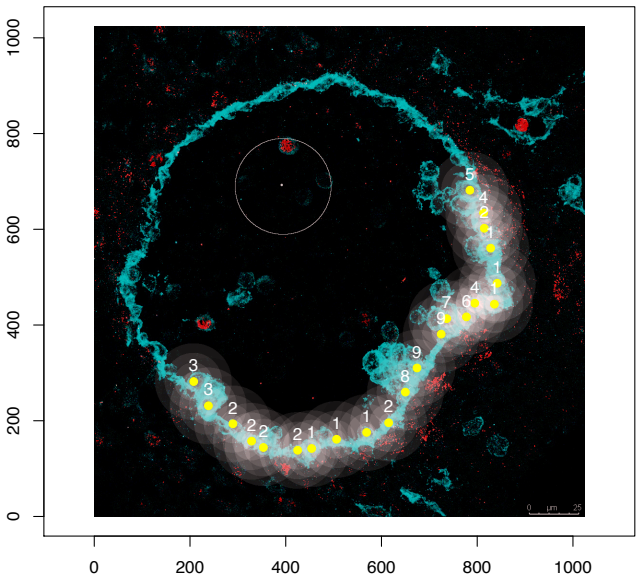

Image: images/DEC_2_yellow.png

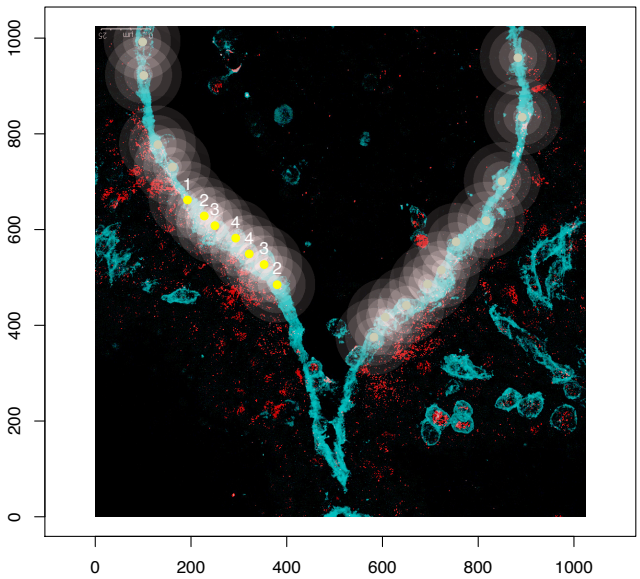

Image: images/DEC_3.png

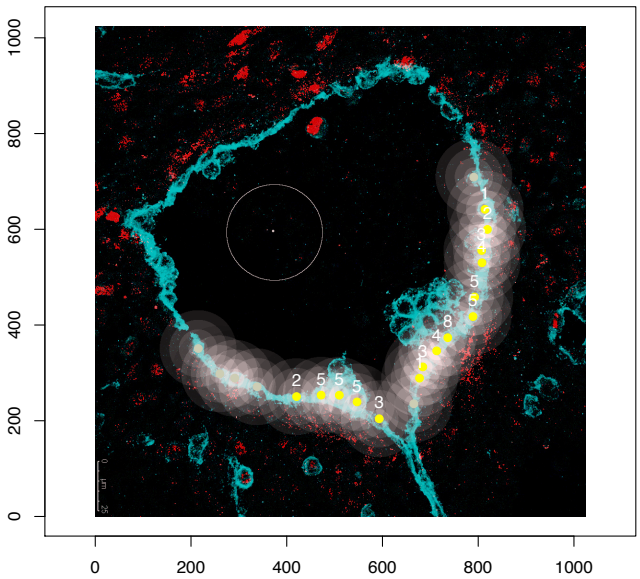

Image: images/DEC_4.png

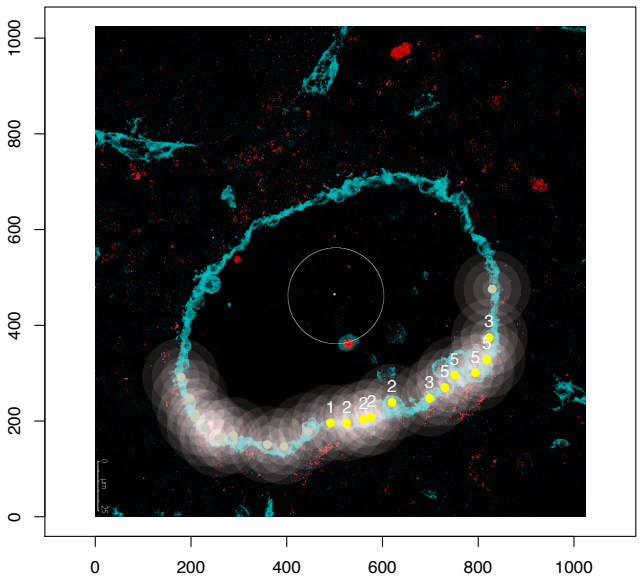

8.2 Differentially expressed genes in pre-HSC-I treated with Ang2 vs ctrl

8.2.1 Up-regulated genes

Ensemble IDs	Gene name	Log_2FC	P-value	Adjusted P-value
ENSMUSG00000043090	Zfp866	8.09	3.02E-22	1.15E-18
ENSMUSG00000061650	Med9	8	1.64E-14	1.44E-11
ENSMUSG00000002871	Tpra1	7.72	1.48E-16	2.11E-13
ENSMUSG00000025077	Dclre1a	7.63	7.94E-14	5.67E-11
ENSMUSG00000051043	Gprc5c	7.53	1.22E-14	1.16E-11
ENSMUSG00000029108	Pcdh7	7.38	3.43E-16	4.35E-13
ENSMUSG00000024970	AI846148	7.19	6.92E-15	7.19E-12
ENSMUSG00000029201	Ugdh	7.19	1.54E-11	6.51E-09
ENSMUSG00000027086	Fastkd1	7.09	1.31E-10	3.84E-08
ENSMUSG00000032531	Amotl2	7.09	2.15E-21	6.15E-18
ENSMUSG00000068966	Zbtb34	7.06	4.10E-14	3.12E-11
ENSMUSG00000030045	Mrpl19	7.03	3.40E-12	1.62E-09
ENSMUSG00000050248	Evc2	7.02	5.94E-17	9.70E-14
ENSMUSG00000047749	Zc3hav1l	7	3.40E-12	1.62E-09
ENSMUSG00000086537	Nespas	6.97	3.93E-11	1.32E-08
ENSMUSG00000021868	Ppif	6.94	1.21E-11	5.31E-09
ENSMUSG00000015290	Ubl4a	6.88	1.24E-12	6.77E-10
ENSMUSG00000048696	Mex3d	6.87	2.74E-13	1.84E-10
ENSMUSG00000045045	Lrfn4	6.82	3.88E-11	1.32E-08
ENSMUSG00000026179	Pnkd	6.68	2.76E-10	7.51E-08
ENSMUSG00000063145	Bbs5	6.64	4.65E-08	7.14E-06
ENSMUSG00000097375	6720427I07Rik	6.63	4.09E-09	8.19E-07
ENSMUSG00000032267	Usp28	6.55	1.41E-12	7.31E-10
ENSMUSG00000021822	Plau	6.52	3.12E-20	7.13E-17
ENSMUSG00000002409	Dyrk1b	6.44	2.53E-11	9.96E-09
ENSMUSG00000028121	Bcar3	6.44	2.58E-10	7.17E-08
ENSMUSG00000026788	Zbtb43	6.43	9.98E-11	3.00E-08
ENSMUSG00000028730	Cfap57	6.43	4.18E-10	1.11E-07
ENSMUSG00000021815	Mss51	6.42	1.97E-08	3.31E-06
ENSMUSG00000028268	Gbp3	6.42	6.06E-08	8.88E-06
ENSMUSG00000024924	Vldlr	6.38	3.32E-13	2.11E-10
ENSMUSG00000032783	Troap	6.37	8.39E-10	2.08E-07
ENSMUSG00000024026	Glo1	6.36	3.46E-09	7.19E-07
ENSMUSG00000004947	Dtx2	6.31	5.25E-11	1.66E-08
ENSMUSG00000036158	Prickle1	6.31	3.08E-11	1.14E-08
ENSMUSG00000024293	Esco1	6.26	5.48E-11	1.69E-08

ENSMUSG00000024824	Rad9a	6.24	2.90E-11	1.10E-08
ENSMUSG00000079108	Srp54b	6.21	3.56E-09	7.25E-07
ENSMUSG00000036523	Greb1	6.18	1.13E-08	2.02E-06
ENSMUSG00000000058	Cav2	6.09	1.04E-07	1.36E-05
ENSMUSG00000030554	Synm	6.06	1.44E-09	3.23E-07
ENSMUSG00000022788	Fgd4	6.04	1.17E-07	1.52E-05
ENSMUSG00000027115	Kif18a	6.04	3.07E-07	3.51E-05
ENSMUSG00000001036	Epn2	6.03	1.05E-12	5.98E-10
ENSMUSG00000023072	Cep89	6.03	1.06E-09	2.46E-07
ENSMUSG00000030861	Acadsb	6.03	7.74E-08	1.09E-05
ENSMUSG00000059897	Zfp930	6.03	1.01E-07	1.34E-05
ENSMUSG00000042202	Slc35e2	6.02	3.68E-11	1.31E-08
ENSMUSG00000028232	Tmem68	6.01	7.44E-09	1.42E-06
ENSMUSG00000039789	Zfp597	6.01	4.69E-08	7.14E-06
ENSMUSG00000060301	2610008E11Rik	6	2.31E-09	5.08E-07
ENSMUSG00000073478	D730003I15Rik	5.99	4.38E-06	0.000340562
ENSMUSG00000046410	Kcnk6	5.93	3.72E-08	5.90E-06
ENSMUSG00000007950	Abhd8	5.83	5.82E-07	6.05E-05
ENSMUSG00000021271	Zfp839	5.83	5.41E-08	8.02E-06
ENSMUSG00000023050	Map3k12	5.83	1.68E-08	2.91E-06
ENSMUSG00000030386	Zfp606	5.82	1.31E-06	0.000117867
ENSMUSG00000040795	Iqcc	5.81	8.68E-08	1.19E-05
ENSMUSG00000034118	Tpst1	5.8	1.75E-07	2.10E-05
ENSMUSG00000036810	Cnep1r1	5.79	3.43E-09	7.19E-07
ENSMUSG00000027164	Traf6	5.73	8.14E-09	1.53E-06
ENSMUSG00000003752	Itpkc	5.71	9.63E-07	9.18E-05
ENSMUSG00000022793	B4galt4	5.7	3.33E-07	3.77E-05
ENSMUSG00000038344	Txlng	5.69	1.01E-09	2.41E-07
ENSMUSG00000021076	Actr10	5.68	2.06E-08	3.41E-06
ENSMUSG00000005107	Slc2a9	5.66	5.62E-07	5.89E-05
ENSMUSG00000021532	Fastkd3	5.65	3.36E-07	3.77E-05
ENSMUSG00000038085	Cnbd2	5.61	4.87E-07	5.20E-05
ENSMUSG00000085148	Mir22hg	5.61	9.82E-07	9.27E-05
ENSMUSG00000024827	Gldc	5.6	2.97E-08	4.78E-06
ENSMUSG00000050357	Carmil2	5.59	4.79E-07	5.16E-05
ENSMUSG00000102850	Gm37082	5.57	8.75E-08	1.19E-05
ENSMUSG00000026664	Phyh	5.55	1.59E-06	0.000140689
ENSMUSG00000029402	Snrnp35	5.55	9.65E-07	9.18E-05
ENSMUSG00000028101	Pias3	5.54	5.56E-07	5.88E-05
ENSMUSG00000056124	B4galt6	5.54	8.56E-08	1.19E-05
ENSMUSG00000024168	Tmem204	5.53	6.22E-08	9.00E-06
ENSMUSG00000090093	Gm14399	5.51	8.12E-07	8.00E-05
ENSMUSG00000026784	Pdss1	5.5	1.72E-06	0.000150326
ENSMUSG00000027939	Nup210l	5.5	4.03E-07	4.43E-05

ENSMUSG00000066595	Mfsd7b	5.47	6.61E-07	6.74E-05
ENSMUSG00000048186	Bend7	5.45	1.13E-05	0.000736248
ENSMUSG00000073758	Sh3d21	5.44	8.40E-06	0.000574555
ENSMUSG00000002688	Prkd1	5.39	1.31E-08	2.30E-06
ENSMUSG00000045691	Thtpa	5.39	1.29E-06	0.000116577
ENSMUSG00000096929	A330023F24Rik	5.38	1.92E-08	3.27E-06
ENSMUSG00000007872	Id3	5.37	8.49E-09	1.56E-06
ENSMUSG00000034731	Dgkh	5.36	5.98E-13	3.59E-10
ENSMUSG00000021411	Pxdc1	5.35	1.63E-06	0.000143507
ENSMUSG00000092416	Zfp141	5.35	6.50E-06	0.000469592
ENSMUSG00000035505	Cox18	5.34	3.35E-06	0.000279143
ENSMUSG00000054893	Zfp667	5.29	7.49E-06	0.000524799
ENSMUSG00000063455	D630045J12Rik	5.29	1.73E-07	2.10E-05
ENSMUSG00000005580	Adcy9	5.25	2.42E-06	0.0002064
ENSMUSG00000024193	Phf1	5.25	2.24E-06	0.000192772
ENSMUSG00000073139	Tmem185a	5.23	6.79E-07	6.87E-05
ENSMUSG00000002732	Fkbp7	5.22	3.81E-06	0.000310911
ENSMUSG00000110393	Gm36445	5.22	9.50E-06	0.000646215
ENSMUSG00000066042	Med18	5.19	4.66E-06	0.000359522
ENSMUSG00000070031	Sp140	5.19	6.37E-05	0.003276115
ENSMUSG00000053965	Pde5a	5.17	1.15E-05	0.000748316
ENSMUSG00000090137	Uba52	5.16	1.56E-07	1.96E-05
ENSMUSG00000048731	Ggnbp1	5.15	3.52E-05	0.001991768
ENSMUSG00000034685	Fam171a2	5.13	1.92E-07	2.28E-05
ENSMUSG00000079557	Mar-02	5.12	6.78E-06	0.000487387
ENSMUSG00000033256	Shf	5.09	2.53E-05	0.001514512
ENSMUSG00000028959	Fastk	5.06	4.20E-08	6.57E-06
ENSMUSG00000000915	Hip1r	5.03	8.31E-07	8.11E-05
ENSMUSG00000063849	Ppcdc	5.03	6.38E-06	0.00046425
ENSMUSG00000078122	F630028O10Rik	5.03	0.000140825	0.006459866
ENSMUSG00000035578	Iqcg	5.02	2.14E-05	0.001306409
ENSMUSG00000055128	Cgrrf1	5.01	1.99E-05	0.001238406
ENSMUSG00000041729	Coro2b	4.98	4.74E-07	5.16E-05
ENSMUSG00000064284	Cdpf1	4.98	4.99E-05	0.002676793
ENSMUSG00000009772	Nuak2	4.94	6.92E-05	0.003527691
ENSMUSG00000020303	Stc2	4.94	4.85E-05	0.002623163
ENSMUSG00000027935	Rab13	4.94	5.02E-06	0.000382333
ENSMUSG00000004105	Angptl2	4.91	1.60E-05	0.001011431
ENSMUSG00000026721	Rabgap1l	4.91	6.17E-06	0.000452769
ENSMUSG00000070822	Zscan18	4.91	7.10E-06	0.000503436
ENSMUSG00000056665	Them6	4.81	0.000272615	0.011120761
ENSMUSG00000024160	Spsb3	4.8	0.000116017	0.005430905
ENSMUSG00000003062	Stard3nl	4.79	5.10E-05	0.002722713

ENSMUSG00000114193	AC122828.4	4.75	0.000120341	0.005587562
ENSMUSG00000032125	Robo4	4.74	1.24E-06	0.000114298
ENSMUSG00000033460	Armcx1	4.74	2.15E-08	3.51E-06
ENSMUSG00000045237	1110012L19Rik	4.74	4.17E-05	0.002301013
ENSMUSG00000020262	Adarb1	4.73	1.72E-07	2.10E-05
ENSMUSG00000037260	Hgsnat	4.73	5.21E-06	0.000394125
ENSMUSG00000027474	Ccm2l	4.72	1.69E-05	0.001057076
ENSMUSG00000040040	Ift88	4.71	1.03E-05	0.000680821
ENSMUSG00000051379	Flrt3	4.71	2.64E-05	0.001571332
ENSMUSG00000048406	B330016D10Rik	4.67	0.000187911	0.008194139
ENSMUSG00000112963	AL513022.1	4.67	0.000394799	0.01498138
ENSMUSG00000061118	Dnajc30	4.6	0.000167193	0.007488953
ENSMUSG00000047098	Rnf31	4.58	3.11E-05	0.001800522
ENSMUSG00000023809	Rps6ka2	4.55	4.93E-08	7.41E-06
ENSMUSG00000032122	Slc37a2	4.55	4.65E-05	0.002528215
ENSMUSG00000036867	Smad6	4.54	3.81E-05	0.002111227
ENSMUSG00000024892	Pcx	4.53	0.000105713	0.005010171
ENSMUSG00000050555	Hyls1	4.53	0.000187959	0.008194139
ENSMUSG00000028698	Pik3r3	4.52	7.68E-06	0.000534805
ENSMUSG00000034220	Gpc1	4.51	2.41E-05	0.001459031
ENSMUSG00000030035	Wbp1	4.49	0.000113588	0.005360997
ENSMUSG00000032109	Nlrx1	4.49	0.000654794	0.022595343
ENSMUSG00000020682	Mmp28	4.46	5.96E-05	0.003092552
ENSMUSG00000015846	Rxra	4.45	3.80E-05	0.002111227
ENSMUSG00000037730	Mynn	4.45	3.96E-06	0.000319483
ENSMUSG00000036966	Spryd3	4.41	9.15E-05	0.004414727
ENSMUSG00000042035	Igsf3	4.38	3.27E-05	0.001885714
ENSMUSG00000068114	Ccdc134	4.37	0.00031322	0.012391561
ENSMUSG00000030688	Stard10	4.36	0.000372351	0.014319853
ENSMUSG00000025993	Slc40a1	4.35	0.000337615	0.013116459
ENSMUSG00000107881	Gm44250	4.35	7.74E-05	0.003876248
ENSMUSG00000041654	Slc39a11	4.34	0.000314617	0.012391561
ENSMUSG00000024164	C3	4.32	7.98E-05	0.00398047
ENSMUSG00000044502	Bod1	4.32	0.00024655	0.010277728
ENSMUSG00000044339	Alkbh2	4.31	0.000384831	0.01470081
ENSMUSG00000066829	Zfp810	4.31	0.000294496	0.011802583
ENSMUSG00000039683	Sdk1	4.3	0.00051382	0.018690883
ENSMUSG00000024875	Yif1a	4.27	0.000170582	0.007610872
ENSMUSG00000030145	Zfp248	4.25	1.10E-05	0.000722019
ENSMUSG00000036036	Zfp57	4.25	3.06E-05	0.001785928
ENSMUSG00000039911	Spsb1	4.25	0.000388178	0.014779231
ENSMUSG00000049521	Cdc42ep1	4.25	9.20E-09	1.67E-06
ENSMUSG00000028364	Tnc	4.24	6.72E-05	0.003442295
ENSMUSG00000045251	Zfp688	4.24	0.00022687	0.009705263

ENSMUSG00000075229	Ccdc58	4.23	8.86E-05	0.004360053
ENSMUSG00000031262	Cenpi	4.22	2.24E-07	2.64E-05
ENSMUSG00000001844	Zdhhc4	4.19	8.09E-05	0.004018726
ENSMUSG00000102428	Pcdhga12	4.19	0.000397552	0.015035895
ENSMUSG00000067787	Blcap	4.18	6.44E-08	9.20E-06
ENSMUSG00000034714	Ttyh2	4.17	0.000627986	0.021868477
ENSMUSG00000059142	Zfp945	4.15	0.000302085	0.012022352
ENSMUSG00000021190	Lgmn	4.14	3.58E-05	0.002011621
ENSMUSG00000031433	Rbm41	4.14	0.000596147	0.021212421
ENSMUSG00000074220	Zfp382	4.14	0.000676195	0.023193689
ENSMUSG00000000325	Arvcf	4.11	0.00033049	0.012883474
ENSMUSG00000024663	Rab3il1	4.11	0.000180103	0.007942593
ENSMUSG00000031292	Cdkl5	4.11	8.58E-07	8.31E-05
ENSMUSG00000053541	Gm4759	4.11	0.000549049	0.019845701
ENSMUSG00000046447	Camk2n1	4.1	0.000796238	0.026059121
ENSMUSG00000037148	Arhgap10	4.09	8.77E-05	0.004337611
ENSMUSG00000102324	Gm19721	4.08	0.001287064	0.03838342
ENSMUSG00000021268	Meg3	4.07	1.06E-11	4.83E-09
ENSMUSG00000045867	Cradd	4.07	0.001346461	0.039535411
ENSMUSG00000038880	Mrps34	4.05	5.33E-05	0.002806456
ENSMUSG00000050730	Arhgap42	4.05	0.000197573	0.008548018
ENSMUSG00000030400	Ercc2	4.04	0.000165965	0.007463181
ENSMUSG00000034312	Iqsec1	4.04	1.26E-06	0.000114779
ENSMUSG00000050846	Zfp623	4.03	0.000152587	0.006916088
ENSMUSG00000058729	Lin9	4.01	0.000180867	0.007945623
ENSMUSG00000018900	Slc22a5	3.98	0.00159762	0.045056828
ENSMUSG00000028690	Mmachc	3.98	0.001109239	0.034522408
ENSMUSG00000038151	Prdm1	3.98	7.98E-06	0.00055212
ENSMUSG00000028576	Ift74	3.97	7.14E-05	0.003624133
ENSMUSG00000010721	Lmbr1	3.96	0.001264772	0.037959123
ENSMUSG00000004994	Ccdc130	3.95	0.000737946	0.02466983
ENSMUSG00000046230	Vps13a	3.95	7.29E-06	0.000513876
ENSMUSG00000024446	Rpp21	3.94	0.001032932	0.032501792
ENSMUSG00000047603	Zfp235	3.94	0.001199206	0.036623866
ENSMUSG00000039990	Edrf1	3.88	0.000240476	0.0102204
ENSMUSG00000072294	Klf12	3.87	0.001586919	0.0448658
ENSMUSG00000039199	Zdhhc1	3.86	0.00149177	0.042811557
ENSMUSG00000029569	Tmem168	3.84	0.000808863	0.026246698
ENSMUSG00000020974	Pole2	3.83	0.000852315	0.027269303
ENSMUSG00000036285	Noa1	3.81	0.000599445	0.021249692
ENSMUSG00000090919	Pabpc4l	3.81	0.001471338	0.042545892
ENSMUSG00000024887	Asah2	3.78	0.000708433	0.02394002
ENSMUSG00000022792	Yars2	3.77	0.000323797	0.01267716
ENSMUSG00000024242	Map4k3	3.76	0.001092403	0.034184738

ENSMUSG00000097048	1600020E01Rik	3.76	0.001637161	0.045945093
ENSMUSG00000023908	Pkmyt1	3.73	0.000909239	0.028928493
ENSMUSG00000028999	Rint1	3.72	3.05E-07	3.51E-05
ENSMUSG00000022515	Anks3	3.71	0.001083948	0.03401332
ENSMUSG00000047909	Ankrd16	3.7	0.000913666	0.028988592
ENSMUSG00000021796	Bmpr1a	3.69	7.20E-07	7.21E-05
ENSMUSG00000045071	E130308A19Rik	3.69	2.12E-05	0.001306409
ENSMUSG00000031983	2310022B05Rik	3.68	0.00028107	0.011344091
ENSMUSG00000041961	Znrf3	3.68	0.000756469	0.025044589
ENSMUSG00000028218	Fam92a	3.66	0.000197207	0.008548018
ENSMUSG00000024845	Tmem134	3.65	0.000617589	0.021704924
ENSMUSG00000026694	Mettl13	3.63	1.66E-05	0.001040665
ENSMUSG00000029161	Cgref1	3.59	0.001196251	0.036623866
ENSMUSG00000035171	1110059E24Rik	3.58	0.000245631	0.010277728
ENSMUSG00000037325	Bbs7	3.58	0.001832755	0.049842197
ENSMUSG00000028648	Ndufs5	3.57	3.50E-05	0.001991768
ENSMUSG00000022747	St3gal6	3.55	3.51E-05	0.001991768
ENSMUSG00000025871	4833439L19Rik	3.55	9.91E-07	9.28E-05
ENSMUSG00000042607	Asb4	3.54	0.001105551	0.034501642
ENSMUSG00000023791	Pigx	3.53	0.001175352	0.036088367
ENSMUSG00000021252	Erg28	3.46	0.000135879	0.006283463
ENSMUSG00000004383	Large1	3.45	0.000504192	0.018600508
ENSMUSG00000042439	Zfp532	3.42	2.89E-05	0.001711057
ENSMUSG00000058240	Cryzl1	3.41	0.000298579	0.011924378
ENSMUSG00000066149	Cdc26	3.37	7.30E-05	0.003675363
ENSMUSG00000022295	Atp6v1c1	3.36	9.81E-06	0.000655433
ENSMUSG00000076435	Acsf2	3.35	0.000832989	0.026876841
ENSMUSG00000041734	Kirrel	3.34	4.96E-05	0.00267234
ENSMUSG00000026273	Mterf4	3.33	0.000755409	0.025044589
ENSMUSG00000000409	Lck	3.31	0.000265287	0.010961749
ENSMUSG00000049960	Mrps16	3.28	9.16E-05	0.004414727
ENSMUSG00000022883	Robo1	3.23	6.17E-09	1.19E-06
ENSMUSG00000062190	Lancl2	3.22	0.000240701	0.0102204
ENSMUSG00000027087	Itgav	3.21	7.74E-07	7.68E-05
ENSMUSG00000037685	Atp8a1	3.13	0.00069442	0.023676602
ENSMUSG00000008035	Mid1ip1	3.11	1.48E-05	0.00094422
ENSMUSG00000033411	Ctdspl2	3.11	9.72E-06	0.000653361
ENSMUSG00000040856	Dlk1	3.09	0.001257557	0.037899266
ENSMUSG00000028134	Ptbp2	3.06	0.000271998	0.011120761
ENSMUSG00000041773	Enc1	3.06	0.000271995	0.011120761
ENSMUSG00000040738	Ints8	3.05	0.000437672	0.016390467
ENSMUSG00000046324	Ermp1	2.99	1.48E-05	0.00094422
ENSMUSG00000079109	Pms2	2.98	0.000246144	0.010277728
ENSMUSG00000038563	Efl1	2.93	3.42E-06	0.000283453

ENSMUSG00000040848	Sft2d2	2.9	0.001412924	0.041064672
ENSMUSG00000018574	Acadvl	2.84	0.001238597	0.037525877
ENSMUSG00000022105	Rb1	2.84	2.93E-05	0.001726417
ENSMUSG00000021458	2010111I01Rik	2.81	0.000165954	0.007463181
ENSMUSG00000063800	Prpf38a	2.77	0.000365742	0.014161042
ENSMUSG00000038188	Scarf1	2.74	4.74E-06	0.000363466
ENSMUSG00000030022	Adamts9	2.73	0.001488095	0.042811557
ENSMUSG00000039523	Cep104	2.68	0.001295533	0.038535373
ENSMUSG00000024349	Tmem173	2.62	0.000603016	0.021258159
ENSMUSG00000028256	Odf2l	2.59	8.92E-05	0.00437343
ENSMUSG00000031365	Zfp275	2.58	9.69E-06	0.000653361
ENSMUSG00000058709	Egln2	2.58	0.000794108	0.026059121
ENSMUSG00000071074	Yipf3	2.58	0.000578743	0.020722275
ENSMUSG00000000605	Clcn4	2.57	0.000408393	0.015394938
ENSMUSG00000020653	Klf11	2.57	0.000373697	0.01432338
ENSMUSG00000023942	Slc29a1	2.57	0.001711235	0.047789067
ENSMUSG00000074794	Arrdc3	2.56	6.49E-07	6.67E-05
ENSMUSG00000022507	1810013L24Rik	2.54	0.001223629	0.037170988
ENSMUSG00000030982	9030624J02Rik	2.5	3.48E-07	3.86E-05
ENSMUSG00000034601	2700049A03Rik	2.48	0.000279453	0.01131884
ENSMUSG00000038102	Trappc11	2.47	9.12E-05	0.004414727
ENSMUSG00000028884	Rpa2	2.45	0.000215623	0.009258814
ENSMUSG00000023805	Synj2	2.35	0.001722756	0.047876679
ENSMUSG00000027490	E2f1	2.35	0.000275435	0.011195814
ENSMUSG00000034135	Sik3	2.35	2.14E-05	0.001306409
ENSMUSG00000038456	Dennd2a	2.32	0.001733929	0.048070237
ENSMUSG00000005505	Kbtbd4	2.3	0.001216004	0.037037849
ENSMUSG00000022994	Adcy6	2.29	3.80E-06	0.000310911
ENSMUSG00000028245	Nsmaf	2.21	3.48E-05	0.001991768
ENSMUSG00000037712	Fermt2	2.15	0.000956264	0.030172494
ENSMUSG00000032826	Ank2	2.12	4.23E-05	0.00232276
ENSMUSG00000109324	Prmt1	2.07	0.001158311	0.035818897
ENSMUSG00000076432	Ywhaq	2.06	0.001341406	0.039535411
ENSMUSG00000021555	Naa35	1.97	0.000453576	0.016875385
ENSMUSG00000041747	Utp15	1.93	0.000917968	0.029044399
ENSMUSG00000023495	Pcbp4	1.92	0.000114054	0.005360997
ENSMUSG00000000378	Ccm2	1.91	0.001399261	0.04077132
ENSMUSG00000000127	Fer	1.9	0.000841242	0.027066676
ENSMUSG00000057469	E2f6	1.9	0.000653443	0.022595343
ENSMUSG00000044562	Rasip1	1.78	3.02E-06	0.000255182
ENSMUSG00000055013	Agap1	1.73	0.000641533	0.022272297
ENSMUSG00000020134	Peli1	1.72	0.000775431	0.025598199
ENSMUSG00000061887	Ssbp3	1.68	0.001831971	0.049842197
ENSMUSG00000006024	Napa	1.59	0.000806395	0.026246698

ENSMUSG00000037851	Iars	1.53	0.000671657	0.023107413
ENSMUSG00000045763	Basp1	1.5	0.000701613	0.02385065

8.2.2 Down-regulated genes

Ensemble IDs	Gene name	Log_2FC	P-value	Adjusted P-value
ENSMUSG00000021904	Sema3g	-7.79	4.53E-24	5.17E-20
ENSMUSG00000027811	4930579G24Rik	-7.19	1.71E-10	4.88E-08
ENSMUSG00000023243	Kcnk5	-6.86	4.34E-15	4.96E-12
ENSMUSG00000015542	Nat9	-6.76	1.13E-09	2.58E-07
ENSMUSG00000027583	Zbtb46	-6.72	4.06E-14	3.12E-11
ENSMUSG00000003721	Insig2	-6.28	2.39E-09	5.15E-07
ENSMUSG00000052155	Acvr2a	-6.28	7.79E-10	1.98E-07
ENSMUSG00000031709	Tbc1d9	-6.2	1.60E-11	6.51E-09
ENSMUSG00000041241	Mul1	-6.13	4.16E-09	8.20E-07
ENSMUSG00000011256	Adam19	-6.06	3.82E-20	7.28E-17
ENSMUSG00000021573	Tppp	-5.83	9.80E-08	1.32E-05
ENSMUSG00000053846	Lipg	-5.83	6.79E-10	1.76E-07
ENSMUSG00000027843	Ptpn22	-5.82	7.05E-06	0.000503276
ENSMUSG00000033233	Trim45	-5.69	1.51E-07	1.92E-05
ENSMUSG00000022240	Ctnnd2	-5.56	2.62E-07	3.05E-05
ENSMUSG00000111291	AC124577.3	-5.18	4.35E-06	0.000340562
ENSMUSG00000072647	Adam1a	-5	5.77E-06	0.00043072
ENSMUSG00000047044	D030056L22Rik	-4.88	0.000146254	0.006682056
ENSMUSG00000032192	Gnb5	-4.84	6.25E-05	0.003232037
ENSMUSG00000022528	Hes1	-4.73	4.29E-05	0.002345439
ENSMUSG00000037032	Apbb1	-4.66	0.000148756	0.006769284
ENSMUSG00000071669	Snx29	-4.63	8.30E-06	0.000571287
ENSMUSG00000031955	Bcar1	-4.6	1.52E-06	0.000136046
ENSMUSG00000062310	Glrp1	-4.58	0.000513827	0.018690883
ENSMUSG00000071176	Arhgef10	-4.58	4.17E-06	0.00033042
ENSMUSG00000027200	Sema6d	-4.45	2.70E-23	1.54E-19
ENSMUSG00000097141	Gm10524	-4.34	0.000313737	0.012391561
ENSMUSG00000045287	Rtn4rl1	-4.21	0.001393941	0.0407202
ENSMUSG00000062184	Hs6st2	-4.19	7.22E-05	0.003646659
ENSMUSG00000056145	AI504432	-4.13	0.000807996	0.026246698
ENSMUSG00000102674	8030442B05Rik	-4.11	0.001569649	0.044598337
ENSMUSG00000045854	Lyrm2	-4.1	0.000505926	0.018600508
ENSMUSG00000026853	Crat	-4.08	0.000119946	0.005587562
ENSMUSG00000029759	Pon3	-3.99	0.00037029	0.01428871
ENSMUSG00000029121	Crmp1	-3.98	1.66E-07	2.06E-05
ENSMUSG00000028899	Taf12	-3.8	0.000560794	0.020206288
ENSMUSG00000034744	Nagk	-3.77	0.000624039	0.021797477
ENSMUSG00000028016	Ints12	-3.56	9.92E-05	0.004742603
ENSMUSG00000021967	Mrpl57	-3.46	4.00E-06	0.000319483

ENSMUSG00000022469	Rapgef3	-3.46	4.55E-11	1.48E-08
ENSMUSG00000039611	Tmem246	-3.37	0.000506458	0.018600508
ENSMUSG00000003865	Gys1	-3.36	9.32E-05	0.004471874
ENSMUSG00000028647	Mycbp	-3.35	0.000564408	0.020272545
ENSMUSG00000047146	Tet1	-3.26	2.41E-05	0.001459031
ENSMUSG00000013076	Amotl1	-3.21	1.01E-09	2.41E-07
ENSMUSG00000053110	Yap1	-3.09	0.00180079	0.049325245
ENSMUSG00000038822	Hace1	-3.02	0.001739228	0.048100389
ENSMUSG00000033400	Agl	-3.01	0.001432614	0.041531248
ENSMUSG00000024975	Pdcd4	-2.98	1.51E-05	0.000956219
ENSMUSG00000030287	Itpr2	-2.97	0.00126619	0.037959123
ENSMUSG00000071757	Zhx2	-2.87	5.56E-06	0.000417593
ENSMUSG00000036902	Neto2	-2.86	0.001170258	0.036028804
ENSMUSG00000035314	Gdpd5	-2.84	2.01E-06	0.000174262
ENSMUSG00000006527	Sfmbt1	-2.82	0.000101104	0.004811714
ENSMUSG00000043065	Spice1	-2.82	0.000292043	0.011745462
ENSMUSG00000055639	Dach1	-2.78	0.000206207	0.008887921
ENSMUSG00000071637	Cebpd	-2.78	8.97E-05	0.004378715
ENSMUSG00000025269	Apex2	-2.75	3.72E-05	0.002080757
ENSMUSG00000028669	Pithd1	-2.72	0.000600915	0.021249692
ENSMUSG00000030604	Zfp626	-2.67	0.000547445	0.019845701
ENSMUSG00000040451	Sgms1	-2.52	5.53E-05	0.002895615
ENSMUSG00000031681	Smad1	-2.48	0.000176006	0.007822346
ENSMUSG00000074211	Sdhaf1	-2.44	0.000738669	0.02466983
ENSMUSG00000060904	Arl1	-2.34	0.000453186	0.016875385
ENSMUSG00000059772	Slx1b	-2.33	0.001568365	0.044598337
ENSMUSG00000070871	Ccnyl1	-2.31	0.001718153	0.047865242
ENSMUSG00000040435	Ppp1r15a	-2.3	0.000140229	0.006458455
ENSMUSG00000019947	Arid5b	-2.28	0.000476575	0.017673516
ENSMUSG00000063894	Zkscan8	-2.26	0.000584211	0.02085267
ENSMUSG00000031631	Cfap97	-2.23	0.000720236	0.024195684
ENSMUSG00000002996	Hbp1	-2.19	0.000265838	0.010961749
ENSMUSG00000026814	Eng	-2.16	3.99E-06	0.000319483
ENSMUSG00000002900	Lamb1	-2.13	3.06E-05	0.001785928
ENSMUSG00000024422	Dhx16	-2.07	0.000409781	0.015396437
ENSMUSG00000072704	Smim10l1	-2.05	5.66E-05	0.002952522
ENSMUSG00000026355	Mcm6	-2.03	3.14E-06	0.000263584
ENSMUSG00000027981	Rnpc3	-2.02	0.001343219	0.039535411
ENSMUSG00000024238	Zeb1	-2	1.48E-07	1.90E-05
ENSMUSG00000034621	Gpatch8	-1.98	5.22E-05	0.002774428
ENSMUSG00000037926	Ssh2	-1.88	1.31E-05	0.000844725
ENSMUSG00000022438	Parvb	-1.87	1.05E-06	9.76E-05
ENSMUSG00000006386	Tek	-1.86	2.47E-05	0.001483887
ENSMUSG00000025597	Klhl4	-1.86	6.10E-06	0.000452656

ENSMUSG00000019578	Ubxn6	-1.85	0.001758331	0.048456352
ENSMUSG00000022136	Dnajc3	-1.82	0.001496576	0.042841838
ENSMUSG00000062960	Kdr	-1.79	0.0007048	0.023887913
ENSMUSG00000022614	Lmf2	-1.78	0.000259512	0.010778723
ENSMUSG00000066877	Nck2	-1.75	0.001160304	0.035818897
ENSMUSG00000035671	Zswim4	-1.74	0.000243279	0.010253637
ENSMUSG00000051817	Sox12	-1.72	0.001760584	0.048456352
ENSMUSG00000018412	Kansl1	-1.71	6.18E-06	0.000452769
ENSMUSG00000051855	Mest	-1.63	4.31E-06	0.000339188
ENSMUSG00000064120	Mocs1	-1.62	0.001646996	0.046107805
ENSMUSG00000061436	Hipk2	-1.61	5.29E-05	0.002795495
ENSMUSG00000005656	Snx6	-1.58	0.000743048	0.024743707
ENSMUSG00000018340	Anxa6	-1.58	0.00078051	0.025691614
ENSMUSG00000025757	Hspa4l	-1.55	0.001332109	0.039418012
ENSMUSG00000034845	Plvap	-1.55	0.000685297	0.023435527
ENSMUSG00000026275	Ppp1r7	-1.51	0.000176719	0.007823605
ENSMUSG00000027649	Ctnnbl1	-1.5	0.001243296	0.037568588